HOLOGRAPHIC ASPECTS OF BLACK HOLES, MATRIX MODELS AND QUANTUM CRITICALITY

OLGA PAPADOULAKI

ISBN/EAN: 978-90-393-6816-9

Printed by Ipskamp Drukkers

Holographic Aspects of Black Holes, Matrix Models and Quantum Criticality

Holografische Aspecten van Zwarte Gaten, Matrixmodellen en Kwantumcriticiteit

(met een samenvatting in het Nederlands)

Proefschrift

ter verkrijging van de graad van doctor aan de Universiteit Utrecht op gezag van de rector magnificus, prof. dr. G.J. van der Zwaan, ingevolge het besluit van het college voor promoties in het openbaar te verdedigen op maandag 28 augustus 2017 des middags te 12.45 uur

door

Olga Papadoulaki

geboren op 3 maart 1990 te Athene, Griekenland

PROMOTOR: Prof. S. Vandoren
COPROMOTOR: Dr. U. Gürsoy

to my family

CONTENTS

PUBLICATIONS xiii

1 INTRODUCTION 1
- 1.1 Holography . . . 1
  - 1.1.1 Holographic Principle . . . 1
  - 1.1.2 Gauge/Gravity duality . . . 2
- 1.2 Black Holes . . . 8
  - 1.2.1 Black Holes in AdS and in AdS/CFT . . . 9
- 1.3 Matrix Models and Liouville String Theory . . . 10
  - 1.3.1 Liouville field theory . . . 11
  - 1.3.2 Matrix Models . . . 13
- 1.4 Quantum Phase Transitions . . . 22
- 1.5 Content of the thesis . . . 24

2 THE BLACK HOLE S-MATRIX FROM QUANTUM MECHANICS 27
- 2.1 Introduction . . . 27
- 2.2 Back-reaction and the Black Hole S-Matrix . . . 29
  - 2.2.1 Derivation of the S-Matrix . . . 30
- 2.3 The model . . . 35
  - 2.3.1 Construction of the model . . . 36
  - 2.3.2 A projective light-cone construction . . . 40
  - 2.3.3 Relation to Matrix Models and two dimensional String Theory 42
- 2.4 Combining the oscillators (partial waves) . . . 43
  - 2.4.1 Time delays and degeneracy of states . . . 45
  - 2.4.2 Exponential degeneracy for the collection of oscillators . . . 47
- 2.5 Discussion . . . 50

3 MATRIX QUANTUM MECHANICS ON $S^1/\mathbb{Z}_2$ 55
- 3.1 The Setup . . . 59
  - 3.1.1 $c = 1$ Liouville Theory on $S^1/\mathbb{Z}_2$ . . . 59
  - 3.1.2 Fermionic orbifold theories . . . 60
  - 3.1.3 Matrix Quantum Mechanics . . . 62
  - 3.1.4 Orbifolding in the Matrix Model Picture . . . 63
- 3.2 The Canonical Partition Function . . . 65
  - 3.2.1 Partition function in terms of eigenvalues . . . 66
  - 3.2.2 Canonical partition function in terms of angles . . . 73
- 3.3 The Grand Canonical Partition Function . . . 77
  - 3.3.1 The Circle . . . 78
  - 3.3.2 Grand Canonical for the regular representation . . . 78
- 3.4 Large orbifold expansions . . . 84
  - 3.4.1 Generic n . . . 84
  - 3.4.2 $n = 0$ . . . 85
  - 3.4.3 $n = N/2$ . . . 86

3.5 Conclusions . . . 87
4 A MAGNETICALLY INDUCED QUANTUM CRITICAL POINT IN HOLOGRAPHY 93
4.1 Introduction and summary . . . 93
4.2 Gravity Set Up . . . 97
4.2.1 Black branes . . . 97
4.2.2 Good singularities and the thermal gas solution . . . 99
4.3 Thermodynamic quantities and the quantum critical point . . . 102
4.3.1 Thermodynamics of the black brane . . . 102
4.3.2 Thermodynamics of the thermal gas . . . 104
4.3.3 Difference of free energies and the quantum critical point . . . 104
4.3.4 Similarities with the Nambu-Jona-Lasinio model . . . 106
4.4 Fluctuations . . . 108
4.4.1 Spectrum in the thermal gas phase . . . 109
4.4.2 Spectrum in the black brane phase . . . 111
4.4.3 Extended probes . . . 111
4.5 Discussion and Outlook . . . 112
A APPENDIX OF CHAPTER 3 117
A.1 Other classes of orbifolds . . . 117
A.2 Oscillator wavefunctions . . . 117
A.2.1 Normal Harmonic Oscilator . . . 118
A.2.2 Inverted Harmonic Oscillator . . . 118
A.2.3 Mehler for parabolic cylinder . . . 120
A.3 Representation in terms of angles (Wilson-lines) . . . 120
A.3.1 Measure . . . 123
A.3.2 Pfaffian in regular representation . . . 123
A.4 Grand Canonical for $n = 0$ . . . 124
A.5 Hilbert transform properties . . . 125
A.6 The Kernel . . . 127
A.6.1 Kernel in Energy basis . . . 127
A.6.2 Kernel in elliptic functions . . . 128
A.6.3 Trace of the kernel . . . 128
A.6.4 1-particle density of states . . . 129
A.7 Approximate methods for large β . . . 130
A.7.1 Circle in angles . . . 131
A.7.2 Generic n in angles . . . 131
A.7.3 Generic n in eigenvalues of M . . . 131
A.7.4 $n = 0$ . . . 132
A.7.5 $n = N/2$ with Hermite polynomials . . . 135
A.7.6 $n = N/2$ with parabolic cylinder functions . . . 137
B APPENDIX OF CHAPTER 4 143

SUMMARY 151
SAMENVATTING 153

ACKNOWLEDGMENTS 155
CURRICULUM VITAE 157

BIBLIOGRAPHY 159

PUBLICATIONS

This thesis is based on the following papers:

- Chapter 4 is based on *A magnetically induced quantum critical point in holography*,
  A. Gnecchi, Gürsoy, O. Papadoulaki, C. Toldo,
  Published in JHEP 1609 (2016) 090
  DOI: 10.1007/JHEP09(2016)090.
  arXiv:1604.04221 [hep-th].

- Chapter 2 is based on *The Black Hole S-Matrix from Quantum Mechanics*[1],
  P. Betzios, N. Gaddam and O. Papadoulaki,
  Published in JHEP 1611 (2016) 131
  DOI: 10.1007/JHEP11(2016)131
  arXiv:1607.07885 [hep-th].

- Chapter 3 is based on *Matrix Quantum Mechanics on the* $S^1/\mathbb{Z}_2$[2],
  P. Betzios, U. Gürsoy and O. Papadoulaki,
  arXiv:1612.04792 [hep-th].

The most part of this thesis is an identical reproduction of the above papers.

1 This paper has also been part of the thesis of N. Gaddam [1] and P. Betzios [2].
2 This paper has also been part of the thesis of P. Betzios [2].

1 INTRODUCTION

In this thesis we will present three seemingly very different models that can be treated in the context of holography. First, in chapter 2 we will present the black hole S-matrix of Gerard 't Hooft, and we will show how by solving a quantum mechanical problem, one can obtain the same S-matrix. Then, in chapter 3 we will present the correspondence between non critical Liouville string theory coupled to $c = 1$ matter and the dual matrix quantum mechanics model. Finally, in chapter 4 we will present an example of correspondence, between a condensed matter system at quantum criticality and a gravitational theory. We would like in this chapter, to give a basic and self-contained introduction of the various physical notions that one needs to be familiar with in order to read this thesis. As well as to emphasise the underlying links among the seemingly unrelated three main chapters.

1.1 HOLOGRAPHY

If one wants to summarise in one word what is the core subject of this thesis, this word would be holography. What we mean by holography broadly is the mapping of a gravitational theory in D dimensions to a quantum mechanics system or quantum field theory in less dimensions. In this section we first present the Holographic Principle by 't Hooft and then we focus on gauge/gravity duality, which is the best understood example of holography to date.

1.1.1 *Holographic Principle*

The holographic principle was first stated by Gerard 't Hooft [3] and then refined by Susskind [4] who combined his ideas with those of Thorn [5] and 't Hooft. The original statement by 't Hooft is that if we want the physical phenomena associated with gravitational collapse to be consistent with the postulates of quantum mechanics, then at a Planckian level our world does not have the degrees of freedom expected in $3 + 1$ dimensions but rather the observable degrees of freedom can be described as if they were Boolean variables defined on a two-dimensional lattice, evolving with time. This idea was inspired by the Bekenstein-Hawking entropy of a black hole, which as we will see later on is given by an area law and it does not scale with the volume as is usually the case with statistical systems –where gravity does not play any role. More generally one can make the statement that our world is a hologram in the sense that its degrees of freedom can be understood as the degrees of freedom of a two dimensional lattice where at each lattice point there is one degree of freedom –one bit of information.

These ideas gave seeds to what we now call gauge/gravity duality. The latter, was initially formulated in the context of D- branes in string theory. Its best understood example is the duality between $\mathcal{N} = 4$ super- Yang-Mills (SYM) field theory at strong coupling and type IIB string theory on $AdS_5 \times S^5$ at weak coupling (supergravity limit). It is also called AdS/CFT[1]. Gauge/gravity duality has been applied to much more general systems than the previous example. For example it can be used even outside the context of string theory, when the field theory is not conformal and the gravity is asympotically locally AdS. In this more general form it can be used to describe physics at strong coupling in condensed matter systems and phenomenological QCD models. In the next subsection we are going to review both the formal and the more applied aspects of gauge/gravity duality.

1.1.2 *Gauge/Gravity duality*

Gauge/Gravity duality refers to the correspondence between a gauge theory and a gravitational theory at some appropriate limit, that we are going to describe in the following. But first we should introduce the large N limit and the 't Hooft coupling that as we will show are essential for the existence of gauge/gravity duality. There is a tremendous number of reviews about gauge/gravity duality both for the applications and the more formal aspects, here we cite only the reviews that we used to write this section [6, 7, 8].

1.1.2.1 *The large N limit and the 't Hooft coupling*

One of the first hints that gauge theories are related to string theories was given by the large N expansion proposed by Gerard 't Hooft [9] as a possible approach to render QCD solvable. Before we move on to present the large N limit, let us first mention that string theory that now is a theory of gravity was first formulated in order to explain the experimental discovery of mesons and hadrons in the 1960's. The idea was to view all these particles as different oscillation modes of a string. This approach was successful in capturing some aspects of the spectrum of those particles. It was later discovered that hadrons and mesons are actually made of quarks and that they are described by quantum chromodynamics (QCD).

QCD, is a gauge theory that has an $SU(3)$ gauge symmetry. This is what we call colors of quarks. The basic characteristic of QCD is that it is strongly coupled at low energies and that its coupling decreases as the energy increases (it is asympotically free). QCD at low energy is strongly coupled and cannot be treated perturbatively. Moreover it is not clear what is an appropriate expansion parameter since the coupling constant is not a free parameter but after renormalisation it is absorbed into defining the scale of the masses. Therefore, we are not able to perturb with respect to it.

1 The term AdS/CFT stands for Anti-de-Sitter space/ Conformal Field Theory since as we will see later on the gravity theory lives in an AdS space and the field theory is conformal in the case of the canonical example given by Maldacena.

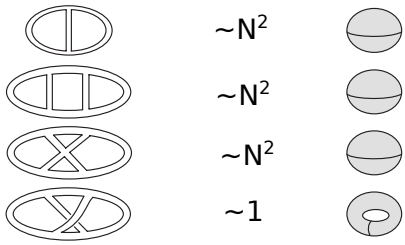

FIGURE 1: Perturbation expansion in powers of $1/N$ and classification with respect to the topology of the graphs.

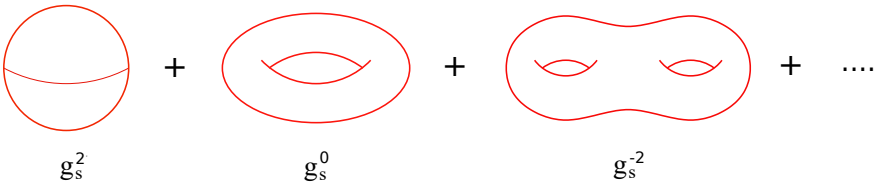

FIGURE 2: Genus expansion of closed oriented strings, g_s is the string theory coupling constant.

To tackle this issue, Gerard 't Hooft in [9] proposed that one can send $N \to \infty$ and the same time to keep fixed $\lambda = g^2 N$, where λ is the 't Hooft coupling and g is the bare coupling constant of the gauge interactions. Now, the 't Hooft coupling is the one that governs the pertubative expansion. The idea is that the gauge theories simplify at large N limit and one can have a well defined perturbation expansion in powers of $1/N$. Indeed, he showed that the correlation functions at this limit have such an expansion. Moreover by introducing the double line notation he classified the various Feynman graphs with respect to their topology –their genus (number of handles in a two dimensional surface)– this is the so called "genus expansion", see Figure 1. It can be shown that the only diagrams that contribute at this limit are the planar[2] ones, since they are of order N^2 and the rest are suppressed by powers of $1/N^2$. Another theory that we find such genus expansion is in perturbation theory of closed oriented strings, see Figure 2. We can match these two by identifying $g_s = 1/N$, where g_s is the string coupling constant. In this case the genus is referred to the different topologies of the two dimensional string worldsheet. This similarity between the gauge theory and the string theory expansion is the strongest indication that there should exist some relation between them. But, this is not enough to tell us which string theory is dual to which gauge theory.

2 They are diagrams that can be draw on a sphere without intersecting themselves.

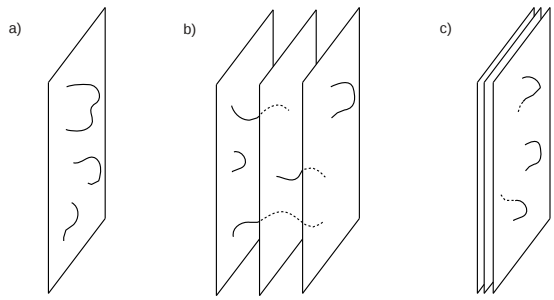

FIGURE 3: In picture a) we see a Dp- brane where open strings can end. In picture b) we see three parallel Dp- branes where open strings stretch among them. In picure c) we see a stack of N coincident Dp- branes where N^2 open strings are stretching on.

1.1.2.2 *AdS/CFT correspondence*

The best way to see the relation between gauge theories and string theories is by studying Dp- branes, where we will be able to show that we can get the two different theories by taking two different limits. The best understood example was given by Maldacena in [10] and it is the one that we are going to describe here. Take a stack of N coincident Dp- branes with N being large. Dp- branes are objects in string theory with p spatial dimensions. We want to describe the low energy excitations of this stack of Dp- branes in two different limits. For simplicity we will restrict to a stack of N coincident $D3$- branes embedded in nine spatial dimensions of IIB string theory, see Figure 3. How strong is the gravitational back-reaction depends on how large N is and on the dimensionless string coupling constant g_s. When

$$\lambda \equiv 4\pi N g_s \ll 1\,, \tag{1.1}$$

the gravitational back-reaction of the $D3$- branes is negligible, since the tension of the N $D3$- branes scales as N/g_s, but the strength of gravity is g_s^2. In this limit the $D3$- branes, just exist in the nine dimensional space parallel to each other and between each pair of them there are open strings stretching, there are N^2 such strings. Since the branes are coincident, the lightest string states are massless. These are the low energy degrees of freedom of the theory. These N^2 massless excitations can be described by $\mathcal{N} = 4$ super Yang-Mills theory. This theory, has an $SU(N)$ symmetry and its matter content transforms in the adjoint representation this allows us to introduce matrix indices for their study. This theory describes excitations that propagate on the three spatial dimensions of the $D3$- branes and has the following Lagrangian density

$$L \sim \frac{N}{\lambda}\mathrm{Tr}\left(F^2 + (\nabla\Phi)^2 + i\bar{\Psi}\not{D}\Psi - i\bar{\Psi}\left[\Phi,\Psi\right] - \left[\Phi,\Phi\right]^2\right)\,, \tag{1.2}$$

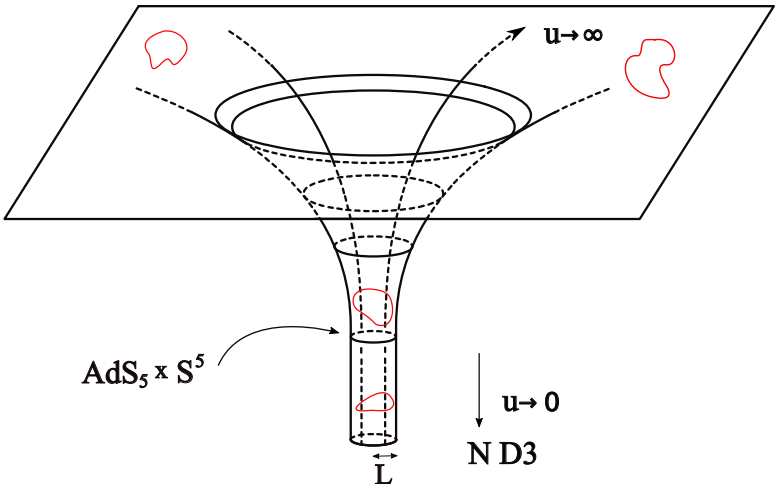

FIGURE 4: In this picture we see the formation of $AdS_5 \times S^5$. The stack of N $D3$- branes gravitationally collapses and forms the infinite throat at $u \to 0$, when we are at the limit (1.3). The $D3$- branes act as sources of closed strings (red closed lines). These closed strings cannot escape from the throat since it is infinite and at this limit the transmission and absorption probabilities are zero thus they decouple from the rest flat space $u \to \infty$. L is the AdS_5 radius and u is the radial coordinate in the ten dimensional flat space time.

where F is the $SU(N)$ field strength, Φ are bosons and Ψ are fermions. Both of them transform under the adjoint representation of $SU(N)$, thus can be written as matrices. The overall trace is over the $SU(N)$ indices. Moreover this theory is supersymmetric with a global $SU(4)$ symmetry (R- symmetry) as well as conformal ($SO(4,2)$). One can see that (1.1) is the 't Hooft coupling. To summarise, the claim is that the low energy excitations of the stack of N $D3$- branes in the limit (1.1) is given by a weakly interacting matrix large N theory.

In the opposite regime

$$\lambda \equiv 4\pi N g_s \gg 1\,, \tag{1.3}$$

the effects of gravity are very strong forcing the N Dp- branes to gravitationally collapse forming a black brane, see Figure 4. By definition the horizon of the black brane is infinitely gravitationally redshifted. Thus for an observer at infinity the low energy excitations of the system are excitations that occur at the near horizon geometry. In our case the near horizon geometry is $AdS_5 \times S^5$ with the following metric

$$ds^2 = L^2\left(\frac{-dt^2 + \sum_{i=1}^{3} dx_i^2 + dr^2}{r^2} + d\Omega_5^2\right). \tag{1.4}$$

The x_i coordinates are along the $D3$- brane spatial dimensions, the radial coordinate r is orthogonal to the $D3$- branes, while the rest five directions form a five sphere.

The horizon is at $r \to \infty$ and the AdS radius L can be related to the string length L_s and the Planck length L_p, $L = \lambda^{1/4} L_s = (4\pi N)^{1/4} L_p$. In particular, in the strong 't Hooft coupling regime (1.3) and at large $N \gg 1$, the radius of curvature L of the $AdS_5 \times S^5$ geometry is very large compared to both the string and the Planck lengths. Thus, we can neglect quantum gravity effects and highly excited string states, so that the near horizon excitations are classical gravitational perturbations of the background (1.4). The AdS_{d+1} space is a maximally symmetric space with isometry group $SO(d,2)$[3].

The conclusion of the above discussion is that the low energy excitations of a stack of N $D3$- branes at the two opposite 't hooft coupling limits are described by two different theories, a gauge theory at weak coupling and a gravity theory at strong coupling.

Maldacena conjectured in [10] that there exists a decoupled set of degrees of freedom that interpolates between these weak and strong coupling descriptions. In the context of $D3$- branes this translates to the following: the classical gravitational dynamics of $AdS_5 \times S^5$ is the strong coupling description of large N $\mathcal{N} = 4$ super Yang-Mills theory. One can notice that the gravitational theory lives in more dimensions than the gauge theory.

There are more examples of such dualities that one can form by choosing different types of branes. Another very important example comes from M- theory, if one takes a stack of large N number of $M2$- branes in $\mathbb{R}^{1,2} \times \mathbb{R}^8/\mathbb{Z}_k$ then the low energy theory is at weak 't Hooft coupling the $2+1$- dimensional gauge theory called ABJM [11] and at strong 't Hooft coupling is the 11- dimensional supergravity on $AdS_4 \times S^7$.

AdS/CFT and more generally gauge/gravity duality is a strong/weak type of duality. Seen in a string theoretical framework it is an open/closed duality, since D-branes can be seen as objects where open strings can end but also as sources of closed strings. In the weak 't Hooft coupling, it is the open strings spectrum that gave us the gauge theory (the open string spectrum does not include the graviton). On the other hand, the equivalent interpretation as closed string sources (graviton is included in this case) gave us the gravitational theory. There are other examples of open/closed duality that hey were discovered even before AdS/CFT. Such an example of open/closed duality is the duality between noncritical string theory and the $c \leq 1$ matrix models[4] that we will study in chapter 3.

1.1.2.3 *Applied Gauge/Gravity Duality*

Now, that we have presented the best understood example of gauge/gravity duality from a string theoretical point of view, we are ready to move towards applications

3 One can notice that the conformal group of a d dimensional conformal field theory is the same as the isometry group of AdS_{d+1} space. This matching of the symmetries justifies, as we will see in 1.1.2.3 in the context of applied AdS/CFT that we ask for the gravity theory to be asympotically locally AdS and to live in one more dimension than the field theory.

4 In this thesis we are going to present the case of $c = 1$ matrix model and Liouville string theory in the form of "old matrix model" where open/closed duality is not essential for our results, but we are going to give a basic presentation of the D- brane interpretation.

of this duality. Although, the duality is not proven mathematically there have been many successful consistency checks. We are at such level of confidence that we use the duality in less restrictive setups and outside the string theoretic framework. By this we mean the following: it is enough to have a gauge field theory that is strongly coupled [5] and has a large number of colors on the one side and a classical gravitational theory at weak coupling and one more dimension that is asymptotically locally AdS on the other. Then the defining relation of the correspondence is [12]:

$$\left\langle e^{\int d^d(x) J(x)\mathcal{O}(x)} \right\rangle_{CFT} = \int \mathcal{D}\phi\, e^{S_{AdS_{d+1}}}\big|_{\phi(x,\partial AdS)=J(x)}\,, \tag{1.5}$$

where, $J(x)$ is the source for the operator $\mathcal{O}(x)$ in the field theory side and $\phi(x,r)$ is the bulk field that lives in the AdS space and whose leading behavior near the boundary corresponds to the source for the operator $\mathcal{O}$. Thus if one wants to compute correlation functions for the operator $\mathcal{O}$ should vary the gravitational action with respect to the dual field ϕ. The matching between the different computations that can be performed at each side can be done using the holographic dictionary below.

∂AdS: CFT	Bulk AdS: Gravity
Global Symmetry	Gauge Symmetry
Temperature	Hawking temperature
chemical potential/charge density	boundary values of the gauge field
Scalar operator $\mathcal{O}_b$	Scalar field $\phi(x,r)$
Energy-Momentum Tensor T_{ab}	Metric Tensor $g_{\mu\nu}$
Global Internal Symmetry Current J_a	Maxwell Field A_μ

This broader definition of gauge/gravity duality allows us to study condensed matter systems such as strange metals and high temperature superconductors [8], where strong coupling and lack of a quasi-particle description renders the usual methods insufficient. Moreover, phenomenological models of QCD were constructed that show agreement with lattice computations and experimental results [13, 14].

In contrast with the example of the previous section, where one follows a top-down approach, starting from string theory and taking appropriate limits to arrive at the quantum field theory and the classical gravity descriptions respectively, in the case of applied holography the approach is more phenomenological. In this case, one just assumes the validity of the duality and proceeds by using the dictionary. This way, one maps the strongly coupled field theoretic problem to a problem described by an effective weakly coupled (classical) gravity theory. This approach is called bottom-up and since the connection through string theory is lacking one can not know the exact field content of the theory. As one can see from the dictionary the only relations that one can get are expectation values and correlation functions of operators. But, still

5 Let us stress that conformality is not essential and can be dropped.

this approach is very useful since these are precisely the observable quantities -the quantities that one can measure in an experiment and the ones that have a physical meaning.

1.2 BLACK HOLES

Black holes are fascinating and mysterious objects that can be observed in nature [15]. At the same time there is huge theoretical interest in them for various reasons that we are going to review in the following paragraphs, such as the well known information paradox. Except of their own very interesting and still not completely understood physics, one can appreciate their usefulness as tools that give access and shed light in the thermodynamic properties and phase transitions of strongly coupled systems in the framework of gauge/gravity duality.

Black holes as astrophysical objects are very dense and they have a singularity at their center that is cloaked by a surface called the event horizon. After something passes through the event horizon classically cannot get out and even the light cannot escape hence the name. One way that a black hole can form is when a very large star has burned all its fuels and cannot support its volume anymore. Then, it undergoes a gravitational collapse shrinking to a tiny size with huge density, this is the so called singularity. The gravitational field around it is huge and it starts "eating" anything that passes through its event horizon even light, making it even more dense. Since black holes are "black" they do not emit any electromagnetic signal outside their event horizon at least classically. The way that scientists detect a black hole is from other astrophysical objects that are forced to orbit around them due to the black hole's huge gravitational field. They accelerate and emit radiation and hence give us the signal that something with huge mass is there.

In the beginning of the 20th century, general relativity was discovered and came to explain in a classical context the gravitational interactions in cosmological scales. Schwarzschild in 1916 found the black hole solution [16]–named after him– as solution of the vacuum Einstein equations. This means that general relativity, allows such singular geometries. What characterises such a solution is a curvature singularity that is cloaked by a horizon. After the black hole has formed, it is characterised only by a handful of parameters. Those are its mass and charges such as the electric charge and the angular momentum. This means that we lost all the information about the in-falling matter that formed the black hole. This property allows us to treat the black hole as a thermodynamic system. Indeed, it was discovered that the three laws of thermodynamics can be translated to the three laws of black hole mechanics [17].

Bekenstein [18] and Hawking [19] argued that the entropy of the black hole scales with the area of the horizon, in contrast with what is expected usually from statistical systems where the entropy scales with the volume[6]. Moreover, Hawking by doing a semi-classical computation discovered that black holes emit thermal radiation [20]. Since the radiation is thermal, after the total evaporation of the black hole, we can-

6 This observation, as we saw led to the formation of the holographic principle since it seems that all the degrees of freedom of the black hole "live" on its horizon.

not recover the information of the particles that created it. Information loss violates unitarity and unitarity is essential for a consistent quantum mechanical theory. This is the well known information paradox. There are many proposals for the solution of the information paradox and the reconciliation of gravity with quantum mechanics. One of them is by Gerard 't Hooft and is based on the black hole S-matrix [21]. The black hole S-matrix is formulated by taking into account the gravitational backreaction that the ingoing particles have on the outgoing ones close to the horizon. We will review the black hole S-matrix in detail in chapter 2, so we are not going to give any more details here.

Another issue is what we mean by the black hole entropy. In the language of statistical physics the entropy counts the microscopic degrees of freedom –microstates– of a system. But what are these microstates that the black hole is composed of? For a theory of quantum gravity to be consistent, it should allow for a microstate counting and this counting should reproduce the area law of the thermodynamic black hole entropy. Such check has only be performed in the context of string theory and for supersymmetric black holes [22]. For this computation supersymmetry was crucial since it makes the microstates insensitive to effects due to changes of the string coupling. The identification of microstates was made using open/closed duality and counting them using the Cardy formula in the conformal field theory side, so still we do not know what are these microstates in the gravitational picture. Due to these reasons there has not yet been performed a microstate counting for the Schwarzschild black hole.

1.2.1 *Black Holes in AdS and in AdS/CFT*

New developments in the study of black holes came with gauge/gravity duality. As we saw AdS/CFT has its seeds in the holographic principle. Black holes are a natural framework for the holographic principle, since a hologram is a two dimensional picture that encodes information about a three dimensional object. Like the black hole entropy is encoded at its horizon and it scales with its area, but encodes all the information about the black hole.

The new insight that AdS/CFT gave us is that now we can have a dual description of the black hole physics in terms of a quantum field theory. Naturally, there are many studies that try to solve the information paradox [23, 24] in this context as well as to count the black hole microstates [25, 26, 27, 28]. There is a drawback, though in this approach, that we can study asymptotically AdS and not asymptotically Minkowski black holes.

On the other hand, in the context of gauge/gravity duality one can use the semiclassical description of black holes to model strongly coupled field theories at finite temperature, charge density, magnetic fields etc. Indeed in chapter 4 of this thesis we are going to use this approach to model a strongly coupled system at finite charge density and under external magnetic field. There are many such studies in the applied AdS/CFT literature, for example we have seen the use of black holes to model

high temperature superconductors, heavy ion colisions, the dehavior of quark-gluon plasma etc.

Since in chapter 4 we are going to use asymptotically Anti-de Sitter black hole solutions arising in four-dimensional $\mathcal{N} = 2$ gauged supergravity, we would like to give a brief and incomplete overview. Gauged supergravity is the low energy effective theory describing string compactifications in the presence of fluxes. Compactifications on a seven dimensional manifold give us four dimensional configurations with a scalar potential. This potential allows for a negative cosmological constant, thus for asymptotically AdS black hole solutions. The solutions that arise at this context are very useful for many reasons [29]. First of all some of them can be embedded in M/string theory and through AdS/CFT can be seen as dual configurations in the context of ABJM [11] theory. In this framework there are recent studies that are trying to count their microstates [25, 26, 27, 28]. Moreover since they are four dimensional, they can be charged and be at finite temperature, by employing the AdS/CFT dictionary, they can be used in studies of $2 + 1$- dimensional condensed matter systems. Indeed they have been used in top down models of holographic superconductors [30, 31, 32]. Going away from the formal AdS/CFT, we see their extensive use also in applied gauge/gravity duality where people use them to explore universal behaviors of transport coefficients as well as to study phase transitions both in top-down and bottom-up models [33, 34, 35].

1.3 MATRIX MODELS AND LIOUVILLE STRING THEORY

Random matrix models have many applications in various fields of theoretical physics. In the context of this thesis we are interested in matrix models from the point of view of string theory. But, first we would like to give some examples of the use of random matrices in other physical problems. The use of matrix models implies the existence of random processes, since usually we turn to them when the matrix size is large.

The first time matrix models where used in physics, was when Wigner [36] realised that the energy levels of large atomic nuclei have the same distribution as the spectrum of eigenvalues of a random Hermitian matrix when the size of the matrix becomes infinite. The importance of this observation lies in the fact that one can use the matrix model approach for any nucleus that is sufficiently large, thus there is an underlying universality. The identification of universal features is very important in the case of chaotic systems and systems with large number of degrees of freedom.

Another natural case that we can use matrix models is when we take the large N limit. As we already saw, since the gauge fields are operators in the adjoint representation of $SU(N)$ they are $N \times N$ unitary matrices. Moreover, if we use the double line notation we can classify the Feynman diagrams according to their topology. In this limit only the planar graphs contribute –the ones that can be drawn on a sphere without intersecting themselves. Furthermore, one can have a diagrammatic expansion in terms of the size of the matrix for each matrix model. These, simplifications although did not solve QCD gave a huge insight in the connection between string theory and gauge theories and as we already saw led to gauge/gravity duality.

In the following subsections we are going to present the connection of matrix models with two dimensional string theory. Again there are numerous reviews, here we cite the ones that we used [37, 38, 39, 40].

1.3.1 *Liouville field theory*

As we know from a basic course in string theory, for a string theory to be consistent we want the Weyl anomaly to cancel. This can happen only for specific dimensions of spacetime. These special dimensions are twenty six for the bosonic case and ten for the supersymmetric one. Moreover in the supersymmetric case we have absence of the tachyonic mode –scalar mode with negative mass– that destabilizes the vacuum in the bosonic case. When the Weyl anomaly is not canceled we can still have meaningful theories, the so called noncritical string theories. Such theories can be interpreted as statistical ensembles of collections of two dimensional surfaces embedded in a D dimensional space. Employing this interpretation we can even allow for breaking of Weyl invariance at the classical level for example by introducing a worldsheet cosmological constant.

String theory is believed to be the theory that describes our world since it produces all possible states that we need, incorporates quantum gravity and at low energies it can reduce to interesting field theories. Moreover, it has the ability to describe many different worlds, but it does not have a mechanism to explain why our world is as it is. One of the reasons that we do not have a more thorough physical understanding of string theory is the difficulty to incorporate non perturbative effects[7] [**?**]. After the discovery of D- branes a lot of progress has been made towards this direction for example through open/closed duality and AdS/CFT. Another road that scientists followed, before the advent of D- branes was discovered, was to try to work in two dimensions where due to reduction of the number of dynamical degrees of freedom the equations and the physics simplify considerably but still interesting phenomena can arise. In this section we are going to follow this second path. We are interested in Liouville field theory coupled to $c = 1$ matter, a non-critical string theory that is equivalent to two dimensional string theory in a linear dilaton background, a critical string theory.

Liouville equation named after Joseph Liouville was studied by him in order to understand the conformal properties of the Riemann surface (especially the uniformization problem[8]). When one quantises the two dimensional gravity the quantum Liouville equation emerges. Starting from the Polyakov formulation of the path integral of string theory for fixed topology, allowing for a cosmological constant term we have,

$$Z = \int [Dg]\,[DX]\, e^{-S[g;X]-\mu_0 \int d^2z\sqrt{g}}\,, \tag{1.6}$$

7 More precisely we do not know what is the true vacuum of the theory.

8 The uniformization theorem says that every simply connected Riemann surface is conformally equivalent to one of the three Riemann surfaces: the open unit disk, the complex plane, or the Riemann sphere. In particular it implies that every Riemann surface admits a Riemannian metric of constant curvature.

where

$$S[g;X] = \int d^2z\sqrt{g}g_{\mu\nu}\partial^\mu X^I\partial^\nu X^I\,, \tag{1.7}$$

$g_{\mu\nu}$ is the metric of the two dimensional worldsheet and X^I are the bosonic matter fields that live there. This integral implies that we have to integrate over all possible topologies and geometries in two dimensions. If one performs a Weyl transformation $g_{\mu\nu} \to e^\sigma g_{\mu\nu}$, then a kinetic term will arise for the scalar field σ at the action due to the fact that the integration measure $Dg_{\mu\nu}$ is not invariant under the Weyl transformation. Exponentiating this anomaly, one arrives at the Liouville action,

$$S_L = \int d^2z\left(\frac{1}{2}\partial_\mu\sigma\partial^\mu\sigma + R\sigma + \mu e^\sigma\right)\,. \tag{1.8}$$

To perform the path integral over the metric, we decompose the fluctuation of the metric into the diffeomorphism v_μ, Weyl transformation σ and the moduli Y. The action and the measure of integration by definition are diffeomorphism invariant. This is a gauge symmetry and we have still leftover gauge invariance that we need to get rid off. We do so by dividing with the volume of the gauge group. Then we are left with integration over the conformal mode and the moduli. To implement this change of variables we employ the Fadeev-Popov method. In the case of critical string theory Weyl symmetry is a gauge symmetry and we can again get rid of it, but in our case we cannot do this due to the anomalies at the integration measure. By choosing to work in the conformal gauge $g_{\mu\nu} = e^\phi\hat{g}_{\mu\nu}$, the partition function of the two dimensional quantum gravity coupled to matter fields is

$$Z = \int [DY]\left[D\phi_{e^\phi\hat{g}_{\mu\nu}}\right][Dbc]\left[DX_{e^\phi\hat{g}_{\mu\nu}}\right]e^{-S[X,\hat{g}]-S[bc,\hat{g}]}\,. \tag{1.9}$$

where b, c are the Fadeev-Popov ghosts. For the Liouville action to emerge we have to integrate over the Liouville mode ϕ, but there is an issue here. The integration measure for ϕ is not Gaussian and it is tricky to integrate over it. In order to bring it to the Gaussian form we have to perform a Jacobian transformation. This is very difficult. Another way to treat this –proposed by David-Distler-Kawai (DDK)– is to guess the Gaussian measure by asking for "locality", "diffeomorphism invariance" and "conformal invariance". Then we get the renormalised Liouville action

$$S = \frac{1}{4\pi}\int d^2z\sqrt{g}\left(\partial_\mu\phi\partial^\mu\phi + QR\phi + 4\pi\mu e^{2b\phi}\right)\,, \tag{1.10}$$

where one can find that $Q = b + b^{-1}$. Moreover, for the metric to be real the central charge of the matter field $c_m \leq 1$.

Let's now present the second interpretation of the $c = 1$ Liouville theory as a critical two dimensional string theory. Let's start by considering the sigma model description of the critical string in general dimensions with arbitrary background fields.

$$S = \frac{1}{4\pi}\int d^2z\sqrt{g}\left(g^{\mu\nu}G_{ab}(X)\partial_\mu X^a\partial_\nu X^b + 2\Lambda^2 T(X) + \frac{1}{2}R\Phi(X)\right)\,, \tag{1.11}$$

where we have put $B_{\mu\nu} = 0$ (the total antisymmetric rank two tensor) and Λ is the cut-off scale of the world sheet. If we ask for the background to be consistent with the string equation of motion then this action has to satisfy conformal invariance. This translates to the vanishing of the beta functions at first order with respect to α'.

$$\begin{aligned} \beta_{\mu\nu}(g) &= R_{\mu\nu} + \nabla_\mu \nabla_\nu \Phi - \frac{1}{4}\partial_\mu T \partial_\nu T \\ \beta(\Phi) &= -R + (\partial_\mu \Phi)^2 - \nabla^2 \Phi + \frac{2(D-26)}{3} - T^2 + \frac{1}{6}T^3 \\ \beta(T) &= \nabla^2 T - \partial_\mu \Phi \partial^\mu T + 4T - T^2 . \end{aligned} \tag{1.12}$$

These beta functions can be seen as equations of motion of the following effective action

$$S = \int d^D x \sqrt{G} e^{-\Phi} \left[R + (\partial_a \Phi)^2 - \frac{2(D-26)}{3} - \frac{1}{4}(\partial_a T)^2 + T^2 - \frac{T^3}{6} \right] . \tag{1.13}$$

If we compare the action (1.11) with the $c = 1$ Liouville action,

$$S = \frac{1}{4\pi} \int d^2 z \sqrt{g} \left(g^{\mu\nu} \partial_\mu \phi \partial_\nu \phi + 2R\phi + 4\pi\mu e^{2b\phi} + g^{\mu\nu} \partial_\mu X \partial_\nu X \right) , \tag{1.14}$$

we see that when $\mu = 0$, they match for: $D = 2$, $G_{ab} = \eta_{ab}$, $\Phi = 4\phi$ and $T = 0$. When $\mu \neq 0$ then we also have the following identification: $\Lambda^2 T = 2\pi\mu e^{2\phi}$. In this case though, the mass-shell condition for the tachyon field is satisfied[9] but the one-loop corrected beta function is not. Since, Liouville theory is by definition conformal invariant we expect that if one includes all orders in α' the beta function will be satisfied. We see that $\Phi = 4\phi$ gives rise to the emergent second dimension the so called Liouville dimension. The inclusion of the tachyonic mode T is very important since as we can see from $\Lambda^2 T = 2\pi\mu e^{2\phi}$, it is analogous to the exponential of the Liouville direction. As we see from (1.11) it imposes an exponential potential at the string theory action, that protects the perturbative string theory from entering the strong coupling regime, thus allowing for a meaningful perturbation theory, see Figure 5.

Using the string theory formulation one can compute the genus one (torus) partition function. One can also quantise semi-classically the theory and compute expectation values of correlators of operators again though at some approximation. The tool that enables us to compute higher genera and non-perturbative contributions is the matrix model approach that we are going to describe in the next subsection.

1.3.2 *Matrix Models*

The $c = 1$ Liouville field theory can be represented by a matrix model. This matrix model comes to life by summing over geometries embedded in one dimension, but as we have already shown the resulting string theory is two dimensional and the extra

9 It is a massless field in the case of two dimensional string theory, it is not really a tachyon.

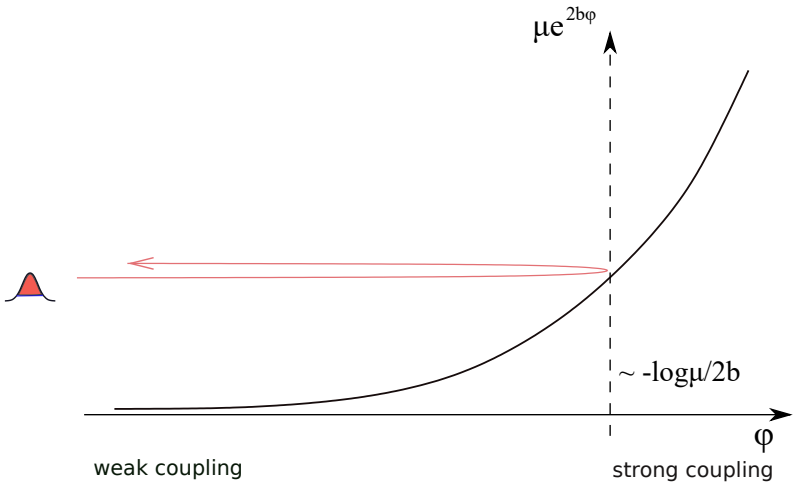

FIGURE 5: In this picture we see the scattering of a tachyon excitation off the tachyon potential $\mu e^{2b\phi}$. When $\phi \to \infty$ (strong coupling), the exponential barrier keeps the string theory perturbations from reaching the strongly coupled region.

dimension comes from the Liouville mode. The role of the matrix model is to map this one dimensional embedding into a non-relativistic quantum mechanics model of free fermions. In this language, in principle one can compute any quantity at all genera.

We parametrize the continuous surfaces by coordinates z_1, z_2. The Euclidean geometry is described by the metric $g_{\mu\nu}(z)$, and the embedding by the scalar field $X(z)$. Then indeed the theory of random surfaces in one embedding dimension is equivalent to two dimensional quantum gravity coupled to a scalar field. This can be seen from the path integral formulation, where we have to sum over all the compact connected geometries and their embeddings,

$$Z = \sum_{topologies} \int [Dg_{\mu\nu}][DX] e^{-S} , \tag{1.15}$$

where we have chosen S to be the simplest covariant action in two dimensions:

$$S = \frac{1}{4\pi} \int d^2z \sqrt{g} \left(g^{\mu\nu} \partial_\mu X \partial_\nu X + R\Phi + 4\lambda \right) . \tag{1.16}$$

As we know in two dimensions the integral of curvature R

$$\frac{1}{4\pi} \int d^2z \sqrt{g} R = 2(1-h) = \chi_{Euler} , \tag{1.17}$$

gives the Euler characteristic χ_{Euler} that depends only on the number of handles h –the genus– of the surface. One can see the surface with h handles as a string theory diagram with h loops. The weighting factor for a surface with h handles is $e^{\Phi(2h-2)}$

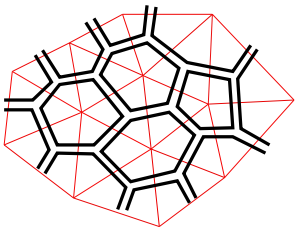

FIGURE 6: In this picture we see the trangulation of a surface. The red lines compose the triangular lattice Λ and the black double lines the dual lattice $\tilde{\Lambda}$.

and we can identify $g_0 = e^{\Phi}$ where g_0 is the string theory coupling. Instead of the continuous approach that we presented in the subsection above, here we are going to sum over discrete approximations to smooth surfaces and then we will take the limit that the lattice spacing goes to zero to get the continuum sum. One way to discretise the surfaces is to triangulate them, see Figure 6 –to approximate the surfaces with a collection of equilateral triangles with side a. Each face of the triangular lattice is considered flat, and the curvature is entirely concentrated at the vertices. Each vertex I of the triangular lattice has a conical singularity with deficit angle $\pi(6 - q_I)/3$, where q_I is the number of triangles that meet at I. Thus, the vertex I has a delta-function of curvature with positive, zero, or negative strength if $q_I \leq 6, = 6, \geq 6$ respectively. In the continuum limit the size of each face becomes infinitesimal, and we can define the smoothed out curvature by averaging over many triangles.

The basic assumption that we made here is that the sum over the handles is equivalent to the sum over the various lattices when we send the lattice spacing to zero. Then the integral over the embeddings $\int [DX]$ is defined as the integral over all possible embeddings of the lattice in the real line. The last piece left to complete the procedure is to specify the weight attached to each configuration. This can be done by discretising the action (1.16) and counting each configuration with weight e^{-S}. The discretised version of (1.15) is

$$Z(g_0, \kappa) = \sum_h g_0^{2(h-1)} \sum_{\Lambda} \kappa^V \prod_{i=1}^{V} \int dX_i \prod_{\langle ij \rangle} G\left(X_i - X_j\right) , \tag{1.18}$$

where Λ is the lattice, $\langle ij \rangle$ is referred to the links of the dual lattice $\tilde{\Lambda}$, V is the number of vertices of the dual lattice, $\kappa \sim e^{\sqrt{3}\lambda a^2/4\pi}$ and $G(X) = e^{-X^2/2}$.

The important observation here is that this partition function is given by the sum of all connected Feynman graphs in the quantum mechanics system of $N \times N$ Hermitian matrices. To make this clearer, let's consider the following partition function

$$Z = \int D^{N^2}\Phi(x) exp\left(-\beta \int_{-T/2}^{T/2} dx \, \mathrm{Tr}\left(\frac{1}{2}(d_x\Phi)^2 + U(\Phi)\right)\right) , \tag{1.19}$$

where $U(\Phi) = \frac{1}{2\alpha'}\Phi^2 - \frac{1}{3!}\Phi^3$, x is the Euclidean time and $\beta = \frac{1}{\hbar}$. The next step is to rescale Φ such that,

$$Z \sim \int D^{N^2}\Phi(x) exp\left(-N\int_{-T/2}^{T/2} dx \,\mathrm{Tr}\,\left(\frac{1}{2}(\frac{d\Phi}{dx})^2 + \frac{1}{2\alpha'}\Phi^2 - \frac{\kappa}{3!}\Phi^3\right)\right), \quad (1.20)$$

where $\kappa = \sqrt{N/\beta}$ is the cubic coupling constant. The sum over all connected graphs is

$$\lim_{T\to\infty} \ln Z = \sum_h N^{2(1-h)} \sum_V \kappa^V \prod_{i=1}^{V} \int_{-\infty}^{+\infty} dx_i \prod_{\langle ij\rangle} e^{-|x_i - x_j|/\alpha'}. \quad (1.21)$$

If we compare (1.18) and (1.21), we can see that they match if we identify X with x –the embedding coordinate– with the Euclidean time. Then, the link factor G is represented here by the one dimensional Euclidean propagator. Moreover, from the one dimensional Euclidean propagator and the identification between X, x one can see that the scaling of X is determined by α'. Finally, the string coupling g_0 is related to the size of the matrix N as $g_0 \sim 1/N$. Due to this identification the free energy expansion for the matrix model, in powers of $1/N^2$ gives a classification in a topological fashion of the surfaces. Then, it looks like we have to keep N finite if we want g_0 to be finite, but we will show that if we take the continuum limit and the same time we send $N \to \infty$, we end up with a finite string coupling g_0. This is the so called double scaling limit.

Let us now, review how one takes the continuum limit. We start by increasing the cubic coupling up to a critical value κ_c. When $\kappa = \kappa_c$, the number of triangles that parametrise a surface goes to infinity and each triangle has become infinitesimal so that each surface is continuous and finite. Moreover, when $\kappa \to \kappa_c$, we define the cosmological constant to be $\Delta = \pi(\kappa_c^2 - \kappa^2)$. Since $\kappa = \kappa_c e^{-\sqrt{3}\lambda a^2/4\pi}$, where λ the physical cosmological constant, we have $\lambda \sim \Delta/a^2$.

We would like to stress here that although we chose to triangulate the surfaces, we could have chosen any other way to discretise the surfaces and again be able to make connection with the matrix quantum mechanics, the only difference would have been the use of a different potential $U(\Phi)$. In the end the way that we discretise the surfaces after we take the double scaling limit should not play any role.

Now that we have shown the connection between the sum of the connected Feynman diagrams of a quantum mechanical system of $N \times N$ Hermitian matrices with the partition function of discretised surfaces, we would like to move to the Hamiltonian formalism and show how the free fermionic theory arises.

Using Hamiltonian formalism the partition function is

$$Z = \left\langle f|e^{-\beta HT}|i\right\rangle, \quad (1.22)$$

where f is the final state, i is the initial state and H is the Hamiltonian. Now, if we take the limit $T \to \infty$ and the final and initial state to be the same we can compute the ground state energy E_0 as follows

$$\lim_{T\to\infty} \frac{\ln Z}{T} = -\beta E_0 . \quad (1.23)$$

Then, since we are interested to compute the partition function for the embedding in the infinite line, the only thing that we need to compute is E_0. To do so first we have to quantise the $SU(N)$ symmetric Hermitian matrix quantum mechanics. The Lorentzian signature Lagrangian is

$$L = \mathrm{Tr}\left(\frac{1}{2}\dot{\Phi}^2 - U(\Phi)\right). \tag{1.24}$$

The Lagrangian is symmetric under rigid rotations $\Phi(t) \to V^\dagger \Phi(t) V$ where $V \in SU(N)$. Now we are going to diagonalise the matrix Φ such that $\Phi(t) = \Omega^\dagger(t)\Lambda(t)\Omega(t)$, where $\Omega \in SU(N)$, the diagonal piece is $\Lambda(t) = diag(\lambda_1(t), ..., \lambda_N(t))$ and the rest $N^2 - N$ angular degrees of freedom are at the Ω pieces. So, then we have

$$\mathrm{Tr}\left(\dot{\Phi}^2\right) = \mathrm{Tr}\left(\dot{\lambda}^2\right) + \mathrm{Tr}\left[\lambda, \dot{\Omega}\Omega^\dagger\right]^2. \tag{1.25}$$

Furthermore we can decompose $\dot{\Omega}\Omega$ in terms of the generators of $SU(N)$, T_{ij}, $\tilde{T}_{ij}$ and H_i. Where T_{ij} is the symmetric traceless piece $M_{ij} = M_{ji} = 1$, $\tilde{T}_{ij}$ is the antisymmetric traceless piece $M_{ij} = -M_{ji} = -i$ and H_i is the diagonal piece that generates the Cartan subalgebra.

$$\dot{\Omega}\Omega^\dagger = \frac{i}{\sqrt{2}}\sum_{i<j}\left(\dot{\alpha}_{ij}T_{ij} + \dot{\beta}_{ij}\tilde{T}_{ij}\right) + \sum_{i=1}^{N-1}\dot{\alpha}_i H_i\,. \tag{1.26}$$

Then (1.24) substituting (1.26) and (1.25) becomes

$$L = \sum_i\left(\dot{\lambda}_i^2 + U(\lambda_i)\right) + \frac{1}{2}\sum_{i<j}(\lambda_i - \lambda_j)^2(\dot{\alpha}_{ij}^2 + \dot{\beta}_{ij}^2)\,. \tag{1.27}$$

Now we should also transform the measure of integration $D\Phi$ in terms of Ω, λ. It takes the form $D\Phi = D\Omega\prod_i d\lambda_i \Delta^2(\lambda)$, where $\Delta^2(\lambda) = \prod_{i<j}(\lambda_i - \lambda_j)$, is the Vandermonde[10] determinant. Due to the Jacobian determinant of the transformation of the measure the kinetic term for the diagonal matrix Λ -the matrix of the eigenvalues- becomes after some manipulations

$$-\frac{1}{2\beta^2\Delta\,(\lambda)}\sum_i\frac{d^2}{d\lambda^2}\Delta\,(\lambda)\,. \tag{1.28}$$

Then the Hamiltonian is

$$H = -\frac{1}{2\beta^2\Delta\,(\lambda)}\sum_i\frac{d^2}{d\lambda^2}\Delta\,(\lambda) + \sum_i U(\lambda_i) + \sum_{i<j}\frac{\Pi_{ij}^2 + \tilde{\Pi}_{ij}^2}{(\lambda_i - \lambda_j)^2}\,. \tag{1.29}$$

Π_{ij} and $\tilde{\Pi}_{ij}$ are conjugate momenta to α_{ij} and β_{ij}. Π_{ij} generates left rotations $\Omega \to A\Omega$ and since the Lagrangian is independent of $\dot{\alpha}_i$ the wave function Ψ should satisfy the following constraints $\Pi_{ii}\Psi = 0$. This translates to the fact that when A is diagonal then the left rotations leave Φ the same.

10 It is totally antisymmetric.

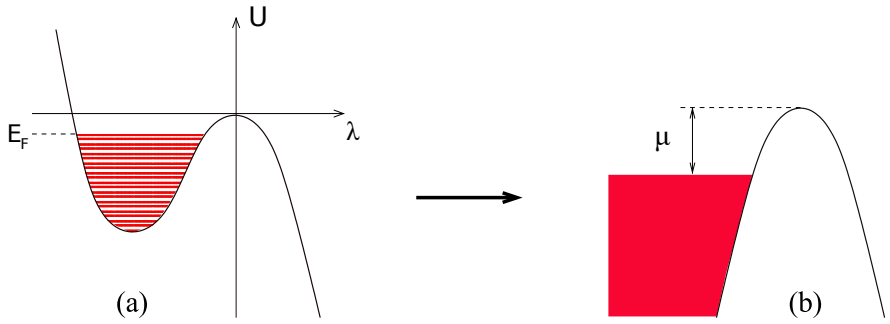

FIGURE 7: In picture (a) we see the cubic potential $U(\lambda)$, on the left of the potential we see the energy levels of the N fermions filling the energy levels up to energy $\mu_F = \epsilon_N$. In picture (b) we see the effect of the double scaling limit that is to focus around the tip of the potential (around the quadratic maximum).

The next step is to find the ground state, such a state should be annihilated by Π_{ij} and $\tilde{\Pi}_{ij}$. This means that it should be in the singlet representation of $SU(N)$. These are symmetric functions that depend only on λ, $\chi_s(\lambda)$. By acting with the Hamiltonian (1.29) we have

$$(\sum_{i=1}^{N} h_i)\Psi(\lambda) = E\Psi(\lambda)\,, \tag{1.30}$$

where E is the energy of the state, $\Psi(\lambda) = \Delta(\lambda)\chi_s(\lambda)$ and $h_i = -\frac{1}{2\beta^2}\frac{d^2}{d\lambda^2} + U(\lambda_i)$. We notice that the wavefunction Ψ is by construction totally antisymmetric and h_i is a non-relativistic single particle Hamiltonian. Then it is clear that finding the partition function for the sum of the discretised surfaces embedded in an infinite line has been reduced to the problem of finding the ground state energy of a system of N free fermions under a potential $U(\lambda)$. This means that we can solve two dimensional string theory through solving a quantum mechanical problem of N non interacting fermions.

Now, we are ready to find E_0. According to what we show above it should be given by $E_0 = \sum_{i=1}^{N}\epsilon_i$ where ϵ_i is the energy of each of the N fermions. Since we are dealing with fermions we cannot have them all at the same energy level, this means that they are going to occupy the first N energy levels of the Hamiltonian h. As we saw $U(\lambda)$ is a cubic potential unbounded from below[11], this means that it does not have bound states. Moreover, uncontrollable non-perturbative processes such as tunneling can occur. But we are interested in the limit where $\beta \to \infty$ -classical limit and in an expansion in $1/\beta^2$. In this limit, there are orbits at the left of the potential that are spaced as $1/\beta$ and their decay time is analogous to $\beta \to \infty$. Thus, at the

11 In the case of $0B$ type "super-string" theory the potential is quartic (double well potential) and it is non-pertubativelly stable [41].

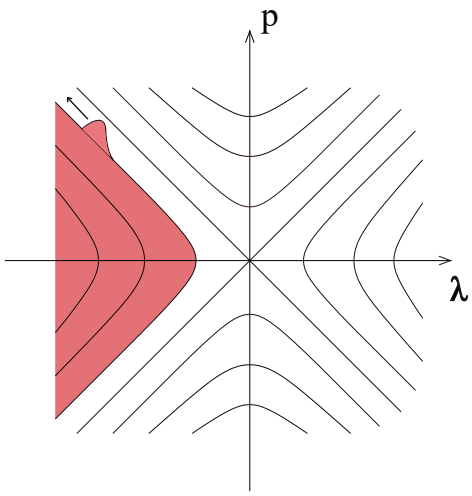

FIGURE 8: In this picture we see the phase space of the free fermions after taking the double scaling limit. The contours are orbits of fixed energy and the pink region is the Fermi sea. The little blob is the scattered tachyon excitation of Figure 5.

expansion in powers of $1/\beta^2$ this instability cannot be probed. Then, each ϵ_i is the energy of each of these levels, see Figure 7. Using the Bohr-Sommerfeld quantisation condition, $\int p_n(\lambda)d\lambda = 2\pi n/\beta$, where $p_n(\lambda) = \sqrt{2(\epsilon_n - U(\lambda))}$ we can find the Fermi sea level $\mu_F = \epsilon_N$.
$\int_{\lambda_-}^{\lambda_+} \sqrt{2(\mu_F - U(\lambda))}d\lambda = \pi N/\beta$, where $\lambda_{-/+}$ are the classical turning points. One can notice that μ_F is increasing as a function of N/β. Both μ_F and E_0 become singular when $N/\beta \to \kappa_c^2$ and $\mu_F = \mu_c$ the latter been the height of the potential barrier. As we saw above, it is at this critical limit that the theory of free fermions is equivalent to quantum gravity in two dimensions. For the fermionic system this critical limit pinpoints the start of spilling of fermions off the barrier. In Figure 8 we see the phase space of the free fermions after we have taken the double scaling limit.

It is important to relate the cosmological constant Δ with the chemical potential $\mu = \mu_c - \mu_F$, since this allows us to express E_0 in terms of Δ. To do so we will need the following relations. First let us define the density of eigenvalues as

$$\rho(\epsilon) = \frac{1}{\beta}\sum_n \delta\left(\epsilon - \epsilon_n\right) , \tag{1.31}$$

then

$$\kappa^2 = \frac{N}{\beta} = \int_0^{\mu_F} \rho(\epsilon)d\epsilon , \tag{1.32}$$

and

$$\lim_{T\to\infty} \frac{-\ln Z}{T} = \beta E = \beta^2 \int_0^{\mu_F} \rho(\epsilon)\epsilon d\epsilon . \tag{1.33}$$

Now, we differentiate (1.32)

$$\frac{\partial \Delta}{\partial \mu} = \pi \rho(\mu_F)\,, \tag{1.34}$$

and we invert it to get μ as a function of Δ. Then we differentiate (1.33) and we have $\frac{\partial E}{\partial \Delta} = \frac{1}{\pi}\beta(\mu - \mu_c)$. After doing the following redefinition of the energy $E \to E + \frac{1}{\pi}\beta\mu_c\Delta$, we get

$$\frac{\partial E}{\partial \Delta} = \frac{1}{\pi}\beta\mu\,. \tag{1.35}$$

Using the WKB relation we get

$$\rho(\mu_F) = \frac{1}{\pi}\int_{\lambda_-}^{\lambda_+} \frac{d\lambda}{\sqrt{\mu_F - U(\lambda)}} \sim -\frac{1}{\pi}\ln\mu + \mathcal{O}\left(1/\beta^2\right)\,. \tag{1.36}$$

Substituting (1.36) in (1.34) we have

$$\Delta = -\mu\ln\mu + \mathcal{O}(1/\beta^2)\,. \tag{1.37}$$

Then, substituting (1.36) in (1.35) we have

$$-\beta E = \frac{1}{2\pi}(\beta\mu)^2\ln\mu + \dots\,. \tag{1.38}$$

Thus, we have related both the cosmological constant Δ of the worldsheet and the ground state energy E with the chemical potential μ. These relations, as we will see in chapter 3 are crucial for the matching of the string theory with the matrix model results. The important observation is that the critical behavior of the density of eigenvalues comes from the part of the integral near the quadratic maximum of the potential. This results to the quantum mechanical theory of free fermions in an inverted harmonic oscillator potential as in Figure 7. One may be concerned because the cubic potential is unstable and as we saw tunneling phenomena can occur. But if one is interested in perturbative effects only, such as an asymptotic genus expansion, then it can be shown that the theory is pertubatively stable, because at this limit $\mu \to 0$ (continuum limit) tunneling phenomena are forbidden.

The observables that one can compute now that we have completely defined our model are the partition function at all genera, correlation functions, expectation values of loop operators that are poking holes into the worldsheet in the dual string theory picture, the S-matrix of scattering states and conserved charges. Moreover, these quantities can be computed also from the Liouville side at the torus level and then one can match with the results from the matrix model. This is important in order to be confident that the matrix model indeed describes the string theory that we want to study. Since the matrix model is much more rich and we can not be sure that they are in one to one correspondence.

The analysis above is for the case of singlet states, if one wants to consider non-singlet excitations has to pay energy $\mathcal{O}(-\log\mu)$, but at the continuum limit $\mu \to$

0, thus these states are completely decoupled from the singlet excitations at the limit of interest. A way to project naturally only to the singlet states is to gauge the matrix model by a non dynamical gauge field A and $D_x\Phi = \partial_x\Phi + [A, \Phi]$, then the Gauss constraint projects on the $U(N)$ singlets. In the model that we described above –embedding in the infinite line– the non-singlets do not contribute and they do not play any role. But, if we allow for periodic Euclidean time $x \sim x + 2\pi R$, then we must allow for twisted boundary conditions for $\Phi(x + 2\pi R) = \Omega\Phi(x)\Omega^{-1}, \Omega \in U(N)$. The propagator is $\left\langle \Phi_i^k(x)\Phi_j^l(x') \right\rangle = \sum_{m=-\infty}^{\infty} \exp(-|x - x' + 2\pi R m|^2)(\Omega^m)_i^l(\Omega^{-m})_j^k$. By a diagrammatic visualisation it can become clear that the sum over m_i is a sum over vortex insertions. Thus, the sum over twisted boundary conditions introduces vortices into the partition sum for the scalar matter field X. The suppression of non-singlet excitations is analogous to the suppression of vortices in two spacial dimensions of a periodic scalar below the Kosterlitz-Thouless transition[12].

For what we have said so far we have not referred at all in D- branes, this is the so called "old matrix model" that was developed in the beginning of the 90s. After the discovery of D- branes in the mid 90s and after the AdS/CFT correspondence, a different perspective on the matrix model was developed. One can interpret the matrix quantum mechanics as the quantum mechanics of a tachyonic field living on a stack of N unstable $D0$- branes, the so called ZZ[13] branes. This tachyon transforms in the adjoint representation of the $U(N)$ gauge group and has the following effective action

$$S_T = \int dt \frac{1}{2} \mathrm{Tr}\,(D_t T)^2 - \mathrm{Tr}\,[V(T)] + \dots, \tag{1.39}$$

where D_t the covariant derivative with respect to the non-dynamical gauge field that lives on the $D0$- brane. The expectation is that the open string dynamics of the ZZ branes describes the pure closed string physics of the Liouville theory at the double scaling limit. This is a realisation of open/closed duality. Since, the $D0$-branes decouple from the closed string dynamics that give gravity, precisely when at the double scaling limit and their effective description (1.39) is the one of the tachyon "field theory". This is the exact equivalent of the AdS/CFT corespondence where we can take the different limits for the stack of N $D3$- branes and at the one case we have $\mathcal{N} = 4$ SYM and in the other gravity on $AdS_5 \times S^5$.

We would like to close this section by presenting the dictionary between the two dimensional dilaton background bosonic string theory and the $c = 1$ matrix model picture, since it gives the global picture of the duality and summarises results that we did not talk about here.

12 It is a transition from bound vortex-antivortex pairs at low temperatures to unpaired vortices and antivortices at some critical temperature.

13 Named after the Zamolodchikov brothers.

String theory	Matrix model
Closed string vacuum	Fermi sea of matrix eigenvalues
Liouville potential $\mu\, e^{2b\phi}$	Inverted oscillator potential
Worldsheet cosmological constant Δ	Chemical potential $-\mu \ln \mu$
Closed strings	Fermi surface density wave quanta
String S-matrix	S-matrix of density waves
$D0$ particle (ϕ: D, X: N)	Matrix eigenvalue λ
Open string tachyon on n D-particles	A block of the matrix M_{ij}
D-branes (X: D, ϕ: N, $S_{bdy} = \mu_B \oint e^{b\phi}$)	Macroscopic loops $\mathrm{tr}[\log(z - M(\lambda))]$
Boundary cosm. const. μ_B	Loop eigenvalue parameter $2z$
D-branes (ϕ: D, X: N, $S_{bdy} = \beta \oint \cos X$)	Eigenvalues outside the Fermi sea
Open string coupling β	Eigenvalue energy $E = -\mu \sin^2 \pi\beta$

Where z symbolises the eigenvalue coordinate, D stands for Dirichlet boundary conditions, N stands for Neumann boundary conditions.

1.4 QUANTUM PHASE TRANSITIONS

In this section we would like to introduce the notion of quantum phase transitions, these are phase transitions that occur at zero temperature $T = 0$ due to quantum fluctuations. In chapter 4 of this thesis, we are going to study them holographically. Here, we will not talk about holography but we are going to present the notion from the condensed matter theory point of view, where the physics is clearer. This section is based on the book [42] about quantum phase transitions by Sachdev.

We consider a lattice system with Hamiltonian $H(g)$, where g is the coupling constant. The ground state energy of this system varies with g and in general when this lattice is finite, the ground state energy is a smooth and analytic function of g. In this case (finite lattice), a non analyticity in the ground state energy can be present if $H(h) = H_0 + gH_1$ and H_0, H_1 commute, which means that although the eigenvalues depend on g the eigenfunctions are independent of g. Then there can be a level-crossing where an excited level becomes the ground state at $g = g_c$. By taking the limit where the finite lattice becomes infinite (continuous), there are more possibilities. For example an avoided level-crossing between the ground and an excited state in a finite lattice could become progressively sharper as the lattice size increases, leading to a non-analyticity at $g = g_c$ in the infinite lattice limit, see Figure 9. Thus, one arrives at the following definition for a quantum phase transition: Any point of non-analyticity in the ground state energy of an infinite lattice system signals a quantum phase transition. The nonanalyticity could be either the limiting

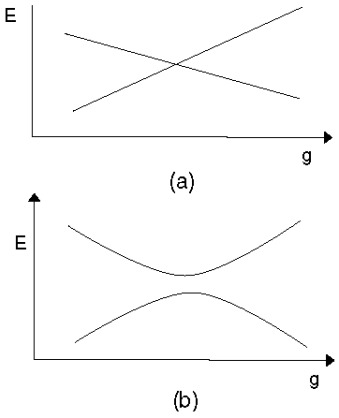

FIGURE 9: In picture (a) we see the case of an actual level crossing and in picture (b) the case of an avoided level crossing. Both graphs in (a) and (b) present the energy levels of a system E_i as functions of the coupling constant g.

case of an avoided level-crossing or an actual level-crossing. The phase transition is usually accompanied by a qualitative change in the nature of the correlations in the ground state.

Although quantum phase transitions occur strictly at $T = 0$ we will see now that they have important impact on the physics at finite temperature. First of all let's see what is the fate of the quantum critical point when we turn on the temperature $T > 0$. There are two possibilities either the non-analyticity vanishes at finite temperature and all the functions are analytic with respect to g close to $g = g_c$, or there is a line of second-order phase transitions[14] that at $T = 0$ ends at the quantum critical point $g = g_c$, see Figure 10.

Phase transitions aside, it is worth noting how the quantum phase transition influences the dynamics of the system at finite temperature. The equilibration time τ_{eq} is defined as the characteristic time in which local thermal equilibrium is established after a weak external perturbation and it is a function of $g - g_c$ and T. This quantity can be used to characterise the dynamics of the system at finite temperature.

At $T = 0$ there is only one characteristic scale that is for example the energy difference between the ground state energy and the first excited state ΔE and depends on $g - g_c$, but at $T \neq 0$ we have a second energy scale, $k_B T$ due to thermal fluctuations. As one can see at Figure 10 there are two distinct regions of thermal equilibration. In the case where $\Delta E > k_B T$, we find long equilibration times which satisfy $\tau_{eq} \gg \frac{\hbar}{k_B T}$. In this case the dynamics of the system become effectively classical. Thus we can use classical equations of motion to describe the re-equilibration dynamics at the time scale τ_{eq}. In the case where $\Delta E < k_B T$, we have the quantum critical region, here we find a short equilibration time given by $\tau_{eq} \sim \frac{\hbar}{k_B T}$. The equilibration time is indepen-

14 A second order phase transition is signaled by a discontinuity in the second derivative of the free energy.

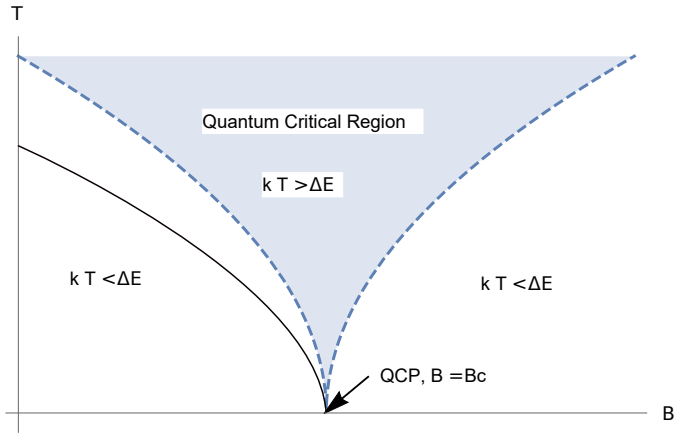

FIGURE 10: In this graph we represent temperature with T, the Boltzmann constant k_B with k and the coupling constant g with B. The light blue region is the quantum critical region (QCR). In QCR both quantum and thermal fluctuations are equally important and the physics is governed by the conformal field theory (CFT) that describes the physics at the quantum critical point (QCP). The boundary of the critical region, shown by the dashed lines, is where the thermal fluctuations kT are of the same order as the intrinsic energy scale ΔE. At the QCP the energy scale vanishes signaling a quantum phase transition (QPT) when the coupling constant B takes a critical value $B = B_c$, since there are no scales the physics at this point is governed by a CFT. The white regions are the ones where the thermal fluctuations are important and the physics is effectively classical. The solid black line symbolises a line of second order phase transitions that can happen at finite temperature T –if they exist– at $T = 0$ they end up at the QCP.

dent of the microscopic energy scale and is determined only by $k_B T$. In this regime, quantum and thermal fluctuations are equally important and to study the dynamics of the system at this phase we cannot use an effectively classical description. Let us point out that the dashed lines are not phase transitions but smooth crossovers and that on these lines the thermal and quantum fluctuations are of the same magnitude. For a pictorial overview see Figure 10.

1.5 CONTENT OF THE THESIS

In this last section of the introduction we would like to give an overview of the content of each chapter.

In chapter 2, we are going to revisit the old black hole S-matrix construction and its new partial wave expansion of 't Hooft. Inspired by old ideas from non-critical string theory and the $c = 1$ Matrix Quantum Mechanics, we reformulate the scattering in terms of a quantum mechanical model –of waves scattering off inverted harmonic oscillator potentials– that exactly reproduces the unitary black hole S-matrix for all spherical harmonics; each partial wave corresponds to an inverted harmonic oscil-

lator with ground state energy that is shifted relative to the s-wave oscillator. Identifying a connection to two dimensional string theory allows us to show that there is an exponential degeneracy in how a given total initial energy may be distributed among many partial waves of the four dimensional black hole.

In chapter 3, we study Matrix Quantum Mechanics (MQM) on the Euclidean time orbifold $S^1/\mathbb{Z}_2$. Upon Wick rotation to Lorentzian time and taking the double-scaling limit this theory provides a toy model for a big-bang/big-crunch universe in two dimensional non-critical string theory where the orbifold fixed points become cosmological singularities. We derive the partition function both in the canonical and grand canonical ensemble in two different formulations and demonstrate a matching between them. We pinpoint the contribution of twisted states in both of these formulations either in terms of bi-local operators acting at the end-points of time or branch-cuts on the complex plane. We calculate, in the matrix model, the contribution of the twisted states to the torus level partition function explicitly and show that it precisely matches the world-sheet result, providing a non-trivial test of the proposed duality. Finally we discuss some interesting features of the partition function and the possibility of realising it as a τ- function of an integrable hierarchy.

In chapter 4, we investigate quantum critical points in a $2+1$- dimensional gauge theory at finite chemical potential χ and magnetic field B. The gravity dual is based on four dimensional $\mathcal{N}=2$ Fayet-Iliopoulos gauged supergravity and the solutions we consider –that are constructed analytically– are extremal, dyonic, asymptotically AdS_4 black branes with a nontrivial radial profile for the scalar field and extremal, magnetically charged, asymptotically AdS_4 acceptable singular solutions with a nontrivial radial profile for the scalar field. We discover a line of second order fixed points $B = B_c(\chi)$ between the dyonic black brane and the extremal "thermal gas" solution with a singularity of good-type, according to the acceptability criteria of Gubser. The dual field theory is a strongly coupled nonconformal field theory at finite charge and magnetic field, related to the ABJM theory deformed by a triple trace operator Φ^3. We find similarities between the behaviour of the VeV $\langle\Phi\rangle$ under magnetic field and that of the quark condensate in $2+1$- dimensional Nambu-Jona-Lasinio models.

2 THE BLACK HOLE S-MATRIX FROM QUANTUM MECHANICS

2.1 INTRODUCTION

The work of Bekenstein [18] and Hawking [20] has spurred extensive research on the so-called "information paradox". The premise of the paradox is that in a collapse of matter forming a black hole, the intermediate state post-collapse is a black hole that can be characterized by a small number of physical parameters (mass, charge, angular momentum, etc.). A semi-classical calculation as the one Hawking originally did, however, suggests that black holes radiate as black bodies, namely with a thermal spectrum. This seems to suggest a gross violation of unitary evolution as all information about the exact in-state that went into forming the black hole appears to have been lost after its evaporation.

The emergence of string theory, holography [21, 43, 4] and gauge/gravity duality [10, 44, 12] has shed significant light on this problem. In fact, it is often claimed that if one were to believe gauge/gravity duality, the paradox is solved "in-principle" as the boundary theory is unitary by construction and the duality states an equivalence (at the level of partition functions) between the gravitational and boundary field theories. Nevertheless, the strength of this claim is questionable [45, 46] and even within the best understood examples of gauge/gravity duality, there is no general consensus on the exact process of information retrieval. Furthermore, the best understood examples of the said duality, while providing for a very useful toolbox, typically involve bulk space-times with a negative cosmological constant and are far from the real world. Technology at this stage is far from established to reliably understand more realistic space-times. Additionally, why intricate details of string theory or the duality may be absolutely necessary for our understanding of the evolution of general gravitational dynamics is not apparent. While the fuzzball program [47, 48, 49, 50, 51] provides some arguments for why stringy details may be important, it is fair to say that there is no general consensus on the matter.

Years before gauge/gravity duality was proposed and was seen as a possible resolution to the information paradox, there was an alternative suggestion by 't Hooft [21, 52, 53]. The proposal was to consider particles of definite momenta "scattering" off a black-hole horizon. These particles were to impact the out-going Hawking quanta owing to their back-reaction on the geometry. With the knowledge that the black hole is made out of a large, yet *finite*, number of in-states, one may scatter particles of varying momenta repeatedly, until all in-states that may have made up the black hole have been exhausted. This led to a construction of an S-matrix that maps in to out states. This matrix was shown to be unitary. A further advancement for spherically symmetric horizons was made recently [54, 55, 56], where a partial

wave expansion allowed for an explicit writing of the S-matrix for each spherical harmonic. This construction presumes that the S-matrix can be split as

$$S_{\text{total}} \;=\; S_{-\infty}\, S_{\text{horizon}}\, S_{+\infty}\,, \tag{2.1}$$

where $S_{\pm\infty}$ correspond to matrices that map asymptotic in-states to in-going states near the horizon and outgoing states near the horizon to asymptotic out-states respectively. And S_{horizon} is the S-matrix that captures all the dynamics of the horizon. The construction is also done in a "probe-limit" in that the back-reaction is not taken to impact the mass of the black hole. Only its effect on outgoing particles is captured. Based on the spherical symmetry it is natural to expand the scatering in spherical harmonics. It is then found that the different waves evolve independently. For a general non-spherically symmetric background such as the Kerr black hole one would have to use a different basis of eigenfunctions in which to expand the scattering. Furthermore, one would need to extend the scattering algebra once one includes extra forces such as the electromagnetic one. A limitation is that the back-reaction calculations ignore transverse effects [57, 58] which grow in increasing importance as we approach Planckian scales. These effects might cause the partial waves to interact. One might claim that this should lead to non-linear interactions between the partial waves. However, the situation is more complex. The algebra is closely related to string theory algebras, where transverse modes would represent motion in the string world sheet itself; there, these are seen to blend with the gauge constraints for the transverse coordinates. The algebra for the dynamical variables is still linear, but the entire algebra for the Poincare group is not.

Inspired by old ideas from non-critical two dimensional string theory [38, 59, 60, 61, 62, 63, 64, 65], we construct a theory—of a collection of quantum mechanical degrees of freedom in an inverted harmonic oscillator potential—that exactly reproduces the S-matrix of 't Hooft for every partial wave; the inverted potential arises naturally to allow for scattering states, as opposed to bound states in a conventional harmonic oscillator. The intrinsically quantum nature of the model dispenses with the critique that the S-matrix of 't Hooft is a "classical" one. In our construction, all the observables (S-matrix elements) are exactly identical to those of 't Hooft's S-matrix. Furthermore, we observe that in-states must contain an approximately constant number density over a wide range of frequencies in order for the scattered out-states to appear (approximately) thermal; this condition was also noted in the two dimensional string theory literature. Finally, we show that our model captures an exponentially growing degeneracy of states. It may be added that aside from the approaches mentioned earlier, there have been many attempts to construct toy-models to study black hole physics [66, 67, 68, 69, 70, 71]. The hope is that "good" toy models teach us certain universal features of the dynamics of black hole horizons. Unfortunately, most of these models are based on assumptions and extrapolations far away from well established physics, while as we mentioned earlier we just combine gravitational back-reaction and quantum mechanics in our work.

This chapter is organized as follows. In the section 2.2, we briefly review gravitational back-reaction and 't Hooft's S-matrix construction along with its partial wave

expansion. Our derivation is slightly different to the one of 't Hooft [54] in that our derivation relies only on the algebra associated to the scattering problem. Therefore, the "boundary conditions" of the effective bounce, as was imposed in 't Hooft's construction is built in from the start via the back-reaction algebra (2.15). In section 2.3, we present our model and compute the corresponding scattering matrix to show that it explicitly matches the one of 't Hooft. In section 2.4, we make an estimate of the high energy behaviour of the total density of states to argue that the model indeed describes the existence of an intermediate black-hole state. We conclude with a discussion and some future perspectives in 2.5.

A BRIEF SUMMARY OF RESULTS: There are two main results of this work: one is a re-writing of the degrees of freedom associated to 't Hooft's black hole S-matrix in terms of inverted harmonic oscillators; this allows us to write down the corresponding Hamiltonian of evolution explicitly. The second, related result is an identification of a connection to two dimensional string theory which in turn allows us to show that there is an exponential degeneracy of how a given total initial energy may be distributed among many partial waves of the four dimensional black hole; much as is expected from the growth of states associated to black hole entropy. At various points in Sections 2.3 and 2.4, we review some aspects of matrix models and two dimensional string theory in detail. While we expect some consequences for these theories based on our current work, we do not have any new results within the framework of two dimensional black holes or matrix models in this chapter.

2.2 BACK-REACTION AND THE BLACK HOLE S-MATRIX

Consider a vacuum solution to Einstein's equations of the form:

$$ds^2 \;=\; 2A\left(u^+,u^-\right)du^+\,du^- + g\left(u^+,u^-\right)\,h\left(\Omega\right)d\Omega^2\,, \tag{2.2}$$

where u^+, u^- are light-cone coordinates, $A\left(u^+,u^-\right)$ and $g\left(u^+,u^-\right)$ are generic smooth functions of those coordinates and $h\left(\Omega\right)$ is the metric tensor depending on only the $(d-2)$ transverse coordinates Ω. It was shown in [58] that an in-going massless particle with momentum p^- induces a shock-wave at its position specified by Ω and $u^- = 0$. The shock-wave was shown to change geodesics such that outgoing massless particles feel a kick—of the form $u^- \to u^- + 8\pi G\, p^-_{\text{in}} \hat{f}\left(\Omega,\Omega'\right)$—in their trajectories at $u^- = 0$, where $\hat{f}$ depends on the spacetime in question. If we were to associate a putative S-matrix to the dynamics of the black hole, the said back-reaction may be attributed to this S-matrix in the following manner. Consider a generic in-state $|\text{in}_0\rangle$ that collapsed into a black hole and call the corresponding out-state after the complete evaporation of the black hole $|\text{out}_0\rangle$. The S-matrix maps one into the other via: $S\;|\text{in}_1\rangle = |\text{out}_1\rangle$. Now the back-reaction effect may be treated as a tiny modification of the in-state as $|\text{in}_0\rangle \to |\text{in}_0 + \delta p^-_{\text{in}}\left(\Omega\right)\rangle$, where $\delta p^-_{\text{in}}\left(\Omega\right)$ is the momentum of an in-going particle at position Ω on the horizon. Consequently, the

action of the S-matrix on the modified in-state results in a different out-state which is acted upon by an operator that yields the back-reacted displacement:

$$S\ \left|\text{in}_0 + \delta p_{\text{in}}^{-}\left(\Omega\right)\right\rangle\ =\ e^{-i\delta p_{\text{out}}^{+}(\Omega')\delta u_{\text{out}}^{-}}\left|\text{out}_0\right\rangle\ , \tag{2.3}$$

where the operator acting on the out-state above is the "displacement" operator written in Fourier modes. Now, we may repeat this modification arbitrarily many times. This results in a cumulative effect arising from all the radially in-going particles with a distribution of momenta on the horizon. Therefore, writing the new in- and out-states—with all the modifications included—as $\left|\text{in}\right\rangle$ and $\left|\text{out}\right\rangle$ respectively, we have

$$\begin{aligned}&\left\langle\text{out}\right|S\left|\text{in}\right\rangle\ = \\ &\left\langle\text{out}_0\right|S\left|\text{in}_0\right\rangle\ \exp\left[-i8\pi G\int d^{d-2}\Omega'\ p_{\text{out}}^{+}\left(\Omega'\right)\ \hat{f}\left(\Omega,\Omega'\right)\ p_{\text{in}}^{-}\left(\Omega\right)\right]\ .\end{aligned} \tag{2.4}$$

Should we now *assume* that the Hilbert space of states associated to the black-hole is completely spanned by the in-going momenta and that the Hawking radiation is entirely spanned by the out-state momenta, we are naturally led to a unitary S-matrix given by

$$\left\langle p_{\text{out}}^{+}\right|S\left|p_{\text{in}}^{-}\right\rangle\ =\ \exp\left[-i8\pi G\int d^{d-2}\Omega'\ p_{\text{out}}^{+}\left(\Omega'\right)\ \hat{f}\left(\Omega,\Omega'\right)\ p_{\text{in}}^{-}\left(\Omega\right)\right]\ . \tag{2.5}$$

There is an overall normalization factor (vacuum to vacuum amplitude) that is undetermined in this construction. The assumption that the black hole Hilbert space of states is spanned entirely by the in-state momenta p_{in}^{-} is equivalent to postulating that the said collection of radially in-going, gravitationally back-reacting particles collapse into a black hole. While this may seem a reasonable assumption, it is worth emphasizing that there is no evidence for this at the level of the discussion so far. We have not modeled a collapsing problem. We will see in Section 2.4 that our proposed model in Section 2.3 provides for a natural way to study this further. And significantly, we give non-trivial evidence that the derived S-matrix possibly models a collapsing black-hole.

2.2.1 *Derivation of the S-Matrix*

We now return to the back-reaction effect at a semi-classical level in order to derive an explicit S-matrix using a partial wave expansion in a spherically symmetric problem. For the back-reacted metric—after incorporating the shift $u^{-}\rightarrow u^{-}+f\left(\Omega,\Omega'\right)$ into (2.2)—to still satisfy Einstein's equations of motion, the following conditions need to hold at $u^{-}=0$ [58]:

$$\begin{aligned}&\frac{A\left(u^{+,-}\right)}{g\left(u^{+,-}\right)}\triangle_{\Omega}f\left(\Omega,\Omega'\right)-\left(\frac{d-2}{2}\right)\frac{\partial_{u^{+}}\partial_{u^{-}}g\left(u^{+,-}\right)}{g\left(u^{+,-}\right)}f\left(\Omega,\Omega'\right)\\ &=\ 8\,\pi\,p_{\text{in}}^{-}\,A\left(u^{+,-}\right)^{2}\,\delta^{(d-2)}\left(\Omega,\Omega'\right)\\ &\partial_{u^{-}}A\left(u^{+,-}\right)=0=\partial_{u^{-}}g\left(u^{+,-}\right)\ ,\end{aligned} \tag{2.6}$$

where $\triangle_\Omega$ is the Laplacian on the $(d-2)$-dimensional metric $h(\Omega)$. We concern ourselves with the Schwarzschild black-hole, written in Kruskal-Szekeres coordinates as

$$ds^2 \;=\; -\frac{32\,G^3\,m^3}{r}e^{-r/2Gm}du^+\,du^- + r^2 d\Omega^2\,. \tag{2.7}$$

For the above metric (2.7), at the horizon $r = R = 2Gm$, the conditions (2.6) were shown [58] to reduce to

$$\triangle_S(\Omega)\,f(\Omega,\Omega') \;:=\; (\triangle_\Omega - 1)\,f(\Omega,\Omega') \;=\; -\kappa\,\delta^{(d-2)}(\Omega,\Omega')\,, \tag{2.8}$$

with the implicit dependence of r on u^+ and u^- given by

$$u^+\,u^- \;=\; \left(1-\frac{r}{2Gm}\right)e^{-r/2Gm}\,, \tag{2.9}$$

and $\kappa = 2^4\,\pi\,e^{-1}\,G\,R^2\,p^-_{\text{in}}$. These seemingly ugly coefficients may easily be absorbed into the stress-tensor on the right hand side of the Einstein's equations. Now, the cumulative shift experienced by an out-going particle, say u^-_{out}, is given by a distribution of in-going momenta on the horizon

$$u^-_{\text{out}}(\Omega) \;=\; 8\pi G R^2\int d^{d-2}\Omega'\,\tilde{f}(\Omega,\Omega')\;p^-_{\text{in}}(\Omega')\,, \tag{2.10}$$

where $\kappa\,\tilde{f}(\Omega,\Omega') = f(\Omega,\Omega')$. Similarly, we have the complementary relation for the momentum of the out-going particle, say p^+_{out} given in terms of the position u^+_{in} of the in-going particle:

$$u^+_{\text{in}}(\Omega) \;=\; -8\pi G R^2\int d^{d-2}\Omega'\,\tilde{f}(\Omega,\Omega')\;p^+_{\text{out}}(\Omega')\,. \tag{2.11}$$

The expressions (2.10) and (2.11) may be seen as "boundary conditions" of an effective bounce off the horizon. However, this intuition is rather misleading and we will refrain from this line of thought. Nevertheless, what is striking to note is that the momentum of the in-state is encoded in the out-going position of the Hawking radiation while the position of the in-state is encoded in the momentum of the out-going Hawking state! However, so far, the quantities $u^\pm_{\text{in/out}}$ are dimensionless while $p^\mp_{\text{in/out}}$ are densities of momenta with mass dimensions four. Therefore, to appropriately interpret these as positions and momenta, we rescale them as $u^\pm_{\text{in/out}} \to R u^\pm_{\text{in/out}}$ and $p^\mp_{\text{in/out}} \to R^{-3} p^\mp_{\text{in/out}}$ [55]. Notwithstanding this rescaling, we continue to use the same labels for the said quantities in order to avoid clutter of notation. Now, using the canonical commutation relations, respectively, for the out and in particles[1]

$$\left[\hat{u}^-(\Omega)\,,\hat{p}^+(\Omega')\right] \;=\; \left[\hat{u}^+(\Omega)\,,\hat{p}^-(\Omega')\right] \;=\; i\,\delta^{(d-2)}(\Omega-\Omega')\,, \tag{2.12}$$

1 To avoid clutter in notation, we drop the in/out labels on positions and momenta of particles. u^+ and u^- always refer to ingoing/outgoing positions, respectively. Consequently, p^- and p^+ are always associated with ingoing/outgoing momenta, respectively.

we may derive the algebra associated to the black hole scattering. We do this in a partial wave expansion—in four dimensions—as

$$\hat{u}^{\pm}(\Omega) = \sum_{lm} \hat{u}^{\pm}_{lm} Y_{lm}(\Omega) \quad \text{and} \quad \hat{p}^{\pm}(\Omega) = \sum_{lm} \hat{p}^{\pm}_{lm} Y_{lm}(\Omega) . \tag{2.13}$$

Working with these eigenfunctions of the two-sphere Laplacian and using (2.8) we can write the back-reaction equations (2.10) and (2.11) as

$$\hat{u}^{\pm}_{lm} = \mp \frac{8\pi G}{R^2 (l^2 + l + 1)} \hat{p}^{\pm}_{lm} =: \mp \lambda \, \hat{p}^{\pm}_{lm} . \tag{2.14}$$

In terms of these partial waves, we may now write the scattering algebra as

$$\left[\hat{u}^{\pm}_{lm}, \hat{p}^{\mp}_{l'm'}\right] = i\delta_{ll'}\delta_{mm'} \tag{2.15}$$

$$\left[\hat{u}^{+}_{lm}, \hat{u}^{-}_{l'm'}\right] = i\,\lambda\,\delta_{ll'}\delta_{mm'} \tag{2.16}$$

$$\left[\hat{p}^{+}_{lm}, \hat{p}^{-}_{l'm'}\right] = -\frac{i}{\lambda}\,\delta_{ll'}\delta_{mm'} . \tag{2.17}$$

A few comments are now in order. Since the different spherical harmonics do not couple in the algebra, we will drop the subscripts of l and m from here on. Furthermore, we see that the shift-parameter λ "morally" plays the role of Planck's constant $\hbar$, but one that is now l dependent. Moreover, we see that wave-functions described in terms of four phase-space variables are now pair-wise related owing to the back-reaction (2.14). Finally, it is important to note that each partial wave does not describe a single particle but a specific profile of a density of particles. For instance, the s-wave with $l = 0$ describes a spherically symmetric density of particles.

Since the operators $\hat{u}^{\pm}$ and $\hat{p}^{\pm}$ obey commutation relations associated to position and momentum operators, we see that the algebra may be realized with $\hat{u}^{-} = -i\lambda\partial_{u^+}$ in the u^+ basis and $\hat{u}^{+} = i\lambda\partial_{u^-}$ in the u^- basis. A similar realization is evident for the momentum operators. Moreover, we may now define the following inner-products on the associated Hilbert space of states that respect the above algebra:

$$\left\langle u^{\pm} \,\middle|\, p^{\mp} \right\rangle = \frac{1}{\sqrt{2\pi}} \exp\left(i u^{\pm} p^{\mp}\right) \tag{2.18}$$

$$\left\langle u^{+} \,\middle|\, u^{-} \right\rangle = \frac{1}{\sqrt{2\pi\lambda}} \exp\left(i \frac{u^{+}u^{-}}{\lambda}\right) \tag{2.19}$$

$$\left\langle p^{+} \,\middle|\, p^{-} \right\rangle = \sqrt{\frac{\lambda}{2\pi}} \exp\left(i\lambda p^{+} p^{-}\right) . \tag{2.20}$$

Using (2.19), for instance, we may write the out-going wave-function—travelling along the coordinate u^- after scattering—in terms of the in-going one travelling along u^+ as

$$\left\langle u^{-} \,\middle|\, \psi \right\rangle =: \psi^{\text{out}}(u^{-}) = \int_{-\infty}^{\infty} \frac{du^{+}}{\sqrt{2\pi\lambda}} \exp\left(-i \frac{u^{+}u^{-}}{\lambda}\right) \psi^{\text{in}}(u^{+}) . \tag{2.21}$$

One can immediately see that this mapping is Unitary just being a fourier transform. To derive another useful form of the S-matrix associated to the scattering, we first move to Eddington-Finkelstein coordinates:

$$u^+ = \alpha^+ e^{\rho^+}\,, \quad u^- = \alpha^- e^{\rho^-}\,, \quad p^+ = \beta^+ e^{\omega^+} \quad \text{and} \quad p^- = \beta^- e^{\omega^-} \tag{2.22}$$

where $\alpha^\pm = \pm 1$ and $\beta^\pm = \pm 1$ to account for both positive and negative values of the phase space coordinates u^+, u^-, p^+ and p^-. The normalization of the wave-function as

$$\begin{aligned} 1 &= \int_{-\infty}^{\infty} \left|\psi\left(u^+\right)\right|^2 du^+ \\ &= \int_{-\infty}^{0} \left|\psi\left(u^+\right)\right|^2 du^+ + \int_{0}^{\infty} \left|\psi\left(u^+\right)\right|^2 du^+ \\ &= -\int_{\infty}^{-\infty} \left|\psi^+\left(-e^{\rho^+}\right)\right|^2 e^{\rho^+} d\rho^+ + \int_{-\infty}^{\infty} \left|\psi^+\left(+e^{\rho^+}\right)\right|^2 e^{\rho^+} d\rho^+ \\ &= \sum_{\alpha=\pm} \int_{-\infty}^{\infty} \left|\psi^+\left(\alpha e^{\rho^+}\right)\right|^2 e^{\rho^+} d\rho^+ \end{aligned} \tag{2.23}$$

suggests the following redefinitions for the wave-function in position and momentum spaces

$$\begin{aligned} \psi^\pm\left(\alpha^\pm e^{\rho^\pm}\right) &= e^{-\rho^\pm/2}\,\phi^\pm\left(\alpha^\pm, \rho^\pm\right) \\ \tilde{\psi}^\pm\left(\beta^\pm e^{\omega^\pm}\right) &= e^{-\omega^\pm/2}\,\tilde{\phi}^\pm\left(\beta^\pm, \omega^\pm\right)\,. \end{aligned} \tag{2.24}$$

Therefore, using (2.21), we may write $\phi^{\text{out}}\left(\alpha^-, \rho^-\right)$ as:

$$\begin{aligned} &\phi^{\text{out}}\left(\alpha^-, \rho^-\right) = \frac{1}{\sqrt{2\pi\lambda}} \int_{-\infty}^{\infty} du^+ e^{\frac{\rho^+ + \rho^-}{2}} \exp\left(-i\frac{u^+ u^-}{\lambda}\right) \phi^{\text{in}}\left(\alpha^+, \rho^+\right) = \\ &\sum_{\alpha^+=\pm} \int_{-\infty}^{\infty} \frac{du^+}{\sqrt{2\pi}} e^{\frac{\rho^+ + \rho^- - \log\lambda}{2}} \exp\left(-i\alpha^+\alpha^- e^{\rho^+ + \rho^- - \log\lambda}\right) \phi^{\text{in}}\left(\alpha^+, \rho^+\right) = \\ &\sum_{\alpha^+=\pm} \int_{-\infty}^{\infty} \frac{dx}{\sqrt{2\pi}} \exp\left(\frac{x}{2} - i\alpha^+\alpha^- e^x\right) \phi^{\text{in}}\left(\alpha^+, x + \log\lambda - \rho^-\right)\,, \end{aligned} \tag{2.25}$$

where in the last line, we introduced $x \coloneqq \rho^+ + \rho^- - \log\lambda$. This equation may be written in matrix form as

$$\begin{aligned} &\begin{pmatrix} \phi^{\text{out}}\left(+, \rho^-\right) \\ \phi^{\text{out}}\left(-, \rho^-\right) \end{pmatrix} = \\ &\int_{-\infty}^{\infty} dx \begin{pmatrix} A\left(+,+,x\right) & A\left(+,-,x\right) \\ A\left(-,+,x\right) & A\left(-,-,x\right) \end{pmatrix} \begin{pmatrix} \phi^{\text{in}}\left(+, x + \log\lambda - \rho^-\right) \\ \phi^{\text{in}}\left(-, x + \log\lambda - \rho^-\right) \end{pmatrix} \end{aligned} \tag{2.26}$$

where we have defined the quantity

$$A\left(\gamma,\delta,x\right) \;:=\; \frac{1}{\sqrt{2\pi}}\,\exp\left(\frac{x}{2}-i\,\gamma\,\delta\,e^{x}\right)\,, \tag{2.27}$$

with $\gamma=\pm$ and $\delta=\pm$. This integral equation may further be simplified by moving to Rindler plane waves:

$$\phi^{\text{out}}\left(\pm,\rho^{-}\right)=\frac{1}{\sqrt{2\pi}}\int_{-\infty}^{\infty}dk_{-}\,\phi^{\text{out}}\left(\pm,k_{-}\right)\,e^{ik_{-}\rho^{-}} \tag{2.28}$$

$$\phi^{\text{in}}\left(\pm,x+\log\lambda-\rho^{-}\right)=\frac{1}{\sqrt{2\pi}}\int_{-\infty}^{\infty}dk_{\tilde{x}}\,\phi^{\text{in}}\left(\pm,k_{\tilde{x}}\right)e^{-ik_{\tilde{x}}\left(x+\log\lambda-\rho^{-}\right)} \tag{2.29}$$

$$A\left(\gamma,\delta,x\right)=\frac{1}{\sqrt{2\pi}}\int_{-\infty}^{\infty}dk_{x}\,A\left(\gamma,\delta,k_{x}\right)e^{ik_{x}\,x}\,. \tag{2.30}$$

This allows us to write the above matrix equation (2.26) as

$$\begin{pmatrix}\phi^{\text{out}}\left(+,k\right)\\ \phi^{\text{out}}\left(-,k\right)\end{pmatrix}= e^{-ik\log\lambda}\begin{pmatrix}A\left(+,+,k\right) & A\left(+,-,k\right)\\ A\left(-,+,k\right) & A\left(-,-,k\right)\end{pmatrix}\begin{pmatrix}\phi^{\text{in}}\left(+,k\right)\\ \phi^{\text{in}}\left(-,k\right)\end{pmatrix} \tag{2.31}$$

where $A\left(\gamma,\delta,k\right)$ can be computed from the inverse Fourier transform of (2.27) using a coordinate change $y=e^{x}$ and the identity

$$\int_{0}^{\infty}dy\,e^{i\sigma y}y^{-ik-\frac{1}{2}}=\Gamma\left(\frac{1}{2}-ik\right)e^{i\sigma\frac{\pi}{4}}\,e^{k\sigma\frac{\pi}{2}}\,,\quad\text{where}\quad\sigma=\pm\,. \tag{2.32}$$

Carrying out this computation, we find the following S-matrix:

$$S\left(k_{l},\lambda_{l}\right)=e^{-ik_{l}\log\lambda_{l}}\begin{pmatrix}A\left(+,+,k_{l}\right) & A\left(+,-,k_{l}\right)\\ A\left(-,+,k_{l}\right) & A\left(-,-,k_{l}\right)\end{pmatrix}= \frac{1}{\sqrt{2\pi}}\Gamma\left(\frac{1}{2}-ik_{l}\right)e^{-ik_{l}\log\lambda_{l}}\begin{pmatrix}e^{-i\frac{\pi}{4}}\,e^{-k_{l}\frac{\pi}{2}} & e^{i\frac{\pi}{4}}\,e^{k_{l}\frac{\pi}{2}}\\ e^{i\frac{\pi}{4}}\,e^{k_{l}\frac{\pi}{2}} & e^{-i\frac{\pi}{4}}\,e^{-k_{l}\frac{\pi}{2}}\end{pmatrix}\,. \tag{2.33}$$

In this expression, we have reinstated a subscript on k and λ to signify that they depend on the specific partial wave in question. One may additionally diagonalize this matrix by noting that

$$A\left(+,+,k\right)\;=\;A\left(-,-,k\right)\quad\text{and}\quad A\left(+,-,k\right)\;=\;A\left(-,+,k\right)\,. \tag{2.34}$$

With this observation, we see that the diagonalization of the S-matrix is achieved via the redefinitions

$$\begin{aligned}
\phi_1^+(k) &= \phi^+(+,k) + \phi^+(-,\rho^+)\,, \\
\phi_2^+(k) &= \phi^+(+,k) - \phi^+(-,k)\,, \\
A_1(k) &= A(+,+,k) + A(+,-,k)\,, \\
A_2(k) &= A(+,+,k) - A(+,-,k)\,.
\end{aligned} \tag{2.35}$$

It may be additionally checked that this matrix is unitary. As already mentioned, while it may not be clear whether this matrix is applicable to the formation and evaporation of a physical black hole, a conservative statement that can be made with certainty is the following: all information that is thrown into a large black hole is certainly recovered in its entirety, at least when the degrees of freedom in question are positions and momenta. It would be interesting to generalize this to degrees of freedom carrying additional conserved quantities like electric charge, etc. On the other hand, there is a certain property of the S-matrix that may be puzzling at first sight. Positive Rindler energies k imply that the off-diagonal elements in the S-matrix are dominant with exponentially suppressed diagonal elements. While negative Rindler energies reverse roles. One way to interpret this feature is to think of an eternal black hole where dominant off-diagonal elements suggest that information about in-going matter from the right exterior is carried mostly by out-going matter from the left exterior. However, in a physical collapse, there is only one exterior. It has been suggested by 't Hooft that one must make an antipodal mapping between the two exteriors to make contact with the one-sided physical black hole; we discuss this issue in Section 2.5.

2.3 THE MODEL

Asking two simple questions allows us to almost entirely determine a quantum mechanical model that corresponds to the black hole scattering matrix of the previous section. The first question is "what kind of a quantum mechanical potential allows for scattering states?" The answer is quite simply that it must be an unstable potential. The second question is "what quantum mechanical model allows for energy eigenstates that resemble those of Rindler space?" The answer, as we will show in this section, is a model of waves scattering off an inverted harmonic oscillator potential. Using this intuition, we will now construct the model and show that it explicitly reproduces the desired S-matrix. Having constructed the model, we will then proceed to compare it to two dimensional string theory models. The construction of our model and intuition gained from a comparison to two dimensional string theory/-matrix quantum mechanics models [59, 62, 65] allows us to study time delays and degeneracy of states in the next section.

Inverted quadratic potentials, at a classical level, fill up phase space with hyperbolas as opposed to ellipses as in the case of standard harmonic oscillator potentials. Since we have a tower of four dimensional partial waves in the black hole picture,

each of them results in a phase space of position and momentum and consequently a collection of inverted harmonic oscillators, one for each partial wave. Since the black hole scattering of 't Hooft mixes positions and momenta, we are naturally led to consider the description of scattering in phase space.

2.3.1 *Construction of the model*

We first start with a phase space parametrized by variables x_{lm} and p_{lm}. To implement the appropriate scattering off the horizon, we start with the same black hole scattering algebra: $[\hat{x}_{lm}, \hat{p}_{l'm'}] = i\lambda\delta_{mm'}\delta_{ll'}$, with $\lambda = c/\left(l^2+l+1\right)$ with $c = 8\pi G/R^2$. We will return to how this parameter might naturally arise in a microscopic setting in Section 2.5. Standard bases of orthonormal states are $|x; l, m\rangle$ and $|p; l, m\rangle$; these are coordinate and momentum eigenstates respectively, with

$$\langle l, m; x|p; l', m'\rangle = \frac{1}{\sqrt{2\pi\lambda}}\, e^{ipx/\lambda}\, \delta_{mm'}\delta_{ll'}\,. \tag{2.36}$$

Since our interest is in the scattering of massless particles, it will turn out to be convenient to use light-cone bases $|u^{\pm}; l, m\rangle$ which are orthonormal eigenstates of the light-cone operators:

$$\hat{u}^{\pm}_{lm} = \frac{\hat{p}_{lm} \pm \hat{x}_{lm}}{\sqrt{2}} \qquad \text{and} \qquad \left[\hat{u}^{+}_{lm}, \hat{u}^{-}_{l'm'}\right] = i\lambda\delta_{ll'}\delta_{mm'}\,. \tag{2.37}$$

While they look similar to creation and annihilation operators of the ordinary harmonic oscillator, $\hat{u}^{\pm}$ are in truth hermitian operators themselves; and are not hermitian conjugate to each other. Therefore, the states $|u^{\pm}; l, m\rangle$ are reminiscent of coherent states. These plus and minus bases will be useful in describing the in and outgoing states of the upside down harmonic oscillator. For definiteness, we will choose for the ingoing states to be described in terms of the $u^{+}_{l,m}$ basis while for the outgoing ones to be in terms of the $u^{-}_{l,m}$ basis. As in the previous section, we will work in the simplification where different oscillators (partial waves) do not interact and will therefore omit the partial wave labels in all places where they do not teach us anything new. Furthermore, as before, from the commutation relations we may define the following inner product on the Hilbert space of states

$$\langle u^{+}|u^{-}\rangle = \frac{1}{\sqrt{2\pi\lambda}}\, \exp\left(\frac{iu^{+}u^{-}}{\lambda}\right), \tag{2.38}$$

that expresses the Fourier transform kernel between the two bases. We may again realize the algebra if $\hat{u}^{-}$ acts on $\langle u^{+}|u^{-}\rangle$ and $\langle u^{+}|x\rangle$ as $-i\lambda\partial_{u^{+}}$ while $\hat{u}^{+}$ acts on $\langle u^{-}|u+\rangle$ and $\langle u^{-}|x\rangle$ as $i\lambda\partial_{u^{-}}$. To endow the model with dynamics, we now turn to the Hamiltonian for each oscillator/partial wave

$$\begin{aligned} H_{lm} &= \frac{1}{2}\left(p^2_{lm} - x^2_{lm}\right) \\ &= \frac{1}{2}(u^{+}_{lm}u^{-}_{lm} + u^{-}_{lm}u^{+}_{lm})\,, \end{aligned} \tag{2.39}$$

which may also be written as

$$H \;=\; \mp i\,\lambda\left(u^{\pm}\partial_{u^{\pm}}+\frac{1}{2}\right) \tag{2.40}$$

in the $u^{\pm}$ bases where we drop the l, m indices. Physically the wave-function can be taken to correspond to a wave coming from the right which after scattering splits into a transmitted piece that moves on to the left and a reflected piece that returns to the right. The other wave function can be obtained from this one by a reflection $x \to -x$. The light-cone coordinates describe these left/right movers and simplify the description of scattering since the Schrödinger equation becomes a first order partial differential equation. Moreover, the energy eigenfunctions are simply monomials of $u^{\pm}$ while in the x representation the energy eigenfunctions are more complicated parabolic cylinder functions. In particular, for each partial wave the Schrödinger equation in light-cone coordinates is:

$$i\,\lambda\,\partial_t\psi_{\pm}\left(u^{\pm},t\right) \;=\; \mp i\,\lambda\,\left(u^{\pm}\partial_{u^{\pm}}+1/2\right)\psi_{\pm}\left(u^{\pm},t\right) \tag{2.41}$$

with solutions

$$\psi_{\pm}\left(u^{\pm},t\right) \;=\; e^{\mp t/2}\,\psi^{0}_{\pm}\left(e^{\mp t}u^{\pm}\right)\,. \tag{2.42}$$

This can also be written in bra/ket notation as:

$$\langle u^{\pm}|\psi^{\pm}(t)\rangle \;=\; \langle u^{\pm}|e^{\frac{i}{\lambda}\hat{H}t}|\Psi^{\pm}_{0}\rangle \;=\; e^{\mp\frac{t}{2}}\langle e^{\mp t}u^{\pm}|\Psi^{\pm}_{0}\rangle\,. \tag{2.43}$$

The time evolution for the basis states is given by

$$\begin{aligned} e^{\frac{i}{\lambda}Ht}|u^{\pm}\rangle \;&=\; e^{\pm\frac{t}{2}}|e^{\pm t}u^{\pm}\rangle \\ \langle u^{\pm}|e^{\frac{i}{\lambda}Ht} \;&=\; e^{\mp\frac{t}{2}}\langle e^{\mp t}u^{\pm}| \\ \langle u^{+}|e^{\frac{i}{\lambda}Ht}|u^{-}\rangle \;&=\; \frac{1}{\sqrt{2\pi\lambda}}e^{-\frac{t}{2}}\exp\left(\frac{i}{\lambda}u^{+}u^{-}e^{-t}\right)\,. \end{aligned} \tag{2.44}$$

In the conventions of Figure 11, it is easy to see that ingoing states can be labelled by the u^{+} axis while the outgoing ones by the u^{-} axis. Since the potential is unbounded, the Hamiltonian has a continuous spectrum. In the u^{+} representation the energy eigenstates with eigenvalue ϵ are

$$\frac{1}{\sqrt{2\pi\lambda}}(u^{+})^{i\frac{\epsilon}{\lambda}-\frac{1}{2}}\,.$$

The singularity at $u^{+}=0$ leads to a two fold doubling of the number of states. This is understood to be arising from the existence of the two regions (I - II) in the scattering diagram. From now on we use $|\epsilon,\alpha^{+}\rangle_{\text{in}}$ and $|\epsilon,\alpha^{-}\rangle_{\text{out}}$ for the in and outgoing energy eigenstates with the labels $\alpha^{+}=\pm$, $\alpha^{-}=\pm$ to denote the regions I and II. While we have four labels, we are still only describing waves in the two quadrants (I-II)

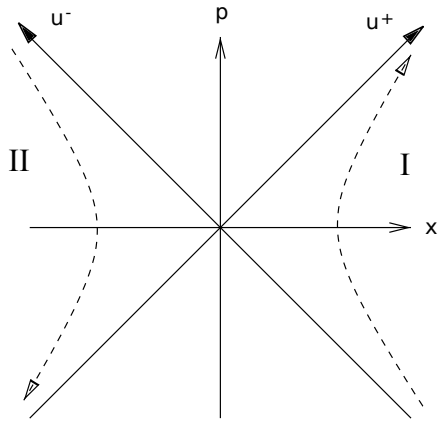

FIGURE 11: The scattering diagram.

with two of them for ingoing waves and two for outgoing ones. The in-states may be written as

$$\langle u^+|\epsilon,+\rangle_{\text{in}} = \begin{cases} \frac{1}{\sqrt{2\pi\lambda}}(u^+)^{i\frac{\epsilon}{\lambda}-\frac{1}{2}} & u^+ > 0 \\ 0 & u^+ < 0 \end{cases}$$

$$\langle u^+|\epsilon,-\rangle_{\text{in}} = \begin{cases} 0 & u^+ > 0 \\ \frac{1}{\sqrt{2\pi\lambda}}(-u^+)^{i\frac{\epsilon}{\lambda}-\frac{1}{2}} & u^+ < 0 \end{cases}$$

describing left and right moving ingoing waves for the regions I and II respectively. Similarly, the natural out basis is written as

$$\langle u^-|\epsilon,+\rangle_{\text{out}} = \begin{cases} \frac{1}{\sqrt{2\pi\lambda}}(u^-)^{-i\frac{\epsilon}{\lambda}-\frac{1}{2}} & u^- > 0 \\ 0 & u^- < 0 \end{cases}$$

$$\langle u^-|\epsilon,-\rangle_{\text{out}} = \begin{cases} 0 & u- > 0 \\ \frac{1}{\sqrt{2\pi\lambda}}(-u^-)^{-i\frac{\epsilon}{\lambda}-\frac{1}{2}} & u^- < 0 \end{cases}$$

to describe the right and left moving outgoing waves for the regions I and II respectively. Therefore, time evolution of the energy eigenstates

$$\langle u^+|\epsilon,+\rangle_{\text{in}}(t) = \frac{1}{\sqrt{2\pi\lambda}}e^{-i\frac{\epsilon}{\lambda}t}(u^+)^{i\frac{\epsilon}{\lambda}-\frac{1}{2}} = \frac{1}{\sqrt{2\pi\lambda}}e^{-\frac{\rho^+}{2}}e^{-i\frac{\epsilon}{\lambda}t}e^{i\frac{\epsilon}{\lambda}\rho^+} \qquad (2.45)$$

implies that they correspond to the Rindler relativistic plane-waves[2] moving with the speed of light in the tortoise-coordinates if we identify the quantum mechanical

2 Normalised in the $u^{\pm}$ basis.

time with Rindler time $t = \tau$ and the inverted harmonic oscillator energy with the Rindler momentum via $\kappa\lambda = \epsilon$. This means that the energy of the eigenstates of the non-relativistic inverted oscillator, when multiplied by λ, can also be interpreted as the energy/momentum of the Rindler relativistic plane waves of the previous section. This allows us to write down any ingoing state in terms of these Rindler plane waves. As we have seen, the unitary operator relating the $u^{\pm}$ representations is given by the fourier kernel (2.38) on the whole line that acts on a state as

$$\psi_{\text{out}}(u^-) \;=\; \left[\hat{\mathcal{S}}\psi_{\text{in}}\right](u^-) = \int_{-\infty}^{\infty} \frac{du^+}{\sqrt{2\pi\lambda}} e^{\frac{-iu^+u^-}{\lambda}} \psi_{\text{in}}(u^+). \tag{2.46}$$

It is now clear that repeating the calculations of the previous section results in the same S-matrix, rather trivially. However, to make the connection to the eigenstates of the inverted harmonic oscillator transparent, we will derive it in a more conventional manner. To represent the action of the kernel on energy eigenstates, we split it into a 2×2 matrix that relates them as follows:

$$\begin{pmatrix} |\epsilon,+\rangle_{out} \\ |\epsilon,-\rangle_{out} \end{pmatrix} = \hat{\mathcal{S}} \begin{pmatrix} |\epsilon,+\rangle_{in} \\ |\epsilon,-\rangle_{in} \end{pmatrix} . \tag{2.47}$$

The fastest method to find each entry is to compute the in-going energy eigenstates in the out-going position basis and vice versa using the insertion of a complete set of states of the form

$$\langle u^-|\epsilon\rangle_{\text{in}} \;=\; \int_{-\infty}^{\infty} du^+ \langle u^-|u^+\rangle\langle u^+|\epsilon\rangle_{\text{in}} \,. \tag{2.48}$$

The results are

$$\langle u^-|\epsilon,\pm\rangle_{\text{in}} \;=\; \lambda^{\frac{i\epsilon}{\lambda}} e^{\frac{\mp i\pi}{4}} e^{\pm\frac{\pi\epsilon}{2\lambda}} \Gamma\left(\frac{1}{2} + i\frac{\epsilon}{\lambda}\right) \frac{(\alpha^-|u^-|)^{-i\frac{\epsilon}{\lambda}-\frac{1}{2}}}{\sqrt{2\pi\lambda}} \tag{2.49}$$

$$\langle u^+|\epsilon,\pm\rangle_{\text{out}} \;=\; \lambda^{\frac{-i\epsilon}{\lambda}} e^{\frac{\pm i\pi}{4}} e^{\pm\frac{\pi\epsilon}{2\lambda}} \Gamma\left(\frac{1}{2} - i\frac{\epsilon}{\lambda}\right) \frac{(\alpha^+|u^+|)^{i\frac{\epsilon}{\lambda}-\frac{1}{2}}}{\sqrt{2\pi\lambda}} \,. \tag{2.50}$$

Each of these equations gives two results for each sign[3] to yield:

$$\begin{aligned} \mathcal{S} \;&= \\ &\frac{1}{\sqrt{2\pi}} \exp\left(-i\,\frac{\epsilon}{\lambda}\,\log\lambda\right) \Gamma\left(\tfrac{1}{2} - i\frac{\epsilon}{\lambda}\right) \begin{pmatrix} e^{-i\frac{\pi}{4}}\, e^{-\frac{\pi\epsilon}{2\lambda}} & e^{i\frac{\pi}{4}}\, e^{\frac{\pi\epsilon}{2\lambda}} \\ e^{i\frac{\pi}{4}}\, e^{\frac{\pi\epsilon}{2\lambda}} & e^{-i\frac{\pi}{4}}\, e^{-\frac{\pi\epsilon}{2\lambda}} \end{pmatrix} \\ &= e^{i\Phi(\epsilon)} \exp\left(-i\,\frac{\epsilon}{\lambda}\,\log\lambda\right) \begin{pmatrix} \frac{e^{-i\pi/4}}{\sqrt{1+e^{2\pi\epsilon/\lambda}}} & \frac{e^{i\pi/4}}{\sqrt{1+e^{-2\pi\epsilon/\lambda}}} \\ \frac{e^{i\pi/4}}{\sqrt{1+e^{-2\pi\epsilon/\lambda}}} & \frac{e^{-i\pi/4}}{\sqrt{1+e^{2\pi\epsilon/\lambda}}} \end{pmatrix} , \end{aligned} \tag{2.51}$$

3 For negative signs, one makes use of $(-1)^{i\epsilon/\lambda-1/2} = e^{-i\pi/2}e^{-\pi\epsilon/\lambda}$.

with the scattering phase $\Phi(\epsilon)$ being defined as

$$\Phi(\epsilon) \;=\; \sqrt{\frac{\Gamma\left(\frac{1}{2}-i\frac{\epsilon}{\lambda}\right)}{\Gamma\left(\frac{1}{2}+i\frac{\epsilon}{\lambda}\right)}}\,. \tag{2.52}$$

Identifying parameters as $k_l\,\lambda_l \;=\; \epsilon_l$, we see that this precisely reproduces the S-matrix derived in the previous section for every partial wave. In this model, it is clear that the competition between reflection and transmission coefficients is owed to the energy of the waves being scattered being larger than the tip of the inverted potential.

2.3.2 *A projective light-cone construction*

Although we had good reason to expect such an inverse harmonic oscillator realization of the black hole S-matrix, there is, in fact, another way to derive it—using what is called a projective light-cone construction. This construction was first studied by Dirac and [72, 73] provide a good modern introduction to the topic. The essential idea is to embed a null hyper-surface inside Minkowski space to study how linear Lorentz symmetries induce non-linearly realized conformal symmetries on a (Euclidean) section of the embedded surface. This allows us to relate the Rindler Hamiltonian -which can then be related directly to the Hamiltonian of the quantum mechanics model that describes the scattering- with the Dilatation operator on the horizon. In a black hole background this construction is of course expected to hold only locally in the near horizon region. We first introduce $x^M \;=\; (x^\mu, x^{d-1}, x^d)$ with $\mu \;=\; 1, .., d-2$ (note that μ is a Euclidean index), where the light-cone coordinates are defined as $x^\pm \;=\; x^d \pm x^{d-1}$. Here, x^d serves as the time coordinate [4]. The Minkowski metric η_{MN} in these coordinates is given as

$$ds^2 \;=\; -dx^+dx^- + dx_\mu dx^\mu\,, \tag{2.53}$$

which has an $SO(d-1,1)$ Lorentz symmetry. There is an isomorphism between the corresponding Lorentz algebra and the Euclidean conformal algebra in $d-2$ dimensions. To state this isomorphism, we first label the $d-2$-dimensional Euclidean conformal group generators as:

$$\begin{aligned}
&P_\mu = i\partial_\mu && \text{corresponding to translations,}\\
&M_{\mu\nu} = i\left(x_\mu\partial_\nu - x_\nu\partial_\mu\right) && \text{to rotations,}\\
&D = ix^\mu\partial_\mu && \text{to dilatations and}\\
&K_\mu = i\left(2x_\mu\left(x^\nu\partial_\nu\right) - x^2\partial_\mu\right) && \text{to special conformal transform.}
\end{aligned} \tag{2.54}$$

The identification is now given as follows:

$$J_{\mu\nu} \;=\; M_{\mu\nu}\,, \quad J_{\mu+} \;=\; P_\mu\,, \quad J_{\mu-} \;=\; K_\mu\,, \quad J_{+-} \;=\; D\,, \tag{2.55}$$

4 The null cone is described by the equation $X^2 = 0$ and a Euclidean section can be given as $x^+ = f(x^\mu)$.

where the $SO(3,1)$ Lorentz generators J_{MN} are given by

$$J_{MN} = x_M p_N - x_N p_M . \tag{2.56}$$

These satisfy the $SO(3,1) \backsimeq SL(2,\mathbb{C})$ algebra. Equation (2.55) is understood as holding on the null hyper-surface, so one needs to solve the constraint equation and express $x^{\pm}$ in terms of x^{μ}. In particular the Dilatation operator on the two dimensional horizon is

$$D = J_{+-} = x_+ p_- - x_- p_+ = \frac{1}{\lambda}\left(u^+ u^- + u^- u^+\right) = \frac{1}{\lambda} H , \tag{2.57}$$

where in the second equality we used $u^{\pm} = x_{\pm}$ to connect to the light-cone coordinates of the previous sub-section and in the third equality, we made use of the back-reaction relations (2.14). Interestingly enough, we see that the Rindler Hamiltonian (Boost generator) together with the backreaction relations gives exactly the Hamiltonian of the inverted oscillator and can also be interpreted as the Dilatation operator on the two dimensional horizon. This identification involves a rescaling of the inverted harmonic oscillator Hamiltonian with λ that is also neatly realized in the relation between the quantum mechanical energy ϵ and the Rindler energy κ to relate the two S-matrices.

This construction via the light-cone projection could possibly shed more light on the relation between the black hole S-matrix and string theoretic amplitudes. In the early papers on black hole scattering [52, 53, 21], a striking similarity between the S-matrix and stringy amplitudes was observed. The role of the string worldsheet was attributed to the horizon itself. It was noted that the string tension was imaginary. In the construction above, we found that the induced conformal symmetry on the horizon is Euclidean and that the Dilatation operator is mapped to the time-evolution operator (Rindler Hamiltonian) of the four dimensional Lorentzian theory. This led us to the unstable potential of the inverse harmonic oscillator. It may well be that the apparently misplaced factors of i in the string tension is owed to the Euclidean nature of conformal algebra on the horizon. It would also be interesting to understand the role of possible infinite-dimensional local symmetries on the horizon/worldsheet [74, 75] from the point of view of the quantum mechanics model, elaborating on the null cone construction. We leave this study to future work.

While the model is seemingly very simple, this is not the first time that such a model has been considered to be relevant for black hole physics [64, 76]. However, previous considerations have found that these models do not correspond to two dimensional black hole formation owing to an insufficient density of states in the spectrum. Refining these considerations with the intuition that each oscillator as considered in this section corresponds to a partial wave of a four dimensional black hole, we find that our model may indeed be directly related to four dimensional black holes. We provide evidence for this in Section 2.4. In order to move on to which, however, it will be very useful for us to review the two dimensional string theory considerations of the past; this is what we now turn to.

2.3.3 *Relation to Matrix Models and two dimensional String Theory*

Hermitian Matrix Quantum Mechanics (MQM) in the inverted harmonic oscillator was studied in connection with $c = 1$ Matrix Model and string theory in two dimensions. For more details, we refer the reader to [38, 39]. Here, we briefly review these results in order to point out various similarities and differences with our work. The Lagrangian of MQM is of the form

$$L \;=\; \frac{1}{2}\mathrm{Tr}\left[(D_t M)^2 + M^2\right] \qquad \text{with} \qquad D_t \;=\; \partial_t - iA_t\,, \tag{2.58}$$

where A_t is a non-dynamical gauge field. The $N \times N$ Hermitian Matrices transform under $U(N)$ as $M \to U^\dagger M U$. The role of the non-dynamical gauge field is to project out the non-singlet states in the path integral. Diagonalization of the matrices results in a Vandermonde factor in the path integral measure:

$$\mathcal{D}M \;=\; \mathcal{D}U \prod_i dx_i \prod_{i<j}(x_i - x_j)^2\,. \tag{2.59}$$

This indicates a natural fermionic redefinition of the wave-functions into Slater determinants (in a first quantised description). The Hamiltonian of the system is, therefore, in terms of N free fermions:

$$\begin{aligned} \hat{H}\tilde{\Psi} &= -\left(\frac{\hbar^2}{2}\sum_{i=1}^{N}\partial_{x_i}^2 + \frac{1}{2}x_i^2\right)\tilde{\Psi}\,, \quad \text{with} \\ \tilde{\Psi}(x_i) &= \prod_{i<j}(x_i - x_j)\Psi(x_i)\,, \end{aligned} \tag{2.60}$$

with $\tilde{\Psi}(x_i)$ being the redefined fermionic wave-functions. Filling up the "Fermi-sea" up to a level μ, allows for a definition of the vacuum. Clearly, all fermions are subject to the same chemical potential μ that is typically considered to be below the tip of the inverted oscillator. A smooth string world-sheet was argued to be produced out of these matrices in a double-scaling limit $N \to \infty, \hbar \to 0$ with an inverse string-coupling related to the chemical potential as $\mu \sim 1/g_s$. In this double-scaling limit, this theory describes string theory on a two dimensional linear dilaton background with coordinates described by time t and the Liouville field ϕ. The matrix model/harmonic oscillator coordinate x is conjugate to the target space Liouville field via a non-local integral transformation [77]. In contrast to this picture, owing to a one-one correspondence between the two dimensional harmonic oscillators and four dimensional partial waves in our model, this integral transform is unnecessary. However, it has been argued in string theory that only the quadratic tip is relevant in this double-scaling limit, even in the presence of a generic inverted potential, emphasizing the universality of the quadratic tip. Whilst we do not have a similar stringy argument, we expect the ubiquitous presence of the quadratic potential to persist in our construction owing to the ubiquitous presence of the Rindler horizon in physical black holes formed from collapsing matter. A modern discourse with emphasis on

the target space interpretation of the matrix model as the effective action of N $D0$ branes may be found in [78]. A natural second quantized string field theory description of the system where the fermionic wave-functions are promoted to fermionic fields may be found in [79, 38, 37] and references therein. A satisfactory picture of free fermionic scattering in the matrix model was given in [59] via the following S-matrix relation:

$$\hat{S} \;=\; i_{b\to f} \circ \hat{S}_{ff} \circ i_{f\to b} \tag{2.61}$$

where even though the asymptotic tachyonic states are bosonic, one is instructed to first fermionize, then scatter the fermions in the inverted quadratic potential and then to bosonize again. The total S-matrix is unitary if the fermionic scattering is unitary and the bosonization spans all possible states. The logic of this expression resembles that of 't Hooft's S-matrix, where one first expands a generic asymptotic state into partial waves, expresses them in terms of near horizon Rindler parameters, scatters them with the given S-matrix that is similar to the one of two dimensional string theory before transforming back to the original asymptotic coordinates. At the level of the discussion now, it may already be noted that one important difference between the two dimensional string-theoretic interpretation of the matrix model and our four dimensional partial wave one is the nature of the transformations that relate asymptotic states to the eigenstates of the inverted harmonic oscillator. Additionally, and perhaps more importantly, in our construction, we have an entire collection of such harmonic oscillators/matrix models parametrised by l, m that conspire to make up a four dimensional black hole. We present concrete evidence for this by studying time-delays and degeneracy of states in Section 2.4. There are further differences between the two dimensional string theories and our construction, in order to present which, we need to proceed to a study of the spectrum of states in our model; this enables us to study growth of states in the two models. Finally, we also comment on a possible second quantization and appropriate MQM interpretation of our model in Section 2.5.

2.4 COMBINING THE OSCILLATORS (PARTIAL WAVES)

On the side of the macroscopic black hole in Section 2.2, the calculation was done in an approximation where there is a pre-existing black hole into which degrees of freedom are thrown (as positions and momenta). It was then evident that the information that was sent into the black hole is completely recovered since the S-matrix was unitary. Furthermore, the back-reaction computation told us exactly how this information is retrieved: in-going positions as out-going momenta and in-going momenta as out-going positions. However, a critical standpoint one may take with good reason would be to say that this is not good enough to tell us if a physical collapse of a black hole and complete evaporation of it is a unitary process. The calculation has not modeled a collapsing problem.

The picture to have in a realistic collapse is that of an initial state that evolves in time to collapse into an intermediate black hole state which then subsequently

evaporates to result in a final state that is related to the initial one by a unitary transformation. Naturally, the corresponding macroscopic picture is that of a strongly time-dependent metric. Heuristically, one may think of the total S-matrix of this process as being split as

$$\hat{S} \;=\; \hat{S}_{\mathscr{I}^- \to \mathrm{hor}^-}\, \hat{S}_{\mathrm{hor}^- \to \mathrm{hor}^+}\, \hat{S}_{\mathrm{hor}^+ \to \mathscr{I}^+} \tag{2.62}$$

where $\hat{S}_{\mathscr{I}^- \to \mathrm{hor}^-}$ corresponds to evolution from asymptotic past to a (loosely defined) point in time when gravitational interactions are strong enough for the collapse to begin, $\hat{S}_{\mathrm{hor}^- \to \mathrm{hor}^+}$ to the piece that captures all the "action"—insofar as collapse and evaporation are concerned—take place and finally $\hat{S}_{\mathrm{hor}^+ \to \mathscr{I}^+}$ represents the evolution of the evaporated states to future infinity. The horizon—being a teleological construction that can be defined only if one knows the global structure of spacetime—has a time dependent size and location in a collapse/evaporation scenario but for us will nevertheless comprise the locus of spacetime points where the back-reaction effects are important. Therefore, we use subscripts $\mathrm{hor}^{\pm}$ to refer to it, at different points in time, in the above heuristic split. Thought of the total evolution this way, it is clear that the most important contribution arises from the part of the matrix that refers to the region in space-time where gravitational back-reaction cannot be ignored. The other pieces are fairly well-approximated by quantum field theory on an approximately fixed background. Nevertheless, in the intermediate stage, the metric is strongly time-dependent.

At the outset, let it be stated that we will not get as far as being able to derive this metric from the quantum mechanics model. We may ask if there are generic features of the black hole that we have come to learn from semi-classical analyses that can also be seen in this model. We will focus on two important qualitative aspects of (semi-classical) black holes:

TIME-DELAY: A physical black hole is not expected to instantaneously radiate information that has been thrown into it. There is a time-delay between the time at which radiation begins to be received by a distant observer compared to the time that in-going information was thrown at it. Given an in-state that collapses into a black hole, we expect that the time-scale associated to the scattering process is of the order GM[5].

In previous studies of two dimensional non-critical string theory, it was found that with a single inverted harmonic oscillator, the associated time-delay is not long enough to have formed a black hole [60, 63, 64]. However, with the recognition that each oscillator corresponds to a partial wave and that a collection of oscillators represents a four dimensional black hole, we see that the time delay associated to each oscillator is the time spent by an in-going mode in the scattering region. This is the time in which the backreaction effect transforms UV modes-localised packets into IR-delocalised ones. In order for one to study the lifetime of the black hole as a single system one needs to combine all these oscillators.

5 More precicely due to dimensional reasons it should scale with a power of GM, with a logarithmic correction due to the relation between tortoise and asymptotic coordinates.

APPROXIMATE THERMALITY: As Hawking famously showed [20], the spectrum of emitted radiation should look largely thermal for a wide range of energies. One way to probe this feature is via the number operator which, for a finite temperature system, can be written as $\langle \hat{N}(\omega) \rangle = \rho(\omega) f(\omega)$ with $\rho(\omega)$ being the density of states and $f(\omega)$ the appropriate thermal distribution for Fermi/Bose statistics. Given that the S-matrix is unitary, we know that this notion of temperature and thermality of the spectrum is only approximate. Notwithstanding this, a detector at future infinity should register this approximately thermal distribution for a large frequency range in order to satisfy the criterion of unitarity together with approximate thermality. To be more precise, if one captures only the reflected or transmitted piece of the waves, the spectrum can be shown to be approximately thermal 2.5. If one tries to capture both, there will still be a relative time delay since the reflected and transmitted pieces do not suffer the same time delay which leads to some period of time until the process reveals its unitary nature.

In what follows, we will study whether the S-Matrix corresponding to our collection of oscillators in the model presented in Section 2.3 displays both these properties. En route we will have to understand the correct way of combining the different oscillators partial waves.

2.4.1 *Time delays and degeneracy of states*

We have seen that the total scattering matrix associated to four-dimensional gravity can be seen as arising via a collection of inverted harmonic oscillators, each with a different algebra differentiated by λ_l in, say, (2.15). One canonical way to study life-times in scattering problems in quantum mechanics is via the time-delay matrix, which is defined as:

$$\Delta t_{ab} = \Re \left(i \sum_c S^\dagger(k_l, \lambda_l)_{ac} \left(\frac{dS(k_l, \lambda_l)}{dk} \right)_{cb} \right) . \tag{2.63}$$

Each matrix element above encodes the time spent by a wave of energy k_l in the scattering region in the corresponding channel. The trace of this matrix, called Wigner's time delay τ_l, captures the total characteristic time-scale associated to the entire scattering process. Said another way, should we start with a generic in-state that undergoes scattering and is then retrieved in the asymptotic future as some out-state, the trace of the above matrix associates a life-time to the intermediate state [80, 81]. For large energies k_l, using $S(k_l, \lambda_l)$ in (2.33), the Wigner time-delay associated to the scattering of a single oscillator can be calculated to scale as $\tau \sim \log(\lambda_l k_l)$. This is the same result as was found in the two dimensional string theory literature [60, 63, 64] and was argued to not be long-enough for black hole formation. Based on these black hole non-formation results in the matrix quantum mechanics, it was suggested that studying the non-singlet sectors would shed light on two dimensional black hole formation[68, 82]. Despite some efforts in relating the adjoint representations with long-string states [76], a satisfactory Lorentzian description is still missing. Anticipating our result prematurely, our model does not suffer from these difficul-

ties as it is to describe a four dimensional black hole with a collection of oscillators. Merely the s-wave oscillator in our model would mimic the singlet sector in matrix quantum mechanics[6].

The above time delay τ may also be interpreted as a density of states associated to the system. The inverted potential under consideration implies a continuous spectrum. In order to discretize which, to derive the density of states, the system must be stabilized—by putting it in a box of size Λ, for instance. Demanding that the wavefunctions vanish at the wall and regulating the result by subtracting any cut-off dependent quantities, the density of states may be computed from the scattering phase Φ defined via $\mathcal{S}(k_l, \lambda_l) = \exp[i\Phi(k_l, \lambda_l)]$ as $\rho(\epsilon_l) = d\Phi/d\epsilon_l$ [83]. The result is exactly the same as what we get from computing the time delay using the scattering matrix (2.33) and the time-delay equation (2.63) to find a Di-Gamma function $\psi^{(0)}$

$$\begin{aligned}\rho(\epsilon_l) \;=\; \tau_l \;&=\; \frac{2}{\lambda_l}\Re\left[\psi^{(0)}\left(\frac{1}{2}-i\frac{\epsilon_l}{\lambda_l}\right)+\log(\lambda_l)\right]\\ &=\; \Re\left[\sum_{n=0}^{\infty}\frac{2}{i\epsilon_l-\lambda_l\left(n+\frac{1}{2}\right)}+\frac{2}{\lambda_l}\log(\lambda_l)\right]\,.\end{aligned} \tag{2.64}$$

This density of states may be used to define a partition function for each partial wave (with Hamiltonian $\hat{H}_{lm}$), where the energy eigenstates contributing to the partition function will have been picked out by the poles of the density $\rho(\epsilon_l)$. However, in our model, we see that there are many oscillators in question. Should we start with an in-state made of a collection of all oscillators instead of a single partial wave, we may first write down the total S-matrix as a product of the individual oscillators as

$$\mathcal{S}_{\text{tot}} \;=\; \prod_{l=0}^{\infty}\mathcal{S}(k_l, \lambda_l)\,, \tag{2.65}$$

assuming that different partial waves do not interact. One may correct for this by adding interaction terms between different oscillators. To compute the time-delay associated to a scattering of some in-state specified by a given total energy involves an appropriately defined Wigner time-delay matrix as

$$\tau_{\text{tot}} \;=\; \text{Tr}\left[\Re\left(-i\left(\mathcal{S}_{\text{tot}}^{\dagger}\right)_{ac}\left(\frac{d\mathcal{S}_{\text{tot}}}{dE_{\text{tot}}}\right)_{cb}\right)\right]\,, \tag{2.66}$$

where this equation makes sense only if we have defined a common time evolution and unit of energy for the total system/collection of partial waves. We will elaborate on this in a while. Now, even in the spherically symmetric approximation, to write the total S-matrix as a function of merely one coarse-grained energy E_{tot} is not a uniquely defined procedure. However, our intuition that each partial wave may be thought of as a single-particle oscillator allows us to compute the density of states in a combinatorial fashion. We will see that the degeneracy of states associated to an intermediate long-lived thermal state arises from the various ways in which one

6 It would be very interesting if higher l modes can be described as non-singlets of a matrix model.

might distribute a given total energy among the many available oscillators. Given a total energy E_{tot}, we now have the freedom to describe many states, each with a different distribution of energies into the various available oscillators. From the poles in the density defined in (2.64), we see that each oscillator has energies quantized as

$$\epsilon_l = \lambda_l \left(n_l + \frac{1}{2} \right) . \tag{2.67}$$

This allows us to measure energies in units of c, where c is defined implicitly via $\lambda_l \left(l^2 + l + 1 \right) = c$. Therefore, in these units, the energies are "quantized" as

$$\frac{\epsilon_l}{c} = \frac{1}{l^2 + l + 1} \left(n_l + \frac{1}{2} \right) . \tag{2.68}$$

Now, given some total energy E_{tot}, we see that any oscillator may be populated with a single particle state carrying energy such that $n_l = E_{\text{tot}} \left(l^2 + l + 1 \right)$, where we leave out the half integer piece for simplicity. Importantly, we see that there exist "special" states coming from very large l-modes even for very small energies. For example, an energy of 1 could arise from a very large l-mode with the excitation given by $n_l = \left(l^2 + l + 1 \right)$. This is rather unsatisfactory for one expects that it costs a lot of energy to create such states. Moreover, there is an interplay between the log term in the growth of states and the behaviour of the DiGamma function that we are unable to satisfactorily take into account. There is an additional problem which is that the energy of each partial wave is measured in different units that are l dependent; this means that they also evolve with different times. We thus conclude that this is not the correct way to combine the different oscillators.

There is a rather beautiful way to resolve all these three problems via a simple change of variables that we turn to next. It will allow us to interpret the above cost of energy as relative shifts of energies with respect to a common ground state. Additionally these relative shifts also cure the above interplay; there will simply be no log term in the density of states. Finally, this will also introduce a canonical time evolution for the entire system, resulting in one common unit of energy.

2.4.2 *Exponential degeneracy for the collection of oscillators*

In order to combine the different oscillators and define a Hamiltonian for the total system we need to get rid of the l dependence in the units of energy used for different oscillators. It turns out that this is possible by rewriting the black hole algebra. Moreover using these new variables, the relation between 't Hooft's black hole S-matrix for an individual partial wave and the one of two dimensional string theory of type II [59] can be made manifest. To make this connection transparent, we again start

with a collection of inverse harmonic oscillators and the following Hamiltonian for the total system

$$\begin{aligned} H_{tot} &= \sum_{l,m} \frac{1}{2} \left(\tilde{p}_{lm}^2 - \tilde{x}_{lm}^2 \right) \\ &= \sum_{l,m} \frac{1}{2} \left(\tilde{u}_{lm}^+ \tilde{u}_{lm}^- + \tilde{u}_{lm}^- \tilde{u}_{lm}^+ \right) , \end{aligned} \tag{2.69}$$

but this time imposing the usual λ-independent commutation relations $[\tilde{u}_{lm}^+ \tilde{u}_{l'm'}^-] = i\delta_{ll'}\delta_{mm'}$. The λ dependence will come through via an assignment of a chemical potential $\mu(\lambda)$ for each oscillator; this assignment is to be thought of as a different vacuum energy for each partial wave. Following [59], one may then derive an S-matrix for this theory. To match this to the one of 't Hooft for any given partial wave, one must identify the chemical potential and energy parameters as $\mu = 1/\lambda$ and the Rindler energy $k = \omega + \mu = \omega + 1/\lambda$. It is worth noting that in the reference cited above, only energies below the tip of the inverted potential were considered, resulting in a dominant reflection coefficient. In contrast 't Hooft's partial waves carry energies higher than the one set by the tip of the potential. Consequently, to make an appropriate identification of two dimensional string theory with the partial wave S-matrix, an interchanging of the reflection and transmission coefficients is necessary. If one were to make a parallelism with the string theory the "string coupling" of each partial wave would scale as $g_s \sim 1/\mu \sim c/(l^2 + l + 1)$. This indicates that as we increase the size of the black hole or we consider higher l partial waves the corresponding string coupling becomes perturbatively small.
Writing out the energies of the various partial waves with the above identification, we have

$$k_l = \omega_l + \frac{l^2 + l + 1}{c} , \qquad \text{and} \qquad E_{\text{tot}}^{\text{Rindler}} = \sum_l k_l . \tag{2.70}$$

At this stage, the labels ω_l are continuous energies. However, discretizing the spectrum as before, by putting the system in a box, we arrive at discrete energies

$$c\, E_{\text{tot}} = \sum_l \left[c \left(n_l + \tfrac{1}{2} \right) + l^2 + l + 1 \right] , \tag{2.71}$$

for every individual oscillator. Without a detour into this two dimensional string theory literature, we may have alternatively arrived at this spectrum from the quantum mechanics model in 2.3 via the following identifications:

$$\epsilon_l \longrightarrow 1 + \lambda_l\, \omega_l \qquad \text{and} \qquad \lambda_l \longrightarrow \frac{1}{\mu_l} . \tag{2.72}$$

While the model presented in Section 2.3 makes the algebra manifest, the above identification of parameters to relate to the model with a λ-independent algebra makes the physical interpretation of the relative shifts in energies between the partial waves

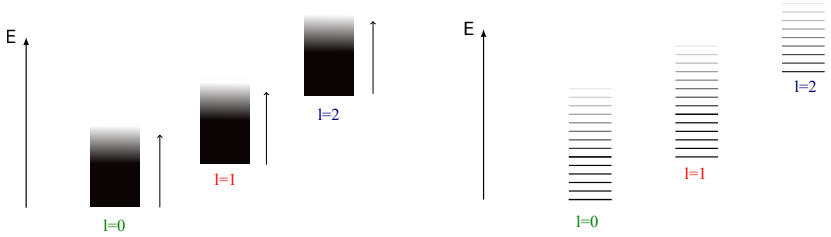

FIGURE 12: Spectrum of the collection of oscillators. The left picture is the continuous spectrum of the collection of inverted oscillators, where each ground state energy depends on the angular momentum of the partial wave to be interpreted as a chemical potential. On the right, we have discretised the spectrum by putting the system into a box.

manifest and allows for a consistent definition of time and energy for the total system.

This allows us to rewrite our S-matrix $S\left(\epsilon_l/\lambda_l\right)$ as a function of two variables ω_l and μ_l as $S\left(\omega_l, \mu_l\right)$. With this change of variables, we recover exactly the S-matrix of two dimensional string theory discussed in the literature and therefore, now allows us to interpret μ as a chemical potential of the theory. However, since μ_l is now l dependent in our collection of oscillators, it gives us a natural way to interpret how the combined system behaves. To excite a very large l oscillator, one first has to provide sufficient energy that is equal to $\mu_l \sim \left(l^2 + l + 1\right)$. Therefore, we naturally see that exciting a large l-oscillator costs energy. The physical spectrum may be depicted as in Figure 12, where we depict an arbitrarily chosen ground-state energy with $E = 0$, each oscillator labeled by l and excitations above them by n_l. The various oscillators are shifted by a chemical potential. And the vacuum is defined to be the one with all Rindler energies k_l set to zero. Now, given an initial state carrying a total energy of E_{tot}, we are left with a degeneracy of states that may be formed by distributing this energy among the many available oscillators. The larger this energy, the more oscillators we may distribute it into and hence the larger the degeneracy. The degeneracy associated to equation (2.71), without the chemical potential shift, is merely asking for the number of sets of all integers $\{n_l\}$ that add up to E_{tot}. These are the celebrated partitions into integers that—as Ramanujan showed—grow exponentially. Clearly, for large total energy, our degeneracy grows similarly at leading order. However, the chemical potential shift slows down the growth polynomially compared to the partitioning into integers owing to the fact that for a given E_{tot}, only approximately $\sqrt{E_{\text{tot}}}$ number of oscillators are available. It is worthwhile to note that, in this simplistic analysis, we have ignored the degeneracy arising from the m quantum number; accounting for which clearly increases the growth of states. We already see that the statistical description of the model supports an exponential growth of density of states. This shares striking resemblance to the Hagedorn growth of density of states in black holes.

As a conservative estimate, we may start with some total energy E_{tot} and a fixed set of oscillators that are allowed to contribute to it. This allows us to sum over the

contribution arising from the $\left(l^2+l+1\right)c^{-1}$ piece in (2.71) to be left with some subtracted total energy $\tilde{E}_{\text{tot}}$ that is to be distributed among the n_l excitations over each of the available oscillators. Clearly, this grows exponentially much as the partitions into integers does, with the subtracted energy $\tilde{E}_{\text{tot}}$. This is given by the famous Hardy-Ramanujan formula for the growth of partitions of integers:

$$p\left(n\right) \sim \exp\left(\pi\sqrt{\frac{2n}{3}}\right). \tag{2.73}$$

Identifying n with the integer part of $\tilde{E}_{\text{tot}}$, we see the desired exponential growth. And considering that the same total energy may be gained from choosing different sets of oscillators to start with, increases this degeneracy further, in equal measure. While imposing the antipodal identification of 't Hooft—which we discuss in Section 2.5—reduces this degeneracy, the exponential growth of states remains. How one may derive the Schwarzschild entropy from this degeneracy requires a truly microscopic understanding of the parameter λ. We suggest a way forward towards the end of this chapter but leave a careful study to future work.

2.5 DISCUSSION

Here, we have constructed a quantum mechanics model that reproduces 't Hooft's black hole S-matrix for every partial wave using which, we provided non-trivial evidence that it corresponds to a black hole S-matrix. Several questions, though, remain unanswered. The only degrees of freedom in question were momenta and positions of ingoing modes. One may add various standard model charges, spin, etc. to see how information may be retrieved by the asymptotic observer.

Dynamically speaking, gravitational evolution is expected to be very complicated in real-world scenarios. We have merely discuss the problem upon the assumption of spherical symmetry. One could also imagine interactions between the different harmonics once the transverse part of the gravitational force becomes dominant. While incorporating these interactions may be very difficult to conceive in gravity, they are rather straightforward to implement in the quantum mechanical model; one merely introduces interaction terms coupling different oscillators. Exactly what the nature of these interactions is, is still left open.

The complete dynamics of the black hole includes a change in mass of the black hole during the scattering process. In this chapter, we chose to work in an approximation where this is ignored. The corresponding approximation in the inverted oscillators is that the potential is not affected by the scattering waves. In reality, of course, the quadratic potential changes due to the waves that scatter off it. The change in the form of the inverted potential due to a scattering mode can be calculated [84]. We hope to work on this in the future and we think that this gives us a natural way to incorporate the changes to the mass of the black hole. Another possible avenue for future work is to realise a truly microscopic description of the S-matrix, either in the form of a matrix model or a non-local spin model having a finite-dimensional Hilbert

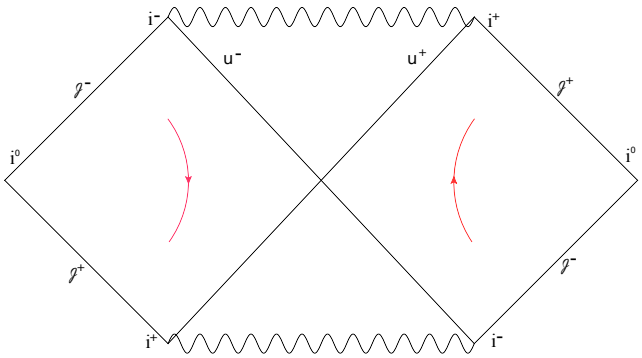

FIGURE 13: The Penrose diagram. Each point in the conformal diagram originally corresponds to a different sphere. After antipodal identification, the points (u^+, u^-) and $(-u^+, -u^-)$ correspond to antipodal points on a common sphere as given in (2.74). The red lines indicate the arrows of time.

space from the outset, where the inverse harmonic potential or emergent $SL(2,\mathbb{R})$ symmetries are expected to arise after an averaging over the interactions between the microscopic degrees of freedom. Some models with these properties can be found in [85, 86, 87, 88].

ANTIPODAL ENTANGLEMENT Unitarity of the S-Matrix demands that both the left and right exteriors in the two-sided Penrose diagram need to be accounted for; they capture the transmitted and reflected pieces of the wave-function, respectively. In the quantum mechanics model, there appears to be an ambiguity of how to associate the two regions I and II of the scattering diagram in Fig. 11 to the two exteriors of the Penrose diagram. We saw, in the previous section, that the quantum mechanical model appears to support the creation of physical black holes by exciting appropriate oscillators. To resolve then the issue of two exteriors, it was proposed that one must make an antipodal identification on the Penrose diagram [55]; see figure 13. Unitarity is arguably a better physical consistency condition for the allowed states than a demand of the maximal analytic extension. The precise identification is given by $x \to Jx$ with[7]

$$J: \quad (u^+, u^-, \theta, \phi) \longleftrightarrow (-u^+, -u^-, \pi - \theta, \pi + \phi) \ . \tag{2.74}$$

Note that J has no fixed points and is also an involution, in that $J^2 = 1$. Such an identification implies that the points u^+, u^- and $-u^+, -u^-$ in the Penrose diagram are just antipodal points of a common sphere, but with no identification among different points of this sphere. Precisely on the horizon, one actually needs to identify the antipodal points of the horizon. This represents the central point of the Penrose diagram for which $u^\pm = 0$. Note that, since external observers can only see positive

7 Note that the simpler mapping of identifying points in I, II via $(u^+, u^-, \theta, \phi) \leftrightarrow (-u^+, -u^-, \theta, \phi)$ is singular on the axis $u^+, u^- = 0$.

u values, the external observer does not notice the antipodal identification on the horizon, he never sees the horizon directly. In particular for the distributions, this means

$$u^{\pm}(\theta,\phi) \;=\; -u^{\pm}(\pi-\theta,\pi+\phi) \quad \text{and} \quad p^{\pm}(\theta,\phi) \;=\; -p^{\pm}(\pi-\theta,\pi+\phi)\;. \tag{2.75}$$

Therefore, noting that the spherical harmonics then obey $Y_{l,m}(\pi-\theta,\pi+\phi) = (-1)^l Y_{l,m}(\theta,\phi)$, we see that only those modes with an l that is odd contribute. Global identifications of the two exteriors have been considered in the past [89, 90, 91] but we emphasize that this proposal is different from these works. The physics of the scattering, with this identification is now clear. In-going wave-packets move towards the horizon where gravitational back-reaction is strongest according to an asymptotic observer. Most of the information then passes through the antipodal region and a small fraction is reflected back. Turning on quantum mechanics implies that ingoing position is imprinted on outgoing momenta and consequently, an highly localised ingoing wave-packet transforms into two outgoing pieces—transmitted and reflected ones—but both having highly localised momenta. Their positions, however, are highly de-localised. This is how large wavelength Hawking particles are produced out of short wavelength wave-packets and an IR-UV connection seems to be at play. Interestingly, the maximal entanglement between the antipodal out-going modes suggests a non geometric microscopic "wormhole" connecting each pair [92]; the large geometric wormhole (Einstein-Rosen bridge) connects the reflected and transmitted Hilbert spaces. Furthermore, as the study of the Wigner time-delay showed, the reflected and transmitted pieces arrive with a time-delay that scales logarithmically in the energy of the in-going wave. One may also wonder why transmitted pieces dominate the reflected ones. It may be that the attractive nature of gravity is the actor behind the scene.

APPROXIMATE THERMALITY: We now turn to the issue of thermality of the radiated spectrum. Given a number density, say $N^{\text{in}}(k)$ as a function of the energy k, we know that there is a unitary matrix that relates it to radiated spectrum. This unitary matrix is precisely the S-matrix of the theory. The relation between the in and out spectra is given by $N^{\text{out}}(k) = S^{\dagger}N^{\text{in}}(k)S$[8]. Using the explicit expression for the S-matrix (2.33), we find

$$N^{\text{out}}_{++}(k) \;=\; \frac{N^{\text{in}}_{++}(k)}{1+e^{2\pi k}} + \frac{N^{\text{in}}_{--}(k)}{1+e^{-2\pi k}} \tag{2.76}$$

$$N^{\text{out}}_{--}(k) \;=\; \frac{N^{\text{in}}_{--}(k)}{1+e^{2\pi k}} + \frac{N^{\text{in}}_{++}(k)}{1+e^{-2\pi k}}\,, \tag{2.77}$$

where N^{in}_{++} and N^{in}_{--} are the in-going number densities from either side of the potential. We see that indeed the scattered pulse emerges with thermal factors $1+e^{\pm 2\pi k}$.

8 This comes about since it is a bilinear having one creation one annihilation operator.

For most of the radiated spectrum to actually be thermal, we see that N^{in}_{++} and N^{in}_{--} must be constant over a large range of energies. This was observed to be the case in the context of two dimensional string theory, starting from a coherent pulse, seen as an excitation over an appropriate Fermi-sea vacuum [60, 63, 64]. In our context, since we do not yet have a first principles construction of the appropriate second quantised theory, this in-state may be chosen. For instance, a simple pulse with a wide-rectangular shape would suffice. One may hope to create such a pulse microscopically, by going to the second quantised description and creating a coherent state. Alternatively, one may hope to realize a matrix quantum mechanics model that realizes a field theory in the limit of large number of particles. After all, we know that each oscillator in our model really corresponds to a partial wave and not a single particle in the four dimensional black hole picture.

SECOND QUANTIZATION V/S MATRIX QUANTUM MECHANICS: Given the quantum mechanical model we have studied in this chapter, we may naively promote the wave-functions ψ_{lm} into fields to obtain a second quantized Lagrangian:

$$\mathcal{L} = \sum_{l,m} \int_{-\infty}^{\infty} du^{\pm} \psi^{\dagger}_{lm}\left(u^{\pm},t\right)\left[i\partial_t + \frac{i}{2}\left(u^{\pm}\partial_{u^{\pm}} + \partial_{u^{\pm}}u^{\pm}\right) + \mu_l\right]\psi_{lm}(u^{\pm},t)\,. \tag{2.78}$$

With a change of variables to go to Rindler coordinates,

$$\psi^{(\text{in/out})}_{lm}(\alpha^{\pm},\rho^{\pm},t) \;=\; e^{\rho^{\pm}/2}\psi_{lm}(u^{\pm}=\alpha^{\pm}e^{\rho^{\pm}},t)\,, \tag{2.79}$$

the Lagrangian becomes relativistic

$$\mathcal{L} = \sum_{l,m}\int_{-\infty}^{\infty} d\rho^{\pm} \sum_{\alpha^{\pm}=1,2} \Psi^{\dagger(\text{in/out})}_{lm}\left(\alpha^{\pm},\rho^{\pm},t\right)\times \left(i\partial_t - i\partial_{\rho^{\pm}} + \mu_l\right)\Psi^{(\text{in/out})}_{lm}\left(\alpha^{\pm},\rho,t\right)\,, \tag{2.80}$$

where the label "in" (out) corresponds to the $+$ ($-$) sign. The form of the Lagrangian being first order in derivatives indicates that the Rindler fields are naturally fermionic. In this description we have a collection of different species of fermionic fields labelled by the $\{l,m\}$ indices. Possible interaction between different harmonics[9] would correspond to interacting fermions of the kind above. The conceptual trouble with this approach is that each "particle" to be promoted to a field is in reality a partial wave as can be seen from the four-dimensional picture. Therefore, second quantizing this model may not be straight-forward [56]. It appears to be more appealing to think of each partial wave as actually arising from an N-particle matrix quantum mechan-

9 Such interactions could be caused by transverse effects, though note that such effects are suppressed as $1/M_{Pl}$.

ics model which in the large-N limit yields a second quantized description. Since N counts the number of degrees of freedom, it is naturally related to c via

$$\frac{1}{N^2} \sim c = \frac{8\pi G}{R^2} \sim \frac{l_P^2}{R^2}\,. \tag{2.81}$$

Therefore, N appears to count the truly microscopic Planckian degrees of freedom that the black hole is composed of. The collection of partial waves describing the Schwarzschild black hole would then be a collection of such N-particle matrix quantum mechanics models. Another possibility is to describe the total system in terms of a single matrix model but including higher representations/non-singlet states to describe the higher l modes. This seems promising because if one fixes the ground state energy of the lowest $l = 0$ (or $l = 1$ after antipodal) oscillator, the higher l oscillators have missing poles in their density of states compared to the $l = 0$, much similar to what was found for the adjoint and higher representations in [93]. Finally we note that we can combine the chemical potential with the oscillator Hamiltonian to get

$$\hat{H}_{\text{tot}} = \sum_{l,m} \left[\frac{1}{2} \left(\hat{p}_{lm}^2 - \hat{x}_{lm}^2 \right) + \frac{R^2}{8\pi G} \left(\hat{L}^2 + 1 \right) \right] , \tag{2.82}$$

with $\hat{L}^2 = \sum_i \hat{L}_i^2$ giving the magnitude of angular momentum of each harmonic. One can then perform a matrix regularisation of the spherical harmonics following [94, 95] which replaces the spherical harmonics $Y_{lm}(\theta, \phi)$ with $N \times N$ matrices $\mathbb{Y}_{lm}$ where $l \leq N - 1$. This naturally sets a cut-off on the spherical harmonics from the onset. To sharpen any microscopic statements about the S-matrix, one might first need to derive an MQM model that regulates Planckian effects.

3

MATRIX QUANTUM MECHANICS ON $S^1/\mathbb{Z}_2$

Little is known in Quantum Gravity about how the space-like singularities in general, and cosmological singularities in particular, can be resolved—if they can be resolved at all. Some of the questions in this context are: is string theory able to provide consistent, non-singular dynamics around such singularities? What is the set of possible initial conditions for the cosmological evolution starting from a big-bang singularity? What are the possible initial wave-functions of the universe at the big-bang? How is the evolution of the universe determined following the big-bang, et cetera. Quantum gravity is, notoriously, a subject where problems vastly outnumber results especially for the physics near spacetime singularities. At short distances strong fluctuations of the metric are expected to cause a breakdown of classical geometry and the notion of space and time might lose their meaning and become emergent concepts of a more fundamental theory. Nevertheless, various efforts to understand the initial conditions of the Universe based on the semi-classical approximation to the path integral were made in the 80's, most notably the no-boundary proposal of Hartle and Hawking [96] and the tunnelling boundary condition of Linde and Vilenkin [97, 98] but it is fair to say we do not have a unique sensible answer to the aforementioned problems.

It is natural to ponder what string theory has to offer in this context, and whether it can resolve these problems or at least provide us with a new perspective. In string/M-theory these fundamental questions have been addressed in the various approximations and using various models in the past. Some notable work includes the study of time dependent orbifolds and the null-brane construction [99, 100, 101, 102, 103, 104, 105], the Bang-Crunch scenarios [106, 107, 108, 109, 110, 111, 112, 113], tachyon condensation [114, 115, 116], constructions attempting to address cosmological singularities via string theory [117, 118, 119, 120, 121, 122, 123], or via AdS/CFT [124, 125, 126, 127, 128, 129] and pre-Big Bang scenarios [130] among many others. For related work on string cosmology with a view towards inflation see [131, 132, 133].

Motivated by these difficult questions, we ask a more modest question in this chapter: What can string theory teach us about the cosmological singularities in the context of a toy model: the two dimensional non-critical string theory or $c = 1$ Liouville theory[1]) [134, 135]? The idea here is the following. Start with the *Euclidean* 2D non-critical string theory with Euclidean time direction, τ, compactified on a circle with radius R. This theory has a well-known dual formulation in terms of Matrix Quantum Mechanics (MQM) of a Hermitean $N \times N$ dimensional matrix M at finite tempera-

1 More precisely $c = 1$ Liouville theory is an exact CFT equivalent to 2D string theory in a linear dilaton and exponential tachyon background in the Liouville direction ϕ. The non-critical is an adjective referring to the number of dimensions.

ture $T = 1/2\pi R$ in a double scaling limit [136, 38, 83]. Now, consider a $\mathbb{Z}_2$ orbifold of the non-critical string theory (NCST) in the Euclidean time direction where one identifies $\tau \sim -\tau$. The following identifications

$$\tau \sim \tau + 2\pi R, \qquad \text{and} \qquad \tau \sim -\tau\,, \tag{3.1}$$

restrict the domain of the Euclidean time to the line segment $0 \leq \tau \leq \pi R$. Upon Wick rotating to Lorentzian time, the fixed points of the orbifold at the points $\tau = 0$ and $\tau = \pi R$ correspond respectively to the big-bang and big-crunch singularities of a toy, cosmological big-bang/big crunch universe in two dimensions. The questions posed above are expected to have a much simpler formulation in this toy universe, since the only non-trivial physical degrees of freedom in the bulk are a massless closed string "tachyon field" in case of the bosonic NCST with an additional RR scalar C_0 in case of supersymmetric type $0B$ NCST [137, 138, 139, 41, 140]. This is to be contrasted with the infinitely many physical excitations of the critical bosonic string in 26 dimensions and supersymmetric string in 10 dimensions. The 2D toy model also enjoys the following great advantage: Resolution of cosmological singularities in string theory is expected to involve not only the full set of corrections in the string length scale α' but also the perturbative corrections in the string coupling constant g_s [141][2]. This seems an insurmountable task for critical string theories (unless one attempts to use the BFSS [142] or related matrix model formulations, as in some of the references above). In the case of 2D NCST however, the dual formulation in terms of Hermitean MQM comes to the rescue. The partition function evaluated via MQM involves at least the full set of perturbative g_s corrections in the dual string theory and in addition a great deal is understood for non-perturbative corrections as well [143, 144, 145, 146].

The duality between 2D NCST and the Hermitean MQM was discovered back in the late 80s [147, 148, 149, 150]. Starting from a Lagrangian of the form

$$\mathcal{L} = \mathrm{tr}\left(\frac{1}{2}\left(\frac{\partial M}{\partial t}\right)^2 + \frac{1}{2\alpha'}M^2 - \frac{\kappa}{3!}M^3\right)\,, \tag{3.2}$$

one considers the web of Feynman diagrams of the matrix M that arise from the cubic interaction vertex. This web of Feynman diagrams then provides the dual lattice of the one obtained from triangulations of a string world-sheet a la 't Hooft [151]. As one increases the bare coupling κ one discovers that the average number of triangles on a given world-sheet begins to diverge at a critical value κ_c. Then, taking the double scaling limit $N \to \infty$, $\kappa \to \kappa_c$ with $N(\kappa_c^2 - \kappa^2)$ kept constant, one obtains a continuum formulation of the 2D string theory in terms of matrix quantum mechanics. The crucial point here is that a *universality* arises in this double scaling limit, that focuses on the tip of the potential provided by the mass term in (3.2). Therefore, the theory dual to the continuum limit of the 2D string theory is just described by Hermitean matrix quantum mechanics with the *inverse harmonic oscillator potential*. In

2 and possibly corrections non-perturbative in g_s.

this duality, the time direction in MQM provides the time direction for the 2D space-time where the string can propagate. In addition, the eigenvalues λ_i of the matrix M provide the extra space-like Liouville direction ϕ in the 2D string theory picture.

In some sense, this duality can be viewed as the oldest example of the open/closed dualities in string theory, much before the famous AdS/CFT correspondence in the case of critical IIB string theory [10]. The lessons learned from AdS/CFT, in particular the role of D-branes in this correspondence, ignited a revival of interest in the old matrix quantum mechanics in the oos. A gauge/gravity type of interpretation focusing on the target space physics arising from the matrix model has been proposed in [152, 153]. According to this picture, MQM describes the field theory living on N $D0$ branes, the ZZ branes found in [154], that sit at the strong coupling end of the Liouville theory. Furthermore, the $0B$ fermionic NCST also admits a non-perturbative formulation where the cubic potential in case of the bosonic NCST is simply replaced by a quartic potential. Therefore, unlike the bosonic theory, $0B$ fermionic NCST is believed to be non-perturbatively stable [41, 140]. One important insight that arises from the D-brane interpretation in the string/matrix duality is the need to introduce a non-dynamical[3] bulk gauge field $A_0(\tau)$ in the matrix path integral. Integration over this gauge field then projects to the singlet sector of the MQM. The gauged matrix model then captures the physics of the so-called linear dilaton background of the 2D string theory.

In this chapter, we consider a toy cosmological universe with a big bang/big crunch singularity in the context of bosonic and $0B$ NCST. As explained above, a natural model that is suitable for this purpose is a space-time where the (Euclidean) time direction is compactified and orbifolded as $S^1/\mathbb{Z}_2$ and coupled to the Liouville direction. If the Euclidean time direction in this model admits an analytic continuation into Lorentzian signature, one can interpret the orbifold singularities as cosmological singularities. One also hopes that information about the initial and final wavefunctions is encoded in the twisted sector of the orbifold that describes states localized at the orbifold fixed points. One can go further and also ask if one can compute the transition amplitude of the universe in this model.

We take the first step toward this aim in this chapter and focus on the calculation of the orbifolded matrix model partition function in *Euclidean* time using the machinery of matrix quantum mechanics. In particular, we show that

- the orbifold operation is represented in the matrix model by the operation $\mathrm{diag}(-1,-1,\cdots,-1,1,1,\cdots,1)\star$ where $\star$ acts on time as $\star t = -t\star$ and with n eigenvalues with the value -1 in the diagonal matrix. Hence, there are $n = 0,\cdots N/2$ distinct orbifold representations on the matrix model. In the T-dual D-instanton picture there are $N-2n$ fractional instantons that are stuck at the orbifold fixed points and n D-particles free to move along the t-directon. We argue that the correct choice corresponds to $n = N/2$, where there are no fractional instantons.

3 This gauge field is necessarily non-dynamical in two dimensions.

- Using the matrix model techniques we calculate the torus partition function in the large R limit for the $n = 0$ and $n = N/2$ representations, especially the twisted state contribution to it, and show that the $n = N/2$ representation matches precisely the result obtained from the world-sheet CFT. This provides a non-trivial check of the equivalence we propose between the orbifold MQM and the orbifold 2D non-critical string theory.

- The calculation of the full orbifold partition function in the canonical ensemble in the large-N limit proves hard. However, we manage to represent the grand-canonical partition function in terms of an integral kernel whose spectrum gives the single-particle density of states. We obtain this density by two independent methods that agree with each other.

- We further discuss certain aspects of this matrix model in connection with the corresponding 2D string theory. Finally we make various comments on how to implement the Wick rotation of the Euclidean time orbifold partition function to Lorentzian signature. We leave the full Lorentzian space-time interpretation of the possible initial and final boundary conditions at the cosmological singularities and a more thorough study of the semi-classical geometry that the matrix model describes, to future work.

The organization of the chapter is as follows. In the next section we first outline the necessary material on the orbifold $c = 1$ Liouville theory. In particular we present the torus partition function of the bosonic, super-affine $0B$ and $0A$ NCSTs including the contribution from the twisted sectors. This is achieved by considering the possible $\mathbb{Z}_2$ orbifolds of these theories and using self consistency CFT techniques that relate the orbifold with the circle CFT at different multiples of the self-dual radius. In this section, we also introduce some more details of Matrix Quantum Mechanics in 3.1.3 and set up our conventions. Finally in section 3.1.4 we make use of the $D0$ brane picture to determine the boundary conditions of the partition function of the dual MQM, in particular we obtain the boundary conditions for the matrix M and the gauge field A consistent with the orbifold projection. Interestingly, we find different representations of the projection classified by an integer[4] $0 \leq n \leq N/2$. Different representations are found to be related via the action of a certain kind of "loop-operator" at the end-points in 3.2.1.3. In section 3.2, we also compute the canonical (finite N) partition function by representing it as a path integral over the eigenvalues of M. In addition we find that this partition function admits a natural continuation into Lorentzian signature, hence provides a possible connection to the cosmological toy universe. In particular it has a nice structure from which the initial and final wavefunctions and the transition amplitude of the toy cosmological space-time can be read off. These wavefunctions are expressed in terms of determinants of eigenvalues of M at $t = 0$ and $t = T$. We further argue that the regular $n = N/2$ representation is the one expected to be dual to the orbifold in section 3.2.1.6. Moreover in section 3.2.2 we provide a dual description in terms of an angular integral

4 This possibility was observed earlier in the unpublished work [155].

with the angles corresponding to the zero modes of the gauge field A.
Section 3.3 is devoted to the computation of the MQM grand partition function for the "regular" $n = N/2$ and $n = 0$ representations. The grand canonical partition function is helpful in taking the double scaling limit [93], hence connecting the MQM partition function to the genus expansion of the dual string theory. This section contains one of our main findings: here we show that the calculation of the grand canonical partition reduces to the computation of the spectrum of an integral kernel which we express in various useful forms. The equations that determine the spectrum of this kernel can be expressed as integral equations. By deforming the contour of integration in these integral equations, we identify contributions to the untwisted and twisted sectors in the free energy of the orbifolded 2D NCST.
It proves hard to evaluate and express these contributions in terms of the dual string theory quantities in the double scaling limit. In section 3.3.2.3 we perform a partial matching of the various expressions for the kernel by computing its trace, from which we can read-off the one-particle density of states that we express as a sum of the usual harmonic oscillator density of states including a twisted state contribution. Finally in section 3.4 and in appendix A.7 we attempt to compute the twisted states at the orbifold end-points by performing a large radius expansion of the canonical partition function. We manage to do this precisely for the $n = 0$ representation and the "regular" $n = N/2$ representation. We discover then that we can perform an exact matching with the torus contribution to twisted states computed in Liouville. The main finding of our work is that the twisted state contribution in the scaling limit involves a Fredholm determinant of the *sine-kernel* which expresses the probability that all the energy eigenvalues taken from a random Hermitian Hamiltonian lie outside the interval $[-\mu, 0]$ and thus form the fermi sea. This is also called the level spacing distribution $E_2(0, \mu)$ in the random matrix theory parlance. The initial and final wavefunctions take the form of "square-roots" of this distribution.
Throughout the text, we discuss similarities and differences with established results in the literature such as the circle and the 2D black hole [136, 156]. We also discuss the possibility of realising the grand canonical partition function as a τ function of an integrable hierarchy with a Pfaffian structure. Finally, in section 3.5 we conclude with what is achieved and provide a look ahead. Several appendices contain the details of our calculations.

3.1 THE SETUP

3.1.1 $c = 1$ *Liouville Theory on* $S^1/\mathbb{Z}_2$

One computes the orbifold partition function at the torus level in string theory as folllows. Let us call the bosonic matter field[5] X restricted to the line segment $-\pi R \leq X < \pi R$ and obeying the following identifications under translation and reflection

$$X \approx X + 2\pi R \;\; \textit{and} \;\; X \approx -X\,. \tag{3.3}$$

5 This field corresponds to the Euclidean time τ in the previous section.

The modular partition function of the theory is (see for example [157])

$$Z_{orb}(R,z) = \frac{1}{2}\left\{Z_{circle}(R,z) + \frac{|\theta_2(z)\theta_3(z)|}{|\eta(z)|^2} + \frac{|\theta_2(z)\theta_4(z)|}{|\eta(z)|^2} + \frac{|\theta_3(z)\theta_4(z)|}{|\eta(z)|^2}\right\}, \quad (3.4)$$

where $Z_{circle}(R,z)$ is the modular partition function for the circle, $\eta(z)$ is the Dedekind η function, θ's are the elliptic functions, R is the radius of the circle and z is the coordinate on the torus. The fist term in (3.4) gives the contribution from the untwisted states and equals half the partition function of the circle. The contribution from the twisted states is given by the R independent part. To obtain the full torus partition function on the orbifold one should couple the ghost and the Liouville modes to (3.4) and integrate over the moduli z

$$\mathcal{Z}_{orb}(R) = -V_\phi \int_{\mathcal{F}} d^2z \left(\frac{|\eta(z)|^4}{2z_2}\right)\left(2\pi\sqrt{z_2}|\eta(z)|^2\right)^{-1} Z_{orb}(R,z)\,, \quad (3.5)$$

where the integral is over the fundamental domain $\mathcal{F}$, the first term in the integrand is the contribution from the ghost sector and the second the contribution from the Liouville modes. V_ϕ is the contribution from the Liouville zero mode, shown to be proportional to the renormalised volume in the Liouville direction $\log\mu_0$ with μ_0 the renormalised string coupling [158]. Upon performing the integral over z one finds the following answer

$$\mathcal{Z}_{orb}(R) = \frac{1}{2}\mathcal{Z}_{circle}(R) + c, \quad (3.6)$$

where c is independent of R and $\mathcal{Z}_{circle}(R)$ is the partition function of the circle coupled to the Liouville mode computed by the worldsheet methods in [158]

$$\mathcal{Z}_{circle}(R) = -\frac{1}{24}\left(R + \frac{1}{R}\right)\ln(\mu_0)\,. \quad (3.7)$$

To determine the constant c for the orbifold partition function one may use the relation between the circle and the orbifold at the self-dual radius [159]:

$$Z_{orb}(R=1,z) = Z_{circle}(R=2,z)\,. \quad (3.8)$$

Then substituting in (3.8) to (3.5) and combining them with (3.7), one finds the final result:

$$\mathcal{Z}_{orb}(R) = -\frac{1}{48}\left(R + \frac{1}{R}\right)\ln(\mu_0) - \frac{1}{16}\ln(\mu_0)\,. \quad (3.9)$$

3.1.2 *Fermionic orbifold theories*

The classification of $\hat{c} = 1$ CFTs has been performed in [160][161]. According to this classification, the continuous lines of theories include two lines of "circular" theories and various orbifolds of these theories. The "circular" theories consist of the circle CFT and a super-affine CFT. The coupling of these "circular" theories to super-Liouville is discussed in [41]. We summarize their results:

- **Circle CFTs**: The usual fermionic circle theory (compact X + Ising) gives rise to two theories when coupled to super-Liouville: $0A$ and $0B$ depending on the GSO projection. Their partition functions are:

$$\begin{aligned} \mathcal{Z}_{cirA}(R) &= -\frac{1}{12\sqrt{2}} \ln \mu_0 \left(2R + \frac{1}{R}\right), \\ \mathcal{Z}_{cirB}(R) &= -\frac{1}{12\sqrt{2}} \ln \mu_0 \left(R + \frac{2}{R}\right). \end{aligned} \tag{3.10}$$

  These theories are interchanged under the T-duality: $R \to 1/R$. At the special radius, $R = 1$ there is enhanced $SU(2) \times SU(2)$ symmetry.

- **Super-Affine CFTs**: The usual super-affine theory is obtained by modding out the usual fermionic circle theory by the following Z_2:

$$(-1)^{F_s} e^{2ip\delta}, \tag{3.11}$$

  where $(-1)^{F_s}$ is defined as $+1$ on the antiperiodic fermions and -1 on the periodic ones. $e^{2ip\delta}$ is a shift operator that shifts by a unit vector on the self-dual lattice. When Coupled to super-Liouville one again obtains two theories: Super-Affine A and Super-Affine B theories with the following partition functions:

$$\begin{aligned} \mathcal{Z}_{cirA}(R) &= -\frac{1}{12} \ln \mu_0 \left(\frac{R}{\sqrt{2}} + \frac{\sqrt{2}}{R}\right), \\ \mathcal{Z}_{cirB}(R) &= -\frac{1}{24} \ln \mu_0 \left(\frac{R}{\sqrt{2}} + \frac{\sqrt{2}}{R}\right). \end{aligned} \tag{3.12}$$

  These theories are both self-dual under $R \to 2/R$. At the self-dual radius $R = \sqrt{2}$, there is an enhanced $SO(3)^2$ symmetry.

Apart from the type o theories, there are other "circular" $\hat{c} = 1$ theories with type I GSO projections. These have been classified in [162]. In addition to the "circular" $\hat{c} = 1$ theories, there are three families of orbifold CFTs [160][161]. Here we are interested in the $0B$ orbifold:

- **Orbifold I**: The first class of orbifolds is obtained by modding out circular theories by:

$$R: \quad X \to -X, \qquad \Psi \to -\Psi. \tag{3.13}$$

  Both the left and right handed fermions on the world-sheet are transformed in order to preserve world-sheet supersymmetry. R as defined above is a symmetry of only the $0B$ theory since in the $0A$ theory states in the Ramond sector have odd fermion number. Therefore one obtains only one orbifold CFT by twisting the $0B$ theory by R. The partition function is obtained by noting the

following two relations [160] which continue to hold after coupling to super-Liouville:

$$\mathcal{Z}_{orbI}(R) = \frac{1}{2}\mathcal{Z}_{cirB}(R) + const, \tag{3.14}$$

and

$$\mathcal{Z}_{orbB}(1) = \mathcal{Z}_{cirB}(2),. \tag{3.15}$$

The result is:

$$\mathcal{Z}_{orbI}(R) = \frac{1}{2}\mathcal{Z}_{cirB}(R) - \frac{1}{8\sqrt{2}}\ln\mu_0\,. \tag{3.16}$$

This orbifold theory is the one that we shall be interested in constructing the matrix model dual.

We also find two other continuous families of orbifold theories, discuss them and present their torus level partition functions in appendix A.1.

3.1.3 *Matrix Quantum Mechanics*

We now provide a very short review of Matrix Quantum Mechanics (MQM). For more details the reader can consult existing reviews in the literature, for example [83, 38, 163]. Gauged MQM is a $0+1$ dimensional quantum mechanical theory of $N\times N$ Hermitian matrices denoted by $M(t)$ and a non dynamical gauge field $A(t)$. The gauge field acts as a Lagrange multiplier and projects onto the singlet representation of the $U(N)$ gauge group. The path integral is defined as (we work in units where $\alpha' = 1$):

$$\begin{aligned}\langle out|in\rangle \quad &= \quad \int \mathcal{D}M(t)\mathcal{D}A(t) \\ &\exp\left[iN\int_{t_{in}}^{t_f} dt\mathrm{Tr}\left(\frac{1}{2}\left(D_t M\right)^2 + \frac{1}{2}M^2 - \frac{\kappa}{3!\sqrt{N}}M^3\right)\right],\end{aligned} \tag{3.17}$$

where $D_t = \partial_t + [A, M]$. This model has a $U(N)$ gauge symmetry. One can diagonalise M by a unitary transformation $M(t) = U(t)\Lambda(t)U^\dagger(t)$ where $\Lambda(t)$ is diagonal and $U(t)$ unitary. One then picks up a Jacobian from the path integral measure for every t

$$\mathcal{D}M = \mathcal{D}U_{Haar}\prod_{i=1}^{N} d\lambda_i \Delta^2(\Lambda), \quad \Delta(\Lambda) = \prod_{i<j}(\lambda_i - \lambda_j). \tag{3.18}$$

This Vandermonde determinant is responsible for many interesting properties of matrix models in general and for MQM it leads to a natural description in terms of fermionic wave-functions. In particular, after projecting to the singlet sector, the

Hamiltonian is found to act on the fermionic wavefunctions $\tilde{\Psi} = \Delta(\lambda)\Psi(\lambda)$ as

$$\left(-\frac{1}{2}\frac{d^2}{d\lambda_i^2} - \tfrac{1}{2}\lambda_i^2 + \frac{\sqrt{\hbar}}{3!}\lambda_i^3\right)\tilde{\Psi}(\lambda) = \hbar^{-1}E\tilde{\Psi}(\lambda), \quad \hbar^{-1} = \frac{N}{\kappa^2}, \tag{3.19}$$

and describes N non interacting fermions in the cubic potential $V(\lambda)$.

To connect this model with 2D string theory one needs to send $N \to \infty$ and tune the cubic potential to a critical value $\kappa \to \kappa_c$, just before the system becomes unstable[6]. The double scaling limit is most easily performed by introducing a chemical potential μ to fill up the fermi-sea. Schematically this goes as follows: One sends $\mu, \hbar \to 0$, while keeping $\frac{\mu}{\hbar} = g_{st}^{-1}$ fixed. A careful treatment will be provided in sections 3.4 and A.7.4. Tuning the system near the critical point is responsible for producing smooth surfaces out of the matrices [83]. In this limit only the local maximum of the potential becomes relevant and the model thus becomes solvable, described in terms of N free fermions in an inverse harmonic oscillator potential. Let us also mention that in the more modern target space approach, MQM is considered as the zero dimensional field theory living on the world volume of N unstable ZZ $D0$- branes and the matrix field $M(t)$ is interpreted as the open string tachyon field [152].

3.1.4 *Orbifolding in the Matrix Model Picture*

We now consider implementation of the orbifolding procedure in MQM[7], that corresponds to the circle orbifolding we discussed in the string theory picture above. The orbifolding procedure is very similar to the one presented in [164]. We start from the Euclidean Partition function on S^1 (the radius is defined via $\beta_c = 2\beta = 2\pi R$) with the following action:

$$S = \int_{-\beta}^{\beta} d\tau \ \mathrm{tr}\left(\frac{1}{2}(D_\tau M)^2 + \omega^2 M^2\right), \tag{3.20}$$

where τ is the Euclidean time variable, $\beta = \pi R$, and the covariant derivative with respect to the gauge group is $D_\tau M = \partial_\tau M - i[A, M]$. Here, anticipating the large N limit in (3.17) we have dropped the interaction term in (3.17) and we have allowed for a more general mass term ω. For real values of ω this action corresponds to the normal harmonic oscillator potential—the inverted one can be obtained upon the analytic continuation $\omega \to i\omega$.
The action (3.20) is invariant under the $U(N)$ gauge transformations:

$$\begin{aligned} M(\tau) &\to U(\tau) M(\tau) U^\dagger(\tau), \\ A(\tau) &\to U(\tau) A(\tau) U^\dagger(\tau) + iU(\tau)\partial_\tau U^\dagger(\tau). \end{aligned} \tag{3.21}$$

6 This cubic potential is always non-perturbatively unstable, but the supersymmetric version of the model ($0B$) has a quartic stable potential and is thus non-perturbatively well defined.

7 This procedure has been worked out in [155].

The theory also has a $\mathbb{Z}_2$ symmetry corresponding to

$$\tau \to -\tau, \qquad M(\tau) \to M(-\tau), \qquad A(\tau) \to -A(-\tau). \tag{3.22}$$

One can gauge this symmetry by projecting to the invariant states. We will use a more general gauging, by combining the reflection symmetry with a $\mathbb{Z}_2$ subgroup of the $U(N)$ gauge group (see also [164]). We define (up to a change of basis- note also that Ω is defined up to a minus sign)

$$\Omega = \begin{pmatrix} -1_{n\times n} & 0 \\ 0 & 1_{(N-n)\times(N-n)} \end{pmatrix} *, \tag{3.23}$$

with $*f(\tau) = f(-\tau)*$, $*\partial_\tau = -\partial_\tau *$, $0 \le n \le \frac{N}{2}$, and then require:

$$\Omega A(\tau)\Omega^{-1} = -A(\tau) + 2n_i\beta\delta_{ij}, \quad \Omega M(\tau)\Omega^{-1} = M(\tau). \tag{3.24}$$

with $n_i \in \mathbb{Z}$ which is allowed since the eigenvalues of A are periodic variables with period β. This term turns out to be unimportant since it can be gauged-away. This procedure naturally splits the matrices into (even/odd) blocks that need to satisfy different boundary conditions. We get

$$M(\tau) = \begin{pmatrix} M_1(\tau) & \Phi(\tau) \\ \Phi^\dagger(\tau) & M_2(\tau) \end{pmatrix}, \quad A(\tau) = \begin{pmatrix} A_1(\tau) & B(\tau) \\ B^\dagger(\tau) & A_2(\tau) \end{pmatrix}. \tag{3.25}$$

One immediately sees that the $n \times n$ M_1, A_1 and the $(N-n)\times(N-n)$ M_2, A_2 matrices should be Hermitian while the $n \times (N-n)$ Φ, B are complex. In addition, consistency with 3.23, 3.24 requires that M_1, M_2, B are even while A_1, A_2, Φ are odd functions of τ. From the gauge transformations (3.21) the ones that are consistent with the action of Ω are

$$U(\tau) = \begin{pmatrix} V_1(\tau) & W_1(\tau) \\ W_2(\tau) & V_2(\tau) \end{pmatrix}, \tag{3.26}$$

with V_1, V_2 even and W_1, W_2 odd.
After orbifolding the fundamental domain is $0 \le \tau \le \beta$. In the bulk of the domain the theory is as before. The changes come from demanding different boundary conditions for the fields in (3.25) imposed at the fixed points $0, \beta$ due to their symmetry. In particular we need to demand

$$A_1(0) = A_2(0) = \Phi(0) = 0 = A_1(\beta) = A_2(\beta) = \Phi(\beta) \tag{3.27}$$

The $U(N)$ gauge group gets broken to $U(n) \times U(N-n)$ at the boundaries, and as we will see the initial and final wavefunctions contain two separate sets of n and $N-n$ fermions. This breaking also means that the zero-modes of A come solely from the off-diagonal elements B.

The two most special cases are[8] $n = 0$ and $n = N/2$. The first is the simplest case where there exist no zero modes of the gauge field, while the second describes the so-called "regular" representation of the orbifold which is expected to give the Matrix Model dual to the orbifold Liouville theory. Further reasoning for why $n = N/2$ is expected to be the correct representation, based on ideas related to deconstruction, is discussed in section 3.2.1.6.

Representations with different n correspond to adding fractional D-instantons at the fixed points. This becomes clear in the T-dual picture. In particular, upon T-dualizing the Euclidean circle to a radius $1/R$ and then orbifolding, the original D_0 branes become D-instantons whose position on the dual circle is governed by the zero mode of the gauge-field. This means that for $n = 0$, $A(\tau) = n_i \frac{\pi}{R}\delta_{ij}$, $n_i \in \mathbb{Z}$ and all the instantons are stuck at the fixed points $0, \pi/R$. For the generic n representation, one has n-zero modes with arbitrary angle in the T-dual circle and thus the configuration contains n-physical instantons at angles θ_i together with $N - 2n$ stuck at the fixed points. This makes clear that the regular $n = N/2$ representation has only physical instantons in the T-dual picture. More discussion about how to connect different representations will follow in section 3.2.1.3.

3.2 THE CANONICAL PARTITION FUNCTION

The partition function for a generic n representation of the orbifold is then obtained by integrating over the non-vanishing components of the matrices M and A in (3.25) at the initial and final points—that are the even components M_1, M_2 and B at $\tau = 0$ and $\tau = \beta$, and performing the path integral of the full matrices between these points. Thus, for a generic n-representation we have,

$$\mathcal{Z} = \int \mathcal{D}B(0)\mathcal{D}B(\beta)\mathcal{D}M_{1,2}(0)\mathcal{D}M_{1,2}(0)\int_{A(0)}^{A(\beta)}\mathcal{D}A(\tau)\int_{M(0)}^{M(\beta)}\mathcal{D}M(\tau)e^{-S}\,. \tag{3.28}$$

The next step is to reduce this matrix integral to an integral over eigenvalues. One can show that

$$\int_{M(0)}^{M'(\beta)}\mathcal{D}A\mathcal{D}M e^{-\int_0^\beta d\tau \mathrm{Tr}\frac{1}{2}(D_\tau M)^2+\frac{1}{2}\omega M^2} = \int_{U(N)}\mathcal{D}U\langle UM'U^\dagger,\beta|M,0\rangle\,. \tag{3.29}$$

In our case the propagator is the (Euclidean) propagator for a matrix harmonic oscillator given by

$$\langle M',\beta|M,0\rangle = \left(\frac{\omega}{2\pi\sinh\omega\beta}\right)^{N^2/2}\exp\left(-\frac{\omega}{2\sinh\omega\beta}\left[(\mathrm{Tr}M^2+\mathrm{Tr}M'^2)\cosh\omega\beta - 2\mathrm{Tr}MM'\right]\right) \tag{3.30}$$

These two equations can be combined beautifully using the Harish-Chandra-Itzykson-Zuber integral

$$\int_{U(N)} DU \exp\left(g\mathrm{Tr}MUM'U^\dagger\right) = \prod_{p=1}^{N-1}(p!)\,g^{-\frac{1}{2}N(N-1)}\frac{\det e^{g\lambda_i\lambda'_j}}{\Delta(\lambda)\Delta(\lambda')} \tag{3.31}$$

8 From now on we assume even N.

that will allow us to reduce the integral to eigenvalues. This is possible since the only term that couples different matrices in the propagator is precisely of the form that can be reduced to eigenvalues via the HCIZ formula.

Before moving on, let us note the following two options: we can either first diagonalise M and then integrate over U using the HCIZ formula or first diagonalise U and then integrate over M. In the orbifold case one also needs to take care about the orbifold projection which is implemented through the block structure of the matrices. In the next section, we will follow the first procedure and compare the results for the circle and orbifold. In section 3.2.2 we will follow the second and in section 3.3.2.3 we will perform a matching between the two methods.

3.2.1 *Partition function in terms of eigenvalues*

To set up our notation, we define $K^E(\lambda_i, \lambda'_j; \beta) = \langle \lambda'_j, \beta | \lambda_i, 0 \rangle$ the Euclidean oscillator propagator as follows

$$\begin{aligned} K^E(\lambda_i, \lambda'_j; \beta) &= \left[\frac{\omega}{2\pi \sinh \omega\beta}\right]^{\frac{1}{2}} \exp\left(-\frac{\omega \cosh \omega\beta}{2 \sinh \omega\beta}\left(\lambda_i^2 + \lambda_j'^2\right) + \frac{\omega \lambda_i \lambda'_j}{\sinh \omega\beta}\right) \\ &= \sum_n \psi_n(\lambda_i)\psi_n(\lambda'_j) q^{n+\frac{1}{2}}, \end{aligned} \tag{3.32}$$

where the second spectral representation is also known as Mehler's formula. In this representation $q = e^{-\omega\beta}$ and $\psi_n(\lambda_i)$ are the Hermite functions. Note that upon analytic continuation $\omega \to i\omega$ the Hermite functions turn into parabolic cylinder functions
$D_\nu(z)$ defined for complex ν, z see Appendix A.2. One can also resolve the inverted oscillator propagator in terms of parabolic cylinder functions from the start [165], the relevant formula is presented in Appendix A.2.3. As we discuss below the possibility of analytically continuing the propagator in the parameters ω, β is the reason we expect to obtain the Lorentzian transition amplitude in this 2D toy universe directly from the Euclidean description.

3.2.1.1 *The circle*

We first review the case of circle [136, 93]. For this partition function on S^1 we just have to demand periodic boundary conditions ($M'(\beta_c) = M(0)$, $\beta_c = 2\beta$)

$$\mathcal{Z}_N = \int \mathcal{D}M(0)\mathcal{D}U_1 \langle U_1 M(0) U_1^\dagger | M(0) \rangle = \frac{1}{N!} \int \prod_{i=1}^N d\lambda_i \det K^E(\lambda_i, \lambda_j), \tag{3.33}$$

where we diagonalised $M(0) = U_2 \Lambda U_2^\dagger$ and integrated over the matrix $U = U_1 U_2^\dagger$. The $\Delta^2(\Lambda)$ in the numerator from the measure of M, canceled the similar term produced by the HCIZ formula. The term $\prod_{p=0}^{N-1} p!$ in the HCIZ formula got canceled by the second integration over the gauge group which is $\int \mathcal{D}U_{Haar} = \frac{\pi^{N(N-1)/2}}{\prod_{p=0}^N p!}$. In

the end the $1/N!$ term is due to the left-over permutation (Weyl) symmetry between the eigenvalues. For more details on factors of N for this and more general cases see [166].
The result is the partition function of N free fermions in the harmonic oscillator potential:

$$\mathcal{Z}_N = \frac{q^{\frac{N^2}{2}}}{\prod_{k=1}^{N}(1-q^k)}, \tag{3.34}$$

with $q = e^{-\omega\beta_c}$. One can also expand this result for large β_c and recover the zero temperature free energy

$$\mathcal{F} = \beta_c\,\omega\,\frac{N^2}{2} = \beta_c E_0 + O(e^{-\omega\beta_c}), \tag{3.35}$$

where $E_0 = \sum_{k=0}^{N-1}\omega(k+\frac{1}{2})$ the vacuum energy of the system of N fermions. In constrast, in the orbifold case at least for the torus contribution we expect a subleading β independent term due to the presence of twisted states since these are localised at the end-points.

3.2.1.2 *The orbifold partition function for generic n*

The orbifold partition function for generic n after we integrate over the propagation becomes

$$\mathcal{Z}_{n,N-n} = \int \mathcal{D}M\mathcal{D}M'\mathcal{D}U\langle UM'U^\dagger,\beta|M,0\rangle, \tag{3.36}$$

with

$$M = \begin{pmatrix} M_1^{(n\times n)} & 0 \\ 0 & M_2^{(N-n)\times(N-n)} \end{pmatrix}, \qquad \mathcal{D}M = \mathcal{D}M_1\mathcal{D}M_2 \tag{3.37}$$

and similarly for M'. We now use the HCIZ formula to evaluate the integral over the unitary matrix U. If we define the eigenvalues of $M_{1,2}$ as x_i, y_i respectively, $\prod_{i=1}^{n} dx_i/n! \equiv d^n x$ and similarly for y, the result is found to be

$$\begin{aligned}\mathcal{Z}_{n,N-n} &= C_{N,n}\int d^n x d^{N-n} y d^n x' d^{N-n} y' \\ &\quad \frac{\Delta_n(x)\Delta_{N-n}(y)}{\Delta_{n,N-n}(x,y)}\det K(\bar{x}_i;\bar{x}'_j)\frac{\Delta_n(x')\Delta_{N-n}(y')}{\Delta_{n,N-n}(x',y')},\end{aligned} \tag{3.38}$$

with

$$\Delta_{n,N-n}(x,y) = \prod_{i=1}^{n}\prod_{j=1}^{N-n}(x_i - y_j)\,. \tag{3.39}$$

First of all we make the following crucial observation: the form of this Euclidean partition functions in (3.28) and (3.38) are appropriate for analytic continuation into the

Lorentzian time. The analytic continuation is obtained simply by changing $\beta = iT$ in the propagator. Therefore, after the analytic continuation we can simply interpret these Lorentzian partition functions as transition amplitudes from an initial state of the universe at $t = 0$ to a final state at $t = T$

$$\langle \psi_f, T|\psi_i 0\rangle = \int D\bar{x} D\bar{x}' \psi_f^*(\bar{x}') \det K^L(\bar{x}, \bar{x}'; T)\psi_i(\bar{x}) , \tag{3.40}$$

where we introduced the compact notation $\bar{x} = (x, y)$. Here the initial and final wave-functions in this toy universe are of the form

$$\psi_i(\bar{x}) = \psi_f(\bar{x}) = \frac{\Delta_n(x)\Delta_{N-n}(y)}{\Delta_{n,N-n}(x,y)} . \tag{3.41}$$

One can rewrite these wavefunctions in the form $\prod_{i,j}(\lambda_i - \lambda_j)^{q_i q_j}$ in terms of fermions having positive ($q_i = +1\,, 1 \leq i \leq n$) and negative ($q_i = -1\,, n+1 \leq i \leq N$) charge (or spin), with same charge fermions "feeling" repulsion and opposite ones attraction. They represent a Coulomb-gas in one dimension. From this point of view, the representation $n = N/2$ is the only one satisfying charge neutrality. Wavefunctions of this form first arised in studies of Quiver Matrix Models [167, 168, 169][9]. Then they reappeared in connection to the description of effective IR superpotentials of $\mathcal{N} = 1$ gauge theories and in studies of supermatrix models (see [170, 171, 172] and references within). If one replaces rational with hyperbolic functions, a similar ratio can also be found in studies of superconformal Chern-Simons theories of Affine $\hat{D}$-type, at the quiver end-nodes [173]. Finally there is recent interest in these wavefunctions [174] in the context of non-Unitary holography.

3.2.1.3 *Changing representations via Loop operators*

One can connect different n representations by inserting operators in the end-points of the path integral of the form $\prod_j (x - y_j)^2$ or $\prod_j 1/(x - y_j)^2$ to lower/raise the value of n. This form of operators is known as loop operators. We first define the loop operator that creates macroscopic holes/boundaries on the worldsheet (this means the string gets attached to a D-brane, the so called FZZT brane) in matrix model language [175, 163, 39, 176, 177]:

$$W(x) = \frac{1}{N} \operatorname{tr} \log(x - M) . \tag{3.42}$$

The function that creates a coherent state of them is:

$$e^{NW(x)} = \det(x - M) = \prod_j^N (x - \lambda_j) . \tag{3.43}$$

In these equations x can be thought of as a chemical potential μ_B (or a boundary cosmological constant). For $c < 1$ theories these operators have been thoroughly

9 In some of these studies the divergence coming from the denominator is avoided, since it has the form $x_i + y_j$ with the variables restricted to be positive. We will regulate this divergence taking the principal value in section 3.3.2.

studied from the matrix model point of view in [176, 177]. The relevant branes are the FZZT branes which extend along the Liouville direction. In our case let us take as an example the operator that transforms the generic n to the $n = 0$ representation

$$\prod_{i}^{n}\prod_{j}^{N-n}(x_i - y_j)^2 = \det\left(M_1 \otimes \mathbb{1}_{N-n\times N-n} - \mathbb{1}_{n\times n}\otimes M_2\right)^2, \tag{3.44}$$

where the determinant is in the tensor product space. Similarly one can transform the generic n representation to the $n = N/2$ by an inverse determinant of the same form. From this expression, it is easy to see that the eigenvalues of M_1 act as chemical potentials for the eigenvalues of M_2 and vice versa and have to be integrated over (they do not represent external parameters as in the familiar computations that involve FZZT branes). The open strings are the ones stretched between the two sets of n and $N-n$ $D0$ branes which can be thought to separate at the end-points due to the breaking $U(N) \to U(n)\times U(N-n)$. Using a Miwa-style representation [178], the authors of [179] found that in the case of the Normal matrix model, these determinants/inverse determinants decrease/increase the closed string tachyon coupling thus deforming the closed string background. Therefore there exist two complementary ways to understand these operators (open/closed duality). In our case let us note that similarly we can write

$$\begin{aligned}&\det\left(M_1 \otimes \mathbb{1}_{N-n\times N-n} - \mathbb{1}_{n\times n}\otimes M_2\right)^2 = \\ &e^{\left[(N-n)\,\mathrm{tr}\log M_1 + n\,\mathrm{tr}\log M_2 - \sum_{k=1}^{\infty} t_k M_2^k - \sum_{k=1}^{\infty}\bar{t}_k M_1^k\right]}\end{aligned} \tag{3.45}$$

where we chose to expand each determinant factor in a different way and $t_k = \mathrm{tr}(M_1^{-k})/k$, $\bar{t}_k = \mathrm{tr}(M_2^{-k})/k$. These are the closed string tachyon couplings in Miwa variables. The logarithmic terms in the exponent appear in versions of the Penner model, for more details one can consult [180]. This description makes clear that there is a backreaction effect where M_1 deforms the closed string background of M_2 and vice versa.

One might furthermore try to use grassmannian/fermionic variables to exponentiate these factors [176, 177]. In particular we get

$$\det\left(M_1 \otimes \mathbb{1}_{N-n\times N-n} - \mathbb{1}_{n\times n}\otimes M_2\right) = \int d\chi^\dagger d\chi e^{\chi^\dagger(M_1\otimes\mathbb{1}_{N-n\times N-n} - \mathbb{1}_{n\times n}\otimes M_2)\chi}, \tag{3.46}$$

with $\chi_{\alpha j}, \chi^\dagger_{\alpha j}$ fermions transforming in the bifundamental representation of $U(n)\times U(N-n)$[10] that exist only at the orbifold endpoints. One can also endow these fermions with a kinetic term (dynamic-loops on the worldsheet) as in [181] that would correspond to the T-dual picture (Neumann conditions for open strings). This construction also indicates that determinants correspond to fermionic open strings streched between the branes, while inverse determinants to bosonic open strings [176,

10 Integrating-in fundamental fermions had been already used in the context of $c = 1$ open string theory in [181].

177, 179]. It would be very interesting to study further our model from this point of view and connect it with various ideas related to FZZT branes in the existing literature and possibly understand non-perturbative effects as well.

3.2.1.4 *The $n = 0$ case*

This is the simplest case, where the zero modes of the gauge field vanish. The line segment partition function for $n = 0$ has a structure similar to the two-matrix model [182, 183].

$$\mathcal{Z}_{0,N} = \int \mathcal{D}M\mathcal{D}M' \langle M', \beta | M, 0\rangle = C_N \int \prod_{i=1}^{N} d\lambda_i d\lambda_i' \Delta(\lambda') \det_{i,j} K^E(\lambda_i; \lambda_j') \Delta(\lambda), \tag{3.47}$$

with C_N a constant. One can also compute the canonical partition in this case using the methods in the appendix of [182] or by direct Gaussian integration to find

$$\mathcal{Z}_{0,N} = \left(\frac{2\pi}{\omega \sinh \omega\beta} \right)^{N^2/2}. \tag{3.48}$$

Defining the partition function of a single harmonic oscillator with open boundary conditions [184]

$$\mathcal{Z}_1^{op} = \int_{-\infty}^{\infty} dx dx' \langle x | x' \rangle = \left(\frac{2\pi}{\omega \sinh \omega\beta} \right)^{\frac{1}{2}}, \tag{3.49}$$

one finds that the $n = 0$ partition function is just N^2 copies of the single particle one

$$\mathcal{Z}_{0,N} = \left(\mathcal{Z}_1^{op} \right)^{N^2}. \tag{3.50}$$

For large $\beta = \beta_c/2$ one again obtains

$$\mathcal{F}_{0,N} = \tfrac{1}{2}\beta_c E_0 + \frac{N^2}{2} \log C + O(e^{-\omega\beta_c}), \tag{3.51}$$

with the β independent term depending on the normalization of the partition function. We evaluate this β-independent term from the canonical partition function in an unambiguous manner in section 3.4 and try to directly perform the double scaling limit.

3.2.1.5 *The $n = N/2$ Case*

As we discussed, the regular $n = N/2$ case is special and expected to be the correct dual of the 2D string theory on the orbifold, see also the discussion in section 3.2.1.6.

In order to facilitate the computation of the partition function in this case, let us first introduce the Cauchy identity

$$\frac{\prod_{i<j}(x_i - x_j)\prod_{i<j}(y_i - y_j)}{\prod_{i,j}(x_i - y_j)} = \det \frac{1}{x_i - y_j}\,. \tag{3.52}$$

Using this identity we can express the $n = N/2$ partition function as

$$\begin{aligned}\mathcal{Z}_n &= C_n \int d^n\bar{x} d^n\bar{x}' \\ &\det_{n\times n}\left(\frac{1}{x_i - y_j}\right) \det_{2n\times 2n}\begin{pmatrix} K^n(x_i, x'_j) & K^n(x_i, y'_j) \\ K^n(y_i, x'_j) & K^n(y_i, y'_j)\end{pmatrix} \det_{n\times n}\left(\frac{1}{x'_i - y'_j}\right)\,.\end{aligned} \tag{3.53}$$

Now one can perform the integration over (x', y') using the extension of Andréief's identity for matrices of different ranks presented in [185]. The result is

$$\mathcal{Z}_n \sim (-1)^n \int d^n x d^n x' \det\begin{pmatrix} K(x_i, x'_j) & (K\bullet N)(x_i, x'_j) \\ (M\bullet K)(x_i, x'_j) & (M\bullet K\bullet N)(x_i, x'_j)\end{pmatrix}, \tag{3.54}$$

where $\bullet$ stands for either the y integration or the y' integration and we defined $M(x_i, y) = \frac{1}{x_i - y}$, $N(y', x_j) = \frac{1}{y' - x'_j}$ to distinguish between these two cases. For example

$$(M\bullet K\bullet N)(x_i, x'_j) = \int dy dy' M(x_i, y) K(y, y') N(y', x'_j)\,. \tag{3.55}$$

Thus, in this way, we manage to trade integrals over n variables with integrals over single variables.
One can also perform the x' integrations using a formula by de Bruijn [186, 173] to get

$$\mathcal{Z}_n \sim (-1)^{n+\frac{1}{2}(n-1)n} \int d^n x \,\mathrm{pf}\, P, \quad P = \begin{pmatrix} P_{11} & P_{12} \\ P_{21} & P_{22}\end{pmatrix}, \tag{3.56}$$

where "pf" stands for the Pfaffian and the four $n \times n$ blocks given by

$$\begin{aligned} P_{11} &= -(K\circ N\bullet K + K\bullet N\circ K), \\ P_{12} &= (K\circ N\bullet K + K\bullet N\circ K)\bullet M, \\ P_{21} &= -M\bullet(K\circ N\bullet K + K\bullet N\circ K), \\ P_{22} &= M\bullet(K\circ N\bullet K + K\bullet N\circ K)\bullet M\,. \end{aligned} \tag{3.57}$$

with the $\circ$ standing for integration over x'. Let us note that the Pfaffian structure we find here is very similar to the one encountered in studies of the affine $\hat{D}$ superconformal Chern-Simons theory in [173] and we followed essentially the same steps in deriving the equation (3.56).

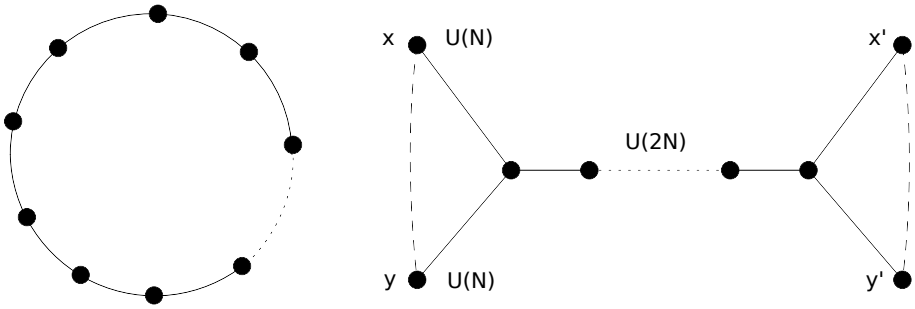

FIGURE 14: The affine $\hat{A}$ and $\hat{D}$ quivers. For the $\hat{D}$ case the nodes in the middle correspond to $U(2N)$, while the end-nodes to $U(N)$ adjoint fields. The connections between the nodes correspond to bi-fundamental fields. In studies of superconformal-chern-simons theories [173], it was found that one can write the partition function integrand as a product of determinants with the end-nodes interacting pairwise as in eq. 3.58.

3.2.1.6 *Deconstruction and Quiver Matrix Models*

There is another important reasoning on why one expects the regular $n = N/2$ representation to be the one related to the orbifold on the Liouville theory. It is based on deconstruction arguments in relation to the study of $c = 1$ CFTs at multiples of the self-dual radius.

In particular a survey of $c = 1$ CFT's shows that the orbifold CFT is related to the critical Ashkin-Teller model [187, 159, 188] that describes two Ising spins coupled by a four spin interaction. The theory at a multiple mR^o_{sd} of the self-dual radius R^o_{sd} has an affine $\hat{D}_m$ symmetry. The reasoning for this is analogous to the one for the affine $\hat{A}_{2m-1}$ symmetry of the circle theory at multiples of the circle self-dual radius $mR^c_{sd} = 2mR^o_{sd}$ and based on studying string propagation on $SU(2)/\Gamma$ with $\Gamma \subset SU(2)$ a finite subgroup of $SU(2)$ (the binary cyclic group $\mathcal{C}_{2n}$ for the circle and the binary dihedral group $\mathcal{D}_n$ for the orbifold).

Deconstruction is a form of discretization of a continuous dimension pioneered in [189]. We will be mostly interested in the proposed description of $c = 1$ string theory, where the dual matrix description for multiples of the self-dual radius on the circle is in terms of an $\hat{A}_{2m+1}$ quiver of matrices and that for the orbifold should similarly expected to be in terms of a $\hat{D}_m$ quiver of matrices [190, 172](see fig. 14). Moreover, in the case of $\hat{A}$-quiver, the partition function can typically be written as the integral of a determinant [167], a fact encountered also in the study of the $\hat{A}$ matrix-quiver of superconformal Chern-Simons theory, where the rational functions are replaced by hyperbolic functions [191]. As we saw in equation (3.33), this is also true for the S^1 partition function for arbitrary radius. Similarly it is known from studies of the ABJM $\hat{D}$-type quiver matrix model, that the partition function has the

structure of a Pfaffian [173]. In particular at the end-nodes x, y of the $\hat{D}$ quiver where the gauge group breaks from $U(2N)$ to $U(N) \times U(N)$[11], one finds a factor

$$\frac{\prod_{i<j} \sinh\left(\frac{x_i - x_j}{2}\right) \sinh\left(\frac{y_i - y_j}{2}\right)}{\prod_{i,j} \sinh\left(\frac{x_i - y_j}{2}\right)} = \det \frac{1}{\sinh\left(\frac{x_i - y_j}{2}\right)} \tag{3.58}$$

which is very similar to our expression (3.41) where the rational functions are replaced by hyperbolic ones. In addition, for the rational case the limit of an infinite number of nodes ($\hat{A}_\infty$ -case), is expected to describe the $c = 1$ infinite line as a limit of the circle at infinite radius and similarly one should expect the infinite line with twisted states at the endpoints to be obtained either taking an infinite radius limit for the orbifold, or equivalently by studying the $\hat{D}_\infty$ quiver.

In the light of this discussion, it becomes more clear why the regular representation should contain the correct description of the orbifold, as it shares the same symmetry breaking at the end-points with the $\hat{D}_m$ quiver-matrix model. Moreover it should also match with it at the corresponding multiples of the self-dual radius. On the other hand this also explains why we were able to write the integrand of the partition function as a Pfaffian. A final property that singles out the regular representation is that this is the only case where the wavefunctions at the endpoints are square integrable on the infinite line $x, y \in (-\infty, \infty)$. In particular taking the generic wavefunction

$$\psi_{n,N}(x, y) = \frac{\Delta_n(x)\Delta_{N-n}(y)}{\Delta_{n,N-n}(x, y)} \tag{3.59}$$

we find that it scales as

$$\begin{aligned} \psi_{n,N} &\sim x_i^{2n-N-1}, \quad for \quad x_i \to \infty \\ \psi_{n,N} &\sim y_j^{N-2n-1}, \quad for \quad y_j \to \infty \end{aligned} \tag{3.60}$$

and thus can be square integrable, $\int |\psi|^2 d^n x d^{N-n} y < \infty$, only for the representation $n = N/2$[12].

3.2.2 *Canonical partition function in terms of angles*

In this section we will follow the other possible method of evaluation of the canonical partition function that involves diagonalising the unitary matrix U and integrating over M.

11 A non-symmetric breaking should probably be understood as containing extra non-perturbative effects which is consistent with the picture of adding D-instantons at the end-points.

12 The divergences at the locii $x_i = y_j$ are regulated below by adopting the principal value prescription.

3.2.2.1 *The circle*

We start again by reviewing the circle case. In equation (3.33) we diagonalise U_1 by a unitary transformation as $U_2 U_1 U_2^\dagger = \delta_{ij} e^{i\theta_j}$ and integrate over $M(0)$ in the path integral to obtain [93]:

$$\begin{aligned}\mathcal{Z}_N &= \int \mathcal{D}M(0)\mathcal{D}U_1 \langle U_1 M(0) U_1^\dagger | M(0)\rangle \\ &= \frac{1}{N!}\int_0^{2\pi}\prod_{k=1}^{N}\frac{d\theta_k}{2\pi}|\Delta(e^{i\theta})|^2 q^{\frac{1}{2}N^2}\prod_{ij}\frac{1}{1-qe^{i(\theta_i-\theta_j)}} \\ &= \frac{1}{N!}\oint\prod_{k=1}^{N}\frac{dz_k}{2\pi i}\det_{i,j}\frac{1}{q^{\frac{1}{2}}z_i - q^{-\frac{1}{2}}z_j},\end{aligned} \tag{3.61}$$

with $z_i = e^{i\theta_i}$, $q = q_c = e^{-\omega\beta_c}$ and in the second line we used the Cauchy identity. The result of the integrations was found [93] to agree with (3.34). The large β_c expansion of this expression can be found in Appendix A.7.1.

3.2.2.2 *The orbifold for generic n*

We now write down the result for the generic n-representation of the orbifold [155]. The details of this calculation are presented in the appendix A.3.

$$\mathcal{Z}_n = \int_0^\pi \prod_k d\theta_k J_n(\theta) I_n(\theta) \tag{3.62}$$

with ($\mathcal{Z}_1^o$ given by eqn. 3.49)

$$\begin{aligned}I_n &= (\mathcal{Z}_1^o)^{\frac{(N-2n)^2}{2}}\prod_i^n\left[\frac{2}{\cosh\tilde{\beta}-\cos\theta_i}\right]^{N-2n} \\ &\quad \prod_{i,j}^n\left[\frac{4}{(\cosh\tilde{\beta}-\cos(\theta_i+\theta_j)(\cosh\tilde{\beta}-\cos(\theta_i-\theta_j)}\right]^{\frac{1}{2}}\end{aligned} \tag{3.63}$$

where $\tilde{\beta} = \omega\beta_c = 2\omega\beta$ and the measure

$$J_n(\theta) = \frac{1}{2^n n!(2\pi)^n}\prod_{i<j}^n \sin^2\left(\frac{\theta_i-\theta_j}{2}\right)\sin^2\left(\frac{\theta_i+\theta_j}{2}\right)\prod_{k=1}^n \sin\theta_k \sin^{2(N-2n)}\left(\frac{\theta_k}{2}\right). \tag{3.64}$$

This looks quite complicated, but as we show in appendix A.3, it can be expressed as the inverse quarter of determinant of the differential operator Q

$$I = \left(\frac{2\pi}{\omega}\right)^{\frac{1}{2}(N-2n)^2}(\det Q)^{-\frac{1}{4}}, \tag{3.65}$$

where

$$Q = -D_0^2 + \omega^2, \qquad D_0 = \partial_0 + i[A, \cdot]\,, \tag{3.66}$$

with a diagonal constant gauge field

$$A = (\pi R)^{-1}\mathrm{diag}(\theta_1, \theta_2, ..., \theta_n, -\theta_1, -\theta_2, ..., -\theta_n, 0, ..., 0)\,. \tag{3.67}$$

This form makes it clear that the angles θ_i can be interpreted in the T-dual picture as the positions of the D-instantons that can move freely. The vanishing θ_i for $i = 2n+1, \cdots N$ correspond to the fractional D-instantons that are stuck at the fixed points. The extra power $1/2$ in (3.65) is due to the orbifold projection.

We also show below that the particular case of $n = N/2$ enjoys a nice Pfaffian structure. Furthermore as a consistency check, one obtains the previous expression (3.48) for $\mathcal{Z}_{n=0}$, since in this case there is no integral to be performed and therefore one just picks up the prefactor. Finally, the large β expansion for generic n can be found in Appendix A.7.2.

3.2.2.3 *The orbifold for $n = N/2$*

For the special $n = N/2$ representation one finds that the canonical partition function can be written in terms of a Pfaffian, as derived in Appendix A.3.2:

$$\mathcal{Z}_n = \frac{1}{n!}\int_0^\pi \prod_{k=1}^n \frac{d\theta_k}{2\pi i}\prod_{k=1}^n \frac{q^{\frac{1}{2}}}{\sqrt{\left(1-qz_k^2\right)\left(1-qz_k^{*2}\right)}}\,\mathrm{pf}\begin{pmatrix} \frac{q^{1/2}(z_i-z_j)}{1-qz_iz_j} & \frac{q^{1/2}(z_i-z_j^*)}{1-qz_iz_j^*} \\ \frac{q^{1/2}(z_i^*-z_j)}{1-qz_i^*z_j} & \frac{q^{1/2}(z_i^*-z_j^*)}{1-qz_i^*z_j^*}\end{pmatrix}, \tag{3.68}$$

with $z_i = e^{i\theta_i}$, $q = e^{-\omega\beta_c}$.
This expression is very interesting. We notice that the terms in the measure take values around the full circle and the square-root leads to branch cuts in the complex z_i plane. One can also exponentiate the measure to obtain an equivalent expression

$$\mathcal{Z}_n = \frac{q^{\frac{n}{2}}}{n!}\int_C \prod_{k=1}^n \frac{dz_k}{2\pi z_k}\prod_{k=1}^n e^{\sum_{j=1}^\infty t_j z_k^{2j} + \sum_{j=1}^\infty t_{-j} z_k^{-2j}}\,\mathrm{pf}\,P, \tag{3.69}$$

with $t_j = t_{-j} = q^j/2j$ and the contour C is the upper-half plane semi-circle.
Comparing this expression with the analogous matrix model description of the 2D black-hole (see [156]) one notices that the couplings t_j act by turning on vortex perturbations or Wilson-lines ($t_k\,\mathrm{tr}\,U^k$) whose strength in our case is determined by the inverse temperature β[13]. Moreover, in our case, all these couplings are related and at large β the most relevant ones are $t_{\pm 1}$ which vanish as $e^{-\omega\beta_c}$. The form of these couplings raises the possibility of encountering a phase transition as one lowers β. Let as also note that these type of perturbations can be encountered also in variants

13 In that case only $t_{\pm 1}$ were turned on and were independent parameters of the model.

of the Gross-Witten-Wadia model [192, 193, 194, 195] that exhibit phase transitions. The form of these couplings thus raises the possibility of encountering a phase transition as one lowers β, but one should keep in mind that for the relevant case of the inverse harmonic oscillator, $\omega = -i$, $q = e^{i\beta_c}$ corresponds to a phase and a more careful study is needed. We should also mention here that based on a generalised version of the FZZ-duality, it is conjectured that higher-windings are related to higher spin generalisations of the 2D black hole [196], where discrete states are liberated as well [197].

Let us finally comment on the possibility of relating this partition function to an integrable hierarchy[14]. If true, this would, on the one hand, indicate that the model is integrable, and on the other hand it would provide us with differential equations for the partition function in terms of its parameters, as in the case of the 2D black hole [156]. To this end, we first note that the couplings t_k act as deformation parameters in a Miwa parametrization. The next step is identifying an appropriate $2n$-free fermion correlator that gives the specific Pfaffian. This Pfaffian structure for free fermions is encountered in BKP/DKP hierarchies, for more information the reader can consult [198, 199, 200] and the references therein. The most important and final difficulty is the fact that the integration is not around the circle but from 0 to π, thus one needs free fermionic correlators with branch cuts like in the Ramond sector. Since the fermionic modes are expanded in semi-integer powers, this means that the fermions live on the double-cover of the z plane, or equivalently in the background of a twisting field, that creates ramification points. In section 3.3.2.2 we find that the natural way to understand the double cover—that turns out to be a torus—is by using a parametrization in terms of Jacobi's elliptic functions.

3.2.2.4 *A non-perturbative symmetry*

It is also easy to check that the partition function for $n = N/2$ admits an exact symmetry upon rotating $\omega \to -i\omega$ and $\beta \to iT$ together. This is because the partition function depends only on the product $\omega\beta$[15]. This can be seen for example from eqn. (3.53) by rescaling the matrix eigenvalues. This property is also shared with the S^1 partition function and furthermore does not hold for any of the other n, that nevertheless just pick phase factors that depend on n.

This symmetry indicates that there is a close connection between the orbifold partition function for an inverted oscillator at Euclidean time and the transition amplitude of the normal oscillator at Lorentzian time and similarly for the cases of the inverted oscillator transition amplitude with the normal oscillator partition function. One can then restrict to the study of two out of the four possibilities.

14 We wish to thank A.Morozov, A.Yu.Orlov and J.van de Leur for discussions related to this possibility.
15 In fact it is also invariant under flipping the sign of $\omega\beta$.

3.3 THE GRAND CANONICAL PARTITION FUNCTION

It is convenient to consider the grand-canonical ensemble instead of the canonical ensemble of the previous section, in order to study the double scaling limit. The canonical partition functions we found in the previous section having the form of determinants and Pfaffians, prove very important in this respect. This is because these forms allow one to pass to the grand-canonical ensemble in a straightforward and rigorous way. The partition function in the grand canonical ensemble is defined by

$$\mathcal{Z}_G = \sum_{N=0}^{\infty} x^N \mathcal{Z}_N, \qquad x = e^{\beta\mu}\,. \tag{3.70}$$

It is a well known in statistical mechanics that it is typically much easier to compute the grand canonical ensemble of fermionic/bosonic[16] gases rather than the canonical one. In the determinant form this is because one can show that [184, 191]

$$\mathcal{Z}_G = \sum_{N=0}^{\infty} \frac{x^N}{N!} \int \prod_{i=1}^{N} d\lambda_i \det K(\lambda_i, \lambda_j) = \det\left(I + x\hat{K}\right)\,, \tag{3.71}$$

where det is a Fredholm determinant. The problem is thus reduced to the computation of the spectrum of a Kernel $\hat{K}$ acting on the space of functions of one variable $f(x)$ as

$$\hat{K}\left[f\right](x) = \int dy K(x,y) f(y)\,. \tag{3.72}$$

Therefore now one needs to solve a one-particle problem. A similar equation exists for Pfaffians [204, 173]

$$\sum_{n=0}^{\infty} x^n \int \frac{d^n x}{n!} (-1)^{\frac{1}{2}(n-1)n} \operatorname{pf} P = \sqrt{\det(\overline{I} - x\,\overline{\Omega}\,P)}, \tag{3.73}$$

where P is a $2n \times 2n$ skew-symmetric matrix consisting of four $n \times n$ blocks P_{ab} $(a, b = 1, 2)$, whose (i, j)-component is $P_{ab}(x_i, x_j)$ satisfying $P_{ba}(x_j, x_j) = -P_{ab}(x_i, x_j)$. The $\overline{\Omega}$ and $\overline{I}$ matrices in (3.73) are defined as,

$$\overline{\Omega} = \begin{pmatrix} 0 & I \\ -I & 0 \end{pmatrix}, \quad \overline{I} = \begin{pmatrix} I & 0 \\ 0 & I \end{pmatrix}. \tag{3.74}$$

Here the Pfaffian on the left-hand side is the finite dimensional one, while the determinanton the right-hand side simultaneously contains a 2×2 determinant and a Fredholm determinant.

16 Also for particles satisfying generalised exclusion statistics [201, 202], this was helpful in studying unoriented strings [203].

3.3.1 *The Circle*

The canonical partition function for the circle is of the form (3.71) thus one directly obtains the result

$$\begin{aligned} \mathcal{Z}_G^c = \det\left(I + x\hat{K}\right), \quad \text{with} \quad K(x,y) &= \sum_{n=0}^{\infty} \psi_n(x)\psi_n(y)q^{n+\frac{1}{2}}, \\ \text{or} \quad K(z,z') = \frac{1}{q^{\frac{1}{2}}z - q^{-\frac{1}{2}}z'}, \quad z &= e^{i\theta}. \end{aligned} \tag{3.75}$$

The eigen-functions are either Hermite functions $\psi_n(x)$ or the polynomials z^n with eigenvalues $\lambda_n = q^{n+\frac{1}{2}}$[17]. The partition function and the grand free energy are thus

$$\begin{aligned} \mathcal{Z}_G^c &= \prod_k \left(1 + xq^{k+\frac{1}{2}}\right), \\ \mathcal{F}_G^c &= -\sum_k \log\left(1 + xq^{k+\frac{1}{2}}\right) \\ &= -\int_{-\infty}^{\infty} d\epsilon \rho_{H.O.}(\epsilon) \log\left(1 + e^{\beta_c(\mu-\epsilon)}\right), \end{aligned} \tag{3.76}$$

where we introduced the inverted oscillator density of states $\rho_{H.O.}(\epsilon) = \frac{1}{\pi}\sum_k \delta(\varepsilon - \varepsilon_k) = -\frac{1}{2\pi} Re\Psi(\frac{1}{2} + i\varepsilon)$, with $\Psi(z)$ the di-gamma function. The derivation of the asymptotic string theory genus expansion from this expression can be found in detail in [38].

3.3.2 *Grand Canonical for the regular representation*

For the regular representation of the orbifold with $n = N/2$, one can pass to the grand canonical ensemble using the pfaffian formula (3.73). We also present the $n = 0$ case with an alternate method in Appendix (A.4). Combining equation (3.56) with 3.73, the result for the regular representation can be written in a nice operator form as

$$\mathcal{Z}_G = \sqrt{\det(\overline{I} + e^{\beta\mu}\widehat{\rho})}, \tag{3.77}$$

with

$$\widehat{\rho} = \begin{pmatrix} \hat{\mathcal{O}}e^{-\beta\hat{H}}\hat{\mathcal{O}}e^{-\beta\hat{H}} & -\hat{\mathcal{O}}e^{-\beta\hat{H}}\hat{\mathcal{O}}e^{-\beta\hat{H}}\hat{\mathcal{O}} \\ -e^{-\beta\hat{H}}\hat{\mathcal{O}}e^{-\beta\hat{H}} & e^{-\beta\hat{H}}\hat{\mathcal{O}}e^{-\beta\hat{H}}\hat{\mathcal{O}} \end{pmatrix}, \tag{3.78}$$

where we defined the bi-local operator $\langle x|\hat{\mathcal{O}}|y\rangle = \frac{1}{\pi(x-y)}$ that acts at the orbifold end-points and $\hat{H}$ the usual harmonic oscillator hamiltonian. The evolution is for

17 One should remember to set $\omega = i$ in case of the inverted harmonic oscillator potential.

$\beta = \beta_c/2$. If we furthermore use the Mehler formula, equation (3.32), we find that this operator acts on the harmonic oscillator wavefunctions (Hermite functions) at the segment endpoints as

$$\langle x|\hat{\mathcal{O}}|\psi_n\rangle = \frac{1}{\pi}\int_\gamma dy \frac{\psi_n(y)}{x-y}\,. \tag{3.79}$$

Now it is important to properly discuss the contour of integration γ since the integrand is singular when $x = y$. This is related also to the problem of the singular nature of the integrals we've encountered so far when two eigenvalues of $M_{1,2}$ coalesce. To avoid the singularity one can adopt an $i\varepsilon$ prescription to go around the singularity either on the positive or negative imaginary plane, and using the Sokhotski-Plemelj theorem

$$\frac{1}{x-y\pm i\varepsilon} = \mp i\pi\delta(x-y) + \mathcal{P}\frac{1}{x-y}, \tag{3.80}$$

one learns that these two independent possibilities are either to encircle the singularity and pick a delta function or to adopt the principal value prescription. It is easy to see that the first prescription of the delta function trivialises the action of $\hat{\mathcal{O}}$ and one just finds eigenfunctions of the matrix kernel as the vectors $v^T = (e^{-\beta\hat{H}}\psi_n, \psi_n)$ and the eigenvalues as $\lambda_n = q^{n+\frac{1}{2}}$, $q = e^{-\omega\beta_c}$. The free energy in this case would then just be one for the circle divided by two (due to the pfaffian/square-root of the determinant).

This makes clear that the prescription that contains the non-trivial twisted state contribution should be the other one, namely the principal value prescription. In addition, this prescription is consistent with the fact that the original integral is for $y \in (-\infty, \infty)$ and the principal value is the natural regulating prescription for the singular kernel $1/(x-y)$ in this range. One can therefore understand the operator $\hat{\mathcal{O}}$ acting as a Hilbert transform to the Harmonic oscillator wavefunctions (see appendix A.5 for the properties of Hilbert transform.)

$$\langle x|\hat{\mathcal{O}}|\psi_n\rangle = \langle x|\psi_n^{\mathcal{H}}\rangle = \frac{1}{\pi}\mathcal{P}\int_{-\infty}^{\infty} dy \frac{\psi_n(y)}{x-y}\,. \tag{3.81}$$

One can also notice that the kernel $\hat{\rho}$ can be written as the square of a more elementary kernel $\hat{\rho} = \hat{\tilde{\rho}}^2$ with[18]

$$\langle x|\hat{\tilde{\rho}}|y\rangle = \frac{1}{\sqrt{2}}\sum_{n=0}^{\infty} q^{\frac{1}{2}(n+\frac{1}{2})} \begin{pmatrix} -\psi_n^{\mathcal{H}}(x)\psi_n(y) & \psi_n^{\mathcal{H}}(x)\psi_n^{\mathcal{H}}(y) \\ \psi_n(x)\psi_n(y) & -\psi_n(x)\psi_n^{\mathcal{H}}(y) \end{pmatrix}. \tag{3.82}$$

One can easily extend these definitions, using from the start parabolic cylinder functions which are the eigenfunctions of the inverse harmonic oscillator and the appropriate Mehler resolution of the propagator, see appendix A.2. It is also possible then

18 Note the similarity with kernels arising in the study of Riemann-Hilbert problems [205, 206, 166].

to wick rotate $\beta = iT$ to discuss the real-time propagator as well. It is also important to note that one can also write the orbifold kernel $\hat{\rho}$ in the energy basis in terms of hypergeometric functions, see appendix A.6.1.

Finally, as an interesting result coming from eqn. (3.78), one can compute the trace of the kernel, if one resolves the operator $\hat{\mathcal{O}}$ in momentum basis as $\langle p_1|\hat{\mathcal{O}}|p_2\rangle = -i\,\mathrm{sgn}\,p_1\delta(p_1-p_2)$ (see appendix A.5). Expressing the oscillator propagator in momentum basis one computes ($\tilde{\beta} = \omega\beta_c$).

$$\mathrm{tr}\,\hat{\rho} = \frac{1}{2\pi\sinh(\tilde{\beta}/2)}\tan^{-1}\frac{1}{\sinh(\tilde{\beta}/2)}\,. \tag{3.83}$$

This is an interesting expression from which we will manage to extract the one-particle density of states -see section 3.3.2.3 - and match it with the analogous expression arising from the representation of the kernel in terms of angles that we now turn to.

3.3.2.1 *Kernel in terms of angles*

One can find an alternative representation of the kernel in terms of angles using equation (3.68). To pass to the grand canonical ensemble in this case we used reference [204] that treats the same structure as we have in terms of angles. The kernel in this description acts to functions $X(\theta)$ as

$$\hat{\rho}\left[\begin{pmatrix}X_1\\X_2\end{pmatrix}\right](\theta) = \int_0^\pi d\mu(\theta')\rho(\theta,\theta')\begin{pmatrix}X_1(\theta')\\X_2(\theta')\end{pmatrix}, \tag{3.84}$$

with the matrix

$$\begin{aligned}\rho(\theta,\theta') &= \begin{pmatrix}\rho_{11}(\theta,\theta') & \rho_{12}(\theta,\theta')\\ \rho_{21}(\theta,\theta') & \rho_{22}(\theta,\theta')\end{pmatrix} = \begin{pmatrix}\rho_{11}(\theta,\theta') & \rho_{11}(\theta,-\theta')\\ -\rho_{11}(-\theta,\theta') & -\rho_{11}(-\theta,-\theta')\end{pmatrix}\\ \rho_{11}(\theta,\theta') &= \frac{1}{q^{-1/2}e^{i\theta}-q^{1/2}e^{i\theta'}} + \frac{1}{q^{1/2}e^{-i\theta}-q^{-1/2}e^{-i\theta'}},\end{aligned} \tag{3.85}$$

and the measure

$$d\mu(\theta') = \frac{d\theta'}{2\pi i}\frac{q^{\frac{1}{2}}}{\sqrt{(1-qe^{2i\theta'})(1-qe^{-2i\theta'})}}, \tag{3.86}$$

that contains two branch-cuts in the complex $z' = e^{i\theta'}$ plane, emanating from four points $z' = \pm q^{\frac{1}{2}}, \pm q^{-\frac{1}{2}}$. For more details see figs. 15, 16. The relevant Riemann surface can be understood by gluing two spheres along two branch-cuts, the resulting surface being a torus. In the next section, we see that this kernel simplifies greatly using Jacobi's elliptic functions.

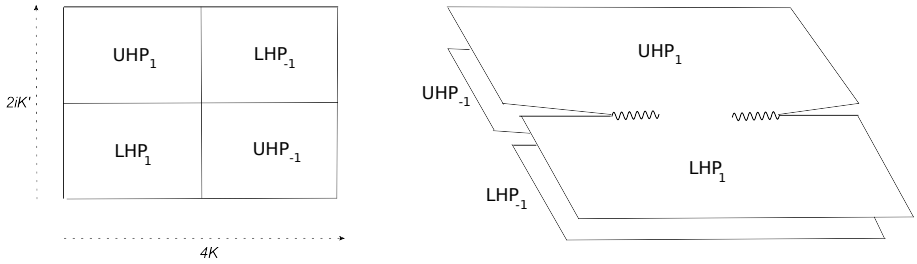

FIGURE 15: The geometry in the complex z plane is of a two-sheeted Riemann surface. The elliptic substitution makes clear that this surface is a torus.

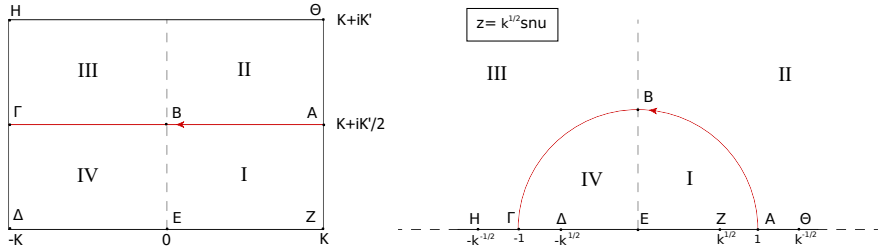

FIGURE 16: The mapping of the rectangle to the upper-half plane via $z = k^{\frac{1}{2}}\,\mathrm{sn}(u,k)$, with a matching of corresponding points. The branch cuts are between $H\Delta$ and $Z\Theta$. Both pictures correspond to the UHP_1 quadrant of 15.

3.3.2.2 *Elliptic function parametrization*

We find that the simplest representation of the kernel follows by going to the double cover and using the doubly periodic elliptic functions. Similar transformations and kernels can be found in studies of Ising, Ashkin-Teller and other models of statistical mechanics [207, 208, 209]. For more details on elliptic functions the reader can consult [210]. In particular we define $z = e^{i\theta} = q^{\frac{1}{2}}\,\mathrm{sn}(u,q)$ with $\mathrm{sn}\,u$ Jacobi's elliptic sine. Note that $q \equiv k = e^{-\omega\beta}$ plays the role of the so-called modulus. With this substitution we find

$$\int_0^{\pi} d\theta\mu(\theta) \to -q^{\frac{1}{2}} \int_{K+iK'/2}^{-K+iK'/2} \frac{du}{2\pi i}, \tag{3.87}$$

which is a great simplification for the measure. To find the new range of integration one can follow picture 16. The eigenvalue equation for the spectrum of the kernel can now be written as follows

$$\lambda \begin{pmatrix} X_1(u) \\ X_2(u) \end{pmatrix} = -q^{\frac{1}{2}} \int_{K+iK'/2}^{-K+iK'/2} \frac{dv}{2\pi i} \begin{pmatrix} \rho_{11}(u,v) & \rho_{11}(u,v+iK') \\ -\rho_{11}(u+iK',v) & -\rho_{11}(u+iK',v+iK') \end{pmatrix} \begin{pmatrix} X_1(v) \\ X_2(v)\,. \end{pmatrix} \tag{3.88}$$

One notices a consistency condition $X_1(u) + X_2(u - iK') = 0$ arising from the matrix equation. We conclude that one need not study a full matrix problem, since the eigenvalue equation reduces to

$$\begin{aligned}\lambda X(u) &= -q^{\frac{1}{2}} \int_{K+iK'/2}^{-K+iK'/2} \frac{dv}{2\pi i} \rho_{11}(u,v) X(v) - q^{\frac{1}{2}} \int_{-K-iK'/2}^{K-iK'/2} \frac{dv}{2\pi i} \rho_{11}(u,v) X(v) \\ &= -q^{\frac{1}{2}} \int_{C_1+C_2} \frac{dv}{2\pi i} \rho_{11}(u,v) X(v), \end{aligned} \tag{3.89}$$

with

$$\rho_{11}(u,v) = \frac{1 - q \,\mathrm{sn}\, u \,\mathrm{sn}\, v}{\mathrm{sn}\, u - q \,\mathrm{sn}\, v}\,. \tag{3.90}$$

Let us also note that the Jacobi's sine and thus the kernel, are doubly periodic with periods $4K$, $2iK'$ i.e. $\mathrm{sn}(u + 4K + 2iK', k) = \mathrm{sn}(u, k)$.

It is interesting to note that had we instead used the closed contour $C_1 + C_2 + C_3 + C_4$ (see fig. 17), we could have then solved the integral equation by picking the poles of the kernel at $\mathrm{sn}\, u = q \,\mathrm{sn}\, v^*$, finding

$$\lambda X(u) = q^{-\frac{1}{2}} \frac{\mathrm{cn}\, u}{\mathrm{cn}\, v^*} X(v^*), \tag{3.91}$$

which is solved by $X(u) = \mathrm{cn}\, u \,\mathrm{sn}^m u,\ m \geq 0$ with eigenvalues $q^{-\frac{1}{2}-m}$(if we demand eigenfunctions that are analytic in the interior of the strip of integration/ interior of unit circle), or by $X(u) = \mathrm{cn}\, u \,\mathrm{sn}^{-m} u,\ m \geq 1$ with eigenvalues $q^{-\frac{1}{2}+m}$ (if we demand eigenfunctions that are analytic in the exterior of the unit circle/strip of integration). This is analogous to the discussion in section 3.3.2, where we find an alternative contour that also gives half the free energy on the circle.

Comparing the integral equation with the contour $C_1 + C_2$ comprising of two horizontal pieces with the one defined via the closed contour $C_1 + C_2 + C_3 + C_4$, we find that we need some extra monodromy data around the torus to relate them. This is also to be expected since, the orbifold we consider is more than half of the circle because of the contributions from the twisted states localized at the fixed points of the orbifold. What we have shown above then means that the information about these twisted states should be contained in the contours $C_3 + C_4$. This contribution can be determined either from the contour integrals around the branch cuts or equivalently from monodromy data around the fundamental cycles of the corresponding torus.

We were not able to solve the Kernel equation including the contribution from the branch-cuts. Therefore we do not have the full-spectrum of the theory in the $n = N/2$ representation. We list different ways of expressing the Kernel equation in Appendix A.6.2. These expressions may be useful to solve obtain the spectrum in future work.

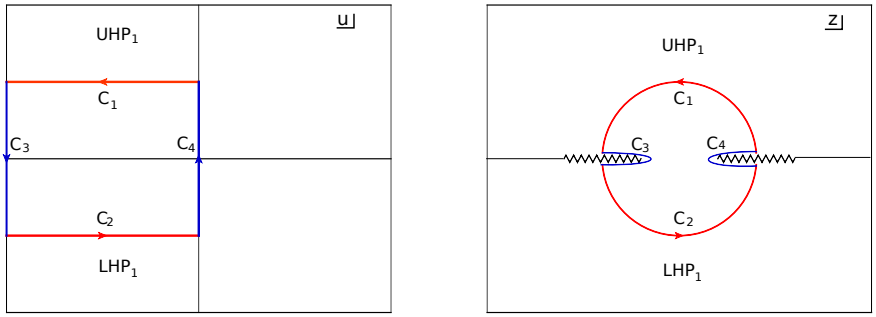

FIGURE 17: The original contour $C_1 + C_2$ is drawn by red lines in the u and z plane. In addition we draw also the two extra segments $C_3 + C_4$ with which the contour can close. In order to relate the closed with the open contour, one needs to know either the contribution around the torus, or the difference of the integral above and below the branch cut.

3.3.2.3 *Trace of the kernel*

A consistency check that can be performed in all the different descriptions we have for the kernel is to compute its trace. From (3.85) and (3.86) we can compute ($\tilde{\beta} = \omega\beta_c$)

$$\begin{aligned} \operatorname{tr}\hat{\rho} &= \frac{1}{\sqrt{2}\sinh(\tilde{\beta}/2)}\int_0^\pi \frac{d\theta}{2\pi}\frac{\sin\theta}{\sqrt{\cosh\tilde{\beta}-\cos(2\theta)}} \\ &= \frac{1}{2\pi\sinh(\tilde{\beta}/2)}\tan^{-1}\frac{1}{\sinh(\tilde{\beta}/2)}\,. \end{aligned} \tag{3.92}$$

This equation matches perfectly with eqn. (3.83), derived from the alternative representation of the kernel and thus provides a good consistency check of the two approaches. This equation is to be contrasted with the one-particle oscillator partition function on the circle

$$Z^{1p}_{H.O.} = \frac{1}{2\sinh\tilde{\beta}/2}\,. \tag{3.93}$$

By rotating $\omega \to -i\omega$, one then finds the inverse oscillator result for the orbifold

$$\begin{aligned} \operatorname{tr}\hat{\rho}_{inv} &= \frac{-1}{2\pi\sin(\omega\beta_c/2)}\tanh^{-1}\left(\frac{1}{\sin(\omega\beta_c/2)}\right) \\ &= \int_0^\pi \frac{d\theta}{2\pi}\frac{\cos(\theta/2)}{\cos(\omega\beta_c)-\cos(\theta)} \end{aligned} \tag{3.94}$$

for more details see appendix A.6.3. This expression has poles as the usual circle partition function for one particle at $\omega\beta_c = 2n\pi$, $n \in \mathbb{Z}$ and also branch cuts emanating from $\omega\beta_c = 2\pi(m+1)$, $m \in \mathbb{Z}$ due to the two logarithms from the inverse hyper-

bolic tangent. One could try to derive the density of states of this partition function using the definition via the Laplace transform

$$\rho_d(\epsilon) = \int_{c-i\infty}^{c+i\infty} \frac{d\beta}{2\pi i} Z(\beta) e^{\beta\epsilon}\,, \tag{3.95}$$

but the branch-cuts pose some difficulty. In particular adding the piece at infinity, the contour will enclose all the poles for $n \leq 0$, which gives the same density of states as in the case of the inverted H.O. but in addition one picks contributions from all the branch cuts for $m \leq -1$. To simplify things, we rewrote this expression as an integral with the integrand having simple poles. Exchanging the integrals, one can formally derive a single particle density of states, $\rho_o^{1p}(\epsilon) = \rho_{H.O.}(\epsilon) + \rho_{twisted}(\varepsilon) + \rho_{Im}(\varepsilon)$, with the "twisted" piece

$$\begin{aligned} \rho_{twisted}(\epsilon) &= \frac{1}{4\pi \sinh(\frac{\epsilon}{\omega}\pi)} \left[Im\,\Psi\left(i\frac{\epsilon}{2\omega} + \frac{1}{4}\right)\right) - Im\,\Psi\left(i\frac{\epsilon}{2\omega} + \frac{3}{4}\right)\right] \\ &= \frac{1}{4\pi \sinh(\frac{\epsilon}{\omega}\pi)} Im \int_0^\infty dt \frac{e^{-i\frac{\epsilon}{\omega}t}}{\cosh(\frac{t}{2})}, \end{aligned} \tag{3.96}$$

with $\Psi(z)$ the digamma function. For more details of this derivation one can see appendix A.6.3. Finally, the density of states contains an extra imaginary piece $\rho_{Im}(\varepsilon)$ (see A.6.3), that might have some interesting interpretation in terms of decaying states, since the decay/tunneling rate of a metastable physical system is related with the imaginary part of the free energy $\Gamma \sim Im\mathcal{F}$ [211].

3.4 LARGE ORBIFOLD EXPANSIONS

The contribution to the partition function from the twisted states can be isolated by considering the limit $\beta \to \infty$. This limit reduces the free energy to the ground state contribution as $\mathcal{F} = \beta_c E_{ground}/2 + \Theta$ and the β-independent constant piece Θ in this expression is the twisted state contribution to the ground state energy of the orbifold.

3.4.1 *Generic n*

One can obtain a closed form expression for this constant piece in the generic n representation of the orbifold, in the formulation in terms of the eigenvalues of M as follows:

$$\Theta = 2\log \int d^{N_1}x \det_{\substack{1\leq i\leq N \\ 1\leq k\leq n \\ 1\leq p\leq N-2n}} \left[\int dy \frac{\psi_{i-1}(y)}{x_k - y} \quad \int dy y^{N-2n-p} \psi_{i-1}(y) \quad \psi_{i-1}(x_k) \right] \tag{3.97}$$

In this expression the determinant is of an $N \times N$ matrix with rows labelled by the index i and the columns separated into three pieces whose size is governed by the

range of k and p. Derivation of this expression can be found in appendix A.7.3. Another expression in the second formulation in terms of eigenvalues of A is presented in Appendix A.7.2. We are unable to obtain the analogous expressions after taking the double scaling (large N) limit however. The latter is necessary to make direct connection to the Liouville theory. In principle, one should be able to express Θ in the grand canonical ensemble. For example it may be possible to obtain it directly using the twisted contribution to the one-particle density of states in equation (3.96). In the previous section we also identified the origin of the twisted state contribution through the contour around the branch cuts in figure 17. However, none of these alternative formulations has practically helped obtaining the final expression in terms of Liouville theory quantities. Instead, we perform the calculation for specific values of n below.

3.4.2 $n = 0$

Starting from the canonical ensemble, we have managed to treat the $n = 0$ representation in terms of even/odd parabolic cylinder functions and write the twisted state contribution in terms of the chemical potential μ. The relevant calculations are presented with detail in appendix A.7.4. This result is found to be

$$\Theta = \frac{1}{2}\int^{\mu} \rho_{H.O.}(\varepsilon)\int^{\mu} \rho_{H.O.}(\varepsilon')\log|\varepsilon-\varepsilon'|d\varepsilon d\varepsilon'. \tag{3.98}$$

One can then use the asymptotic form $\rho_{H.O.}(\varepsilon) = \frac{1}{\pi}\left(-\log\varepsilon + \sum_{m=1}^{\infty}\mathcal{C}_m\varepsilon^{-2m}\right)$ of the density of states to derive the asymptotic genus expansion, which we now describe. In particular one defines the cosmological constant $\Delta = \pi(\kappa_c^2 - \kappa^2)$ that is related to the *renormalised string coupling* μ_0 as $\Delta = -\mu_0\log\mu_0$ in the limit $\kappa \to \kappa_c$. One then fills up states up to the chemical potential μ. The relevant equations are

$$N = \frac{1}{\hbar}\int^{\mu} d\varepsilon\rho_{H.O.}(\varepsilon)\,, \quad \frac{\partial\Delta}{\partial\mu} = \pi\rho(\mu)\,. \tag{3.99}$$

One can invert the second equation above, to find $\mu(\mu_0)$ in an asymptotic expansion whose first term is $\mu = \mu_0$, see [38]. After that we can use an asymptotic expansion of the twisted states $\Theta(\mu)$ and turn it into an asymptotic expansion in the renormalised string coupling μ_0.

$$\begin{aligned}\Theta = \mu_0^2\left(\frac{11}{8} - \frac{\pi^2}{24} + \left(\frac{\pi^2}{12} - \frac{11}{4}\right)\log\mu_0 + \frac{7}{4}\log^2\mu_0 - \frac{1}{2}\log^3\mu_0\right)\\ -\frac{1}{24}\left(1+\frac{\pi^2}{6}\right)\log\mu_0 + \frac{1}{\mu_0^2}\left(\frac{259}{11520} + \frac{7}{2880}\left(\frac{\pi^2}{3} - 7\right)\log\mu_0\right)\mathcal{O}(\mu_0^{-4}),\end{aligned} \tag{3.100}$$

with μ_0 the renormalised string coupling. One notices that the torus contribution is not the same as in equation (3.9).

3.4.3 $n = N/2$

We will now finally treat the case that provides the matching between Liouville theory and the matrix model. For the regular representation $n = N/2$ the generic expression in (3.97) simplifies as

$$\Theta = \tfrac{1}{2}\log\det O_{ij}, \qquad O_{ij} = 2\int_{-\infty}^{\infty} dxdy \frac{\psi^+(\varepsilon_i,x)\psi^-(\varepsilon_j,y)}{x-y}\,. \tag{3.101}$$

We have calculated this expression using both the Hermite functions and the delta-function normalised even and odd parabolic cylinder functions which are the eigenfunctions of the inverted oscillator, see appendix A.2. Details of the calculation of (3.101) are presented in appendices A.7.5 and A.7.6 respectively. For the normal oscillator one finds that the result can be expressed in terms of a determinant of *sine-kernel*, see A.110. For the inverted oscillator the result is in terms of continuous labels

$$O(\varepsilon_1,\varepsilon_2) = \frac{1}{\pi}|\Gamma(1/4+i\varepsilon_1/2)\Gamma(3/4+i\varepsilon_2/2)|\varepsilon^{\pi(3\varepsilon_2+\varepsilon_1)/4}\frac{\sinh\left(\frac{1}{4}\pi(\varepsilon_2-\varepsilon_1)\right)}{\varepsilon_1-\varepsilon_2}\,. \tag{3.102}$$

Substituting this in (3.101), we see that the determinant becomes the product of diagonal pieces times the determinant of the $\sinh(\varepsilon_1-\varepsilon_2)/(\varepsilon_1-\varepsilon_2)$. It is easy to see that the diagonal pieces do not contribute to the $1/\mu$ expansion in the double scaling limit, only giving contributions to non-perturbative terms in μ. Therefore the twisted state contribution to the perturbative expansion in $g_s = 1/\mu_0$ is determined by the kernel of the operator $\sinh(\varepsilon_1-\varepsilon_2)/(\varepsilon_1-\varepsilon_2)$ in the double-scaling limit. We should also remember to solve $\mu(\mu_0)$ to derive the correct asymptotic expansion.

It is, as far as we know, not possible to calculate the spectra of this kernel with the currently available methods. However the determinant of sine kernel where one replaces $\sinh(\varepsilon_1-\varepsilon_2)$ with $\sin(\varepsilon_1-\varepsilon_2)$ is possible to be calculated in an asymptotic fashion as was done in the 70s[212, 213]. Luckily, we can make the replacement $\epsilon \to i\epsilon$ in (3.102), hence transform the $\sinh(\Delta\epsilon)/\Delta\epsilon$ kernel into $\sin(\Delta\epsilon)/\Delta\epsilon$ kernel by considering the following, alternative calculation. The canonical partition function (3.38) with the propagator (3.32) is invariant under $\omega \to i\omega$, $\beta \to -i\beta$.

This is because one can Wick rotate the integrals over the matrix eigenvalues as $x_i \to e^{-i\pi/4}x_i, y_i \to e^{-i\pi/4}y_i$ in the partition function. To see this consider the integral along the contour $C = (-\infty,\to\infty)\cup(\infty,\infty e^{-i\pi/4})\cup(\infty e^{-i\pi/4},-\infty e^{-i\pi/4})\cup(-\infty e^{-i\pi/4},-\infty)$ where the second and the last pieces are on the indicated arcs at infinity. One can see that there are no poles inside this contour C as follows. The only possible poles could arise from the denominator in the initial and final wave functions in (3.41). However these poles can easily be avoided by rotating xs and x's (and similarly ys and y's) in pairs. Also, there are no possible divergences at the arcs at infinity, $|x| = \infty$, in the $n = N/2$ partition function we are interested in here because the wave functions, (3.41) decay at infinity in this case[19]. Finally, one shows

19 Note that this part of the argument would fail for the partition functions with $n < N/2$.

that possible divergence that could arise from the $\det K(\bar{x}, \bar{x}')$ in (3.38) on the infinite arcs in contour C are also absent because one can expand

$$\det K = \sum_r \Psi_r(\bar{x})\Psi_r(\bar{x}')e^{i\beta E_r} \tag{3.103}$$

where the N-fermion wave functions Ψ_r are constructed out of products of the the parabolic cylinder wave-functions, and the latter are convergent on the particular infinite arcs $(\infty, \infty e^{-i\pi/4})$ and $(-\infty e^{-i\pi/4}, -\infty)$, as can be seen from appendix A.2. We conclude that the integral on the contour C vanishes, thus one can Wick-rotate $x_i \to e^{-i\pi/4}x_i$, $y_i \to e^{-i\pi/4}y_i$ in the partition function giving rise to the symmetry under $\omega \to i\omega$, $\beta \to -i\beta$.

Thus, one could calculate the twisted state contribution in the Lorentzian path integral instead of the Euclidean partition function. The only difference that this makes for the twisted state contribution coming from (3.102) is to replace the energies $\epsilon \to i\epsilon$, thus transforming[20] the sinh into the sine kernel. This is also the result for the normal oscillator. Therefore the result, remarkably, boils down to the computation of a Fredholm-determinant of *sine-kernel* which is a well known object in random matrix theory that corresponds to the probability that all the energy eigenvalues are outside the energy range $(-\mu, 0)$ and thus form the fermi sea. This object has been computed with various approaches such as inverse scattering, toeplitz determinants and the Riemann-Hilbert method. Some basic references are [212, 213]. This calculation is reviewed in appendix A.7.6.3 and results in

$$\begin{aligned} \Theta &= \frac{1}{4}\log E_2(0;(0,\mu_0)) = \\ &= -\frac{1}{32}\mu_0^2 - \frac{1}{16}\log\mu_0 + \frac{1}{48}\log 2 + \frac{3}{4}\zeta'(-1) + O\left(\frac{1}{\mu_0^{2m}}\right) . \end{aligned} \tag{3.104}$$

We observe that the twisted state contribution to the torus level partition function $-\frac{1}{16}\log\mu_0$ matches precisely the world-sheet result (3.9). This provides a non-trivial check of the duality we propose between the $n = N/2$ representation of the orbifold matrix quantum mechanics and the 2D non-critical string theory on $S^1/\mathbb{Z}_2$.

3.5 CONCLUSIONS

In this chapter we considered the quantum mechanics of an $N \times N$ dimensional Hermitean matrix M compactified on Euclidean time τ and orbifolded by a $\mathbb{Z}_2$ action that contains the reflection $\tau \to -\tau$, which we also embedded into the gauge group. We provided evidence that this MQM on the $S^1/\mathbb{Z}_2$ orbifold in the large-N limit constitutes a good toy model for a Bang-Crunch universe in the context of 2D string theory. This is because the orbifold MQM admits a natural analytic continuation

20 One may be ask how come the twisted state contributions in the Euclidean and Lorentzian path integrals give rise to different expressions. After all twisted states that are localized on the fixed points are not supposed to see the signature of time. This should be true at the non-perturbative level. Asymptotic expansions can differ, which is the well known Stokes phenomenon.

into Lorentzian time as shown in equation (3.40) and in the double scaling limit the theory becomes dual to 2D string theory with space-like singularities at Lorentzian time $t = 0$ and $t = T$. The space-like dimension of this 2D string theory is given by the Liouville direction that is made out of the eigenvalues of M in the dual MQM description.

PARTITION FUNCTION - The information that one can practically extract from the Liouville description of this theory is rather limited at the moment. In particular we managed to compute the torus contribution to the partition function including the contribution of the twisted states by indirect consistency methods as shown in section 3.1.1. On the other hand, we believe that the description of the theory in terms of MQM provides an alternative, richer point of view.

As a first step, we focused on calculating the partition function of the orbifolded MQM. We found that the orbifolding operation in the MQM description can be given in terms of different representations labeled by a parameter $0 \leq n \leq N/2$ (with even N). These representations arise from possible embeddings of $\mathbb{Z}_2$ into the $SU(N)$ gauge group. We argued why the "regular" representation with $n = N/2$ is preferred. We also showed that the different representations are connected by the action at the orbifold fixed points of operators resembling loop operators in section 3.2.1.3. These operators should correspond to changing the number of stretched open strings between the two sets of n, $N - n$ $D0$ branes.

We calculated both the canonical and the grand canonical partition functions using two different formulations. The first formulation involves first integrating over the gauge field and represents the partition function as an integral over the eigenvalues λ_i of the matrix M. The final expression for an arbitrary representation n is given in equation (3.38). This representation is useful since as we show in equation (3.40) the integrand can be naturally decomposed into a piece localized at $\tau = 0$, a transition amplitude from $\tau = 0$ to $\tau = \beta$ and a piece localized at $\tau = \beta$. This form of the partition function therefore admits a natural rotation into Lorenzian time where the first and the last pieces are naturally identified with the initial and final wave-functions of the toy cosmological universe, and the middle piece with the transition amplitude from the big-bang to the big-crunch. These wave functions depend on the orbifold index n, hence in some sense provide us with a classification of possible bang/crunch universes in this toy model and hence it is crucial to understand the role of n from the string theory side as well. We also note a similarity of our wavefunctions with the ones arising in the work of Dijkgraaf/Vafa on "negative branes" and supermatrix models, see [174]. We do not develop these observations further here. One should be really careful about whether the Wick rotation into Lorentzian time applies smoothly near the singularities/end points in time. Finally, there is always the possibility of inserting excited states at the initial and final states of the universe. Nevertheless, this description suggests an intriguing general qualitative prescription for how to make sense of quantum gravity in a bang/crunch cosmology: express the theory in terms of a dual open-string description, evaluate the orbifold partition function in Euclidean

time to obtain a decomposition into pieces that contain the initial state, transition and the final state, and finally Wick rotate into Lorentzian time.

The second formulation of the partition function involves first integrating over the matrix M and expressing the result in terms of the eigenvalues of the gauge field A. This method gives an alternative form for the partition function in terms of Wilson lines, the zero modes of the gauge field. The final expression for an arbitrary representation n is given in equation (3.62). This formulation clarifies the meaning of the index n: as shown in (3.67), in the T-dual picture, n corresponds to the number of free D-instantons -free to move along the time direction. There also exists $N-2n$ fractional D-instantons stuck at the fixed points of the orbifold. Thus there are no fractional D-instantons in the regular representation with $n = N/2$ and there are only fractional instantons in the $n = 0$ representation.

The $n = N/2$ partition function in this formulation contains a measure which can be thought as containing vortex/Wilson line perturbations of arbitrary order in the form of $\exp\sum_k t_k \left(\operatorname{tr} U^k + \operatorname{tr} U^{-k}\right)$ with $t_k = q^k/2k$. Similar deformations are encountered also in versions of the GWW model [192, 193] which has a third order phase transition, as well as in the proposed matrix model description of the $SL(2,\mathbb{R})/U(1)$ 2D black hole [156]. In contrast, in our case these deformations include all windings and are temperature or radius dependent, which is a quite interesting novel characteristic. In addition it is expected that the higher-windings we find are related to higher spin generalisations of the 2D black hole [196], where discrete states are liberated as well [197]. These discrete states are remnants of the higher-spin excitations that exist in higher dimensions [163, 39] and it is not unnatural to expect their presence due to the orbifolding and breaking of the gauge group that liberates $SU(N)$ non-singlet states near the end of time. The closed string twisted states should then be thought of as a condensate of both the tachyon and those extra states. The possible presence of these states due to the temperature dependent higher winding perturbations can thus lead to quite interesting and rich physics once we manage to compute the partition function or other observables for finite orbifold size R.

The two formulations should of course be equivalent. Even though we have not managed to find a direct change of variables that would relate the two in the canonical ensemble, the equivalence can be partially demonstrated at the level of the grand canonical ensemble. Indeed, in both formulations it is possible to go to the grand canonical ensemble and express it in terms of a square root of a Fredholm determinant of a one-particle kernel $\hat{\rho}$. The spectrum of this Kernel then determines the full non-perturbative answer. We checked the equivalence of the two formulations by explicitly matching the trace of this Kernel in the two cases, see equations (3.83) and (3.92).

TWISTED STATES - A central focus of our work is the contribution of the twisted states to the orbifold partition function. Since these states are localized at the fixed points of the orbifold that are supposed to become the cosmological singularities under Wick rotation, they are expected to contain crucial information on the string dynamics around these points. The twisted states are clearly marked in the torus

partition function of the Liouville theory. Their contribution is given by the constant (R-independent) terms in section 3.1.1. One can isolate this contribution in the dual MQM partition function in the first formulation (in terms of eigenvalues of M) by taking the large $\beta = \pi R$ limit. This limit, essentially decouples the propagation from the wavefunctions/states at the endpoints in time and focuses on the ground state channel contribution to the free energy. The radius independent piece has the form of determinant operators and was denoted by Θ in section 3.4. We were able to explicitly express and compute Θ in terms of 2D string theory parameters in the $n = 0$ and $n = N/2$ representations. This provided the exact matching with the Liouville theory prediction for the torus for the $n = N/2$ representation.

It is also interesting to single out the twisted state contribution directly at the level of the grand canonical ensemble. In particular we worked out the regular $n = N/2$ representation and found that they should manifest in the spectrum of the one particle kernel $\hat{\rho}$ which can be determined solving an integral equation. In the first formulation, section 3.3.2, the presence of extra twisted states was understood through the action of *Hilbert transform operators* at the endpoints. The large β limit, again decouples the Hamiltonian propagation from these operators and "zooms in" at the endpoints in time.

In the second formulation (in terms of eigenvalues of A), we isolated this contribution in section 3.3.2.2. Here the integral is defined on a complex plane with two branch cuts, or alternatively on a two-torus. One obtains precisely half the free energy for MQM on S^1 if one ignores the contribution to the contour of integration around these branch cuts, or alternatively the monodromy around the fundamental cycles of the corresponding torus. Hence in this description the twisted states should be contained in these branch-cut or monodromy contributions. Moreover, let us note that from the Matrix model picture it is clear that these extra contributions can generically lead to both radius dependent together with radius independent terms in the free energy.

We also note that in both formulations, the partition function looks very similar to a four point correlation function: in the first formulation it can be thought of as a correlator between two bi-local operators and in the second as containing four twist operators creating the two branch cuts.

FUTURE DIRECTIONS - In this chapter we focused on the closed string asymptotic expansion of the partition function. We have found that the matrix model also contains a wealth of non-perturbative information.

It will be interesting to understand further the contribution of the fractional instantons present in other representations, which we expect to be non-perturbative in g_{st}.

Let us also note that the structure of the partition function in terms of Wilson lines, is very reminiscent of τ functions of BKP/DKP Hierarchies [198, 199] and it may be very interesting to pursue this connection. For further progress in this direction, one should study free fermions and τ-functions in the presence of twist fields.

Some other interesting calculations we look forward to perform in the future include the disk one point function and the annulus correlation function for two macroscopic loops. Such quantities will be very good probes of the singularities at the endpoints of time.

Furthermore, we should develop the target space picture of our construction further by using the relation between the matrix eigenvalues and the Liouville coordinate ϕ. A description of the initial state in collective field theory variables might prove useful here. A natural question in this context is, what is the spatial extend of the 2D universe near the singularities? Is our theory describing one of the known metrics in the 2D string theory literature? The previous probes we mentioned could also help in giving answers to these questions.

As a final observation we recall that [214, 215] the horizon and the singularity of the 2D black hole is exchanged under T-duality and that there is a relation between the 2D cosmology with the 2D black hole [216]. This can be shown at least at the classical level, for the Lorentzian 2D black hole [217, 218] described by the $SL(2,\mathbb{R})/U(1)$ WZW coset. It is interesting to note that the Hilbert transform operators at the endpoints in time commute with the $SL(2,\mathbb{R})$ generators of linear fractional transformations and that the description of the kernel on the torus has a manifest $SL(2,\mathbb{Z})$ symmetry. In addition, based on the fact that we have a combination of radius dependent vortex perturbations together with radius independent twisted states, it would be very interesting to investigate whether we can similarly relate our setup with a 2D black hole with a possible interpretation of the twisted states as black hole microstates. To this end, it is encouraging that the contribution of the end-point wavefunctions to the canonical free energy takes the form of an entropy $S \sim \mathrm{tr}\, log\rho_{twisted}$ (or $S = N \log 2$ for the normal oscillator), which is also the logarithm of the probability of forming the fermi-sea from an ensemble of random hermitean hamiltonians (taking the double scaling limit of the inverted oscillator). For all these reasons it would be extremely interesting to investigate similar $S^1/\mathbb{Z}_2$ orbifolds in higher dimensions[21].

21 In the context of the 4D Schwarzschild black hole analogous *Lorentzian* Z_2 involutions that involve time reversal have found a recent interest in [219], this case will be treated in the next chapter.

4

A MAGNETICALLY INDUCED QUANTUM CRITICAL POINT IN HOLOGRAPHY

4.1 INTRODUCTION AND SUMMARY

Quantum criticality is proposed to play a fundamental role in solution to important open problems in physics, such as the high T_c superconductivity [42, 220]. Strongly interacting fixed points can be obtained by tuning a certain coupling in these systems such as the pressure, the doping fraction or the magnetic field to a critical value, see e.g. [42] for multiple examples. The characteristic energy scale ΔE that governs the spectrum of fluctuations in these systems vanishes as one approaches this critical point. If the critical point corresponds to second or higher order then this results in a conformal field theory as an effective theory governing the dynamics around criticality. Quantum phase transitions essentially happen in two different ways. It can correspond to a level crossing or a limiting case of an avoided level crossing. The second case appears to be more common in the condensed matter systems [220].

On the other hand, the AdS/CFT correspondence [10, 44, 12] has been proven, over the last two decades, to be one of the most effective methods in addressing the strongly interacting critical phenomena. In this chapter, we take this route to analyse quantum phase transitions at strong coupling, from a dual holographic point of view. As an example of a strongly interacting field theory one may consider the ABJM model [11], deformed by a bosonic, gauge invariant triple trace operator Φ^3, and placed at finite charge q and magnetic field B. The theory we consider in this chapter is related to this model. In fact, we define the precise theory through the dual gravitational background [221, 222] that are analytic solutions to $\mathcal{N} = 2$ $U(1)$-gauged (Fayet–Iliopoulos) supergravity in four dimensions [223]. The aforementioned triple trace deformation corresponding to a scalar field $\varphi(r)$ with a particular profile in the holographic coordinate r, that is determined by an integration constant b, which can be thought of as the value of the VeV of the corresponding bosonic gauge invariant operator Φ. Thus, the solutions we consider in this chapter are governed by three parameters: the VeV b, the charge q (alternatively, the chemical potential χ), and the magnetic field B. Had this solution to $\mathcal{N} = 2$ $U(1)$-gauged (Fayet–Iliopoulos) supergravity in four dimensions been completely equivalent to the corresponding $M2$-brane solution in eleven dimensions, would one confidently identify the field theory with the deformed ABJM model mentioned in the beginning of this paragraph. However, instabilities may arise for the scalar fields which are left outside of the truncation to four dimensions [224, 225, 226]. Therefore, in the most general case the field theories dual to our solutions are strongly coupled, non conformal theories placed at finite charge q and magnetic field B that can be obtained from the ABJM model by such deformations.

Four dimensional $\mathcal{N} = 2$ Fayet–Iliopoulos gauged supergravity allows for the existence of black branes in asymptotically locally AdS_4 space, preserving two real supercharges (1/4- BPS states)[227]. Their generalization to non-supersymmetric and finite temperature solutions were first constructed in [228, 229]. There has been a lot of progress, recently, on holography for BPS solutions in AdS_4 from gauged Supergravity, leading to the microstate counting of 1/4- BPS black holes entropy [26], [25, 28, 27]. In these examples there exist an AdS_2 factor in the near horizon region of the supersymmetric solution, corresponding to an IR fixed point to which the conformal UV theory flows, as a result of the topological twist induced at the AdS_4 boundary by the presence of magnetic fields. Another related line of investigations in the literature involve a holographic study of the ABJM type models deformed by dynamical flavors [230, 231]. The latter paper [231] also reports similar quantum critical behaviour in the ABJM model deformed by dynamical flavor degrees of freedom. Finally, dilatonic, charged and dyonic black-branes have been investigated in the holographic context in a series of papers by Goldstein et al [232, 233] and [234].

We focus on two different types of such solutions in this chapter: the first one is an asymptotically AdS, extremal and dyonic[1] black brane solution with a horizon at a finite locus $r = r_h$. We denote this solution with a subscript "BB" below. The second type of solution is horizonless dyonic "thermal gas" solution that can be obtained by sending the horizon r_h to a singularity r_s. We denote this solution with a subscript "TG" below. Generically it is insufficient to treat these latter type of singular solutions in the classical gravity approximation. However, as shown in [235], if the singularity can always be cloaked by a horizon, the two-derivative gravity approximation is able to capture interesting IR physics in the dual CFT at vanishing string coupling g_s (corresponding to large N in the dual gauge theory)[2]. We find that this latter requirement results in the following non-trivial conditions:

$$q_{TG} = 0, \qquad b_{TG} = \pm 2^{-\frac{7}{4}} \sqrt{|B|}\,. \tag{4.1}$$

Having imposed these conditions on the TG solution, we then seek for possible phase transitions between the BB and the TG branches by considering the difference of free energies between these branches $\Delta F = F_{BB} - F_{TG}$.

We find that this difference indeed vanishes at the critical locus

$$|B| = B_c(\chi) = \frac{4\sqrt{2}}{3}\chi^2\,. \tag{4.2}$$

1 We consider a theory in which two abelian electric-magnetic gauge fields are present. Our main subject of investigation will be systems that are electrically charged with respect to the first gauge field and magnetically charged with respect to the second. Even though they are not dyonic under the same gauge field, we use a broader definition of dyonic systems and we refer to them as possessing generic electric and magnetic charges.

2 We elaborate on details of the criteria in section 4.2.2.

As one approaches this locus, the difference of free energies vanishes quadratically and the difference of magnetizations and the VeVs of the scalar operator vanish linearly,

$$\Delta F \approx \frac{3\sqrt{3}}{2}\frac{(B-B_c)^2}{\chi}\,, \qquad \Delta M \approx \frac{3\sqrt{3}}{2}\frac{B-B_c}{8\chi}\,, \qquad \Delta b \approx \frac{3\sqrt{3}}{16}\frac{(B-B_c)}{\chi} \tag{4.3}$$

signaling a *second order* quantum critical point. In particular, as we show below, the two solutions become the same as B approaches B_c. The *order parameter* of this critical behavior can then be identified as either the magnetization or the VeV of the scalar operator. The magnetization behaves linearly in B in the BB phase and as $\sqrt{B}$ in the TG phase:

$$m_{BB} = \frac{3\sqrt{3}}{\sqrt{2}}\frac{B}{|\chi|}, \qquad m_{TG} = 3\,2^{-\frac{5}{4}}\sqrt{|B|}sgn(B)\,, \tag{4.4}$$

exhibiting a discontinuity in the derivative with respect to both B and χ at the critical point. Similar scaling arise when one considers the VeV $\langle\Phi\rangle$ in the BB and the TG phases, as we show in section 4.3. At this point, one should emphasize that there is no independent source for the operator Φ in the dual theory. Therefore the VeV is completely set by the intensive variables B and χ (chemical potential corresponding to electric charge q) at vanishing T.

It is tempting to relate the phase coalescence we find here to a confinement- deconfinement type critical behaviour as usually is the case with the Hawking-Page type transitions between a black brane and a thermal gas geometry. However, we show in section 4.4.3 that this expectation is false. In particular, we calculate the Polyakov loop holographically, and show that it is finite on both backgrounds. A computation of the quark anti-quark potential supports this conclusion. Finally, we determined the holographic entanglement entropy between a region and its complement in the dual field theory and observed that the thermal gas also corresponds to a "deconfined" state in the corresponding field theory along with the black brane phase. As we argue in section 4.3.4, the critical point is more similar to formation of quark condensate in the three dimensional Nambu-Jona-Lasinio models with magnetic field, rather than a confinement-deconfinement type transition.

We also consider the spectrum of fluctuations around these two type of solutions and find that the spectrum is continuous with no normalisable zero energy excitations in the TG phase and continuous in the BB phase. These findings are discussed in section 4.4 and they are in accord with the expectations from quantum critical points mentioned above. In particular, the boundary of the *quantum critical region* in the phase space should be determined by the condition $\Delta T \sim T \sim \Delta E$ and ΔE should vanish as one approaches the critical point. Just by dimensional analysis one can determine the boundary of the quantum critical region on a fixed χ slice of the phase diagram as $T \propto (B-B_c)^p / B_c^{p-1/2}$ where p is a positive real number which we do not determine here. The expected phase diagram on fixed χ slice is shown in figure 18.

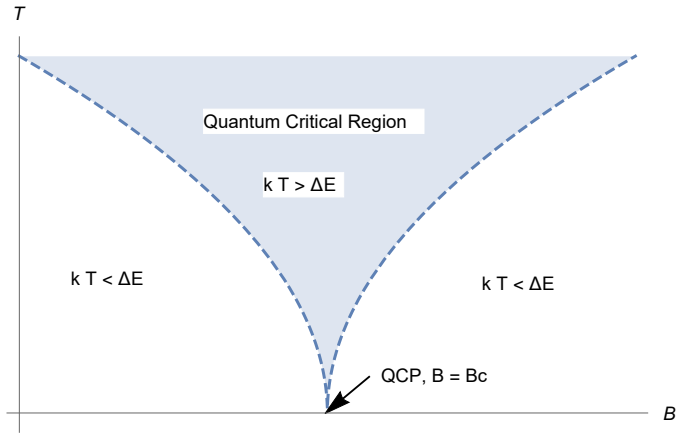

FIGURE 18: The quantum critical region on a fixed χ slice. The boundary of the critical region, shown by the dashed line, is where the thermal fluctuations are of the same order as the intrinsic energy scale ΔE. The latter vanishes as one approaches the critical point, signaling a quantum phase transition.

The rest of the chapter is organized as follows. In the next section we describe the gravity setting and introduce the dyonic black brane background. In particular section 4.2.2 discusses the singular limit of these black branes and outlines construction of the thermal gas backgrounds with a "good" type singularity. We derive the good singularity condition (4.1) in this section. In section 4.3, we study the thermodynamics of the system in the mixed ensemble defined by finite electric chemical potential χ and magnetic field B at vanishing temperature and establish the presence of the quantum critical point. At the end of this section, in subsection 4.3.4, we compare our findings with similar phenomena observed in $2+1$ dimensional Nambu-Jona-Lasinio models. In particular we discuss qualitative similarities and dissimilarities in the profile of the condensate between our holographic model and the NJL models. In section 4.4 we consider fluctuations around our backgrounds obtained by exciting point-like fields and extended objects such as a Nambu-Goto string and minimal surfaces. Here we show that the quantum criticality we find is not associated with a confinement-deconfenement type. Finally in section 4.5 we discuss the various implications of our findings in regard to applications in particle physics and condensed matter. We also give an outlook of the various routes one can extend our investigations. Several appendices detail our calculations.

4.2 GRAVITY SET UP

Our starting point is the Einstein-Maxwell-scalar theory with two gauge fields and one real scalar field, ($\kappa^2 = 8\pi G_N$)

$$I = \frac{1}{\kappa^2}\int \sqrt{-g}\quad d^4x\quad \left(\frac{R}{2} - \frac{1}{2}\partial_\mu\varphi\partial^\mu\varphi - e^{\sqrt{6}\varphi}\xi^3 F^0_{\mu\nu}F^{0\,\mu\nu} - \frac{3}{\xi}e^{-\sqrt{2/3}\varphi}F^1_{\mu\nu}F^{1\,\mu\nu} - V_g(\varphi)\right) + S_{GH}\,. \tag{4.5}$$

This action is identical to the bosonic action of an $\mathcal{N}=2$ sector of $\mathcal{N}=8$ gauged supergravity, obtained by truncating the $SO(8)$ gauging to the $U(1)^4$ Cartan subgroup and further restricting to the diagonal $U(1)$ [221]. In the language of $\mathcal{N}=2$ gauged supergravity it corresponds to a Fayet-Iliopoulos, or R-symmetry gauging where the $U(1)_R \in SU(2)_R$ symmetry is made local. Moreover, the field content can be seen as a no-axions truncation of the $\mathcal{N}=2$ Supergravity special geometry described by the prepotential $F = -2i\sqrt{X^0(X^1)^3}$ [222], with the identification $z = X^0/X^1 = e^{\sqrt{3/8}\varphi}$. The Gibbons- Hawking term is

$$S_{GH} = -\frac{1}{\kappa^2}\int d^3x\sqrt{-h}\Theta\,, \tag{4.6}$$

where h_{mn} is the induced metric at the boundary and Θ is the trace of the extrinsic curvature of the boundary given by $\Theta_{\mu\nu} = -\frac{1}{2}(\nabla_\mu n_\nu + \nabla_\nu n_\mu)$; n^μ is the unit normal vector at the boundary pointing outwards. The theory is specified by two constants ξ_0, ξ_1, a coupling g, and a scalar potential

$$\begin{aligned} V_g(\varphi) &= -\frac{3}{\ell^2_{AdS}}\cosh\left(\sqrt{\frac{2}{3}}\varphi(r)\right)\,, \qquad \ell^2_{AdS} = \frac{3\sqrt{3}}{2g^2\sqrt{\xi_0(\xi_1)^3}}\,, \\ \xi &= \sqrt{3\xi_0/\xi_1} \end{aligned} \tag{4.7}$$

where ℓ_{AdS} is the AdS length scale. The theory admits a (supersymmetric) AdS_4 vacuum at the $\varphi = 0$ locus. At this extremum the scalar field has mass $m^2_\varphi \ell^2_{AdS} = -2$, satisfying the Breitenlohner-Freedman bound. In particular, the mass of the scalar fits in the window $-\frac{9}{4} < m^2_\varphi\ell^2_{AdS} < -9/4+1$ that allows for mixed boundary conditions for the scalar field at the boundary [236, 237]. From this point on we set $\xi_0 = 1/\sqrt{2}, \xi_1 = 3/\sqrt{2}$, $g=1$ thus $\xi = 1$, $\ell_{AdS} = 1$. In particular the radial direction r will be considered as dimensionless below. One can easily recover the dimension of a given object by inserting appropriate powers of ℓ_{AdS} if needed.

4.2.1 *Black branes*

We consider static, spherically symmetric black brane solutions of (4.5) supported by two *magnetic* gauge fields

$$A^\Lambda = \frac{1}{4}p^\Lambda(xdy - ydx)\,, \qquad \Lambda = 0,1\,, \tag{4.8}$$

where x and y are the two spatial directions.

For reasons explained in section 4.3 we are rather interested in *dyonic* solutions with one electric and one magnetic charge, obtained by an electric-magnetic duality transformation only on the gauge field A^0. After the transformation the gauge fields are given by,

$$\tilde{F}^0 = \frac{q}{2(r-3b)^2} dr \wedge dt\,, \qquad F^1 = \frac{B}{2} dx \wedge dy\,. \tag{4.9}$$

The charges of the dualized configuration are related to the original one (4.8) by

$$q(p_0) = -p^0 \equiv q \qquad B(p^1) = p^1 \equiv B\,. \tag{4.10}$$

The duality transformation leaves the metric invariant, hence the solution is of the form as in [228, 229]. We use the parameterization as in [237]. The metric is

$$ds^2 = -\frac{f(r)}{\sqrt{H_0(r)H_1^3(r)}} dt^2 + \sqrt{H_0(r)H_1^3(r)} \left(\frac{dr^2}{f(r)} + r^2(dx^2+dy^2) \right) \tag{4.11}$$

with

$$H_0(r) = 1 - \frac{3b}{r}\,, \quad H_1(r) = 1 + \frac{b}{r}\,, \quad f(r) = \frac{c_1}{r} + \frac{c_2}{r^2} + r^2 H_0(r) H_1(r)^3\,, \tag{4.12}$$

while the metric coefficients are related to the charges as

$$c_1 = \frac{(p^0)^2 - (p^1)^2}{2b}\,, \qquad c_2 = \frac{(p^0)^2 + 3(p^1)^2}{2}\,. \tag{4.13}$$

The scalar field has a radial profile

$$e^{\sqrt{8/3}\varphi} = \frac{r+b}{r-3b}\,. \tag{4.14}$$

which, from its asymptotic expansion at the boundary $r \to \infty$

$$\varphi = \frac{\varphi_-}{r} + \frac{\varphi_+}{r^2} + O(1/r^3)\,, \tag{4.15}$$

reveals that it satisfies mixed boundary conditions: $\varphi_+ = \frac{1}{\sqrt{6}}\varphi_-^2$. From the holographic point of view this corresponds to the insertion of a multi trace deformation in the field theory [238, 239, 240, 236], which, in this case, is given by a triple trace deformation$\lambda\,\Phi^3$, with $\Delta_\Phi = 1$, $\lambda = \frac{1}{\sqrt{6}}$. The dual operator corresponds to $\Phi \sim Tr[Z_1^\dagger Z^1 - W^\dagger W]$, obtained after the identification of the bi-fundamental matter of the boundary theory as $Z^2 = W^1 = W^2 = W$ [241], giving an $\mathcal{N} = 2$ truncation of ABJM. Multi traces are products of single trace operators, normalized canonically [238] such that $\langle \mathcal{O} \rangle = \mathcal{O}(N^0)$ as $N \to \infty$. Due to large-N factorization, there is no mixing at leading order between single and multi trace operators.

It is important to note that the dyonic solution above is a solution of (4.5) with the modified kinetic terms for the gauge fields[3]

$$\mathcal{L}_{FF}^{Dual} = -e^{-\sqrt{6}\varphi}\tilde{F}^0_{\mu\nu}\tilde{F}^{0\,\mu\nu} - 3e^{-\sqrt{2/3}\varphi}F^1_{\mu\nu}F^{1\,\mu\nu}\,. \tag{4.16}$$

We note that, in the holographic dual field theory we interpret q as the charge density and B as the magnetic field. Reinserting the dimensions, the correct identification is given by

$$q_{ft} = q\,\ell_{AdS}, \qquad e\,B_{ft} = B/\ell_{AdS}, \tag{4.17}$$

where e is the electron charge in the dual $2+1$ dimensional field theory. Finally, we provide an expression for the chemical potential associated with the conserved electric charge q, see Appendix B.1.1 for details. The chemical potential is given by

$$\chi = -\int_{r_h}^{\infty}\tilde{F}^0_{tr}dr = -\frac{q}{2(r_h - 3b)}\,, \tag{4.18}$$

which we identify as the *electric chemical potential* after the aforementioned duality transformation.

4.2.2 *Good singularities and the thermal gas solution*

In addition to the black brane solution we described in the previous section, the action (4.5) supports thermal gas type solutions [13], that are horizonless solutions with vanishing entropy. These solutions can be obtained from the black brane by sending the horizon location to the singularity, that are located at the zeros of the functions $H_0(r)$ and $H_1(r)$ in 4.12:

$$r_s = 3b \quad for \quad b > 0\,, \qquad\qquad r_s = -b \quad for \quad b < 0\,. \tag{4.19}$$

These solutions have curvature singularities that are expected to be resolved in the embedding to the full string theory. These solutions may still be acceptable in the $3+1$ dimensional supergravity reduction that we work with here. In the AdS/CFT context, these solutions are dual to a well-defined state in the dual field theory if these singularities satisfy the Gubser's criteria [235]. Indeed, such singular solutions which satisfy the criteria of [235] are shown to correspond to the confined phase in the dual QCD-like gauge theories in [14, 13].

The Gubser criterion requires the singular solution be obtainable from a black-hole in the limit that the horizon approaches the singularity $r_h \to r_s$. To be specific, we consider $b > 0$. The criterion can be expressed in different ways depending on which parameters in the solution one keeps constant, that will eventually correspond to the choice of the thermodynamic ensemble. As it will become clear in the next section, we find appropriate to work with the mixed ensemble where we keep constant the magnetic charge B and the electric chemical potential χ, defined in (4.18). Thus, the

3 The potential and the Einstein-Hilbert term remain invariant.

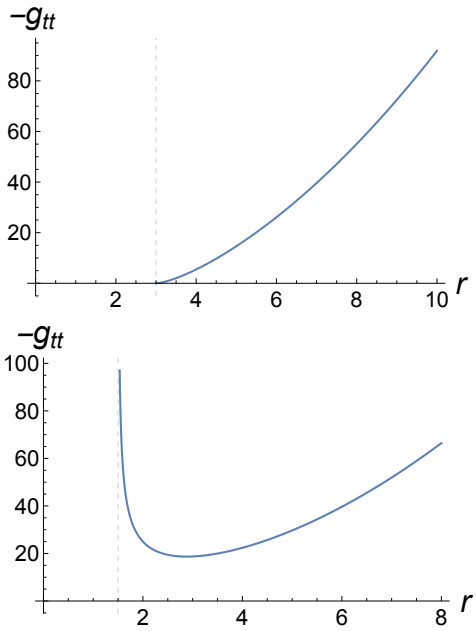

FIGURE 19: Example of warp factor $-g_{tt}$ for a good singularity (left: $B = 8\sqrt{2}$, $\chi = 1$, $r_h = 3b = 3$) and a bad one (right: $B = 1$, $q = 5$, $b = 0.5$). The dashed line indicates the location of the singularity. This coincides with the horizon, $r_h = r_{sing}$, in the plot at the top (good singularity); in this case there is no region where $-g'_{tt}(r) < 0$. In the plot at the bottom (bad singularity), on the contrary, there exists a region where $-g'_{tt}(r) < 0$ (for instance $r < 2$). In both cases of good and bad singularities, the warp factors g_{yy} and g_{xx} go to zero at $r = r_{sing}$ and the curvature invariants such as the Kretschmann scalar $R_{\mu\nu\rho\sigma}R^{\mu\nu\rho\sigma}$ diverge at $r = r_{sing}$.

black brane solution is specified in terms of (b, B, q). Consider the family of black branes with horizon $r_h = 3b + \epsilon$, for small ϵ. For $b > 0$, the horizon r_h satisfies $f(r_h) = 0$ where f is defined in (4.12). This equation, with $r_h = 3b + \epsilon$, can be analytically solved in B. For small epsilon $\epsilon \ll 1$, one finds

$$|B| = 8\sqrt{2}b^2 + \frac{(6b^2 + \chi^2)\epsilon}{\sqrt{2}b} + \mathcal{O}(\epsilon^2)\,. \tag{4.20}$$

This is an analytic expression valid for $\epsilon > 0$, which determines the horizon of the black brane. Under the crucial assumption that the magnetization χ remains finite (see Sec. 4.3.2), we analytically continue eq. $f(r_h) = 0$ to $\epsilon = 0$ and we take this limit as the defining relation of the "good singularity". Namely, we define the thermal gas as the subset in parameter space (B, b_{TG}, χ) defined by

$$b_{TG} = 2^{-\frac{7}{4}}\sqrt{|B|}\,. \tag{4.21}$$

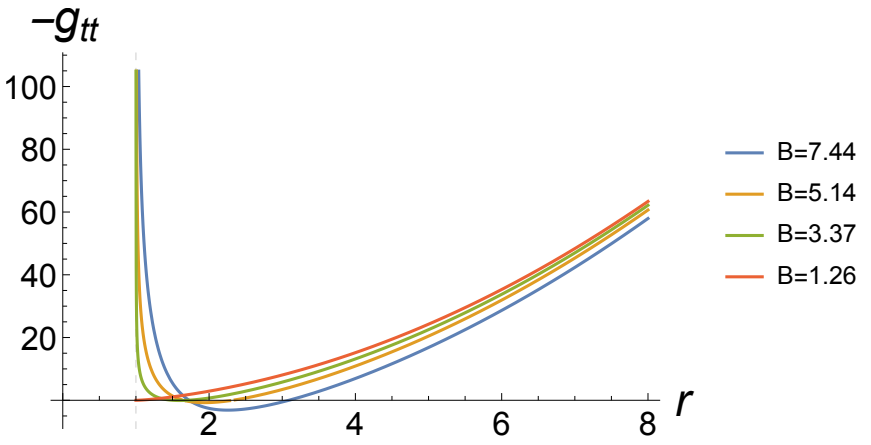

FIGURE 20: Example of warp factor $-g_{tt}$ for black branes (blue, orange and green lines) and good singularity (red line). The curves corresponds to $b = 0.33$ and $\chi = 1$ and are drawn for the following values of magnetic charge: $B = 7.44, 5.14, 3.37, 1.26$. In all cases the singularity is located at $r = r_s = 1$; here the curvature invariants such as the Kretschmann scalar $R_{\mu\nu\rho\sigma}R^{\mu\nu\rho\sigma}$ diverge. The plot shows the family of black branes approaching the good singularity solution (thermal gas) as B approaches the value given by (4.21), at fixed b and χ. In the limit, the horizon is pushed to the singularity $r_s = 3b = r_h$.

Using (4.18), we find that the charge of the thermal gas solution q_{TG} vanishes linearly in the limit $\epsilon \to 0$:

$$q_{TG} = -2\chi\,\epsilon \to 0\,. \tag{4.22}$$

Notice that for the thermal gas the dependence on χ drops from the metric:

$$\begin{aligned} ds^2_{TG} &= -e^{-\sqrt{6}\varphi}(r^2+6br+21b^2)dt^2 + e^{\sqrt{6}\varphi}dr^2(r^2+6br+21b^2)^{-1} + \\ &\quad e^{\sqrt{6}\varphi}(r-3b)^2(dx^2+dy^2)\,, \\ e^{\sqrt{6}\varphi} &= \left(\frac{r+b}{r-3b}\right)^{3/2}\,. \end{aligned} \tag{4.23}$$

Since B, b are related, a suitable set of parameters for the thermal gas is (B, χ, T), where T is the temperature of the gas. Together with χ, they are moduli of the thermal gas solution. Notice it has the same number of parameters as the black brane non-singular solution.

Before concluding this section, let us mention the fact that the definition for a good singularity requires that the gravitational force acting on an uncharged probe particle is always attractive. More precisely, the radial motion of an uncharged particle with

zero angular momentum and energy E is determined by the equation (see for example [242])

$$\frac{1}{2}\left(\frac{dr}{d\tau}\right)^2 - V_{eff}(r) = \frac{1}{2}E^2\,, \tag{4.24}$$

where the effective potential is given by

$$V_{eff}(r) = -\frac{1}{2}g_{tt}\,. \tag{4.25}$$

Hence the requirement that the force on a probe particle is never repulsive translates in $-dg_{tt}/dr > 0$ throughout the spacetime. We illustrate this in Figure 19. In Figure 20, instead, we show how a good singularity (red line) can be obtained as a limit of regular black brane configurations, by tuning the value of the magnetic field B (blue, yellow and green lines are non extremal black branes with two regular horizons).

4.3 THERMODYNAMIC QUANTITIES AND THE QUANTUM CRITICAL POINT

4.3.1 *Thermodynamics of the black brane*

Thermodynamic properties of gravity solutions in asymptotic Anti de Sitter space can be obtained via holographic renormalization of the on-shell action and gravitational stress-energy tensor. We have derived these quantities in Appendix B.1.1, to which we refer for the following relations and identities.

The free energy of any black brane solution of Sec. 4.2.1 is

$$F_{BB} = M_{BB} - TS_{BB} + q_{BB}\chi\,, \tag{4.26}$$

where M_{BB} is the mass of the black brane

$$M_{BB} = \frac{B^2 - q_{BB}^2}{4b_{BB}}\,, \tag{4.27}$$

T , S_{BB} are its temperature and entropy, q_{BB} is the electric charge carried by the black brane, χ is the chemical potential given in equation (4.18). We are interested in the thermodynamics of these solutions in the mixed ensemble, defined by the free energy relation

$$dF_{BB} = -S_{BB}dT + q_{BB}d\chi + m_{BB}dB\,, \tag{4.28}$$

therefore the independent thermodynamic variables are T, χ and B.

Furthermore, we will restrict to the case of vanishing temperature, $T = 0$. In order to eliminate r_h, q and b in the expressions we will make use of (4.18), the horizon equation $f(r_h) = 0$ (f is as in (4.12)) and the extremality condition $f'(r_h) = 0$.

We obtain two interesting ways to express the free energy. First, we can solve the aforementioned equations in terms of B and q and obtain:

$$B^2 = \frac{1}{2}\left(-5b^4 - 12b^3 r_h - 6b^2 r_h^2 + 4b r_h^3 + 3r_h^4\right), \tag{4.29}$$

$$q^2 = \frac{27b^4}{2} + 18b^3 r_h - 3b^2 r_h^2 - 6b r_h^3 + \frac{3r_h^4}{2}. \tag{4.30}$$

Substitution in (4.26) then gives

$$F_{BB} = \frac{1}{4}(5r_h - 7b)(b + r_h)^2. \tag{4.31}$$

This form is useful to check the zeros of the free energy. The function in (4.31) clearly has a quadratic zero at $r_h = -b$, which corresponds to the singularity when $b < 0$, and this gives a consistency check. When $b > 0$, it appears there is another zero at $r_h = 7b/5$, however this value for r_h is smaller than the actual singularity $r_s = 3b$, so in fact the free energy has only one zero that is given by $r_h = -b$. It is also clear from the formula above that the free energy is positive definite.

It is more appropriate, for thermodynamic studies, to express the free energy in terms of the correct variables of the mixed ensemble, namely (T, B, χ). To do so we just need to solve the equations above, this time in terms of χ and B. We obtain the following expressions:

$$r_h = \frac{9B^2 + 160\chi^4}{64\sqrt{6}|\chi|^3}, \tag{4.32}$$

$$q_{BB} = \frac{-9B^2 + 32\chi^4}{8\sqrt{6}\chi^2}\,\mathrm{sgn}(\chi), \tag{4.33}$$

$$b_{BB} = \sqrt{\frac{3}{2}}\frac{32\chi^4 - 3B^2}{64|\chi|^3}. \tag{4.34}$$

These solutions are valid only for $\chi \neq 0$. The free energy of the black brane then follows as,

$$F_{BB} = \frac{27B^2 + 32\chi^4}{24\sqrt{6}|\chi|}. \tag{4.35}$$

This form also makes it obvious that the free energy of the black brane is positive definite. Now one can check the first law of thermodynamics (4.28). The charge density q should be obtained as

$$q_{BB} = \left.\frac{\partial F_{BB}}{\partial \chi}\right|_{B,T}. \tag{4.36}$$

This indeed matches (4.33) perfectly, hence the first law is satisfied. This provides another non-trivial check on our calculations. Finally, the magnetization of the black brane solution is obtained as

$$m_{BB} = \left.\frac{\partial F_{BB}}{\partial B}\right|_{\chi,T} = 3\sqrt{\frac{3}{2}}\frac{B}{|\chi|}. \tag{4.37}$$

We find that the magnetization of the black brane grows linearly with B.

4.3.2 *Thermodynamics of the thermal gas*

As explained in section 4.2.2, the thermal gas solution is obtained from the black brane by sending the horizon r_h to one of the singularities. In the following, in particular, we take $b > 0$[4]. Consider then the limit of a black brane with horizon $r_h = 3b + \epsilon$, as $\epsilon \to 0$. In the grand canonical ensemble the states have fixed magnetic potential, thus $\chi_{TG} = \chi_{BB} = \chi$, which remains finite in this limit. As explained in section 4.2.2, this requirement implies the following relation between the parameter b_{TG} of the thermal gas and the magnetic field B

$$b_{TG} = +2^{-\frac{7}{4}}\sqrt{|B|}\,, \tag{4.38}$$

and it also leads to a vanishing electric charge, $q_{TG} = 0$, see equation (4.22). The temperature of the thermal gas is a moduli parameter, which can be set to any positive value. To match the black brane solution above, then, we choose $T_{TG} = 0$. The entropy for the thermal gas also vanishes in this limit as,

$$S_{TG} = 16\pi 2^{-\frac{21}{8}}|B|^{\frac{3}{4}}\sqrt{\epsilon} \to 0\,. \tag{4.39}$$

In the appendix B.1.1 we compute the thermal gas free energy by holographic renormalization. We have verified that the same result is obtained by substituting in equation (4.26) the expressions (4.22) and (4.39), and imposing the defining relation (4.38). We arrive at

$$F_{TG} = M_{TG} = \frac{B^2}{4b_{TG}} = 2^{-\frac{1}{4}}|B|^{\frac{3}{2}}\,. \tag{4.40}$$

This result is clearly consistent with the first law of thermodynamics: the charge of the thermal gas solution obtained by the variation with respect to χ trivially vanishes, just like (4.22). Moreover, the magnetization is given by

$$m_{TG} = \left.\frac{\partial F_{BB}}{\partial B}\right|_{\chi,T} = 3\cdot 2^{-\frac{5}{4}}\sqrt{|B|}\,\mathrm{sgn}(B)\,. \tag{4.41}$$

We note the qualitative difference between the black brane (4.37) and the thermal gas (4.41) magnetization: the former is linear in B whereas the latter grows like the square root of B.

4.3.3 *Difference of free energies and the quantum critical point*

In the work presented so far, we have introduced all relevant physical quantities needed to study the thermodynamics phase space. We will proceed now to investigate possible phase transitions between black brane and thermal gas solutions.

4 Good singularities with $b < 0$ require $B = 0$ instead, thus, in this ensemble (in which the magnetic field is fixed) they do not compete with regular black branes, the latter generically having $B \neq 0$.

In order to determine whether a phase transition occurs, we consider the difference of free energies (4.35) and (4.40):

$$\Delta F = F_{BB} - F_{TG} = \frac{27B^2 + 32\chi^4}{24\sqrt{6}|\chi|} - 2^{-\frac{1}{4}}|B|^{\frac{3}{2}}\,. \tag{4.42}$$

We note that it is even under $B \to -B$ and $\chi \to -\chi$ independently. This means, as it should be, that the free energy is C-even and P-even. We can consider analogous checks for the difference of magnetizations

$$m = \left.\frac{\partial \Delta F}{\partial B}\right|_{\chi,T} = \frac{3\sqrt{6}}{8}\frac{B}{|\chi|} - 3\,2^{-\frac{5}{4}}\sqrt{|B|}\,\mathrm{sgn}(B)\,, \tag{4.43}$$

which is C-even and P-odd, and the difference of electric charges

$$q = \left.\frac{\partial \Delta F}{\partial \chi}\right|_{B,T} = q_{BB} = \frac{-9B^2 + 32\chi^4}{8\sqrt{6}\chi^2}\,\mathrm{sgn}(\chi)\,, \tag{4.44}$$

yielding that the total charge is P-even and C-odd.

Finally, we find that the free energies of the TG and the BB phases become equal at

$$|B_c| = \frac{4\sqrt{2}}{3}\chi^2\,, \tag{4.45}$$

corresponding to the zero of (4.42). Therefore, for every value of χ (except $\chi = 0$) we find a non-analytic behaviour in the free energy at a finite magnetic field given by (4.45). Quite interestingly, this non-analytic behaviour is of *second order*. In fact, by expanding the difference of free energy (4.42) near the critical point, we obtain

$$\Delta F = 3\sqrt{\frac{3}{2}}\frac{(B - B_c)^2}{|\chi|} + \mathcal{O}(B - B_c)^3\,. \tag{4.46}$$

In order to exhibit the discontinuity in the free energy we can directly compare the free energies and their derivatives at the critical point. We find that, even though the free energies and their first derivatives are continuous between the two phases, the second derivative jumps by an excess amount $\frac{3}{8}\sqrt{3/2}/|\chi|$ from the TG phase to the BB phase at $B = B_c$. Our example corresponds to the limiting case of an avoided level crossing, in the sense that the TG phase always wins over the BB phase everywhere in the phase space except the critical point $B = B_c$ where their free energies become equal. This is still called a "quantum phase transition" according to the definition utilised in [220]. However we avoid using the term "transition", as it sounds more appropriate for an actual level crossing.

The excess magnetization (4.43) can be expanded near the critical point as,

$$\Delta m = 3\sqrt{\frac{3}{2}}\frac{(B - B_c)}{8|\chi|} + \mathcal{O}(B - B_c)^2\,, \tag{4.47}$$

showing that the difference of magnetization between the two phases vanishes linearly at the critical point. We note that the excess charge also vanishes, although quadratically, precisely at the critical point:

$$\Delta q = -3\sqrt{\frac{3}{2}}\frac{(B-B_c)^2}{\chi^2}\,\mathrm{sgn}(\chi) + \mathcal{O}(B-B_c)^2\,. \tag{4.48}$$

These results are another non-trivial check of our previous calculations. It is indeed expected that, at a second order critical point, two competing solutions become the same (as opposed to a first order point where two different, competing states coexist). The solutions we consider are completely specified by S, m and q. The entropies S_{BB} and S_{TG} vanish at the critical point (to check that S_{BB} vanish one has to impose on the black brane parameters (4.32)-(4.34) the criticality condition (4.45)), hence they are the same. As we have seen in (4.47) the magnetizations also become the same. For consistency of a second order critical point then the charges should also become the same. Since the charge of thermal gas vanishes, the critical behaviour then should happen when the charge of the black brane also vanishes, as nicely confirmed above.

The difference between the vacuum expectation values of the condensates in the thermal gas phase, b_{TG} in (4.38) and the black brane phase, b_{BB} in (4.34) also vanishes linearly as

$$\Delta b = b_{TG} - b_{BB} = \frac{3\sqrt{3}}{16}\frac{(B-B_c)}{\chi} + \mathcal{O}(B-B_c)^2\,. \tag{4.49}$$

4.3.4 *Similarities with the Nambu-Jona-Lasinio model*

Our results may find interesting applications in particle physics, regarding dynamical mass generation and spontaneous flavor symmetry breaking in $2+1$ dimensional gauge theories under external magnetic fields (see [243] and the references therein). It is well known that magnetic field acts as a catalyst of chiral condensate in $3+1$ dimensional gauge theories with massless fermions [244, 245]. As shown in [246, 247], it also acts as a catalyst for the flavor symmetry breaking $U(2) \to U(1)\times U(1)$ in similar $2+1$ dimensional gauge theories, with fermions in a 4- component reducible Dirac representation. These theories are generalized and extensively studied in vector like, large-N_f Nambu-Jona-Lasinio (NJL) models, as reviewed in [243]. There, the spontaneous symmetry breaking pattern becomes $U(2N_f) \to U(N_f)\times U(N_f)$. We observe that our results for the scaling of the condensate in the two phases ''BB'' and ''TG'', given by equations (4.34) and (4.38), are in striking similarity with the results obtained in these effective models [243].

In the absence of magnetic fields, the flavor condensate in NJL models vanish when the quartic fermion coupling g is smaller than a critical value g_c. For $g > g_c$ a fermion mass term is dynamically generated and the condensate becomes nonzero [243]. Its strength σ_0 is proportional to the difference $g - g_c$. This breaks the flavor symmetry as described above. Now we would like to compare this with our values for the

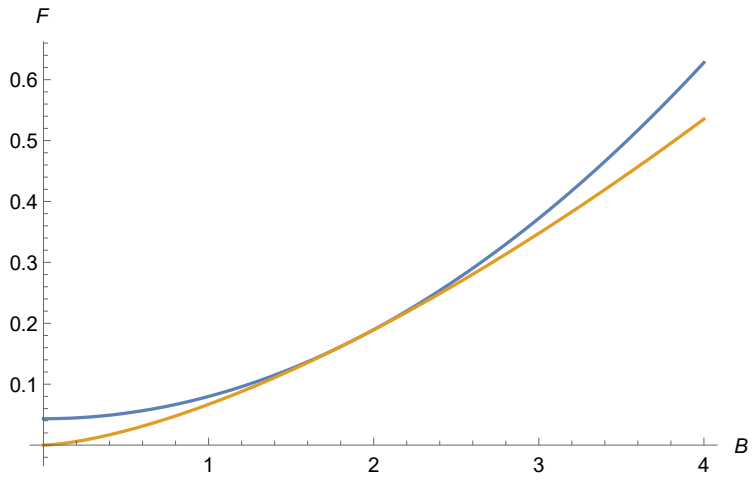

FIGURE 21: Plot of the free energies of the black brane and the solitonic solution for $\chi = 1$, as functions of B, the blue line is the black brane and the yellow line is the thermal gas. The thermal gas is thermodynamically favoured everywhere in the (B, χ) region. At the critical line, defined as $B = \frac{4\sqrt{2}}{3}\chi^2$, black brane and thermal gas coincide.

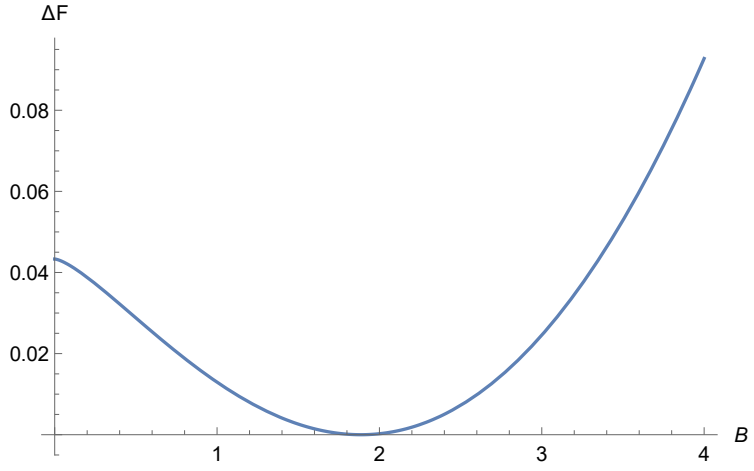

FIGURE 22: Plot of the difference of the the two free energies for $\chi = 1$, as function of B.

condensate in the two phases (4.34) and (4.38) at $B = 0$. First of all, we see that the condensate vanishes in the TG phase, therefore the phase with $g > g_c$ of the NJL model could only be identified with the black brane phase:

$$\sigma_0 = b_{BB}\Big|_{B=0} = \sqrt{\frac{3}{2}}\frac{|\chi|}{2}\,. \tag{4.50}$$

It is therefore tempting to identify the chemical potential χ with the difference of the 4- fermion coupling and the critical coupling, i.e. $g - g_c$, for $g > g_c$. As explained in [243], two qualitatively different phases arise when B is turned on. In the phase analogous to our black brane phase, the condensate scales as

$$\sigma_{NJL,1} \approx \sigma_0 \left(1 + \frac{B^2}{12\sigma_0^4}\right), \tag{4.51}$$

for $B \ll \sigma_0^2$, which qualitatively agrees with the scaling we have found in (4.34):

$$\sigma_{BB} \equiv b_{BB}\Big|_{B\neq 0} = \sigma_0 \left(1 - \frac{B^2}{384\sigma_0^4}\right), \tag{4.52}$$

which is valid for any value B. The second phase is obtained in the region $g \to g_c$ which corresponds to $\chi/\sqrt{B} << 1$ limit. In this limit the TG phase definitely wins over the BB phase, as can be seen from (4.42), which is the only phase where scaling of the condensate becomes independent of χ, (4.21)

$$\sigma_{TG} \equiv b_{TG} = 0.297\sqrt{B}\,, \tag{4.53}$$

whereas the NJL model result is

$$\sigma_{NJL,2} = 0.446\sqrt{B}\,, \tag{4.54}$$

again, in qualitative agreement. We note that this qualitative agreement is non-trivial, for it cannot be deduced only by dimensional analysis, as the condensate in our case could have scaled with an arbitrary power of the ratio B/χ^2.

4.4 FLUCTUATIONS

Another support to our findings, namely presence of quantum criticality at the locus $B = B_c(\chi)$, comes from the study of the theory's spectrum.

Let's consider the spectrum of fluctuations obtained by acting with a bosonic operator $\mathcal{O}_\Delta$ on the vacuum. This can be determined holographically, by studying the fluctuations of the dual bosonic bulk field with mass $m^2 = \Delta(3-\Delta)$, on the gravity background corresponding to the field theory's vacuum.

Below we consider the special case of fluctuations with $m^2 = 0$, both on the thermal gas (TG) and the black brane (BB) backgrounds. The spectrum is given by solutions corresponding to energy eigenvalues ω, which are normalizable both in the ultra-violet ($r \to \infty$) and in the infra-red regime (namely $r \to r_s$ on the TG solution, and $r \to r_h$ on the BB solution). For simplicity we set $\vec{k} = 0$ in the following. The fluctuation equation can be obtained from the action

$$\begin{aligned} S_{fluc} &= \int d^4x \sqrt{-g} g^{\mu\nu} \partial_\mu \phi \partial_\nu \phi^* = \\ &= \int dr d^3x \sqrt{-g} \left\{ g^{rr} |\partial_r \xi_\omega(r)|^2 + \omega^2 g^{tt} |\xi_\omega(r)|^2 \right\}, \end{aligned} \tag{4.55}$$

where we set $\phi(r,x) = \xi_\omega(r)e^{-i\omega t}$. The first term above can be removed by integration by parts and renormalizing away the boundary term [248], the second term is required to be finite for finite energy fluctuations. Thus, the spectrum is obtained by solving the fluctuation equation

$$\xi''_\omega(r) + \frac{d}{dr}\log(\sqrt{-g}g^{rr})\xi'_\omega(r) - \omega^2 g^{tt}g_{rr}\xi_\omega(r) = 0\,, \tag{4.56}$$

and requiring

$$\lim_{r_{UV}\to\infty} \omega^2 \int_{r_{UV}}^{r_{IR}} dr\sqrt{-g}g^{00}|\xi_\omega(r)|^2 < \infty\,, \tag{4.57}$$

on the solution. Here r_{UV} denotes a UV cut-off and r_{IR} is either r_s or r_h depending on the background. Potential divergences in the integral above arise both in the UV and in the IR. For backgrounds with no horizon, requirement of square integrability in these two limits typically results in a discrete spectrum $\omega = \omega_n$, see for example [13].

4.4.1 *Spectrum in the thermal gas phase*

We are going to address the question whether there exists normalizable solutions (according to the normalizability requirement above) with energy ω arbitrarily close to 0. If such solutions can be found, then there is a continuum of states starting just above the vacuum $\omega = 0$. For $\omega \ll 1$ the solution can be obtained perturbatively as $\xi_\omega(r) = \xi_0 + \omega^2\delta\xi_\omega + \mathcal{O}(\omega^4)$. Since the expression in (4.57) is already quadratic in ω we can safely drop the second term and consider solutions to (4.56) with $\omega = 0$. The solution can be obtained analytically in this limit as

$$\xi_0(r) = C_1 + C_2\int_\infty^r \frac{dr'}{\sqrt{-g}g^{rr}} = C_1 + C_2\int_\infty^r \frac{dr'}{r'^2 f(r')}\,, \tag{4.58}$$

where $C_{1,2}$ are integration constants and we used the ansatz (4.11). The solution with $C_1 \neq 0$ is not normalizable near the UV because the limit in (4.57) diverges linearly in r_{UV}. Therefore we set $C_1 = 0$. This solution with $C_2 \neq 0$ is clearly normalizable in the UV as the result of the integration in (4.57) is proportional to r_{UV}^5.

Now let us look at what happens near the IR. For $b > 0$ the singularity is given by $r_s = 3b$. The TG solution with a good type of singularity at that point is given by setting the parameters as (4.1) in (4.11). One then shows that

$$r^2 f(r) = (r-3b)((r+b)^3 - B^2/(2b)) = 48b^2\epsilon^2 + \mathcal{O}(\epsilon^3)\,, \tag{4.59}$$

where we set $r = 3b + \epsilon$ and expand near $\epsilon = 0$ in the second equation. To obtain this double zero it is crucial to use the second condition in (4.1), namely $b = 2^{-7/4}\sqrt{|B|}$. Otherwise one obtains a single zero: $f \to \mathcal{O}(\epsilon)$. Therefore the solution behaves as $\xi_0 \sim \epsilon^{-1}$ near the singularity and the integral in (4.57) diverges as ϵ^{-2}. We conclude that *there are no normalizable excitations with $\omega = 0$ in the TG phase.*

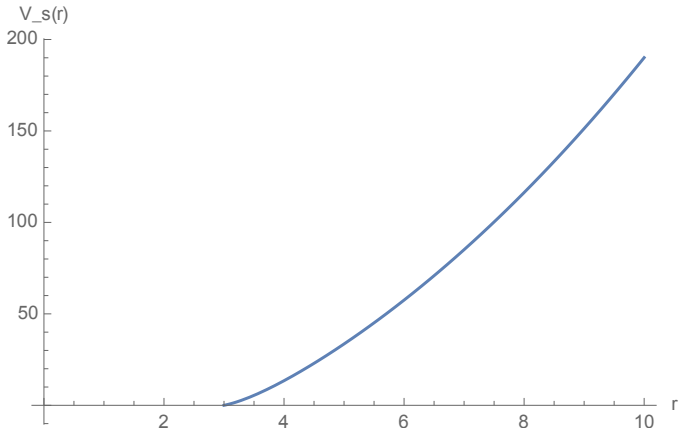

FIGURE 23: We plot the Schrodinger potential for fluctuations around the thermal gas solution for the choice of $b = 1$. The potential vanishes as r approaches the singularity located at $3b$. Therefore the potential has the same qualitative features as the $-g_{tt}$ factor plotted in the right figure in 19.

It is instructive to consider what would have happened had we released the condition $b = 2^{-7/4}\sqrt{|B|}$ on the TG solution. If we keep b arbitrary then the blackening factor has a single zero as mentioned above. Then the solution would behave as $\xi_0 \sim \log\epsilon$ and the integral in (4.57) would have a finite limit as $\epsilon\log^2(\epsilon)$ plus a constant. Thus, one would have obtained a normalizable excitation with $\omega = 0$. This should not happen for consistency of the entire picture and we learn that the condition (4.1) is essential for this.

Finally, we note that the fluctuation equation (4.56) can be put in a Schrödinger form

$$-\frac{d\Psi(r)}{dr^2} + V_s(r)\Psi(r) = \omega^2\Psi(r)\,, \tag{4.60}$$

and defining,

$$\xi_\omega = \left(g^{rr}\sqrt{-g}\right)^{-\frac{1}{2}}\Psi\,, \tag{4.61}$$

where $g_{\mu\nu}$ is the metric of the thermal gas solution given by (4.23). Luckily one obtains an analytic expression for the Schrödinger potential in the r-variable as

$$V_s(r) = \frac{(3b-r)\left(21b^2+6br+r^2\right)\left(279b^4-54b^3r+b^2r^2-4br^3-2r^4\right)}{(b+r)^5}\,. \tag{4.62}$$

We plot this potential for a choice of $b = 1$ in figure 23. Note that the potential vanishes as r approaches the singularity located at $r = 3b$. This does not mean however that there exists massless states: as we have shown above states with $\omega = 0$

does not have square-normalizable wave-functions. Thus the thermal gas solution supports a continuous spectrum with no normalisable $\omega = 0$ excitations. We also note that the Schrödinger potential enjoys the same qualitative features with the $-g_{tt}$ factor plotted in the top figure in 19.

4.4.2 *Spectrum in the black brane phase*

In contrast to the thermal gas phase above, one can show that there exist normalizable fluctuations with arbitrarily small frequency ω in the black brane phase. The easiest argument is as follows. The analog of the normalizable modes in the black brane with Lorentzian signature are the quasi-normal modes (QNM). They are fluctuations on the black brane background with infalling boundary conditions on the horizon and vanishing Dirichlet boundary conditions on the boundary. At finite T, the QNM spectrum is typically given by separated poles on the lower complex frequency plane, the lowest QNM having $|\omega| \sim T$, therefore one can think of these fluctuations as gapped, see for example the review paper [249]. If we view the extremal brane as the $T \to 0$ limit of a finite T black brane background, then we indeed find modes with arbitrarily small energy in the spectrum [250][251]. This argument is robust as long as one keeps an arbitrarily small but finite $T = \epsilon$ as an IR cut-off. Then the lowest QNM indeed has an arbitrarily small energy $|\omega| \propto \epsilon$ and the separation between the QNMs are also of the same order, $|\Delta\omega| \sim \epsilon$. In the strict $T \to 0$ limit however, multiple QNMs accumulate at the origin of the ω complex plane producing a branch-cut [250][251]. This is in accordance with the holographic correspondence as one expects branch-cuts in the retarded Green's function in a strongly interacting conformal field theory at vanishing temperature.

4.4.3 *Extended probes*

We have also studied the solutions of string-like extended objects in our backgrounds. We summarize here our findings; the details are presented in Appendix B.2. It is important to study extended objects on our backgrounds because the corresponding field theory quantities such as the *Polyakov loop*, the *Wilson loop* and the *entanglement entropy* may potentially be considered as order parameters of the critical behavior we found in section 4.3.

In section B.2.1 we calculate the action of a Nambu-Goto string wrapped on the Euclidean time direction and extending in the holographic direction from the boundary to the origin in our geometries. We studied this on both backgrounds where the origin corresponds to the horizon in the case of the Euclidean black brane, and to the singularity r_s in the case of the thermal gas. the exponential of this string action corresponds to the Polyakov loop in the corresponding field theory [252]. We find that, with a proper renormalization at the boundary, the area swiped by the string is finite on both backgrounds, whereas it should be infinite on the thermal gas and finite on the black brane, had these two geometries corresponded to confined (deconfined) phases of the corresponding field theory.

Secondly, in section B.2.2 we studied the string that is attached on the boundary at two points $-l/2$ and $+l/2$ on the x-axis, and hanging down towards the origin. Action of this string corresponds to the potential $V_{q\bar{q}}$ between a quark-antiquark pair located at $x = -l/2$ and $+l/2$ [253, 254]. Thus, this potential should grow with l in a confining phase. We find however that on the thermal gas phase the $V_{q\bar{q}}$ remains finite and it approaches to a constant as l increases. Therefore this phase does not exhibit a confining behaviour.

The entanglement entropy of a region A with its complement on the boundary theory is obtained in the holographic dual by studying the area of a space-like minimal surface that ends on the boundary of region A [255]. This quantity may also act as an order parameter in confinement-deconfinement type transitions [256]. We investigate this possibility in Appendix B.2.3 where we study the space-like minimal surfaces on the thermal gas background. We find that the connected surfaces always have an area smaller than the corresponding disconnected surfaces with the same boundary conditions. This means that the thermal gas, as the black brane, always correspond to a deconfined state in the corresponding field theory.

We found that none of these quantities provides an order parameter for the phase transition, as they exhibit the same qualitative behaviour both on the black brane and the thermal gas phases. On the other hand, this negative statement provides a valuable insight on the nature of the critical point, namely that it *does not correspond to a confinement-deconfinement type transition.*

4.5 DISCUSSION AND OUTLOOK

Our main result is a second order type critical behaviour in the free energy at vanishing temperature, between an electrically and magnetically charged black brane and a magnetically charged, horizonless thermal gas solution, in the Einstein-Maxwell-scalar theory defined by the action (4.5). Both geometries asymptote to AdS_4 near the boundary, and we work in a mixed ensemble where the magnetic charge B and the electrostatic potential χ are held fixed, and the temperature T is set to zero. Quite conveniently, both the backgrounds and the physical quantities such as the thermodynamic potentials can be obtained analytically in our study. Moreover, the action can be embedded in M-theory [222]. The critical point we find is somewhat trivial from the gravity point of view, as we *define* the thermal gas solution by a limiting procedure where the horizon is sent to the singularity. It is then obvious that these two solutions become the same in this limit. However, it is quite non-trivial from the boundary field theory point of view, since when expressed in terms of the physical variables, χ and B the critical behavior takes place at a finite value of B and χ and $T = 0$. Hence, it corresponds to a line of quantum critical points in the phase space, that can be parametrized by χ or B, as in equation (4.45).

Our dual field theory is a $2+1$ dimensional, strongly coupled gauge theory related to the deformed ABJM model [11] as explained in section 4.1. From a bottom-up perspective we have a nonconformal, strongly coupled gauge theory in $2+1$ dimensions at finite chemical potential χ and magnetic field B, holographically defined by the

gravity solution. The gauge group $U(1)^2$ in the gravitational theory corresponds to part of the global R-symmetry of the boundary field theory, and this group is weakly gauged to produce background magnetic and electric fields. The theory is also deformed by a bosonic triple trace operator[5]—that corresponds to the bulk scalar φ—whereby breaking the conformality of the theory and initiating an RG flow. The theory is non-conformal even at vanishing B and χ. This is clear from the running of the scalar φ when $b \neq 0$. Therefore we are dealing with a non-conformal strongly coupled gauge theory that contains both fermionic and bosonic fields in the adjoint representation of the gauge group. It is important to note however, that the deformation of the field theory by the operator Φ^3 is not relevant, in fact it is classically marginal, since the engineering dimension of this operator is three by dimensional analysis. It is also important to note that the source corresponding to the the operator Φ is set to zero in the field theory, see the discussion on page 12 of [236]. Therefore the only dimensionful scales in the theory, at vanishing temperature, are the electrostatic potential χ and the magnetic field B.

Below we discuss the implications of our findings in the holographic dual field theory and in supergravity.

NATURE OF THE QUANTUM CRITICAL POINT: First of all, as we showed in section 4.4.3 by studying the Polyakov loop, the quark potential and the entanglement entropy, the quantum critical point we find here does *not* correspond to a confinement-deconfiement type transition. However, it may correspond to spontaneous breaking of a flavor symmetry in the dual field theory. We already noted similarities between our findings and the earlier studies in $2+1$ dimensional Nambu-Jona-Lasinio models in section 4.3.4. In particular we observed that the dependence of the VeV of the scalar operator follows a similar pattern observed in these studies: there is agreement between the square-root scaling in the TG phase and the near critical region of the NJL model, as well as between the scaling in the BB phase and the $g > g_c$ region of the NJL model. There is one important difference in the latter case however. Comparison of equations (4.51) and (4.52) shows that while the magnetic field tends to increase the value of the condensate in the NJL model, it tends to destroy the condensate in our holographic model. The former phenomenon is called the *magnetic catalysis* [244, 245], a phenomenon well-established by perturbative and effective field theory calculations (see [243] for a recent review, see also a study of the phenomenon in the ABJM type models in [230]). Decrease of the condensate with B in confining $3+1$ dimensional gauge theories above the deconfinement temperature has also been observed both on the lattice [257], in the Sakai-Sugimoto model [258, 259] and in the hard-wall model [260], and it was termed the *inverse magnetic catalysis*. The same phenomenon also occurs in $2+1$ dimensions, as studies on the lattice, the NJL model and the NJL with Polyakov loop shows [261]. What we find here is the inverse magnetic catalysis at vanishing temperature in a holographic

5 As discussed in footnote **??**, we interpret the scalar field as having mixed boundary conditions. Other choices are possible for the bulk solution under consideration, leading to different holographic interpretations that are not of interest in this work.

dual of a strongly interacting gauge theory. One should understand this phenomenon from a microscopic point of view. We suspect that both strong interactions and non-conformality of our theory is essential in this respect. Firstly, as one can show in perturbative studies quite generally, there is no inverse magnetic catalysis when the interactions are weak [244, 245]. Secondly, even the strongest interactions cannot allow for a condensate, hence a fermion mass term, when the underlying theory is conformally invariant.

IMPLICATIONS FOR THE ABJM-TYPE MODELS: Regardless of the discussion above, it would be interesting to investigate possible patterns of flavor symmetry breaking in the ABJM model under magnetic field directly from the microscopic point of view. As discussed in [11] the superpotential enjoys a full $SU(4)$ flavor symmetry obtained by combining the $SU(2) \times SU(2)$ symmetry that rotates the A and B type superfield doublets separately, and the $SU(2)_R$ R-symmetry. The breaking $SU(4) \to SU(2) \times SU(2)$—that is very similar to the pattern in the NJL model above—would take place through the formation of a condensate in a non-conformal cousin of ABJM. This can happen either spontaneously through strong interactions, or explicitly with aid of an external magnetic field.

When the $\mathcal{N} = 2$ Supergravity theory considered here is embedded in $\mathcal{N} = 8$ Supergravity (as required if one is interested in ABJM as the dual theory), the stability of the gravity configuration needs to be discussed taking into account the full $\mathcal{N} = 8$ theory. In particular, it was shown in [225] that the $AdS_2 \times \mathbb{R}^2$ vacua are unstable in the $\mathcal{N} = 8$ theory for generic values of the parameters. These instabilities arise because charged scalars of the $\mathcal{N} = 8$ theory do not satisfy the AdS_2 BF bound. Notice that, in our analysis, also the supersymmetric configuration is thermodynamically disfavoured with respect to the thermal gas, at $T = 0$. This can be interpreted in the dual theory as the supersymmetric vacuum being disfavoured with respect to a scalar field condensate. In order to understand the BPS magnetic solution in the context of ABJM one should analyze the instability of such specific background along the lines of [224, 225, 226]. This will be left for future work.

APPLICATIONS TO CONDENSED MATTER THEORY: Despite its exotic nature, the ABJM theory at finite charge density comes very close to various realistic applications in two (spatial) dimensional condensed matter systems such as the cuprate superconductors and the various strongly coupled strange metals, see [7, 262, 263, 264] for reviews. The field theory we consider is a non-conformal, strongly coupled field theory related to ABJM in the manner explained in section 4.1. When put under external magnetic fields, this theory is quite interesting in view of condensed matter applications. It is long argued that resolution to the various puzzles concerning high T_c superconductivity may be associated with the presence of a quantum critical point under the superconducting dome [42]. Connections between superconductivity [243] and spontaneous symmetry breaking in the NJL type effective theories are also well-known, and our observations above may be interesting from this point of view. All in all, it remains to be seen whether the quantum criticality we found may serve as

a proxy for a strongly interacting quantum critical point that may underlie high T_c superconductivity. To explore this issue it is crucial to study our system at finite T and to introduce a scalar that is charged under the $U(1)$. It is also crucial to study correlators of e.g. composite fermionic operators and explore their behaviour near the quantum critical point.

Finally, it is very interesting to explore the fate of the phase that we found, in the regime of finite temperature. In particular we would like to know if there exists a phase separation line in the (T, B) plane, at fixed χ, of second order that ends on the quantum critical point in the vanishing T limit. It is also conceivable that the critical behavior we find extends into a true second order phase transition at finite T domain. Moreover, we would like to find what is the precise shape of the crossover lines that separate the critical and non-critical regions shown in figure 18. We plan to address these questions in the future.

OPEN QUESTIONS IN THE SUPERGRAVITY CONTEXT: Last but not least, our study raises interesting questions directly in the context of supergravity. First of all, our ensemble includes BPS solutions [227]. One may wonder how the BPS brane decays into the thermal gas solution, despite being stable with respect to small fluctuations in charge[6]. In general, supersymmetric solutions saturate a BPS bound of the form $M \geq |Q|$. For zero temperature solutions, the mass coincides with the system's free energy in the canonical ensemble. Thus, one explains the stability of the supersymmetric solution in the thermodynamic phase space. We considered however a *mixed canonical-grand canonical* ensemble, where the free energy is given by (4.26), thus saturation of the BPS bound is no more equivalent to non-perturbative thermodynamic stability. With the choice of this ensemble, we indeed find that in most of the parameter space except the locus of the critical point, the thermal gas is thermodynamically dominant at vanishing temperature.

It is interesting to ask if the thermal gas itself preserves any supersymmetry, and if so if it preserves more supersymmetries than the black brane. In this case, the thermodynamically favoured solution would be the most supersymmetric one. In order to address this question, one has to embed the theory we considered in $\mathcal{N} = 2$ $U(1)$-gauged Supergravity (a truncation of $\mathcal{N} = 8$ $SO(8)$ gauged theory where only the diagonal $U(1)$ in the Cartan of $SO(8)$ is gauged). Here, however, an electric-magnetic duality transformation affects not only the Maxwell fields, but also the gauging parameters. Such a transformation has been performed in [265] in the black hole case; the analogue, black brane 1/4- BPS constraint obtained with this transformation is $3B - q = 0$. One can then see that the thermal gas, having $q = 0$, cannot preserve supersymmetry for $B \neq 0$ (we find that the thermal gas cannot be supersymmetric for either choice of Killing spinors studied in the literature [221, 265, 266]). We

6 This can be done, for instance by computing the permittivity of the solution, defined as

$$\varepsilon = \left(\frac{\partial Q}{\partial \phi}\right)_T .$$

For the BPS configuration this quantity is positive, denoting stability with respect to charge fluctuations: the chemical potential of the black brane increases as a result of placing more charge on it.

cannot exclude less conventional duality transformations on the gauging that acts differently than in [265], but, since the origin of magnetic gauging parameters in M-theory is less understood [267], the analysis of these scenarios goes beyond the scope of the present analysis.

Finally, a pressing question relates to possible resolution of the thermal gas singularities in the full string theory. It will be very interesting to see if the singularities at $r = 3b$ and $r = -b$ can be excised through an enhançon mechanism found in the study of $D1$-$D5$ and $D2$-$D6$ systems, see [268].

APPENDIX OF CHAPTER 3

A.1 OTHER CLASSES OF ORBIFOLDS

Here we present the rest of the supersymmetric orbifold theories for completeness.

- **Orbifold II**: The second class of orbifolds are obtained by modding out super-affine theories by the same reflection symmetry as above. One has the following relations [160]:

$$\mathcal{Z}_{orbsaA,B}(R) = \frac{1}{2}\mathcal{Z}_{saA,B}(R) + const_{A,B} \tag{A.1}$$

and the following relation at the special radius [160]:

$$\mathcal{Z}_{orbsaA,B}(\sqrt{2}) = \mathcal{Z}_{cirA,B}(\sqrt{2})\,. \tag{A.2}$$

The partition functions are:

$$\begin{aligned} \mathcal{Z}_{orbsaA}(R) &= \frac{1}{2}\mathcal{Z}_{saA}(R) - \frac{1}{8}\ln\mu_0 \\ \mathcal{Z}_{orbsaB}(R) &= \frac{1}{2}\mathcal{Z}_{saB}(R) - \frac{1}{8}\ln\mu_0 \end{aligned} \tag{A.3}$$

These theories are seperately self dual under $R \to 2/R$.

- **Orbifold III**: The third class of orbifolds are obtained by twisting the circular theories by $(-1)^{F_s}R$. Note that this is only a symmetry in the oA theory. One obtains,

$$\mathcal{Z}_{orbA}(R) = \frac{1}{2}\mathcal{Z}_{cirA}(R) + const \tag{A.4}$$

and

$$\mathcal{Z}_{orbA}(1) = \mathcal{Z}_{saA}(2) \tag{A.5}$$

The result is:

$$\mathcal{Z}_{orbA}(R) = \frac{1}{2}\mathcal{Z}_{cirA}(R) - \frac{1}{8\sqrt{2}}\ln\mu_0 \tag{A.6}$$

We observe that orbA and orbB theories are exchanged under T-duality.

A.2 OSCILLATOR WAVEFUNCTIONS

We provide this section as a collection of the relations between various representations of normal/inverted harmonic oscillator wavefunctions.

A.2.1 *Normal Harmonic Oscilator*

We define the normal harmonic oscillator time independent Schroendinger equation $\hbar, m = 1$

$$\tfrac{1}{2}\left(-\partial_x^2 + \omega^2 x^2\right)\psi_n = \varepsilon_n \psi_n \,. \tag{A.7}$$

The Kronecker delta normalised eigenfunctions are

$$\psi_n(x) = \frac{1}{\sqrt{2^n n!}}\left(\frac{\omega}{\pi}\right)^{\frac{1}{4}} e^{-\frac{1}{2}\omega x^2} H_n(\sqrt{\omega}x) = \frac{1}{\sqrt{n!}}\left(\frac{\omega}{\pi}\right)^{\frac{1}{4}} D_n(\sqrt{2\omega}x)\,. \tag{A.8}$$

These wavefunctions satisfy Mehler's formula for the propagator (in real time)

$$\left(\frac{\omega}{2\pi i \sin\omega T}\right)^{\frac{1}{2}} e^{\frac{i\omega}{2\sin\omega T}\left[\left(\lambda_i^2+\lambda_j'^2\right)\cos\omega T - 2\lambda_i\lambda_j'\right]} = \sum_n \psi_n(\lambda_i)\psi_n(\lambda_j')e^{-i\omega(n+\frac{1}{2})T},$$

which we analytically continued to Euclidean time via $T = -i\beta$ to obtain equation (3.32).

A.2.2 *Inverted Harmonic Oscillator*

We want to solve the inverse harmonic oscillator time independent Schroendinger equation. Take the normal harmonic oscillator equation and let $\omega \to i$, and $x \to x/\sqrt{2}$. One then needs to solve:

$$\left(\partial_x^2 + \frac{x^2}{4}\right)\psi = \varepsilon\psi\,. \tag{A.9}$$

This is a particular form of the Weber differential equation

$$\left(\partial_z^2 + \nu + \tfrac{1}{2} - \frac{z^2}{4}\right)\psi = 0\,. \tag{A.10}$$

The solutions are the Parabolic cylinder functions (equivalently expressed via Whittaker functions W)

$$\begin{aligned} D_\nu(z) &= 2^{\frac{\nu}{2}+\frac{1}{4}} z^{-\frac{1}{2}} W_{\frac{\nu}{2}+\frac{1}{4},-\frac{1}{4}}(\frac{z^2}{2}), \\ D_{-\nu-1}(iz) &= 2^{\frac{-\nu}{2}-\frac{1}{4}} e^{i\pi/4} z^{-\frac{1}{2}} W_{\frac{-\nu}{2}-\frac{1}{4},-\frac{1}{4}}(-\frac{z^2}{2})\,. \end{aligned} \tag{A.11}$$

where $D_\nu(z), D_{-\nu-1}(\pm iz)$ are linearly independent. We are in the specific case where $\nu = i\varepsilon - \frac{1}{2}$, $ix^2 = z^2$, thus

$$\begin{aligned} D_{i\varepsilon-\frac{1}{2}}(e^{i\frac{\pi}{4}}x) &= \frac{2^{\frac{i\varepsilon}{2}} e^{-i\pi/8}}{x^{\frac{1}{2}}} W_{\frac{i\varepsilon}{2},-\frac{1}{4}}(\frac{ix^2}{2}), \\ D_{-i\varepsilon-\frac{1}{2}}(e^{i\frac{3\pi}{4}}x) &= \frac{2^{\frac{-i\varepsilon}{2}} e^{i\frac{3\pi}{8}}}{x^{\frac{1}{2}}} W_{\frac{-i\varepsilon}{2},-\frac{1}{4}}(-i\frac{x^2}{2}), \end{aligned} \tag{A.12}$$

are the two linearly independent solutions in our case and there is a degeneracy in the continuous energy spectrum. It is easy to see that they are also formally obtainable from the normal harmonic oscillator upon substituting $x \to x/\sqrt{2}$, $\omega = \pm i$ and $n = \pm i\varepsilon - \frac{1}{2}$, the normalization is different though.

Another useful basis of solutions are the delta function normalised even/odd parabolic cylinder functions [165] which we will denote by $\psi^{\pm}(\varepsilon, z)$

$$\begin{aligned}
&\psi^{+}(\varepsilon, x) = \\
&\left(\frac{1}{4\pi\sqrt{(1+e^{2\pi\varepsilon})}}\right)^{\frac{1}{2}} 2^{1/4}|\frac{\Gamma(1/4+i\varepsilon/2)}{\Gamma(3/4+i\varepsilon/2)}|e^{-ix^2/4}{}_1F_1(1/4-i\varepsilon/2, 1/2; ix^2/2) \\
&= \frac{e^{-i\pi/8}}{2\pi}e^{-\varepsilon\pi/4}|\Gamma(1/4+i\varepsilon/2)|\frac{1}{\sqrt{|x|}}M_{i\varepsilon/2,-1/4}(ix^2/2) \\
&\psi^{-}(\varepsilon, x) = \\
&\left(\frac{1}{4\pi\sqrt{(1+e^{2\pi\varepsilon})}}\right)^{\frac{1}{2}} 2^{3/4}|\frac{\Gamma(3/4+i\varepsilon/2)}{\Gamma(1/4+i\varepsilon/2)}|xe^{-ix^2/4}{}_1F_1(3/4-i\varepsilon/2, 3/2; ix^2/2) \\
&= \frac{e^{-3i\pi/8}}{\pi}e^{-\varepsilon\pi/4}|\Gamma(3/4+i\varepsilon/2)|\frac{x}{|x|^{3/2}}M_{i\varepsilon/2,1/4}(ix^2/2)\,.
\end{aligned} \tag{A.13}$$

Their normalisation is

$$\int_{-\infty}^{\infty} dx \sum_{a=\pm} \psi^a(\varepsilon_1, x)\psi^a(\varepsilon_2, x) = \delta(\varepsilon_1 - \varepsilon_2), \tag{A.14}$$

and

$$\int_{-\infty}^{\infty} d\varepsilon \sum_{a=\pm} \psi^a(\varepsilon, x_1)\psi^a(\varepsilon, x_2) = \delta(x_1 - x_2)\,. \tag{A.15}$$

The relation with the previous basis can be established using the following equations

$$\begin{aligned}
&D_{i\varepsilon-\frac{1}{2}}(e^{i\pi/4}x) = \\
&\frac{\sqrt{\pi}2^{i\varepsilon/2}e^{-i\pi/8}}{\Gamma(3/4-i\varepsilon/2)\sqrt{x}}M_{i\varepsilon/2,-1/4}(ix^2/2) - \frac{2\sqrt{\pi}2^{i\varepsilon/2}e^{-i\pi/8}}{\Gamma(1/4-i\varepsilon/2)\sqrt{x}}M_{i\varepsilon/2,1/4}(ix^2/2) \\
&D_{-i\varepsilon-\frac{1}{2}}(e^{i3\pi/4}x) = \\
&\frac{\Gamma(1/2-i\varepsilon)}{\sqrt{2\pi}}\left[e^{-\varepsilon\pi/2}e^{i\pi/4}D_{i\varepsilon-\frac{1}{2}}(e^{i\pi/4}x) + e^{\varepsilon\pi/2}e^{-i\pi/4}D_{i\varepsilon-\frac{1}{2}}(-e^{i\pi/4}x)\right].
\end{aligned} \tag{A.16}$$

A.2.3 *Mehler for parabolic cylinder*

The delta-function normalised odd/even parabolic cylinder functions $\psi^{\mp}(\varepsilon, x)$ satisfy the following formula [165]:

$$\begin{aligned}\langle x|e^{-2iTH}|y\rangle &= \int_{-\infty}^{\infty} d\varepsilon e^{i\varepsilon T} \sum_{a=\pm} \psi^a(\varepsilon, x)\psi^a(\varepsilon, y) \\ &= \frac{1}{\sqrt{4\pi i \sinh T}} \exp \frac{i}{4}\left[\frac{x^2+y^2}{\tanh T} - \frac{2xy}{\sinh T}\right], \end{aligned} \tag{A.17}$$

which is the analogue of Mehler's formula for the real-time ($T = -i\beta$) inverted H.O. propagator with the Hamiltonian A.9. This holds for $-\pi < ImT < 0$ or $ImT = 0$ with $ReT \neq 0$. To prove it one can use the general expression (7.694) in [269].
An equivalent expression can be found also in the basis of $D_{i\varepsilon-\frac{1}{2}}(z), D_{-i\varepsilon-\frac{1}{2}}(iz)$ using (7.77.3) of [269]

$$\begin{aligned}&\langle x|e^{-2iTH}|y\rangle = \\ &\frac{1}{\sqrt{4\pi i \sinh T}} \exp \frac{i}{4}\left[\frac{x^2+y^2}{\tanh T} - \frac{2xy}{\sinh T}\right] \\ &= \int_{-\infty}^{\infty} d\varepsilon e^{i\varepsilon T} \frac{e^{-\frac{1}{2}\varepsilon\pi}}{4\pi\cosh(\varepsilon\pi)} \\ &\left[D_{i\varepsilon-\frac{1}{2}}(e^{i\frac{\pi}{4}}x)D_{-i\varepsilon-\frac{1}{2}}(e^{i\frac{3\pi}{4}}y) + D_{i\varepsilon-\frac{1}{2}}(-e^{i\frac{\pi}{4}}x)D_{-i\varepsilon-\frac{1}{2}}(e^{i\frac{3\pi}{4}}y)\right], \end{aligned} \tag{A.18}$$

with the same restrictions in T. These expressions are most well suited to compute the transition amplitude in real time. To recover the Euclidean, inverted H.O. expression one needs to set $T = -i\beta$ in the above, (note that they will hold for $R < 1$, otherwise one needs to change the contour of integration to make them well behaved).

A.3 REPRESENTATION IN TERMS OF ANGLES (WILSON-LINES)

Instead of integrating out U one can first integrate out the M's in the expression

$$\mathcal{Z}_{n,N} = \int \mathcal{D}M\mathcal{D}M'\mathcal{D}U\langle UM'U^{\dagger}, \beta|M, 0\rangle = \int \mathcal{D}U I(U)\,. \tag{A.19}$$

If we define $A = 1/\tanh(\omega\beta)$, $B = 1/\sinh(\omega\beta)$, and remember to use blocks for the matrices after orbifolding we get

$$\begin{aligned} I(U) &= \omega^{-\frac{1}{2}(N-2n)^2}\left(\frac{B}{2\pi}\right)^{N^2/2}\int dM_1 dM_2 dM_1' dM_2' e^T, \quad U = \begin{pmatrix} U_1 & U_{12} \\ U_{21} & U_2 \end{pmatrix}, \\ K &= -\frac{A}{2}\mathrm{tr}(M_1^2 + M_1^{2\prime}) + B\mathrm{tr}(M_1 U_1 M_1' U_1^{\dagger} + M_1 U_{12} M_2' U_{12}^{\dagger}) + (1 \leftrightarrow 2)\,. \end{aligned} \tag{A.20}$$

Now the $U's$ are complex but satisfy certain conditions

$$\begin{aligned} U_1U_1^\dagger + U_{12}U_{12}^\dagger &= U_2U_2^\dagger + U_{21}U_{21}^\dagger = 1, \quad U_{12}U_{12}^\dagger = U_{21}U_{21}^\dagger \\ U_1U_{21}^\dagger + U_{12}U_2^\dagger &= U_2^\dagger U_{21} + U_{12}^\dagger U_1 = 0, \end{aligned} \tag{A.21}$$

and can be diagonalised by bi-unitary transformations such that they leave the measure invariant. We thus use the unitary matrices V_1, V_1', V_2, V_2' to get[1]

$$\begin{aligned} U_1 &= V_1 C V_1'^\dagger, \quad U_2 = V_2 \begin{pmatrix} C & 0 \\ 0 & 1 \end{pmatrix} V_2'^\dagger, \\ U_{12} &= -V_1(D,0)V_2'^\dagger, \quad U_{21} = V_2 \begin{pmatrix} D \\ 0 \end{pmatrix} V_1^\dagger, \end{aligned} \tag{A.22}$$

with

$$C_{ij} = \cos\theta_i \delta_{ij}, \quad D_{ij} = \sin\theta_i \delta_{ij}, \quad 0 \le \theta_i \le \frac{\pi}{2}. \tag{A.23}$$

This can be also easily achieved after exponentiation of the zero mode of A that has only non-zero the diagonal components of the off-diagonal blocks.
Since the measure of M's is invariant under a unitary transformation, we can write the four matrix coupling term of K as

$$\mathrm{tr}(M_1 C M_1' C + M_1 D R D + R D M_1' D + R C R' C + S S'^\dagger C + S^\dagger C S' + T T') \tag{A.24}$$

where we have written M_2 and M_2' (which are $(N-n)\times(N-n)$ matrices) as

$$M_2 = \begin{pmatrix} R & S \\ S^\dagger & T \end{pmatrix}, \quad M_2' = \begin{pmatrix} R' & S' \\ S'^\dagger & T' \end{pmatrix} \tag{A.25}$$

with R, R' $n \times n$ matrices. Integration over T, T' will yield a constant factor

$$(2\pi)^{(N-2n)^2} \tag{A.26}$$

Integrations over S, S' yield

$$(2\pi)^{2n(N-2n)} \prod_i^n \left(\frac{B^2}{1 + B^2 \sin^2\theta_i} \right)^{N-2n} \tag{A.27}$$

and integrations over R, M_1 give

$$(2\pi)^{2n^2} \prod_{i,j} \left(\frac{1}{(1 + B^2\sin^2(\theta_i + \theta_j)(1 + B^2 \sin^2(\theta_i - \theta_j)} \right)^{\frac{1}{2}} \tag{A.28}$$

1 Note that any complex matrix can diagonalized by bi-unitary transformations. Also the first line of equation A.21 implies that $U_1U_1^\dagger$ and $U_{12}U_{12}^\dagger$ can be simultaneously diagonalized.

Thus altogether we get

$$I = \left(\frac{2\pi B}{\omega}\right)^{\frac{(N-2n)^2}{2}} \prod_i^n \left[\frac{B^2}{1+B^2\sin^2\theta_i}\right]^{N-2n} \prod_{i,j}^n \left[\frac{B^4}{(1+B^2\sin^2(\theta_i+\theta_j)(1+B^2\sin^2(\theta_i-\theta_j)}\right]^{\frac{1}{2}} \tag{A.29}$$

It is also useful to massage this expression into

$$I = \left[\frac{2\pi B}{\omega}\right]^{\frac{(N-2n)^2}{2}} \prod_i^n \left[\frac{2}{\cosh\tilde{\beta}-\cos\theta_i}\right]^{N-2n} \prod_{i,j} \left[\frac{4}{(\cosh\tilde{\beta}-\cos(\theta_i+\theta_j)(\cosh\tilde{\beta}-\cos(\theta_i-\theta_j)}\right]^{\frac{1}{2}} \tag{A.30}$$

where now the angles run $0 \le \theta_k \le \pi$ and $\tilde{\beta} = 2\omega\beta = \omega\beta_c$.
One can also express the part of the integrand of the canonical partition function that is not coming from the measure as the determinant of a differential operator Q,

$$I = \left(\frac{2\pi}{\quad}\right)^{\frac{1}{2}(N-2n)^2} (\det Q)^{-\frac{1}{4}}, \tag{A.31}$$

where Q is a differential operator on a circle of length 2β.

$$Q = -D_0^2 + {}^2 = -\partial_0^2 + 2i\alpha\partial_0 + \alpha^2 + \omega^2, \tag{A.32}$$

where α is a constant gauge field in the adjoint representation related to θ as $\theta_i = \alpha_i\beta$. Q acts on the matrices M as

$$[Q, M] = \partial_0 M + i[\alpha, M] \tag{A.33}$$

and

$$[\alpha, M]_{ij} = \alpha^{adj}_{ij,kl} M_{kl} = \alpha_{ik}M_{kj} - M_{ik}\alpha_{kj} \tag{A.34}$$

$$(UMU^\dagger)_{ij} = \exp[i\beta\alpha]^{adj}_{ij,kl} M_{kl}, \tag{A.35}$$

with

$$\alpha^{adj}_{ij,kl} = \alpha_{ik}\delta_{jl} - \alpha_{lj}\delta_{ik}, \qquad \exp[i\beta\alpha]^{adj}_{ij,kl} = U_{ik}U^\dagger_{lj}. \tag{A.36}$$

Thus in the momentum representation one can write

$$\det\left(-D_0^2 + {}^2\right) = \det_{matrix} \prod_{n=-\infty}^{\infty} \left[\left(\frac{2\pi n}{\beta} - \alpha^2\right)^2 + {}^2\right] = \tag{A.37}$$

$$= \det_{matrix} 2\left(\cosh(\beta) - \cos(\beta\alpha)\right), \tag{A.38}$$

where α is a matrix and the determinant is with respect of this matrix structure. If the gauge field is $A_{N\times N} = diag(\alpha_1, \alpha_2, ..., \alpha_n, -\alpha_1, -\alpha_2, ..., -\alpha_n, 0, ..., 0)$, then $\alpha^{adj}_{ij,kl} = (\alpha_i - \alpha_j)\delta_{ik}\delta_{jl}$ and A.31 equals A.30.

A.3.1 *Measure*

One needs also to compute the measure for $\mathcal{D}U$. This is achieved by defining the metric on the tangent space of the group $ds^2 = \mathrm{tr}(UdU^\dagger UdU^\dagger)$ and then computing its determinant to get $(0 \le \theta_i \le \pi)$

$$J_n(\theta) = \frac{1}{2^n n!(2\pi)^n}\prod_{i<j}^{n}\sin^2\left(\frac{\theta_i-\theta_j}{2}\right)\sin^2\left(\frac{\theta_i+\theta_j}{2}\right)\prod_{k=1}^{n}\sin\theta_k\sin^{2(N-2n)}\left(\frac{\theta_k}{2}\right). \tag{A.39}$$

One finds that this is exactly the measure on the symmetric space of positive curvature defined as the coset $\frac{SU(N_1+N_2)}{SU(N_1)\times SU(N_2)\times U(1)}$ (Cartan Class $AIII$) [270] with $N_1 \equiv n, N_2 \equiv (N-n)$. Again we see that $n = N/2$ is special and the measure simplifies. The normalization factor $(2\pi)^n$ corresponds to the stability group $U(1)^{\otimes n}$ and the factor $(2^n n!)$ to the discrete Weyl-group [271].

A.3.2 *Pfaffian in regular representation*

In the case of $n = N/2$ we find

$$\mathcal{Z}_n = \int_0^\pi \prod_i d\theta_i J_n(\theta)\prod_{i,j}^{n}\left(\frac{4}{(\cosh\tilde{\beta}-\cos(\theta_i+\theta_j)(\cosh\tilde{\beta}-\cos(\theta_i-\theta_j)}\right)^{\frac{1}{2}} \tag{A.40}$$

where the angles are in $0 \le \theta_i \le \pi$.

One then unfolds the denominator using for example

$$\frac{1}{\cosh\tilde{\beta}-\cos(\theta_i+\theta_j)} = \frac{2q}{(1-qz_iz_j)(1-qz_i^*z_j^*)}, \quad q = e^{-\tilde{\beta}},\ z_i = e^{i\theta_i} \tag{A.41}$$

and similarly the measure

$$J_n = \frac{1}{i^n 2^{2n^2} n!(2\pi)^n}\prod_{i<j}^{n}(z_i-z_j)(z_i-z_j^*)(z_i^*-z_j)(z_i^*-z_j^*)\prod_{k}^{n}(z_k-z_k^*) \tag{A.42}$$

We then define $z_i = e^{i\theta_i}$, $\bar{z}_{1..2n} = (z_{1..n}, z^*_{1..n})$. The partition function now is

$$\mathcal{Z}_n = \frac{1}{n!}\int_0^\pi \prod_{k=1}^{n}\frac{d\theta_k}{2\pi i}\frac{2^{-\frac{1}{2}}}{\sqrt{(\cosh(\tilde{\beta})-\cos(2\theta_k))}}\prod_{i<j}^{2n}\frac{q^{1/2}(\bar{z}_i-\bar{z}_j)}{1-q\bar{z}_i\bar{z}_j} \tag{A.43}$$

From this form, one can use Schur's Pfaffian identity [272, 273]

$$\prod_{i<j}^{2n} \frac{x_i - x_j}{1 - x_i x_j} = \mathrm{pf}\left(\frac{x_i - x_j}{1 - x_i x_j}\right)_{1\le i,j\le 2n} \tag{A.44}$$

for $x_i = q^{\frac{1}{2}} \bar{z}_i$ to compactly write

$$\mathcal{Z}_n = \frac{1}{n!}\int_0^{\pi} \prod_{k=1}^{n} \frac{d\theta_k}{2\pi i} \prod_{k=1}^{n} \frac{q^{\frac{1}{2}}}{\sqrt{\left(1 - q z_k^2\right)\left(1 - q z_k^{*2}\right)}} \mathrm{pf}\begin{pmatrix} \frac{q^{1/2}(z_i - z_j)}{1 - q z_i z_j} & \frac{q^{1/2}(z_i - z_j^*)}{1 - q z_i z_j^*} \\ \frac{q^{1/2}(z_i^* - z_j)}{1 - q z_i^* z_j} & \frac{q^{1/2}(z_i^* - z_j^*)}{1 - q z_i^* z_j^*} \end{pmatrix} \tag{A.45}$$

This is the expression that we use in the main text. This structure has appeared in connection with Ginibre's orthogonal ensemble, for more details see [274, 204] and references within.

A.4 GRAND CANONICAL FOR $n = 0$

The grand canonical partition function for $n = 0$ is a partial-theta

$$\mathcal{Z}_G = \sum_{N=0}^{\infty} x^N Q^{\frac{N^2}{2}} \tag{A.46}$$

with $Q = Z_1^{op}$ the 1-particle partition function with open boundary conditions and $x = e^{\beta\mu}$ the chemical potential. Little is known about partial theta functions as compared to the usual theta functions. In [275] one is able to find the proof for the following formula originally found by Ramanujan

$$\begin{aligned} \sum_{N=0}^{\infty} x^N Q^{\frac{N^2}{2}} &= \prod_{n=1}^{\infty}\left(1 - \frac{x}{f(n)}\right) \\ \frac{1}{f(n)} &= -Q^{n-\frac{1}{2}}\left(1 + y_1(n) + y_2(n) + \mathcal{O}(Q^{\frac{3}{2}n(n+1)})\right) \end{aligned} \tag{A.47}$$

with y's computable in a recursive fashion

$$\begin{aligned} y_1(n) &= \frac{\sum_{j=n}^{\infty}(-1)^j Q^{\frac{1}{2}j(j+1)}}{\sum_{j=0}^{\infty}(-1)^j(2j+1)Q^{\frac{1}{2}j(j+1)}} \\ y_2(n) &= \frac{\left(\sum_{j=n}^{\infty}(j+1)(-1)^j Q^{\frac{1}{2}j(j+1)}\right)\left(\sum_{j=n}^{\infty}(-1)^j Q^{\frac{1}{2}j(j+1)}\right)}{\left(\sum_{j=0}^{\infty}(-1)^j(2j+1)Q^{\frac{1}{2}j(j+1)}\right)^2} \\ y_3(n) &= \ldots \end{aligned} \tag{A.48}$$

It is amusing to note that these terms resemble the rotational partition function of diatomic molecules [276]. It is also easy to see that for large segment as $\beta \to \infty$, $Q \to q_c^{\frac{1}{2}}$ and $y_n \to 0$ leaving

$$\mathcal{Z}_G \approx \prod_{n=0}^{\infty} \left(1 + x q_c^{\frac{1}{2}(n+\frac{1}{2})} \right) \tag{A.49}$$

We thus observe that the leading contribution is half the one of the circle in the large radius limit. Finally, it would be interesting to study further the thermodynamic properties of equation A.47, since it is in a form (entire function) that the Lee-Yang theorem can apply [276]. In particular a sum of positive terms does not allow for a phase transition - no zeros for x on the positive real axis, thus a phase transition is only possible if $f(n)$ can change sign for some value of β.

A.5 HILBERT TRANSFORM PROPERTIES

In this Appendix we collect some of the properties of the Hilbert transform which can be found in [277].
The Hilbert transform on the real line $x \in \mathbb{R}$ of a function $f(x)$ is defined as

$$\mathcal{H}[f](x) = \frac{1}{\pi} \mathcal{P} \int_{-\infty}^{\infty} \frac{f(y)dy}{x-y} \tag{A.50}$$

with $\mathcal{P}$ denoting the principal value. Some properties of the transform are

- The Hilbert transform commutes with complex conjugation $(\mathcal{H}[f])^* = \mathcal{H}[f^*]$.
- It satisfies linearity $\mathcal{H}[af_1 + bf_2] = a\mathcal{H}[f_1] + b\mathcal{H}[f_2]$.
- The linearity of the Hilbert transform also means that if one has a series expansion of a function $f = \sum_k f_k$ then $\mathcal{H}[f] = \sum_k \mathcal{H}[f]_k$.
- It has the parity property of exchanging even with odd functions.
- The Hilbert transform relates the real and imaginary part of a function (Kramers-Kronig relations). As an example if $f(z) = g + ih$ is analytic in the upper half complex plane then $h(x) = -\mathcal{H}[g](x)$ and thus $\int_{-\infty}^{\infty} g\mathcal{H}[g]dx = 0$. Moreover $\mathcal{H}[g](x) = h[x]$.
- The combination with fourier transform $\mathcal{F}$ gives $\mathcal{F} \circ \mathcal{H}[f](x) = -i\,\mathrm{sgn}(x)\mathcal{F}[f](x)$.
- $\mathcal{H}^2 = -I$ and thus the inverse is $\mathcal{H}^{-1} = -\mathcal{H}$. The eigenvalues of the Hilbert transform are $\lambda = \pm i$.
- The Hilbert transform is skew adjoint $\mathcal{H}^\dagger = -\mathcal{H}$.

- If $g(x) = \mathcal{H}[f](x)$ then $\mathcal{H}[f](ax+b) = \mathrm{sgn}(a)g(ax+b)$. Generically the Hilbert transform commutes with translation and positive dilations but anti-commutes with reflection.
- The Hilbert transform commutes with the derivative operator.
- The Hilbert transform commutes with $SL(2,\mathbb{R})$ generators i.e with unitary operators U_g on the space $L^2(\mathbb{R})$ acting as

$$U_g^{-1} f(x) = (cx+d)^{-1} f\left(\frac{ax+b}{cx+d}\right), \quad \left\{ g = \begin{pmatrix} a & b \\ c & d \end{pmatrix} : a,b,c,d \in \mathbb{R},\ ad-bc=1 \right\}. \tag{A.51}$$

Moreover the following properties hold:
For an integer $n \geq 0$, $g(x) = \mathcal{H}[f](x)$

$$\mathcal{H}[x^n f(x)] = x^n g(x) - \frac{1}{\pi} \sum_{k=0}^{n-1} x^k \int_{-\infty}^{\infty} t^{n-1-k} f(t) dt \tag{A.52}$$

Hardy:

$$\int_{-\infty}^{\infty} dx \mathcal{H}[f](x) g(x) = -\int_{-\infty}^{\infty} dx f(x) \mathcal{H}[g](x) \tag{A.53}$$

Hardy-Poincare-Bertrand:

$$\frac{1}{\pi}\mathcal{P}\int_{-\infty}^{\infty} \frac{f(x)dx}{x-t} \frac{1}{\pi}\mathcal{P}\int_{-\infty}^{\infty} \frac{g(y)dy}{y-x} = \frac{1}{\pi}\mathcal{P}\int_{-\infty}^{\infty} g(y)dy \frac{1}{\pi}\mathcal{P}\int_{-\infty}^{\infty} \frac{f(x)dx}{(x-t)(y-x)} - f(t)g(t) \tag{A.54}$$

One can define projection operators as follows:

$$P_{\pm} = \frac{1}{2}\left(I \pm i\mathcal{H}\right) \tag{A.55}$$

Then one can easily see that they satisfy the properties of projection operators (idempotent conditions) $P_{\pm}^2 = P_{\pm}$.

A.6 THE KERNEL

A.6.1 *Kernel in Energy basis*

One can write down the form of the kernel in energy eigen-states and try to diagonalise from there. One has (after symmetrising appropriately):

$$\langle m|e^{-\frac{\beta}{2}\hat{H}}\hat{\mathcal{O}}e^{-\frac{\beta}{2}\hat{H}}|n\rangle = \\ \frac{2^{3+\frac{m+n}{2}}}{\sqrt{m!n!}}\frac{e^{-\frac{\omega\beta}{2}(m+n+1)}\sqrt{\pi}}{n-m}\left[\frac{1}{\Gamma(-m/2)\Gamma(\frac{-n+1}{2})}+\frac{1}{\Gamma(-n/2)\Gamma(\frac{-m+1}{2})}\right]. \tag{A.56}$$

To prove this formula one first has to compute $\langle m|\hat{\mathcal{O}}|n\rangle$ and it is easier to do so in momentum basis where the Hilbert transform just becomes a signum function, see appendix A.5

$$\langle m|\hat{\mathcal{O}}|n\rangle = -i\int_{-\infty}^{\infty}dp\,\mathrm{sgn}(p)\psi_m(p)\psi_n(p) \tag{A.57}$$

with $\psi_m(p)$ the Hermite functions. Note that this is non-zero only if m,n are odd/even or even/odd respectively. One can also form the full kernel by computing the element:

$$\langle n_1|e^{-\frac{\beta}{2}\hat{H}}\hat{\mathcal{O}}e^{-\beta\hat{H}}\hat{\mathcal{O}}e^{-\frac{\beta}{2}\hat{H}}|n_2\rangle = \frac{\pi 2^{6+\frac{n_2+n_1}{2}}}{\sqrt{n_1!n_2!}}e^{-\frac{\omega\beta}{2}(n_1+n_2+1)}\times \\ \sum_m \frac{2^m e^{-\omega\beta(m+1/2)}}{m!(n_1-m)(m-n_2)}\left(\frac{1}{\Gamma(-n_1/2)\Gamma(\frac{-m+1}{2})}\frac{1}{\Gamma(-m/2)\Gamma(\frac{-n_2+1}{2})}+perm\right) \tag{A.58}$$

Now this kernel can be non-zero only if both $n_{1,2}$ are even or odd and the states that run through the sum are then only odd or even respectively. In either case, only one term contributes in the sum and in particular for $n_{1,2}$ odd we get ($q=e^{-\omega\beta_c}$):

$$\langle n_1|\hat{\rho}|n_2\rangle = \frac{q^{\frac{1}{4}(n_1+n_2+2)}2^{6+\frac{n_2+n_1}{2}}}{\Gamma(\frac{-n_1}{2})\Gamma(\frac{-n_2}{2})\sqrt{n_1!n_2!}}\times \\ \frac{n_2\,{}_2F_1\left(\frac{1}{2},-\frac{n_1}{2};1-\frac{n_1}{2};q\right)-n_1\,{}_2F_1\left(\frac{1}{2},-\frac{n_2}{2};1-\frac{n_2}{2};q\right)}{n_1{}^2n_2-n_1n_2{}^2}, \tag{A.59}$$

while for $n_{1,2}$ even

$$\langle n_1|\hat{\rho}|n_2\rangle = \frac{q^{\frac{1}{4}(n_1+n_2+2)}2^{6+\frac{n_2+n_1}{2}}}{\Gamma(\frac{-n_1+1}{2})\Gamma(\frac{-n_2+1}{2})\sqrt{n_1!n_2!}}\frac{q^{\frac{n_2}{2}}B_q\left(\frac{1}{2}-\frac{n_2}{2},-\frac{1}{2}\right)-q^{\frac{n_1}{2}}B_q\left(\frac{1}{2}-\frac{n_1}{2},-\frac{1}{2}\right)}{4(n_1-n_2)}$$

which can also be rewritten in terms of ${}_2F_1$. From this expression we can also match the formulas in A.7.5 for $\hat{\mathcal{O}}^2$ if we set $\beta=0$.

A.6.2 *Kernel in elliptic functions*

One can massage a bit the integral equation (3.89), by adding/subtracting information from the second sheet. In terms of the torus this means to form (the parentheses in both sides of the equation stand for the even/odd case)

$$\lambda\left(X(u)\,(\pm)\,X(u+2K)\right) = -2q^{\frac{1}{2}}\int_{C_1+C_2}\frac{dv}{2\pi i}\begin{pmatrix} q\,\mathrm{sn}\,v\,\mathrm{cn}^2\,u \\ \mathrm{sn}\,u\,\mathrm{dn}^2\,v\end{pmatrix}\frac{X(v)}{\mathrm{dn}^2\,v-\mathrm{cn}^2\,u}, \tag{A.60}$$

where the denominator can be also written as $\mathrm{sn}^2\,u - q^2\,\mathrm{sn}^2\,v$. One can bring this equation into the following final form

$$\lambda X_{(\pm)}(u) = -q^{\frac{1}{2}}\int_{C_1+C_2}\frac{dv}{2\pi i}\begin{pmatrix} q\,\mathrm{sn}\,v\,\mathrm{cn}^2\,u \\ \mathrm{sn}\,u\,\mathrm{dn}^2\,v\end{pmatrix}\frac{X_{(\pm)}(v)}{\mathrm{dn}^2\,v-\mathrm{cn}^2\,u} \tag{A.61}$$

with $X_{(\pm)}(u) = X(u)\,(\pm)\,X(u+2K)$.

A.6.3 *Trace of the kernel*

The trace of the kernel can be computed to be (also using equation 3.78)

$$\begin{aligned}\mathrm{tr}\,\hat{\rho} &= \frac{1}{\sqrt{2}\sinh(\tilde{\beta}/2)}\int_0^\pi\frac{d\theta}{2\pi}\frac{\sin\theta}{\sqrt{\cosh\tilde{\beta}-\cos(2\theta)}} \\ &= \frac{1}{2\pi\sinh(\tilde{\beta}/2)}\tan^{-1}\frac{1}{\sinh(\tilde{\beta}/2)}\end{aligned} \tag{A.62}$$

Due to the branch-cut structure of this expression, it is useful to represent this function in terms of an integral with the integrand having simple poles

$$\mathrm{tr}\,\hat{\rho} = \frac{1}{2\pi\sinh(\tilde{\beta}/2)}\arctan\left(\frac{1}{\sinh(\tilde{\beta}/2)}\right) = \int_0^\pi\frac{d\theta}{2\pi}\frac{\cos(\theta/2)}{\cosh(\tilde{\beta})-\cos(\theta)} \tag{A.63}$$

(keep in mind that $\tilde{\beta} = \omega\beta_{circle} = 2\omega\beta_{orb}$). To discuss the inverse oscillator one needs to set $\omega \to -i\omega$. One then finds

$$\mathrm{tr}\,\hat{\rho}_{inv} = \frac{-1}{2\pi\sin(\omega\beta_c/2)}\tanh^{-1}\left(\frac{1}{\sin(\omega\beta_c/2)}\right) = \int_0^\pi\frac{d\theta}{2\pi}\frac{\cos(\theta/2)}{\cos(\omega\beta_c)-\cos(\theta)} \tag{A.64}$$

An analogous formula for the circle is [93]

$$Z^{inv}_{circ}(\beta_c) = \sum_{k=0}^{\infty} e^{i\omega\beta_c(k+\frac{1}{2})} = \frac{i}{2\sin(\omega\beta_c/2)} = \int_0^\pi\frac{d\theta}{2\pi}\frac{1}{\cos(\omega\beta_c/2)-\cos(\theta)}$$

(A.65)

If we define the twisted partition function [93]

$$Z(\theta,\beta_c)=\frac{1/2}{\cos\omega\beta_c-\cos\theta} \tag{A.66}$$

we understand both results as a 1-particle partition function derived from averaging over twist angles with a different weight for the orbifold and circle (after extending due to symmetry the integrals for $\theta'\in[-\pi,\pi]$). Another useful representation is

$$Z(\theta,\beta_c)=\int_{-\infty}^{+\infty}d\epsilon\, e^{-\beta_c\epsilon}\rho(\theta,\epsilon)=\frac{1}{\sin\theta}\int_{-\infty}^{+\infty}d\epsilon\, e^{-\beta_c\epsilon}\frac{\sinh\frac{\epsilon}{\omega}(\pi-\theta)}{\sinh\frac{\epsilon}{\omega}\pi} \tag{A.67}$$

which holds for $0<\theta<2\pi$ and $\rho(\theta,\epsilon)$ is the twisted density of states. From this one finds a closed formula for the twisted dos:

$$\rho(\theta,\epsilon)=\frac{\sinh\frac{\epsilon}{\omega}(\pi-\theta)}{\sinh\frac{\epsilon}{\omega}\pi\sin\theta} \tag{A.68}$$

and also an expression that gives away the spectrum

$$\rho(\theta,\epsilon)=\sum_{m=-\infty}^{\infty}e^{im\theta}\rho^{(m)}(\epsilon)=\frac{1}{\pi}\sum_{k=0}^{\infty}\sum_{m=-\infty}^{\infty}\frac{e^{im\theta}(\frac{|m|+1}{2}+k)}{(\frac{\epsilon}{\omega})^2+(k+\frac{|m|+1}{2})^2}+\delta(\theta)\log\Lambda^2 \tag{A.69}$$

note in particular the logarithmic divergence at $\theta=0$ that is regulated putting a wall at some cutoff Λ and neglecting any cutoff dependent quantities in the double scaling limit. In this equation $\rho^m(\varepsilon)=-\frac{1}{\pi}Re\Psi(i\frac{\varepsilon}{\omega}+\frac{|m|+1}{2})$ is the Hydrogen atom density of states (discrete spectrum) which should be contrasted with the H.O. density of states $\rho_{H.O.}(\varepsilon)=-\frac{1}{2\pi}Re\Psi(i\frac{\varepsilon}{\omega}+\frac{1}{2})$.

A.6.4 *1-particle density of states*

From the partition function $Z(\beta)$, one computes the density of states using

$$\rho_d(\epsilon)=\int_{c-i\infty}^{c+i\infty}\frac{d\beta}{2\pi i}Z(\beta)e^{\beta\epsilon} \tag{A.70}$$

The difficulty in our case is that one needs again to study very well the pole and branch cut structure of the integrand. We will instead try to use the integral representation for the partition function of the orbifold to write

$$\rho_o(\epsilon)=\frac{1}{2}\int_{c-i\infty}^{c+i\infty}\frac{d\beta_c}{2\pi i}\int_0^{\pi}\frac{d\theta}{2\pi}\frac{\cos(\theta/2)}{\cos(\omega\beta_c)-\cos(\theta)}e^{\beta_c\epsilon} \tag{A.71}$$

with c an infinitesimal positive regulator. Interchanging the integrations one picks the poles at the negative β_c axis $\beta_c=2n\pi\pm\theta$ and sums over the residues. There

is a catch when $\theta \to 0$, since then two poles merge and the singularity pinches the contour. In any case, the same singularity appears also in the analogous formula of the circle A.65 and will just reproduce the irrelevant logarithmic divergence. The result is

$$\rho_o(\epsilon) = \int_0^\pi \frac{d\theta}{2\pi} \frac{\cos(\theta/2)}{\sin(\theta)} \frac{\sinh \frac{\epsilon}{\omega}(\pi-\theta)}{\sinh \frac{\epsilon}{\omega}\pi} = \int_0^\pi \frac{d\theta}{2\pi} \cos(\theta/2)\rho(\theta,\epsilon) \quad \text{(A.72)}$$

It is thus easy to see that this result is equivalent to the one we would get if we just integrate over the twisted dos with the appropriate weight. Now this integral can be performed indefinite to get a result in terms of hypergeometric functions ${}_2F_1$. Taking the limit $\theta \to 0$ and subtracting the expected logarithmic divergence, we find a finite piece

$$\begin{aligned}
&\rho^0(\varepsilon) = \\
&\frac{1}{4\pi}\left(i\pi - 2\gamma + \frac{e^{-\pi\frac{\epsilon}{\omega}}}{\sinh(\pi\frac{\epsilon}{\omega})}\Psi\left(-i\frac{\epsilon}{\omega}+\frac{1}{2}\right) - \frac{e^{\pi\frac{\epsilon}{\omega}}}{\sinh(\pi\frac{\epsilon}{\omega})}\Psi\left(i\frac{\epsilon}{\omega}+\tfrac{1}{2}\right)\right) \\
&= \frac{i}{2} - \frac{1}{2\pi}\gamma - \frac{1}{2\pi} Re\Psi\left(i\frac{\epsilon}{\omega}+\frac{1}{2}\right) + i\frac{1}{2\pi}\frac{\cosh(\pi\frac{\epsilon}{\omega})}{\sinh(\pi\frac{\epsilon}{\omega})} Im\,\Psi\left(i\frac{\epsilon}{\omega}+\tfrac{1}{2}\right),
\end{aligned} \quad \text{(A.73)}$$

that contains the H.O. dos $\rho_{HO}(\epsilon) = -\frac{1}{2\pi} Re\Psi\left(i\frac{\epsilon}{\omega}+\frac{1}{2}\right)$, and imaginary pieces. From the π limit we get[2]

$$\rho^\pi(\epsilon) = \frac{1}{4\pi\sinh(\frac{\epsilon}{\omega}\pi)}\left[Im\,\Psi\left(i\frac{\epsilon}{2\omega}+\frac{1}{4}\right) - Im\,\Psi\left(i\frac{\epsilon}{2\omega}+\frac{3}{4}\right)\right] \quad \text{(A.74)}$$

One then notices that the 1-particle orbifold density of states is $\rho_o(\epsilon) = \rho_{H.O.}(\epsilon) + \rho_{twisted} + \rho_{Im}(\varepsilon)$, with the twisted piece

$$\begin{aligned}
\rho_{twisted}(\epsilon) &= \frac{1}{4\pi\sinh(\frac{\epsilon}{\omega}\pi)}\left[Im\,\Psi\left(i\frac{\epsilon}{2\omega}+\frac{1}{4}\right) - Im\,\Psi\left(i\frac{\epsilon}{2\omega}+\frac{3}{4}\right)\right] \\
&= \frac{1}{4\pi\sinh(\frac{\epsilon}{\omega}\pi)} Im \int_0^\infty dt \frac{e^{-i\frac{\epsilon}{\omega}t}}{\cosh(\frac{t}{2})}
\end{aligned} \quad \text{(A.75)}$$

where we used the integral representation of the digamma function.

A.7 APPROXIMATE METHODS FOR LARGE β

Here we give more details on the large β approximation to the canonical partition function.

2 One nice thing to note is that the twisted part of the dos does not require a cutoff in accordance with the discussion in [93].

A.7.1 *Circle in angles*

It is easy to expand formula 3.61 for large β_c to find

$$\mathcal{Z}_N \approx q^{\frac{1}{2}N^2} \frac{1}{N!} \int_0^{2\pi} \prod_{k=1}^{N} \frac{d\theta_k}{2\pi} |\Delta(e^{i\theta})|^2 (1+\mathcal{O}(q)) = q^{\frac{1}{2}N^2}(1+\mathcal{O}(q)) \quad \text{(A.76)}$$

where one can use the Selberg integral [278] to perform the integration that cancels the factorial.
Thus we find again $\mathcal{F} = \beta_c E_0 + \mathcal{O}(e^{-\beta_c \omega})$.

A.7.2 *Generic n in angles*

One can expand eq. 3.62 for large β and relating $q_c = q_o^2$ to find

$$\begin{aligned} \mathcal{Z}_n &\approx q_c^{\frac{(N-2n)^2}{4}} q_c^{N-2n} q_c^{n^2} (1+\mathcal{O}(q_c)) \int_0^{\pi} \prod_k d\theta_k J_n(\theta) \\ &= q_c^{\frac{N^2}{4}} (1+\mathcal{O}(q_c)) \frac{1}{n!} \prod_{j=0}^{n-1} \frac{\Gamma(1+j)\Gamma(2+j)\Gamma(N-2n+1+j)}{\Gamma(N-n+j+1)}, \end{aligned} \quad \text{(A.77)}$$

where we used again the Selberg integral to compute the integral. We find that the leading in β_c term will give half the Free-energy of the circle for any n.

A.7.3 *Generic n in eigenvalues of M*

We start by the following generalization of the Cauchy identity [279]

$$\frac{\prod_{i<j}^{n}(x_i - x_j) \cdot \prod_{a<b}^{N-n}(y_a - y_b)}{\prod_{i=1}^{n}\prod_{a=1}^{N-n}(x_i - y_a)} = (-1)^{n(N-2n)} \det \begin{pmatrix} \frac{1}{x_1-y_1} & \cdots & \frac{1}{x_1-y_{N-n}} \\ \vdots & \ddots & \vdots \\ \frac{1}{x_n-y_1} & \cdots & \frac{1}{x_n-y_{N-n}} \\ y_1^{N-2n-1} & \cdots & y_{N-n}^{N-2n-1} \\ \vdots & \ddots & \vdots \\ y_1^0 & \cdots & y_{N-n}^0 \end{pmatrix}. \quad \text{(A.78)}$$

where on the right hand side, the upper $N \times N-n$ submatrix and the lower $(N-2n) \times n$ submatrix are given respectively by

$$\left(\frac{1}{x_i - y_a}\right)_{\substack{1\le i\le n \\ 1\le a\le N-n}}, \quad (y_a^{N-2n-p})_{\substack{1\le p\le N-2n \\ 1\le a\le N-n}}. \quad \text{(A.79)}$$

One can now perform the y integrations to obtain

$$\int d^n x d^{N-n} y \det_{N-n\times N-n} \begin{pmatrix} \left(\frac{1}{x_i - y_a}\right)_{\substack{1\le i\le n \\ 1\le a\le N-n}} \\ \left(y_a^{N-2n-p}\right)_{\substack{1\le p\le N-2n \\ 1\le a\le N-n}} \end{pmatrix} \det_{N\times N} \psi_{i-1}(\bar{x}_j)\,. \tag{A.80}$$

It is reassuring to check that the formula reproduces correctly the cases of $n = 0$ and $n = N/2$. One can then perform one extra integration to reach the formula eqn. 3.97 of the main text.

A.7.4 $n = 0$

For the $n = 0$ representation, we define $Dx = \prod_k^N dx_k/N!$ and expand in multi-particle fermionic wavefunctions

$$\begin{aligned} Z_N &= \int DxDy\Delta(x)\Delta(y) \det_{ij} K(x_i, y_j) \\ &= \int DxDy\Delta(x)\Delta(y) \prod_k K(x_k, y_k) \\ &= \int DxDy\Delta(x)\Delta(y) \sum_{E_n} e^{-\beta E_n} \Psi_{E_n}(x_k)\Psi_{E_n}(y_k) \end{aligned} \tag{A.81}$$

with $\Psi_{E_n}(y_k)$ the multiparticle energy eigenfunctions $\langle E_n | y_1, y_2, ...y_N\rangle$. This in the $\beta \to \infty$ limit gives

$$\begin{aligned} Z &= e^{-\beta E_{ground}} \left(\int Dx\Delta(x)\Psi_{ground}(x_k) \right)^2 \\ &= e^{-\beta E_{ground}} \left(\int Dx \det_{i,k}(x_k^{i-1}) \det_{j,k}(\psi_{j-1}(x_k)) \right)^2 \\ &= e^{-\beta E_{ground}} \left(\det_{ij} \int dx (x^{i-1}\psi_{j-1}(x)) \right)^2 \end{aligned} \tag{A.82}$$

with $\psi_i(x_k)$ the single-particle wavefunctions and we used Andreief identity [186] to turn the integral over N variables to an integral over a single one. The Free energy is

$$\mathcal{F} = +\tfrac{1}{2}\beta_c E_{ground} - 2\log \det_{0\le i,j\le N} \int dx (x^{i-1}\psi_{j-1}(x)) \tag{A.83}$$

where the second term can be interpreted as a radius independent contribution of states at the endpoints written as a determinant of a matrix F_{ij}. One needs to compute the following integrals

$$\begin{aligned} F^+_{nm} &= \int_{-\infty}^{\infty} dx x^{2n-2}\psi_{2m-2}(x) \to \int_{-\infty}^{\infty} dx x^{2n-2}\psi^+(\varepsilon_{m-1}, x) \\ F^-_{nm} &= \int_{-\infty}^{\infty} dx x^{2n-1}\psi_{2m-1}(x) \to \int_{-\infty}^{\infty} dx x^{2n-1}\psi^-(\varepsilon_{m-1}, x) \end{aligned} \tag{A.84}$$

where we have indicated the corresponding expressions for the normal and the inverse H.O. To compute this contribution for the inverse harmonic oscillator we will use the odd/even parabolic cylinder $\psi^{\pm}$ functions of appendix A.2. We define $\alpha = \frac{1}{4} - i\frac{\varepsilon}{2}$ and use the following integral (c is an infinitesimal regulating parameter)

$$\begin{aligned} I &= \int_0^\infty dx x^{2n} e^{-i\frac{x^2}{4}} {}_1F_1\left(\alpha;\gamma;\frac{ix^2}{2}e^{ic}\right) = \\ &= 2^{2n} e^{\frac{i\pi}{4}(2n+1)}\Gamma(n+\frac{1}{2}) {}_2F_1\left(\alpha;n+\frac{1}{2};\gamma;2e^{ic}\right) \end{aligned} \tag{A.85}$$

This can be proven using Mellin-Barnes representations for hypergeometric functions. We then get

$$F^+_{nm} = 2^{2n-1} e^{\frac{i\pi}{4}(2n-1)} C_+(\varepsilon)\Gamma(n-\frac{1}{2}) {}_2F_1\left(\alpha, n-\frac{1}{2};\frac{1}{2};2e^{ic}\right) \tag{A.86}$$

$$F^-_{nm} = 2^{2n+1} e^{\frac{i\pi}{4}(2n+1)} C_-(\varepsilon)\Gamma(n+\frac{1}{2}) {}_2F_1\left(\alpha+\frac{1}{2}, n+\frac{1}{2};\frac{3}{2};2e^{ic}\right) \tag{A.87}$$

using the following identity for the hypergeometric functions

$$F(a,b;c;z) = (1-z)^{c-a-b} F\left(c-a, c-b; c; \frac{z}{z-1}\right) \tag{A.88}$$

we find

$$\begin{aligned} F^+_{mn} &= 2^{2n-1} e^{\frac{i\pi}{4}(2n-1)} C_+(\varepsilon_{m-1})(-1)^{n-1} e^{i\pi\alpha}\Gamma(n-\frac{1}{2}) \\ &\quad {}_2F_1\left(\frac{1}{2}-\alpha, 1-n; \frac{1}{2}; 2e^{-ic}\right) = \\ &= 2^{2n-1} e^{\frac{i\pi}{4}(2n-1)} C_+(\varepsilon_{m-1})(2)^{n-1} e^{i\pi\alpha}\sqrt{\pi} \\ &\times \sum_{k=0}^{n-1} \frac{\Gamma\left(\frac{1}{2}-\alpha+n-1-k\right)}{\Gamma\left(\frac{1}{2}-\alpha\right)} \frac{\Gamma\left(n-\frac{1}{2}\right)}{\Gamma\left(n-\frac{1}{2}-k\right)} \frac{(n-1)!}{(n-1-k)!} \frac{\left(-\frac{1}{2}\right)^k}{k!} = \\ &= \frac{2^{2n-1} e^{\frac{\pi}{4}\varepsilon_{m-1}} |\Gamma(\alpha_{m-1})|}{2^{\frac{5}{4}}\sqrt{\pi}} \sum_{k=0}^{n-1} a_k(n) \varepsilon_{m-1}^{n-1-k} \end{aligned} \tag{A.89}$$

where a_k depends only on n. Similarly,

$$\begin{aligned} F^{-}_{nm} &= 2^{2n+1} e^{\frac{i\pi}{4}(2n+1)} C_{-}(\varepsilon_{m-1})(-1)^{n-1} e^{i\pi(\alpha+\frac{1}{2})} \Gamma(n+\frac{1}{2}) \\ & \quad {}_2F_1\left(1-\alpha, 1-n; \frac{3}{2}; 2e^{-ic}\right) = \\ &= 2^{2n+1} e^{\frac{i\pi}{4}(2n+1)} C_{-}(\varepsilon_{m-1})(2)^{n-1} e^{i\pi(\alpha+\frac{1}{2})} \frac{\sqrt{\pi}}{2} \\ &\times \sum_{k=0}^{n-1} \frac{\Gamma\left(\frac{1}{2}-\alpha+n-\frac{1}{2}-k\right)}{\Gamma(1-\alpha)} \frac{\Gamma\left(n+\frac{1}{2}\right)}{\Gamma\left(n+\frac{1}{2}-k\right)} \frac{(n-1)!}{(n-1-k)!} \frac{\left(-\frac{1}{2}\right)^k}{k!} = \\ &= \frac{2^{2n} e^{\frac{\pi}{4}\varepsilon_{m-1}} |\Gamma\left(\alpha_{m-1}+\frac{1}{2}\right)|}{2^{\frac{3}{4}}\sqrt{\pi}} \sum_{k=0}^{n-1} b_k(n) \varepsilon_{m-1}^{n-1-k} \end{aligned} \tag{A.90}$$

with $b_0 = 1$. After using determinantal properties, we find that

$$\ln\left(\det F^{+}_{mn}\right) = \sum_{i<j} \ln\left(\varepsilon_{i-1} - \varepsilon_{j-1}\right) + \sum_i f_i \tag{A.91}$$

$$\ln\left(\det F^{-}_{mn}\right) = \sum_{i<j} \ln\left(\varepsilon_{i-1} - \varepsilon_{j-1}\right) + \sum_i g_i \tag{A.92}$$

with,

$$f_i = \frac{\pi}{4}\varepsilon_{i-1} + \ln|\Gamma\left(\frac{1}{4} - \frac{i\varepsilon_{i-1}}{2}\right)|, \qquad g_i = \frac{\pi}{4}\varepsilon_{i-1} + \ln|\Gamma\left(\frac{3}{4} - \frac{i\varepsilon_{i-1}}{2}\right)| \tag{A.93}$$

Note that as $\varepsilon \to \infty$

$$f(\varepsilon) + g(\varepsilon) = \ln(2\pi) - \frac{1}{2}\ln\left(1 + e^{-2\pi\varepsilon}\right) = \ln(2\pi) - \frac{1}{2}e^{-2\pi\varepsilon} + \ldots \tag{A.94}$$

contributing only non perturbative terms.
Introducing the density of states, one obtains a quite simple result for the twisted state contribution

$$\Theta = \frac{1}{2}\int^{\mu} \rho(\varepsilon) \int^{\mu} \rho(\varepsilon') \log|\varepsilon - \varepsilon'| d\varepsilon d\varepsilon' \tag{A.95}$$

where $\rho(\varepsilon)$ is the density of states:

$$\rho(\varepsilon) = \frac{1}{\pi}\left(-\log\varepsilon + \sum_{m=1}^{\infty} \mathcal{C}_m \varepsilon^{-2m}\right) \tag{A.96}$$

the coefficients $\mathcal{C}_m$ are known in terms of Bernoulli numbers. To compute this quantity we take one derivative wtr to μ to get

$$\frac{\partial\Theta}{\partial\mu} = \rho(\mu)\int_{-\infty}^{0} d\varepsilon \rho(\varepsilon+\mu)\log|\varepsilon| \tag{A.97}$$

In this expression one needs to put a cutoff Λ at the lower part of integration and compute it as a series expansion in $1/\mu$. After one computes A.95, one has to express it in terms of the cosmological constant Δ in order to be able to compare with the Liouville result (see section 3.4). One needs to use

$$\frac{\partial \Delta}{\partial \mu} = \pi \rho(\mu)\,, \tag{A.98}$$

and the renormalised cosmological constant μ_0 that plays the role of the string coupling, defined via

$$\Delta = -\mu_0 \log \mu_0\,. \tag{A.99}$$

In the end Θ can be found in terms of μ_0 as:

$$\begin{aligned}\Theta &= \mu_0^2\left(\frac{11}{8} - \frac{\pi^2}{24} + \left(\frac{\pi^2}{12} - \frac{11}{4}\right)\log\mu_0 + \frac{7}{4}\log^2\mu_0 - \frac{1}{2}\log^3\mu_0\right) \\ &- \frac{1}{24}\left(1+\frac{\pi^2}{6}\right)\log\mu_0 + \frac{1}{\mu_0^2}\left(\frac{259}{11520} + \frac{7}{2880}\left(\frac{\pi^2}{3} - 7\right)\log\mu_0\right)\mathcal{O}(\mu_0^{-4})\,.\end{aligned} \tag{A.100}$$

One notices that the torus contribution is not the same as in equation 3.9.

A.7.5 $n = N/2$ *with Hermite polynomials*

For the regular case we get (the measures contain appropriate factorials)

$$Z = \int dx dx' dy dy' \det_{i,j} \frac{1}{x_i - y_j} \det_{i,j} \frac{1}{x'_i - y'_j} \det_{2n\times 2n} K(x,y;x',y') \tag{A.101}$$

which in the $\beta \to \infty$ limit gives

$$\mathcal{F} = \tfrac{1}{2}\beta_c E_{ground} - 2\log \int d^n x d^n y \det_{i,j} \frac{1}{x_i - x'_j} \det_{2n\times 2n} \psi_{i-1}(\bar{x}_j) \tag{A.102}$$

with $\bar{x} = (x,y)$. One can use Moriyama's formula for unequal ranks in the appendix of [185] to get

$$\Theta = 2\log \int d^n x \det_{\substack{1\le i\le 2n \\ 1\le k\le n}} \left[\int dy \frac{\psi_{i-1}(x_k)}{x_k - y} \quad \psi_{i-1}(x_k)\right] \tag{A.103}$$

As we have dicussed, one can also integrate x's to find

$$\Theta = 2\log\left[\mathrm{pf}_{2n\times 2n} O_{ij}\right] \tag{A.104}$$

with the antisymmetric

$$O_{ij} = \int dx dy \frac{\psi_{i-1}(x)\psi_{j-1}(y) - \psi_{i-1}(y)\psi_{j-1}(x)}{x-y}\,. \tag{A.105}$$

Similarly to the main text we will adopt the principal value prescription. This gives

$$O_{i,j} = \int_{-\infty}^{\infty} dx \psi_{i-1}(x)\psi_{j-1}^{\mathcal{H}}(x) - \psi_{i-1}^{\mathcal{H}}(x)\psi_{j-1}(x) = 2\int_{-\infty}^{\infty} dx \psi_{i-1}(x)\psi_{j-1}^{\mathcal{H}}(x) \tag{A.106}$$

with $\psi^{\mathcal{H}}$ the Hilbert transform of ψ and in the second line we used that the Hilbert transform is skew-adjoint. For the Pfaffian we have the formula $\log[\mathrm{pf}\, A\, \mathrm{pf}\, B] = \frac{1}{2}\,\mathrm{tr}\log A^T B$. where we want to apply it for the case $A = B = O$ with $O^T = -O$ so that we get

$$\Theta = \tfrac{1}{2}\,\mathrm{tr}\log\left(-O^2\right) \tag{A.107}$$

One notices that the matrix O is just twice the Hilbert transform operator $\hat{\mathcal{O}}$ in the energy basis. It is a real antisymmetric matrix with imaginary eigenvalues. Also, since $\mathcal{H}^2 = -1$ (see appendix A.5), we immediately find $\Theta = \frac{1}{2}\,\mathrm{tr}\log 4\hat{I} = N\log 2$. To be more explicit, if we perform the integrals we can rewrite O as:

$$O_{m,n} = 2\langle m|\hat{\mathcal{O}}|n\rangle = \pm 4\frac{2^{2+\frac{m+n}{2}}}{\sqrt{m!n!}}\frac{\sqrt{\pi}}{n-m}\left[\frac{1}{\Gamma(-m/2)\Gamma(\frac{-n+1}{2})} + \frac{1}{\Gamma(-n/2)\Gamma(\frac{-m+1}{2})}\right] \tag{A.108}$$

with $0 \le m, n \le N-1$. In this expression, only one of the two terms inside the brackets can be non-zero when m-odd, n-even or vice versa, the odd/odd even/even pieces are zero. The overall $\pm$ is because the hermite functions are eigenfunctions of the fourier transform with eigenvalues $\pm 1, \pm i$ and one finds an overall factor $(-i)^{m+n+1}$, when going to momentum space in order to calculate the integral. Using this we can form O^2 as (this now holds for n_1, n_2 together odd/even!)

$$O^2_{n_1 n_2} = \frac{2^{n_1/2+n_2/2+3}\sqrt{\pi}}{\sqrt{n1!n2!}(n_1-n_2)}\left[\frac{1}{\Gamma(-\frac{n_1}{2})\Gamma(\frac{-n_2+1}{2})} - \frac{1}{\Gamma(-\frac{n_2}{2})\Gamma(\frac{-n_1+1}{2})}\right]. \tag{A.109}$$

In this expression, we find that the only non-zero terms are the diagonal. This is also consistent with the appropriate limit of the full energy-basis kernel A.58. Near the diagonal this expression approaches the *sine-kernel*

$$O^2_{n_1 n_2} \approx -\frac{4\sin\pi(n_1-n_2)}{\pi(n_1-n_2)}. \tag{A.110}$$

Taking the limit $n_2 \to n_1$ we find

$$\Theta = \tfrac{1}{2}\,\mathrm{tr}\log\left(-O^2\right) = \tfrac{1}{2}\sum_{k=0}^{N-1}\log\left[(\Psi(-k/2) - \Psi(1/2-k/2))\,\frac{2\sin\pi k}{\pi}\right]. \tag{A.111}$$

The expression in brackets has only real part. One also finds

$$\lim_{k\to\mathbb{N}} \left(\Psi(-k/2) - \Psi(1/2-k/2)\right) \frac{2\sin \pi k}{\pi} = 4, \quad \forall k \in \mathbb{N}, \tag{A.112}$$

and thus we recover the expected $\Theta = N \log 2$ which pinpoints to the fact that we just count the total entropy of a two state system at the endpoints, due to the spin up/down nature of the wavefunctions. It is tempting to pass to continuous variables via the dos $\rho_{H.O.}(\varepsilon) = -\frac{1}{\pi}\sum_k \delta(\varepsilon - \varepsilon_k)$ which for the inverse H.O. clicks when $-i\varepsilon = k + \frac{1}{2}$. The result is

$$\Theta = \tfrac{1}{2}\int^{\mu} d\varepsilon \rho_{H.O.}(\varepsilon) \log\left[\left(\Psi(\frac{1}{4}+\frac{i\varepsilon}{2}) - \Psi(\frac{3}{4}+\frac{i\varepsilon}{2}\right)\frac{2\cosh(\pi\varepsilon)}{\pi}\right], \tag{A.113}$$

with the term in the logarithm looking conspicuously similar to the twisted dos equation A.75. One should be very careful though, since the normalization of the Hermite functions after rotating is different compared to the one of the parabolic cylinder functions and one should really perform the computation from the start using the inverse H.O. eigenfunctions.

A.7.6 $n = N/2$ *with parabolic cylinder functions*

Here we perform the same computation using the delta-function normalised even and odd parabolic cylinder functions of appendix A.2 which are eigenfunctions of the inverted oscillator. Since the spectrum is now continuous, we can imagine obtaining a discrete spectrum by putting a cutoff/wall at Λ which is then send to infinity. We again adopt the principal value prescription whenever fourier transforming.

We compute[3]

$$\begin{aligned}\langle \varepsilon_1|O|\varepsilon_2\rangle &= 2\int_{-\infty}^{\infty} dxdy \frac{\psi^+(\varepsilon_1,x)\psi^-(\varepsilon_2,y)}{x-y} = \\ &= 4\int_0^{\infty} dx \int_0^{\infty} dy \frac{\psi^+(\varepsilon_1,x)y\psi^-(\varepsilon_2,y)}{x^2-y^2}\,.\end{aligned} \tag{A.114}$$

This expression is non zero and the integrand is even both in x and y. One can then exponentiate again the denominator using the Fourier transform of the sign function. This gives

$$O(\varepsilon_1,\varepsilon_2) = -2i\int_{-\infty}^{\infty} dt\, \mathrm{sgn}(t) I^+(t) I^-(t) = -4\Re\left[i\int_0^{\infty} dt I^+(t) I^-(t)\right] \tag{A.115}$$

where,

$$I^+(t) = \int_0^{\infty} dx \psi^+(x) e^{-i\frac{1}{2}tx^2}\,, \quad I^-(t) = \int_0^{\infty} dy y \psi^-(y) e^{+i\frac{1}{2}ty^2}\,. \tag{A.116}$$

3 Only the energy dependence is important in the overall normalisation of this object.

The advantage is that now one can compute the resulting integrals using [269]

$$\begin{aligned}\int_0^\infty du e^{-su}u^{b-1}\,{}_1F_1(a,c,ku) &= \Gamma(b)s^{-b}\,{}_2F_1(a,b,c,ks^{-1}),\\ &\quad \Re s>\Re k,\ \Re s>0,\ b>0\,;;|s|>|k|\,,\\ &= \Gamma(b)(s-k)^{-b}\,{}_2F_1(c-a,b,c,\frac{k}{k-s}),\\ &\quad \Re s>\Re k,\ \Re s>0,\ b>0\,;;|s-k|>|k|\end{aligned}$$

Or even the following simpler form that can be obtained from the expression above if $k=1, b=c$

$$\int_0^\infty du e^{-su}u^{c-1}\,{}_1F_1(a,c,u)=\Gamma(c)s^{-c}(1-s^{-1})^{-a}\,,\qquad \Re c>0\,,\quad \Re s>1\,. \tag{A.117}$$

Using an infinitesimal regulator e^{ic} we can find for $I^+(\epsilon_1,t)$ with $t>\frac{1}{2}$

$$\begin{aligned}I^+(\varepsilon_1,t) &= N_1(\varepsilon_1)\int_0^\infty \frac{du}{\sqrt{2u}}e^{-i(\frac{1}{2}+t)ue^{ic}}\,{}_1F_1(1/4-i\varepsilon_1/2,1/2;iue^{ic})\\ &= N_1(\varepsilon_1)\sqrt{\frac{\pi}{2}}(it+\frac{i}{2})^{-1/2}\,{}_2F_1(1/4-i\varepsilon_1/2,1/2,1/2,\frac{e^{ic}}{\frac{1}{2}+t})\,,\end{aligned} \tag{A.118}$$

with $N_1(\varepsilon)=\left(\frac{1}{4\pi\sqrt{(1+e^{2\pi\varepsilon})}}\right)^{\frac{1}{2}}2^{1/4}|\frac{\Gamma(1/4+i\varepsilon/2)}{\Gamma(3/4+i\varepsilon/2)}|^{\frac{1}{2}}$.

For $I^-(\epsilon_2,t)$, we now have (with $t<-\frac{1}{2}$),

$$\begin{aligned}I^-(\varepsilon_2,t) &= N_2(\varepsilon_2)\int_0^\infty du\sqrt{2u}e^{-i(\frac{1}{2}-t)ue^{ic}}\,{}_1F_1(3/4-i\varepsilon_2/2,3/2;iue^{ic})\\ &= N_2(\varepsilon_2)\sqrt{\frac{\pi}{2}}(-it+\frac{i}{2})^{-3/2}\,{}_2F_1(3/4-i\varepsilon_2/2,3/2,3/2,\frac{e^{ic}}{\frac{1}{2}-t})\,,\end{aligned} \tag{A.119}$$

with $N_2(\varepsilon)=\left(\frac{1}{4\pi\sqrt{(1+e^{2\pi\varepsilon})}}\right)^{\frac{1}{2}}2^{3/4}|\frac{\Gamma(3/4+i\varepsilon/2)}{\Gamma(1/4+i\varepsilon/2)}|^{\frac{1}{2}}$. We now encounter a form of non-perturbative ambiguity which has to do with the possible analytic continuations of these hypergeometric functions. In particular, the hypergeometric functions ${}_2F_1(a,b,c,z)$ have branch points at $z=(0,1,\infty)$ and thus the integrals A.118, A.119 have branch points at $t=(\infty,\frac{1}{2},-\frac{1}{2})$ and $t=(-\infty,-\frac{1}{2},\frac{1}{2})$ respectively. We will now assume working in some undetermined branch and naively analytically continue these equations for complex t. In the next subsection we are going to split the t integral into sections and find what are the exact conditions (which sheet to choose) in order to match the result we find here.

We will now introduce the following change of variables $z = 1/(\frac{1}{2}+t), t = (2-z)/2z$. By shifting the corresponding hypergeometric function and performing the integral we get

$$\begin{aligned} O(\varepsilon_1,\varepsilon_2) &= -2\pi N_1(\varepsilon_1)N_2(\varepsilon_2)e^{\frac{1}{2}(\varepsilon_1+\varepsilon_2)\pi}\Re\left[i\int_0^2 dz(z-1)^{-1+\frac{1}{2}i(\varepsilon_1-\varepsilon_2)}\right] \\ &= -2\pi N_1(\varepsilon_1)N_2(\varepsilon_2)e^{\frac{1}{2}(\varepsilon_1+\varepsilon_2)\pi}\Re\left[\int_{-1}^1 \frac{du}{u}u^{+\frac{1}{2}i(\varepsilon_1-\varepsilon_2)}\right] \\ &= 4\pi N_1(\varepsilon_1)N_2(\varepsilon_2)e^{\frac{1}{2}(\varepsilon_1+\varepsilon_2)\pi}\left[\frac{1-e^{\frac{1}{2}(\varepsilon_2-\varepsilon_1)\pi}}{\varepsilon_1-\varepsilon_2}\right]. \end{aligned} \tag{A.120}$$

where the last expression holds when $\Im\varepsilon_1 > \Im\varepsilon_2$ and one can derive a similar one in case $\Im\varepsilon_1 < \Im\varepsilon_2$ by exchanging $\varepsilon_1 \leftrightarrow \varepsilon_2$ with an overall minus sign[4]. We expect that our analytically continued result is valid for some specific branch. A different branch would give a different normalization. This difference in normalization we expect to play a role in the contribution of non-perturbative states as discussed in the main text. The result can also be written as

$$\begin{aligned} O(\varepsilon_1,\varepsilon_2) &= \frac{2e^{(\varepsilon_1+\varepsilon_2)\pi/2}}{(1+e^{2\pi\varepsilon_2})^{1/4}(1+e^{2\pi\varepsilon_1})^{1/4}}\left|\frac{\Gamma(1/4+i\varepsilon_1/2)}{\Gamma(3/4+i\varepsilon_1/2)}\frac{\Gamma(3/4+i\varepsilon_2/2)}{\Gamma(1/4+i\varepsilon_2/2)}\right|^{\frac{1}{2}} \\ &\times \frac{1-e^{(\varepsilon_2-\varepsilon_1)\pi/2}}{\varepsilon_1-\varepsilon_2} \\ &= \frac{1}{\pi}|\Gamma(1/4+i\varepsilon_1/2)\Gamma(3/4+i\varepsilon_2/2)|e^{\pi(3\varepsilon_2+\varepsilon_1)/4} \\ &\times \frac{\sinh\left(\frac{1}{4}\pi(\varepsilon_2-\varepsilon_1)\right)}{\varepsilon_1-\varepsilon_2}. \end{aligned} \tag{A.121}$$

A.7.6.1 *Calculation of the integrals for segments*

We will now perform a consistency check and understand better our branch choice. We split the integrals into sections with respect to the branch points. We demand that the parameter t is real and we drop the regulator. Then we indeed find a result that differs for different sections of t. The sections are $(-\infty,-1/2)\cup(-1/2,1/2)\cup(1/2,\infty)$. We have computed the integrals for each section by taking the limit at the branch points sending a small parameter to zero (ex. we integrate up to $1/2+\epsilon$ and then we send $\epsilon\to 0$). The results are (to be multiplied with the normalization prefactors $N(\epsilon_1)$, $N(\epsilon_2)$)

- For the section $(0,1/2)$:

$$I^+(t) = \frac{\sqrt{2\pi}e^{\frac{\pi\epsilon_1}{2}}\left(\frac{2}{2t+1}-1\right)^{+\frac{1}{2}i\epsilon_1}}{(1-4t^2)^{1/4}} \tag{A.122}$$

4 These cases probably form different elements of the discrete matrix above and below the diagonal, since the poles of the inverted oscillator dos are at $\Im\varepsilon_1 = n_1 + \frac{1}{2}$. The matrix is then appropriately real and antisymmetric

$$I^-(t) = \frac{\sqrt{2\pi}e^{\frac{\pi\epsilon_2}{2}}\left(\frac{2}{2t+1}-1\right)^{-\frac{1}{2}i\epsilon_2}}{(1-4t^2)^{3/4}} \tag{A.123}$$

- For the section $(1/2,\infty)$:

$$I^+(t) = \frac{(1-i)\sqrt{\pi}\left(\frac{2t-1}{2t+1}\right)^{\frac{i\epsilon_1}{2}}}{(4t^2-1)^{1/4}} \tag{A.124}$$

$$I^-(t) = -\frac{(1-i)\sqrt{\pi}\left(\frac{2t-1}{2t+1}\right)^{-\frac{1}{2}(i\epsilon_2)}}{(4t^2-1)^{3/4}} \tag{A.125}$$

One can similarly obtain the rest of the sections by $t \to -t$.

One can now notice that A.122, A.124 are the same expression if one chooses $-1 = e^{-i\pi}$ and A.123, A.125 are the same if we chose $-1 = e^{i\pi}$. This choice corresponds to picking a specific branch. We already know that the spectrum of the inverted oscillator is twofold degenerate and our choice just means that the even/odd modes live in a different sheet of the complex energy plane. After changing variables $z = 1/\frac{1}{2} + t$ this choice gives the same integral and result as in A.120

A.7.6.2 *The sine/sinh kernel*

It is now easy to see that since $O(\varepsilon_1,\varepsilon_2) = A(\varepsilon_1)K^{sinh}(\varepsilon_1-\varepsilon_2)B(\varepsilon_2)$, the only interesting asymptotic contribution comes from the kernel in the middle. The diagonal normalization factors can be shown to contribute non-perturbatively, since they do not admit an $1/\varepsilon$ expansion and scale for large ε as $e^{a\varepsilon}$ with a a parameter depending on the branch we choose. The kernel whose spectrum we want to compute is the analytic continuation of the very well studied sine kernel $K^{sine}(\varepsilon_1,\varepsilon_2) = \frac{\sin(\frac{1}{4}\pi(\varepsilon_1-\varepsilon_2))}{\varepsilon_1-\varepsilon_2}$ for which various results exist in the literature in relation to its spectrum and Fredholm determinants [212, 213].

One way of computing its determinant is to discretise and bring it into a Toeplitz form. In our case one can put a cutoff Λ and then use the density of states of the inverted oscillator $i\varepsilon_j = j + \frac{1}{2}$ which is equidistant, or equivalently analytically continue in ω. Then calculating the determinant of the sine kernel with support on an energy segment one finds that it can be represented as a Toeplitz determinant in a scaling limit

$$\begin{aligned} \det K^{sine}|_{-\infty}^{-\mu} &= \det\left(1-K^{sine}|_{-\mu}^{0}\right), \quad \Leftrightarrow \lim_{N\to\infty} N \det C_{j-k}, \\ \text{with} \quad C_{j-k} &= \delta_{jk} - \frac{\sin(\frac{\pi\mu}{2N}(j-k))}{\pi(j-k)} \end{aligned} \tag{A.126}$$

We will now discuss some properties of this fredholm determinant, and provide an asymptotic evaluation for large μ, with which we can match the torus contribution to the twisted states.

A.7.6.3 *Level spacings*

The level spacing distribution $E_\beta(n,\mu)$ of Random matrices is the probability that the interval $(0,\mu)$ contains exactly n eigenvalues [280]. In our case these will be energy eigenvalues and the random matrix is the Hamiltonian. Thus the Hilbert transform operator effectively randomizes the energy eigenvalues of the system which are to be drawn from an ensemble (GUE/GOE/GSE). The parameter β denotes the ensemble and for us $\beta = 2$ (GUE). We first define $D(\mu;\lambda) = \det\left(1-\lambda K^{sine}\right)$. We also define $K_\pm = K^{sine}(x,y) \pm K^{sine}(x,-y)$ and similarly $D_\pm(\mu;\lambda) = \det\left(1-\lambda K^{\pm}\right)$. For the other ensembles, β , the kernel is a matrix. Then one has [280]

$$E_2(n;(0,\mu)) = \frac{(-1)^n}{n!}\frac{\partial D(\mu;\lambda)}{\partial\lambda^n}|_{\lambda=1} \tag{A.127}$$

and for the other ensembles one can again find formulas involving $E_\pm$ $D_\pm$. We will now use the asymptotic formulas in the literature for the level spacings as $\mu\to\infty$ much like what we want for the asymptotic expansion of string theory $\mu\to\infty$. We provide here the more general result/conjecture for arbitrary β, n [281] that correctly reproduces the proven result for $n=0,\beta=2$ [212, 213]

$$\begin{aligned}\log E_\beta(n;(0,\mu)) \sim_{\mu\to\infty} -\beta\frac{\mu^2}{16} + (\beta n+\beta/2-1)\frac{\mu}{2}\\ + \left[\frac{n}{2}(1-\beta/2-\beta n/2) + \frac{1}{4}(\beta/2+2/\beta-3)\right]\log\mu + ...\end{aligned} \tag{A.128}$$

We now need to remember that the Pfaffian is the square root of the determinant and that we need to divide our result by an extra factor of 2, since we want to match the bosonic string theory partition function, that has support on the one side of the potential. After taking these into account, one finds the twisted state contribution

$$\Theta = \frac{1}{4}\log E_2(0;(0,\mu)) = -\frac{1}{32}\mu^2 - \frac{1}{16}\log\mu + \frac{1}{48}\log 2 + \frac{3}{4}\zeta'(-1) + O\left(\frac{1}{\mu^{2m}}\right). \tag{A.129}$$

We see that we correctly capture only closed string contributions with even higher powers of $1/\mu$ and some of these coefficients can be found in [212]. Moreover this formula predicts that there is no-logarithmic divergence coming from the genus 0 spherical contribution. As a bonus, it is interesting to note that one can make the same computation with orthogonal or symplectic matrices in GOE, GSE which can be found to receive open string corrections with odd powers in μ. These results might be relevant for the unoriented string theory on the orbifold, where odd powers of μ are known to appear and orthogonal/symplectic symmetries to be relevant.

A.7.6.4 *Properties of the sine kernel*

The sine kernel has some remarkable properties some of which which we list here

- Its eigenfunctions are the prolate spheroidal functions and some asymptotic forms of the spectrum exist.
- The Christoffel Darboux (CD) kernels approach the sine kernel in a scaling limit that focuses on the bulk of the spectrum.
- As with all the CD kernels it is a self-reproducing kernel, it obeys $K * K = K$.
- It is the band-limited version of the Dirac delta distribution. To understand this better, let $f \in L^2(\mathbb{R})$ a function whose fourier transform has support on the segment $[-\pi b, \pi b]$ (band limited functions) Then the sine kernel is an orthogonal projection to this space since

$$\int_{-\infty}^{\infty} dy \frac{\sin(\pi b(x-y))}{\pi(x-y)} f(y) = \frac{1}{\sqrt{2\pi}} \int_{-\pi b}^{\pi b} e^{ix\xi} \mathcal{F}[f](\xi) d\xi \tag{A.130}$$

- Moreover one can further consider functions $f \in L^2([-s, s])$. This gives both energy and time band limited functions (in our case $s \sim \mu$ is the energy-band limit while $b = 1/4$ is a "time-band" limiting). This is called a compression of the sine kernel and gives a trace class operator.
- It is easy to see that it is the natural regulating description of the dirac-δ function we were expecting to have (for O^2), since at the discrete level we encountered the identity operator δ_{nm} and we were filling eigenvalues up to the size of the matrix N. It also allows for a rigorous understanding of limiting the energy and defining the fermi surface which corresponds to filling all the negative energy states up to a band below 0 corresponding to the chemical potential $-\mu$.

B

APPENDIX OF CHAPTER 4

B.1 ON-SHELL ACTION VIA HOLOGRAPHIC RENORMALIZATION AND BACKGROUND SUBTRACTION

B.1.1 *On-shell action via holographic renormalization*

In this section we compute the on-shell action for our configurations. In doing so, we plug in the action (4.5) the solutions of the equations of motion and perform the integration over all space. Since the quantity $S_{on-shell}$ obtained this way is per se divergent, we need to resort to the techniques of holographic renormalization (see for instance [282, 283, 284, 285]). We therefore add to the action (4.5) appropriate counterterms that we denote by

$$S_{on-shell,ren} = S_{on-shell} + S_{ct} \,. \tag{B.1}$$

The counterterms we need to add are functions of boundary curvature invariants, hence they do not alter the bulk equations of motion. The prescription for such terms is spelled out for example in [236] (see also [286] for a related computation). They are constructed from the boundary Ricci scalar $\mathcal{R}_3$ and a function $\mathcal{W}(\varphi)$ of the scalar fields, called superpotential:

$$S_{ct} = \frac{1}{4\pi G}\int_{\partial M} d^3x\sqrt{h}\left(\frac{\ell_{AdS}}{2}\mathcal{R}_3 - \mathcal{W}(\varphi)\right) . \tag{B.2}$$

In this expression, h is the determinant of the induced metric at the boundary ∂M, h_{ab}, and $\mathcal{R}_{3,ab}$ is its Ricci curvature. For the black brane the curvature of the boundary is zero, hence the first addendum vanishes identically. The superpotential $\mathcal{W}$ appearing in (B.2) satisfies the following relation:

$$V_g(\varphi) = \frac{1}{2}\left(-\frac{3}{2}\mathcal{W}^2 + g^{ij}\partial_i\mathcal{W}\partial_j\mathcal{W}\right) . \tag{B.3}$$

The crucial point in the computation of counterterms for mixed boundary condition is the fact that the superpotential relation (B.3) fixes the function $\mathcal{W}(\varphi)$ up to finite terms, that would in principle affect the renormalized physical quantities. Indeed, to completely fix this finite term one needs an additional requirement, namely that the holographic renormalization be derived via a well-defined variational principle. As explained in [236], only one specific choice of finite term (thus of $\mathcal{W}$, satisfying (B.3)) satisfies this requirement[1]. Following the prescription of [236] and the work [237]

1 It has been noticed in [237] that, when the boundary conditions enforce a marginal deformation, the finite part of the counterterm $\mathcal{W}$ can be equivalently determined by taking the superpotential $\mathcal{W} \equiv \mathcal{W}_{flow}$ that drives the flow of the scalar fields, $\varphi' = \partial_\varphi \mathcal{W}_{flow}$ of the solution. See [237] for more details.

we find that the correct superpotential counterterm one has to use for our solutions (both branes and thermal gas) is

$$\mathcal{W}(\varphi) = \frac{2}{\ell_{AdS}}\left(1+\frac{\varphi^2}{2}+\frac{1}{6\sqrt{6}}\varphi^3+\mathcal{O}(\varphi^4)\right), \tag{B.4}$$

the finite part being given by the φ^3 term.

The action obtained here requires specific boundary conditions on the vector fields: these are exactly imposing fixed electric chemical potential and fixed magnetic charge. Let us mention the fact that imposing fixed electric charge would amount in adding the finite Hawking-Ross boundary term [287]

$$S_{HR} = \frac{1}{4\pi G}\int_{\partial M} d^3x\sqrt{h}\, n_a F^{ab} A_b\,, \tag{B.5}$$

where n_a is an outward pointing vector normal to the boundary. Since we have decided to work in the mixed ensemble (with fixed electric chemical potential and fixed magnetic charge) we do not need to make such an addition.

We are now ready to perform the computation of the on-shell action. We first start by noticing that, making use of the Einstein's equations of motion, the action (4.5) can be rewritten in terms of the Ricci tensor components plus the integrals over the kinetic terms of the gauge fields:

$$S_{on-shell} = \frac{\mathcal{V}\beta}{4\pi}\int_{r_h}^{\infty} dr\sqrt{-g}\left[(R^y_y+R^t_t)/2+\mathcal{I}_{\Lambda\Sigma}F^{\Lambda}_{\mu\nu}F^{\Sigma\,\mu\nu}\right]+S_{GH}\,. \tag{B.6}$$

We first impose a radial cutoff r_0 that should be sent to infinity after integration. The extrema of integration are r_h and r_0. The total on shell action takes the form

$$\begin{aligned} S_{on-shell} = {} & \frac{\mathcal{V}\beta}{8\pi}\left(-\tfrac{3}{4}\left(2c_1-8b^3\right)-\tfrac{3c_1b+c_2}{4(r_h-3b)}-\tfrac{3c_1b-3c_2}{4(r_h+b)}\right)+ \\ & +\tfrac{\mathcal{V}\beta}{8\pi}\left(3b^2r_h-r_h^3+6b^2r_0-2r_0^3\right), \end{aligned} \tag{B.7}$$

where β comes from the integration in the time direction. For the solution at hand, the computation of the counterterm using (B.4) gives

$$S_{ct} = \frac{\beta\mathcal{V}}{4\pi}\left(\frac{1}{4}\left(2c_1-8b^3\right)-3b^2r_0+r_0^3\right). \tag{B.8}$$

Plugging in (B.7) and (B.8) in (B.1) we see that the divergencies cancel, giving a finite result for the on-shell action. Using the horizon equation $f(r_0)=0$, we can recast (B.1) in the following form:

$$S_{os,ren} = \frac{1}{16\pi}\beta\mathcal{V}\left(3(3b-r_h)(b+r_h)^2-2c_1\right). \tag{B.9}$$

At this point we can directly rewrite the on-shell action in terms of the thermodynamic potentials. The mass of the system can be computed from the renormalized stress energy tensor τ^{ab}

$$\tau^{ab} = \frac{2}{\sqrt{h}}\frac{\delta S_{ren}}{\delta h_{ab}}\,. \tag{B.10}$$

The following expression gives the conserved charge associated with the boundary Killing vector K_b (σ^{ab} is the induced metric on the spacelike section Σ of the boundary and u_a is the unit normal vector to Σ):

$$Q_K = \int_\Sigma d^2x\sqrt{\sigma}u_a\tau^{ab}K_b\,. \tag{B.11}$$

The mass of the system is then obtained for $K = \partial_t$ and one finds

$$M = Q_{\partial_t} = -\frac{1}{4\pi}\frac{c_1}{2}\,. \tag{B.12}$$

This expressions coincides with the mass computed via the AMD procedure [288, 289]. The temperature T is

$$T = \frac{1}{4\pi}\frac{df(r)}{dr}\bigg|_{r_h}\frac{1}{\sqrt{H_0(r)H_1^3(r)}}\bigg|_{r_h} = \frac{-12b^2r_h - c_1 + 4r_h^3}{4\pi\sqrt{(r_h-3b)\,(b+r_h)^3}}\,, \tag{B.13}$$

and the entropy density reads

$$S = \frac{Area}{4\kappa^2} = \frac{r_h^2\sqrt{H_0(r_h)H_1^3(r_h)}}{4\kappa^2}\,. \tag{B.14}$$

The magnetostatic potential m_B and the electrostatic one χ respectively read

$$m_B = -\int_{r_h}^{\infty} G_{1,tr}dr\,, \qquad \chi = -\int_{r_h}^{\infty} F_{0,tr}dr\,. \tag{B.15}$$

The field G_Λ is the dual of the field strength $F = dA$ and it is defined in this way:

$$G_{tr,\Lambda} = \frac{1}{4}\epsilon_{trxy}\frac{\partial\mathcal{L}}{\partial F^\Lambda_{xy}} = \epsilon_{trxy}I_{\Lambda\Sigma}F^{xy,\Sigma} \tag{B.16}$$

with Levi Civita tensor

$$\epsilon_{\mu\nu\rho\sigma} = e^a_\mu e^b_\nu e^c_\rho e^d_\sigma\epsilon_{abcd}\,, \qquad \epsilon_{0123} = 1\,. \tag{B.17}$$

With $\epsilon_{trxy} = h^2(r)$ and $F^\Lambda_{xy} = \frac{p^\Lambda}{2}$ one gets $G_{tr,\Lambda} = \frac{I_{\Lambda\Sigma}p^\Sigma}{2h^2}$, hence

$$\chi = \frac{q}{2\,(3b-r_h)}\,, \qquad m_B = \frac{3B}{2\,(b+r_h)}\,. \tag{B.18}$$

Having all the conserved quantities and the potential defined, one can check that the first law of thermodynamics is satisfied:

$$dM = TdS - \chi dq + mdB\,, \tag{B.19}$$

and the (renormalized) on-shell action $S_{on-shell,ren}$ coincides with the free energy for the mixed ensemble

$$\frac{S_{on-shell,ren}}{\beta} = \frac{I}{\beta} = M - TS + \chi q\,. \tag{B.20}$$

B.1.2 *Background subtraction method*

We will now illustrate the background subtraction method for the free energy computation. The appropriate background should have the same boundary asymptotics of the solution taken into consideration and, in addition to it, it has zero AMD mass.

Obviously, we should subtract the same background from the two solutions that we want to compare. Using different backgrounds would result in a finite piece that comes from the difference between the two backgrounds.

For our specific example, such a background turns out to be the domain wall solution with metric

$$\mathrm{d}s^2 = -r^2\sqrt{H_0(r)H_1^3(r)}\,\mathrm{d}t^2 + \frac{\mathrm{d}r^2}{r^2\sqrt{H_0(r)H_1^3(r))}} + r^2\sqrt{H_0(r)H_1^3(r)}\,\mathrm{d}\sigma^2\,, \tag{B.21}$$

and area element

$$\mathrm{d}\sigma^2 = \mathrm{d}x^2 + \mathrm{d}y^2\,. \tag{B.22}$$

Furthermore, the background has zero magnetic and electric charges $F_{\mu\nu} = (0,0,0,0)$ and the same asymptotic expansion for the scalar field at infinity.

To compute the finite on-shell action we subtract the on-shell action of the background from the on-shell action of the black brane. We can use the same rewriting (B.6) used in the previous section. Since for the background configuration the electric and the magnetic charges are zero, the on-shell action can be written as a whole as an integral of the Ricci tensor component R_t^t. One can then expand the difference around $r_0 \to \infty$. The result is given in terms of a finite part and subleading terms that go to zero as $r_0 \to \infty$.

$$I = \frac{\beta\mathcal{V}}{4\pi}\left(\frac{9b^3 + 15b^2 r_h + 3br_h^2 - 2c_1 - 3r_h^3}{4}\right) + \mathcal{O}({r_0}^{-1}) \tag{B.23}$$

This quantity coincides with the renormalized on shell action (B.9), and the free energy F is the finite part divided by β, which is exactly $F = M - TS + q\chi$. Hence in this case the background subtraction gives the same result as the holographic renormalization.

B.1.3 *On-shell action for the thermal gas solution*

As we show in a previous section the way we acquire the acceptable thermal gas solution is to take the limit $r_h \to r_s$. Likewise to compute the on-shell action we will perform the same procedure as in the black brane case but the limits of integration will be $r_s + \epsilon$, $\epsilon \to 0$ and $r \to \infty$. After the subtraction of the background one finds

$$F_{sol} = M_{ADM,sol} = -\frac{c_1}{8\pi}\,. \tag{B.24}$$

All the rest thermodynamic quantities are computed as in the black brane but taking the limit $r_h \to r_s$.

As one can notice, we have found the thermodynamic quantities and the free energy as functions of r_h, c_1, b, using the $T = 0$ condition we can express them in terms of the actual thermodynamical variables $T = 0, \chi, B$.

B.2 EXTENDED OBJECTS

B.2.1 *Polyakov loop*

The action of a Euclidean string propagating on the background is given by

$$I_{NG} = \frac{1}{4\pi\alpha'}\sqrt{\det(\partial_\alpha X^\mu \partial_\beta X^\nu g_{\mu\nu})}d\sigma d\tau\,, \tag{B.25}$$

where $g_{\mu\nu}$ is the Euclidean metric of the target space. This area diverges in an asymptotically AdS space-time and the renormalization procedure is standard [253]. After renormalization, the area on the Euclidean black brane background is obviously finite because the near horizon geometry is flat corresponding to the origin in the Euclidean signature. The area on the thermal gas background can be obtained by choosing a gauge $\sigma = r$, $\tau = t_E$ where t_E is the imaginary time. Then one obtains $\det(\partial_\alpha X^\mu \partial_\beta X^\nu g_{\mu\nu}) = g_{tt}g_{rr} = 1$ where we used (4.11) with $t = it_E$. Thus, after renormalization of the UV divergence, we again find a finite area for the Nambu-Goto string on the thermal gas, even though there is a singularity at $r = r_s$.

B.2.2 *The quark potential*

We consider a string embedded in the thermal gas background that is attached on the boundary at two points separated by a distance l. A typical geometry minimizing (B.25) with this boundary condition is a curve that ends on the boundary $r = \infty$ at the points $(x, y) = (\pm l/2, 0)$ and hangs down the interior of the geometry making a turning point at $r = r_0$, see for example [290]. The on-shell action is proportional to the quark-antiquark potential on the boundary and the latter can be put in a form[290]

$$V_{q\bar{q}} = H(r_0)\, l - 2d(r_0) \tag{B.26}$$

where

$$d(r_0) = 2\int_{r_0}^{\infty} dr \frac{G(s)}{H(s)}\left(\sqrt{H^2(r) - H^2(r_0)} - H(s)\right) - 2\int_{3b}^{r_0} drG(r)\,, \tag{B.27}$$

with $H^2 = g_{tt}g_{xx}$ and $G^2 = g_{tt}g_{rr}$. On our backgrounds these quantities simplify as $G^2(r) = 1$ and $H^2(r) = f(r)r^2$ where f is defined in (4.12). On a confining background, as l increases, the turning point of the string, r_0 approaches to a final value $r = r_f$ located deeper in the interior of the geometry where $d(r_f)$ and $c(r_f)$ attain

finite values. Therefore, one obtains linear confinement in (B.26). On our thermal gas geometry this point corresponds to the singularity $r_f = 3b$. In order to explore the behavior of the function H near this point we set $r_0 = 3b + \epsilon$ and expand for small ϵ. The blackening factor f on the thermal gas can be put in the form

$$f(r) = H_0(r)\left(r^2 H_1^3(r) - \frac{B^2}{2br}\right), \tag{B.28}$$

where H_0 and H_1 are defined in (4.12). Using this expression and the good singularity condition (4.1) we obtain

$$H(r_0) = r_0^2 f(r_0) \to 4\sqrt{3}b\epsilon\,, \tag{B.29}$$

in the limit $\epsilon \to 0$. Therefore, we find that $d(r_0)$ in (B.26) remains finite as $r_0 \to 3b$ as l increases, whereas $H(r_0)$ vanishes linearly in this limit. This means that the only way confinement may arise from (B.26) is by l diverging faster than $1/\epsilon$. The latter is given by [290]

$$l = 2\int_{r_0}^{\infty} dr \frac{G(r)}{H(r)} \frac{H(r_0)}{\sqrt{H^2(r) - H^2(r_0)}} = 2\int_{r_0}^{r_1} \frac{\sqrt{f(r_0)r_0^2}}{f(r)r^2} \frac{dr}{\sqrt{f(r)r^2 - f(r_0)r_0^2}}\,. \tag{B.30}$$

Changing integration variable $r = 3b + \epsilon, r_0 = 3b + \epsilon_0$, to focus near the singularity, we find

$$l = \int_{\epsilon_0}^{\infty} \frac{d\epsilon}{4\sqrt{6}\sqrt{\epsilon - \epsilon_0} + \cdots}\,, \tag{B.31}$$

that always remains finite. We conclude that the string is not confining on the thermal gas solution.

B.2.3 *Entanglement Entropy*

Entanglement entropy can be employed to check if the thermal gas is a confining background. For a confining background there are two possible minimal surfaces with the same end points on the boundary. When confinement occurs the favoured minimal surface is the two disconnected straight lines extending from the endpoints of the line segment inside the bulk. In the deconfined phase the minimal surface is the curved line that connects the two endpoints. In the following we identify: $h(r)^2 = r^2\sqrt{H_0(r)H_1^3(r)}$. We divide the boundary region into two parts A and B (A's complement), where A is defined as: $l/2 < x < l/2$ and $0 < y < \infty$. By parametrizing this two dimensional surface with (x, y) we can write down the action that should be minimized as

$$A = L\int_{-l/2}^{l/2} dx h\left(r\left(x\right)\right)^2 \sqrt{1 + \frac{\left(\partial_x r\left(x\right)\right)^2}{U\left(r\left(x\right)\right)^2 h\left(r\left(x\right)\right)^2}}\,. \tag{B.32}$$

One notices that the Lagrangian does not depend explicitly on x, hence the quantity

$$H = -\frac{h(r)^2}{\sqrt{1+\frac{(\partial_x r)^2}{U(r)^2 h(r)^2}}}\,, \tag{B.33}$$

is conserved. If r^* is the minimal value of r with respect to x, $\partial_x r|_{r^*} = 0$, then

$$H = -h\left(r^*\right)^2\,, \tag{B.34}$$

but H is a constant and always equals $-h\left(r^*\right)^2$. Thus we can solve B.33 for $\partial_x r$,

$$\partial_x r = U(r)h(r)\sqrt{\frac{h(r)^4}{h(r^*)^4}-1}\,. \tag{B.35}$$

We can now compute the length l that minimizes the area B.32 as a function of r^*,

$$\frac{l}{2} = \int_{r^*}^{r^\infty} dr \frac{1}{U(r)h(r)\sqrt{\frac{h(r)^4}{h(r^*)^4}-1}}\,, \tag{B.36}$$

where r^∞ is the UV cut-off. Eliminating l from the B.32, we find for the connected surface

$$A^{con} = \frac{L}{2G_{N4}}\int_{r^*}^{r^\infty} dr \frac{h(r)^3}{h(r^*)^2 U(r)}\frac{1}{\sqrt{\frac{h(r)^4}{h(r^*)^4}-1}}\,. \tag{B.37}$$

The area for the disconnected case is simply,

$$A^{dis} = \frac{L}{2G_{N4}}\int_{r_0}^{r^\infty} dr \frac{h(r)}{U(r)}\,, \tag{B.38}$$

where r_0 is infinitesimally close to the singularity.

Plotting the difference between B.37 and B.38 $A^{con} - A^{dis}$ as a function of l for all values of B and χ we find that the connected minimal surface is always favoured, leading to the conclusion that thermal gas always corresponds to a deconfined phase.

SUMMARY

In this thesis we present three seemingly very different models that can be treated in the context of holography. First, in chapter 2 we present the black hole S-matrix of Gerard 't Hooft, and we show how by solving a quantum mechanical problem, one can obtain the same S-matrix. Then, in chapter 3 we present the correspondence between non critical Liouville string theory coupled to $c = 1$ matter and the dual matrix quantum mechanics model. In this framework, we build a toy model of two dimensional cosmology that describes a big-bang/ big-crunch universe. Finally, in chapter 4 we use holography to model a $2 + 1$- dimensional strongly coupled theory under external magnetic field and under finite charge density at zero temperature. We then, discover a line of second order quantum critical points by comparing thermodynamically dual gravitational solutions. In the following we would like to present in more details the subject of each chapter.

In the introduction 1, we give a basic and self-contained account of the various physical notions that one needs to be familiar with in order to read this thesis. Specifically, we present the holographic principle as stated by Gerard 't Hooft and Leonard Susskind. This is the primary idea behind Gauge/Gravity duality. We then present, the best understood example of holography –first discovered by Maldacena– which states that gravity on AdS_5 is dual to strongly coupled $\mathcal{N} = 4$ super Yang-Mills gauge theory. Next, we present the dictionary of applied gauge/gravity duality, that is relevant for chapter 4 and some examples that applied gauge/gravity duality has been of use. Concluding this subsection, we move on to the physics of black holes, where we first define and describe real world astrophysical black holes. Afterwards, we comment in the difficulty to connect consistently gravity with quantum mechanics and we state the information paradox. This part is relevant for chapter 2. Then, we briefly present how one can use black hole physics in the context of holography in order to study strongly coupled field theories (this is relevant for chapter 4) and vice-versa. Subsequently, we move on to the correspondence between Liouville string theory and matrix quantum mechanics, where we introduce Liouville field theory and matrix models as well as how to take an appropriate limit –the so called double scaling limit– to show that matrix quantum mechanics are dual to Liouville string theory. We end this subsection, by giving a precise dictionary between the two pictures. Finally, we present quantum criticality and quantum phase transitions that are relevant for chapter 4, from the point of view of condensed matter theory.

In chapter 2, we revisit the old black hole S-matrix construction and its new partial wave expansion of 't Hooft. Inspired by old ideas from non-critical string theory and the $c = 1$ Matrix Quantum Mechanics, we formulate the scattering in terms of a quantum mechanical model –of waves scattering off inverted harmonic oscillator potentials– that exactly reproduces the unitary black hole S-matrix for all spherical harmonics; each partial wave corresponds to an inverted harmonic oscillator with

ground state energy that is shifted relative to the s-wave oscillator. Identifying a connection to two dimensional string theory allows us to show that there is an exponential degeneracy in how a given total initial energy may be distributed among many partial waves of the four dimensional black hole.

In chapter 3, we study Matrix Quantum Mechanics (MQM) on the Euclidean time orbifold $S^1/\mathbb{Z}_2$. Upon Wick rotation to Lorentzian time and taking the double-scaling limit this theory provides a toy model for a big-bang/big-crunch universe in two dimensional non-critical string theory where the orbifold fixed points become cosmological singularities. We derive the MQM partition function both in the canonical and grand canonical ensemble in two different formulations and demonstrate agreement between them. We pinpoint the contribution of twisted states in both of these formulations either in terms of bi-local operators acting at the end-points of time or branch-cuts on the complex plane. We calculate, in the matrix model, the contribution of the twisted states to the torus level partition function explicitly and show that it precisely matches the world-sheet result, providing a non-trivial test of the proposed duality. Finally, we discuss some interesting features of the partition function and the possibility of realising it as a τ-function of an integrable hierarchy.

In chapter 4, we investigate quantum critical points in a $2+1$- dimensional gauge theory at finite chemical potential and magnetic field. The gravity dual is based on four dimensional $\mathcal{N}=2$ Fayet-Iliopoulos gauged supergravity and the solutions we consider –that are constructed analytically– are extremal, dyonic, asymptotically AdS_4 black branes with a nontrivial radial profile for the scalar field and extremal, magnetically charged, asymptotically AdS_4 acceptable singular solutions with a nontrivial radial profile for the scalar field. We discover a line of second order fixed points at a critical value of the magnetic field between the dyonic black brane and the extremal "thermal gas" solution with a singularity of good-type, according to the acceptability criteria of Gubser. The dual field theory is a strongly coupled nonconformal field theory at finite charge and constant external magnetic field, related to the ABJM theory deformed by a triple trace operator. We find similarities between the behaviour of the vacuum expectation value of the scalar operator under magnetic field and that of the quark condensate in $2+1$- dimensional Nambu-Jona-Lasinio models.

SAMENVATTING

In dit proefschrift presenteren we drie schijnbaar verschillende modellen die door middel van holografrie beschreven kunnen worden. In hoofdstuk 2 presenteren we de S-matrix van een zwart gat volgens Gerard 't Hooft en vervolgens laten we zien hoe die afgeleid kan worden door een kwantum mechanisch probleem op te lossen. In hoofdstuk 3 presenteren we de correspondentie tussen een niet kritische Liouville snaar theorie gekoppeld aan $c = 1$ materie en een duale matrix kwantum mechanica model. In deze constructie bouwen wij een speelgoed model van een twee dimensionale kosmologie model dat een big-bang/big-crunch universum beschrijft. In hoofstuk 4 eindigen we met een toepassing van holografie op een $2 + 1$ dimensionale sterk gekoppelde theorie onder de invloed van een extern magnetisch veld met een eindige ladingsdichtheid op de nul temperatuur. Als een resultaat ontdekken we dat er een lijn is van tweede orde kwantum kritische punten door thermodynamisch duale gravitatie oplossing te vergelijken. We zullen niet diper ingaan op elk hoofdstuk.

In de introductie 1, geven we een basische en complete beschrijving van de physiche concepten die men moet kennen om dit profschrift te kunnen doorgronden. We presenteren, met name, het holografisch princie geformuleerd door Gerard 't Hooft en Leonard Susskind. Dit is het centrale idee achter de Ijk/Gravitatie dualiteit. Vervolgens presenteren we het best begrepen voorbeeld van holografie -ontdekt door Maldacena- dat aantoont dat gravitatie op AdS_5 duaal is aan een sterk gekoppeld $\mathcal{N} = 4$ super Yang-Mills ijk theorie. Daarna presenteren we thet woordenboek van de toegepaste gravitatie/ijk dualiteit dat relevant is voor hoofdstuk 4 en sommige voorbeelden waarbij de dualiteit belangrijk was. We eindigen dit onderdeel en gaan door met de natuurkunde van zwarte gaten, waar we eerst de astrofysische zwarte gaten definieÃ«ren en beschrijven. Vervolgens geven we comentaar op de moeilijkheidsgraad van het probleem om en connectie te maken tussen gravitatie en kwantum mechanica en geven we een beschrijving van het informatie paradox. Dit is relevant voor hoofdstuk 2. Daarna geven we een korte beschrijving van de wijze waarmee zwarte gat natuurkunde gebruikt kan worden om sterk gekoppelde systemen te beschrijven in de context van holografie en vice-versa. Vervolgens gaan we naar de correspodentie tussen Liouville snaar theorie en matrix kwantum mechanica door de ze te introduceren en aan te tonen hoe men een correct limiet te nemen - de double scaling limiet- om de dualiteit te bevestigen. We eindigen door het specifiek woordenboek tussen de twee te geven. Als laatste presenteren we, vanuit het oogpunt van gecondenseerde materie, kwantum kritikaliteit and kwantum fase transities die relevant zijn voor hoofdstuk 4.

In hoofdstuk 2 behandelen we de oude S-matrix van een zwart gat met de nieuwe partieele golf expansie van 't Hooft. Geinsipireerd door oude ideen uit niet kritische snaar theorie en de $c = 1$ matrix kwantum mechanica formuleren we de verstrooing in termen van het kwantum mechanica model -golven verstrooien van geinverteerde

harmonische oscillator potentialen- die precies de unitaire zwarte gat S-matrix reproduceert voor alle sferisch harmonische functies; elke partiele golf correspondeert met een geinverteerde harmonische oscillator met grontoestands energie die is verschoven ten opzichte van de s-golf oscillator. Het identificeren van een verbinding naar de twee dimensionale snaar theorie staat ons toe om aan te tonen dat er een exponentiele ontaarding is in de wijze waarmee de totale begins energie verdeeld kan worden over de vele partiele golven van het vier dimensionale zwart gat.

In hoofdstuk 3 bestuderen we de Matrix Kwantum Mechaninca (MQM) op de Euclidische tijd orbifold $S^1/\mathbb{Z}_2$. Na een Wick rotatie richting Lorentz tijd en een dubbeleschaal limiet geeft deze theorie een speelgoed model voor een big-bang/big-crunch universum in twee dimensionale niet-kritische snaar theorie waar de orbifold stabiele dekpunten kosmologische singulariteiten vormen. We leiden de MQM partitie functie af zowel in de canonical als de grand canonica ensemble in twee verschillende formuleringen en tonen aan dat ze overeenkomen. We duiden aan wat de contributies zijn van de twisted toestanden zijn allebei de formuleringen zowel gebruik makend van bi-lokale operatoren werkend op de eind punten van de tijd als vertakkingslijnen in het complexe vlak. In het matrix model berekenen we expliciet de contributie van de twisted toestanden op de torus level partitie functie en laten we zien dat het overeenkomt met het wereldschappen resultaat. Dit is dan een niet triviale test van de voorgestelde dualiteit. We beindigen met een discussie van sommige interessante eigenschappen van de partitie functie en de mogelijkheid om het te realiseren als een τ-functie van een integreerbare hierarchie.

In hoofdstuk 4 onderzoeken we de kwantum kritieke punten in een $2+1$ dimensionale ijktheorie met een eindig chemisch potentiaal en magnetisch veld. De gravitatie duaal is gebaseerd op een vier dimensionale $\mathcal{N}=2$ Fayet-Iliopoulos geijkte supergravity en de oplossingen die we bekijken -die analytisch geformuleerd zijn- zijn extremal, dyonische en asymptotische AdS_4 zwarte branen met een niet triviaal radiaal profiel voor het scalair veld en extremal, magnetisch geladen, asymptotische AdS_4 geaccepteerde singulaire oplosingen met een niet triviaal radiaal profiel voor het scalair veld. We ontdekken een lijn van tweede orde stabiele dekpunten op een kritische waarde van magnetisch veld tussen het dyonische zwarte braan en de extremal "thermisch gasöplossing met een singulariteit van het goede-soort, volgens de criteria van Gubser. De duale velden theorie is een sterk gekoppelde niet-conforme velden theorie met eindige lading en constant extern magnetisch veld, gerelateerd aan de ABJM theorie gedeformeerd door een drievoudig spoor operator. We vinden overeenkomsten tussen het gedrag van de grondtoestand excitatiewaarde van de scalaire operator onder de invloed van een extern veld and dat van een quark condensaat in $2+1$ dimensionaale Nambu-Jona-Lasinio modellen.

ACKNOWLEDGMENTS

I would like to thank my supervisor Umut Gürsoy for giving me the opportunity to work with him. Especially, I would like to thank him for his encouragement to work on different topics and to pursue my own research interests, as well as for discussing about many different physics problems. I would also like to thank my formal adviser, Stefan Vandoren, with whom I really enjoyed talking about physics in multiple occasions.

Next, I would like to thank my collaborators, Alesandra Gnecchi, Chiara Toldo, Marcos Crichigno, Nava Gaddam and Panos Betzios. It was and it still is a pleasure to work and discuss with you. My knowledge of physics would have not been the same without all the interactions that we had.

I would also like to thank the rest of the ITF members for creating such friendly and relaxed atmosphere in the institute and making it an ideal place for one to study physics. Especially, I would like to thank Lars Fritz and Henk Stoof for answering many questions relating to condensed matter physics. Phil Szepietowski, for being always available and genuinely enjoying discussing any physics problem as well as for trying to understand any question and being able to give an answer or a useful insight. Gerard 't Hooft, for inspiring Nava, Panos and myself to work on the physics of black holes and let us see a glimpse of his deep knowledge, intuition and understanding of physics. Bernard de Wit for patiently trying to help Nava, Panos and myself by decoding information from old papers. David Vegh for his useful tips. Also, I would like to thank Dio Anninos for the nice chats that we had and for his contagious enthusiasm for physics. Special thanks to Wanda Verweij-van Schaik, for being the best secretary possible and for always replying to my emails no matter the day or time and trying to give all possible help.

I am especially grateful to Jorgos Papadomanolakis, Jules Lamers and Aron Jansen for translating all the Dutch documents for me these four years. And especially to Jorgos for translating the summary of this thesis in Dutch.

Moreover, I would like to thank my office mates Aron, Marcos and Simon Gentle, for all the nice discussions that we had both for physics and life in general.

These four years in Utrecht, would have been duller without meeting Nava, Irina, Marcos, Sarah, Phil, Polina, Yiannis, Sofia and Simon. I want to thank you for all the nice moments that we shared.

I want to thank Denia Polydorou and Panos for being my paranymphs. And especially Denia for coming here all the way from Uppsala for my defense. Moreover, I would like to thank her for being so enthusiastic and for popping to my office to discuss physics when she was a master student in Utrecht.

Last but not least, I would like to thank my parents Vasilis and Maria for their constant emotional and in the beginning of my studies also financial support and my brother Mihalis. Moreover, I would like to thank the rest members of my family for

different reasons that they know. Finally, I would like to thank Panos for being my partner both in research and life and for being so supportive all these years.

CURRICULUM VITAE

I was born on the 3rd of March 1990 in Athens, Greece. I attended the Music Gymnasium and Lyceum of Sparta from where I graduated in July 2007. I subsequently enrolled in the Physics Department of National and Kapodistrian University of Athens and obtained a BSc in Physics degree in July 2012. My bachelor thesis with title "On holographic Renormalisation and AdS/CFT correspondence" was supervised by Prof A. Lahanas. Afterwards, I was enrolled in the Department of Applied Mathemtics and Theoretical Physics of Cambridge University, where I was awarded a Master of Advance Studies degree in Theoretical Physics in July 2013. In September 2013, I assumed a PhD candidate position in the Institute for Theoretical Physics of Utrecht University under the supervision of Dr. U. Gürsoy. This thesis is an account of the work that has been accomplished since then.

BIBLIOGRAPHY

[1] N. K. Gaddam, PhD Thesis (2016).

[2] P. Betzios, PhD Thesis (2017).

[3] G. 't Hooft, in *Salamfest 1993:0284-296* (1993) pp. 0284–296, arXiv:gr-qc/9310026 [gr-qc] .

[4] L. Susskind, J. Math. Phys. **36**, 6377 (1995), arXiv:hep-th/9409089 [hep-th] .

[5] C. B. Thorn, in *The First International A.D. Sakharov Conference on Physics Moscow, USSR, May 27-31, 1991* (1991) pp. 0447–454, arXiv:hep-th/9405069 [hep-th] .

[6] O. Aharony, S. S. Gubser, J. M. Maldacena, H. Ooguri, and Y. Oz, Phys. Rept. **323**, 183 (2000), arXiv:hep-th/9905111 [hep-th] .

[7] S. A. Hartnoll, *Strings, Supergravity and Gauge Theories. Proceedings, CERN Winter School, CERN, Geneva, Switzerland, February 9-13 2009*, Class. Quant. Grav. **26**, 224002 (2009), arXiv:0903.3246 [hep-th] .

[8] S. A. Hartnoll, A. Lucas, and S. Sachdev, (2016), arXiv:1612.07324 [hep-th] .

[9] G. 't Hooft, The Large N Expansion in Quantum Field Theory and Statistical Physics. Edited by BREZIN E ET AL. Published by World Scientific Publishing Co. Pte. Ltd., 1993. ISBN# 9789814365802, pp. 80-92 , 80 (1993).

[10] J. M. Maldacena, Int. J. Theor. Phys. **38**, 1113 (1999), [Adv. Theor. Math. Phys.2,231(1998)], arXiv:hep-th/9711200 [hep-th] .

[11] O. Aharony, O. Bergman, D. L. Jafferis, and J. Maldacena, JHEP **10**, 091 (2008), arXiv:0806.1218 [hep-th] .

[12] E. Witten, Adv. Theor. Math. Phys. **2**, 253 (1998), arXiv:hep-th/9802150 [hep-th] .

[13] U. Gursoy, E. Kiritsis, and F. Nitti, JHEP **02**, 019 (2008), arXiv:0707.1349 [hep-th] .

[14] U. Gursoy and E. Kiritsis, JHEP **02**, 032 (2008), arXiv:0707.1324 [hep-th] .

[15] B. Abbott, R. Abbott, T. Abbott, M. Abernathy, F. Acernese, K. Ackley, C. Adams, T. Adams, P. Addesso, R. Adhikari, *et al.*, Physical Review Letters **116**, 241103 (2016).

[16] K. Schwarzschild, in *Sitzungsberichte der Königlich Preussischen Akademie der Wissenschaften zu Berlin, Phys.-Math. Klasse, 424-434 (1916)* (1916).

[17] J. M. Bardeen, B. Carter, and S. W. Hawking, Commun. Math. Phys. **31**, 161 (1973).

[18] J. D. Bekenstein, Phys. Rev. **D7**, 2333 (1973).

[19] S. W. Hawking, Phys. Rev. **D13**, 191 (1976).

[20] S. W. Hawking, *In *Gibbons, G.W. (ed.), Hawking, S.W. (ed.): Euclidean quantum gravity* 167-188*, Commun. Math. Phys. **43**, 199 (1975), [,167(1975)].

[21] G. 't Hooft, Int. J. Mod. Phys. **A11**, 4623 (1996), arXiv:gr-qc/9607022 [gr-qc] .

[22] A. Strominger and C. Vafa, Phys. Lett. **B379**, 99 (1996), arXiv:hep-th/9601029 [hep-th] .

[23] K. Papadodimas and S. Raju, Phys. Rev. Lett. **112**, 051301 (2014), arXiv:1310.6334 [hep-th] .

[24] K. Papadodimas and S. Raju, Phys. Rev. **D89**, 086010 (2014), arXiv:1310.6335 [hep-th] .

[25] K. Hristov, A. Tomasiello, and A. Zaffaroni, JHEP **05**, 057 (2013), arXiv:1302.5228 [hep-th] .

[26] F. Benini, K. Hristov, and A. Zaffaroni, (2015), arXiv:1511.04085 [hep-th] .

[27] S. M. Hosseini and A. Zaffaroni, (2016), arXiv:1604.03122 [hep-th] .

[28] F. Benini and A. Zaffaroni, JHEP **07**, 127 (2015), arXiv:1504.03698 [hep-th] .

[29] C. Toldo, *Anti-de Sitter black holes in gauged supergravity. Supergravity flow, thermodynamics and phase transitions*, Ph.D. thesis, Utrecht U. (2014-12-31).

[30] N. Bobev, A. Kundu, K. Pilch, and N. P. Warner, JHEP **03**, 064 (2012), arXiv:1110.3454 [hep-th] .

[31] S. S. Gubser, S. S. Pufu, and F. D. Rocha, Phys. Lett. **B683**, 201 (2010), arXiv:0908.0011 [hep-th] .

[32] S. S. Gubser, C. P. Herzog, S. S. Pufu, and T. Tesileanu, Phys. Rev. Lett. **103**, 141601 (2009), arXiv:0907.3510 [hep-th] .

[33] A. Gnecchi, U. Gursoy, O. Papadoulaki, and C. Toldo, JHEP **09**, 090 (2016), arXiv:1604.04221 [hep-th] .

[34] O. DeWolfe, S. S. Gubser, O. Henriksson, and C. Rosen, Phys. Rev. **D95**, 086005 (2017), arXiv:1609.07186 [hep-th] .

[35] O. DeWolfe, O. Henriksson, and C. Rosen, Phys. Rev. **D91**, 126017 (2015), arXiv:1410.6986 [hep-th] .

[36] E. P. Wigner, in *Mathematical Proceedings of the Cambridge Philosophical Society*, Vol. 47 (Cambridge Univ Press, 1951) pp. 790–798.

[37] Y. Nakayama, International Journal of Modern Physics A **19**, 2771 (2004).

[38] I. R. Klebanov, in *Spring School on String Theory and Quantum Gravity (to be followed by Workshop) Trieste, Italy, April 15-23, 1991* (1991) arXiv:hep-th/9108019 [hep-th] .

[39] E. J. Martinec, in *9th Frontiers of Mathematical Physics Summer School on Strings, Gravity and Cosmology Vancouver, Canada, August 2-13, 2004* (2004) pp. 403–457, [,403(2004)], arXiv:hep-th/0410136 [hep-th] .

[40] S. Yu. Alexandrov, *Matrix Quantum Mechanics and String Theory in Two Dimensions in Non-trivial Fund*, Ph.D. thesis, CEA Saclay, SPhT (2003).

[41] M. R. Douglas, I. R. Klebanov, D. Kutasov, J. M. Maldacena, E. J. Martinec, and N. Seiberg, , 1758 (2003), arXiv:hep-th/0307195 [hep-th] .

[42] S. Sachdev, *Quantum phase transitions* (Wiley Online Library, 2007).

[43] G. 't Hooft, Nucl. Phys. **B256**, 727 (1985).

[44] S. S. Gubser, I. R. Klebanov, and A. M. Polyakov, Phys. Lett. **B428**, 105 (1998), arXiv:hep-th/9802109 [hep-th] .

[45] S. Mathur, "Confusions and questions about the information paradox & The fuzzball paradigm for black holes," `http://www.physics.ohio-state.edu/~mathur/confusions2.pdf`, `http://www.physics.ohio-state.edu/~mathur/faq2.pdf`, [Discussion on Samir Mathur's webpage - http://www.physics.ohio-state.edu/ mathur/].

[46] S. D. Mathur, *Strings, Supergravity and Gauge Theories. Proceedings, CERN Winter School, CERN, Geneva, Switzerland, February 9-13 2009*, Class. Quant. Grav. **26**, 224001 (2009), arXiv:0909.1038 [hep-th] .

[47] S. D. Mathur, *The quantum structure of space-time and the geometric nature of fundamental interactions. Proceedings, 4th Meeting, RTN2004, Kolymbari, Crete, Greece, September 5-10, 2004*, Fortsch. Phys. **53**, 793 (2005), arXiv:hep-th/0502050 [hep-th] .

[48] I. Bena and N. P. Warner, *Winter School on Attractor Mechanism (SAM 2006) Frascati, Italy, March 20-24, 2006*, Lect. Notes Phys. **755**, 1 (2008), arXiv:hep-th/0701216 [hep-th] .

[49] V. Balasubramanian, J. de Boer, S. El-Showk, and I. Messamah, *Strings, supergravity and gauge theories. Proceedings, European RTN Winter School, CERN, Geneva, Switzerland, January 21-25, 2008*, Class. Quant. Grav. **25**, 214004 (2008), arXiv:0811.0263 [hep-th] .

[50] K. Skenderis and M. Taylor, Phys. Rept. **467**, 117 (2008), arXiv:0804.0552 [hep-th] .

[51] S. D. Mathur, (2008), arXiv:0810.4525 [hep-th] .

[52] G. 't Hooft, (1991).

[53] G. 't Hooft, in *International Conference on Fundamental Aspects of Quantum Theory to Celebrate the 60th Birthday of Yakir Aharonov Columbia, South Carolina, December 10-12, 1992* (1992).

[54] G. 't Hooft, (2015), arXiv:1509.01695 [gr-qc] .

[55] G. 't Hooft, (2016), 10.1007/s10701-016-0014-y, arXiv:1601.03447 [gr-qc] .

[56] G. 't Hooft, (2016), arXiv:1605.05119 [gr-qc] .

[57] P. C. Aichelburg and R. U. Sexl, Gen. Rel. Grav. **2**, 303 (1971).

[58] T. Dray and G. 't Hooft, Nucl. Phys. **B253**, 173 (1985).

[59] G. Moore, M. R. Plesser, and S. Ramgoolam, Nuclear Physics B **377**, 143 (1992).

[60] K. Schoutens, H. L. Verlinde, and E. P. Verlinde, Phys. Rev. **D48**, 2670 (1993), arXiv:hep-th/9304128 [hep-th] .

[61] E. P. Verlinde and H. L. Verlinde, Nucl. Phys. **B406**, 43 (1993), arXiv:hep-th/9302022 [hep-th] .

[62] S. Yu. Alexandrov, V. A. Kazakov, and I. K. Kostov, Nucl. Phys. **B640**, 119 (2002), arXiv:hep-th/0205079 [hep-th] .

[63] J. L. Karczmarek, J. M. Maldacena, and A. Strominger, JHEP **01**, 039 (2006), arXiv:hep-th/0411174 [hep-th] .

[64] J. J. Friess and H. L. Verlinde, (2004), arXiv:hep-th/0411100 [hep-th] .

[65] J. M. Maldacena and N. Seiberg, JHEP **09**, 077 (2005), arXiv:hep-th/0506141 [hep-th] .

[66] C. G. Callan, Jr., S. B. Giddings, J. A. Harvey, and A. Strominger, Phys. Rev. **D45**, 1005 (1992), arXiv:hep-th/9111056 [hep-th] .

[67] G. W. Gibbons and P. K. Townsend, Phys. Lett. **B454**, 187 (1999), arXiv:hep-th/9812034 [hep-th] .

[68] V. Kazakov, I. K. Kostov, and D. Kutasov, Nuclear Physics B **622**, 141 (2002).

[69] J. M. Magan, (2016), arXiv:1601.04663 [hep-th] .

[70] A. Jansen and J. M. Magan, (2016), arXiv:1604.03772 [hep-th] .

[71] S. Banerjee, J.-W. Bryan, K. Papadodimas, and S. Raju, JHEP **05**, 004 (2016), arXiv:1603.02812 [hep-th] .

[72] S. Rychkov, (2016), arXiv:1601.05000 [hep-th] .

[73] S. Weinberg, Phys. Rev. **D82**, 045031 (2010), arXiv:1006.3480 [hep-th] .

[74] S. W. Hawking (2015) arXiv:1509.01147 [hep-th] .

[75] S. W. Hawking, M. J. Perry, and A. Strominger, Phys. Rev. Lett. **116**, 231301 (2016), arXiv:1601.00921 [hep-th] .

[76] J. Maldacena, Journal of High Energy Physics **2005**, 078 (2005).

[77] G. Moore and N. Seiberg, International Journal of Modern Physics A **7**, 2601 (1992).

[78] J. McGreevy and H. Verlinde, Journal of High Energy Physics **2003**, 054 (2004).

[79] P. Ginsparg and G. W. Moore, arXiv preprint hep-th/9304011 **9** (1992).

[80] M. S. de Bianchi, Open Physics **10 (2)**, 282 (2012), arXiv:1010.5329v3 [quant-ph] .

[81] C. de Carvalho and H. Nussenzveig, Physics Reports **364**, 83 (2002).

[82] T. Banks, arXiv preprint arXiv:1506.05777 (2015).

[83] V. Kazakov, in *Cargese Study Institute: Random Surfaces, Quantum Gravity and Strings Cargese, France, May 27-June 2, 1990* (1990).

[84] C. Asplund and D. Berenstein, (2010), arXiv:1009.4667 [hep-th] .

[85] A. Kitaev, "A simple model of quantum holography," `http://online.kitp.ucsb.edu/online/entangled15/kitaev/`, `http://online.kitp.ucsb.edu/online/entangled15/kitaev2/`, [Talks at KITP, April 7, 2015 and May 27, 2015].

[86] D. Anninos, S. A. Hartnoll, L. Huijse, and V. L. Martin, Class. Quant. Grav. **32**, 195009 (2015), arXiv:1412.1092 [hep-th] .

[87] D. Anninos, F. Denef, and R. Monten, JHEP **04**, 138 (2016), arXiv:1512.03803 [hep-th] .

[88] J. Maldacena and D. Stanford, (2016), arXiv:1604.07818 [hep-th] .

[89] G. W. Gibbons, Nucl. Phys. **B271**, 497 (1986).

[90] N. G. Sanchez and B. F. Whiting, Nucl. Phys. **B283**, 605 (1987).

[91] M. K. Parikh, I. Savonije, and E. P. Verlinde, Phys. Rev. **D67**, 064005 (2003), arXiv:hep-th/0209120 [hep-th] .

[92] J. Maldacena and L. Susskind, Fortsch. Phys. **61**, 781 (2013), arXiv:1306.0533 [hep-th] .

[93] D. Boulatov and V. Kazakov, Int. J. Mod. Phys. **A8**, 809 (1993), arXiv:hep-th/0012228 [hep-th] .

[94] B. de Wit, J. Hoppe, and H. Nicolai, Nucl. Phys. **B305**, 545 (1988).

[95] W. Taylor, Rev. Mod. Phys. **73**, 419 (2001), arXiv:hep-th/0101126 [hep-th] .

[96] J. B. Hartle and S. W. Hawking, Physical Review D **28**, 2960 (1983).

[97] A. Vilenkin, Physics Letters B **117**, 25 (1982).

[98] A. D. Linde, Lettere al Nuovo Cimento (1971-1985) **39**, 401 (1984).

[99] H. Liu, G. Moore, and N. Seiberg, arXiv preprint gr-qc/0301001 (2002).

[100] H. Liu, G. W. Moore, and N. Seiberg, JHEP **10**, 031 (2002), arXiv:hep-th/0206182 [hep-th] .

[101] H. Liu, G. W. Moore, and N. Seiberg, JHEP **06**, 045 (2002), arXiv:hep-th/0204168 [hep-th] .

[102] V. Balasubramanian, S. F. Hassan, E. Keski-Vakkuri, and A. Naqvi, Phys. Rev. **D67**, 026003 (2003), arXiv:hep-th/0202187 [hep-th] .

[103] M. Fabinger and J. McGreevy, JHEP **06**, 042 (2003), arXiv:hep-th/0206196 [hep-th] .

[104] D. Robbins and S. Sethi, JHEP **02**, 052 (2006), arXiv:hep-th/0509204 [hep-th] .

[105] E. J. Martinec, D. Robbins, and S. Sethi, JHEP **08**, 025 (2006), arXiv:hep-th/0603104 [hep-th] .

[106] S. Elitzur, A. Giveon, D. Kutasov, and E. Rabinovici, JHEP **06**, 017 (2002), arXiv:hep-th/0204189 [hep-th] .

[107] B. Craps and B. A. Ovrut, Phys. Rev. **D69**, 066001 (2004), arXiv:hep-th/0308057 [hep-th] .

[108] N. Turok, M. Perry, and P. J. Steinhardt, Phys. Rev. **D70**, 106004 (2004), [Erratum: Phys. Rev.D71,029901(2005)], arXiv:hep-th/0408083 [hep-th] .

[109] D. Z. Freedman, G. W. Gibbons, and M. Schnabl, *The new cosmology. Proceedings, Conference on Strings and Cosmology, College Station, USA, March 14-17, 2004, and Mitchell Symposium on Observational Cosmology, College Station, USA, April 12-16, 2004*, AIP Conf. Proc. **743**, 286 (2005), [,286(2004)], arXiv:hep-th/0411119 [hep-th] .

[110] B. Craps, S. Sethi, and E. P. Verlinde, JHEP **10**, 005 (2005), arXiv:hep-th/0506180 [hep-th] .

[111] B. Craps, A. Rajaraman, and S. Sethi, Phys. Rev. **D73**, 106005 (2006), arXiv:hep-th/0601062 [hep-th] .

[112] T. Ishino and N. Ohta, Phys. Lett. **B638**, 105 (2006), arXiv:hep-th/0603215 [hep-th] .

[113] M. Blau and M. O'Loughlin, JHEP **09**, 097 (2008), arXiv:0806.3255 [hep-th] .

[114] J. McGreevy and E. Silverstein, JHEP **08**, 090 (2005), arXiv:hep-th/0506130 [hep-th] .

[115] Y. Hikida and T.-S. Tai, JHEP **01**, 054 (2006), arXiv:hep-th/0510129 [hep-th] .

[116] Y. Nakayama, S.-J. Rey, and Y. Sugawara, (2006), arXiv:hep-th/0606127 [hep-th] .

[117] I. Antoniadis, C. Bachas, J. Ellis, and D. Nanopoulos, Nuclear Physics B **328**, 117 (1989).

[118] F. Larsen and F. Wilczek, Phys. Rev. **D55**, 4591 (1997), arXiv:hep-th/9610252 [hep-th] .

[119] L. Cornalba, M. S. Costa, and C. Kounnas, Nucl. Phys. **B637**, 378 (2002), arXiv:hep-th/0204261 [hep-th] .

[120] B. Craps, D. Kutasov, and G. Rajesh, JHEP **06**, 053 (2002), arXiv:hep-th/0205101 [hep-th] .

[121] M. Berkooz, B. Craps, D. Kutasov, and G. Rajesh, JHEP **03**, 031 (2003), arXiv:hep-th/0212215 [hep-th] .

[122] I. Florakis, C. Kounnas, H. Partouche, and N. Toumbas, Nucl. Phys. **B844**, 89 (2011), arXiv:1008.5129 [hep-th] .

[123] C. Krishnan and S. Roy, Phys. Rev. **D88**, 044049 (2013), arXiv:1305.1277 [hep-th] .

[124] N. Turok, B. Craps, and T. Hertog, (2007), arXiv:0711.1824 [hep-th] .

[125] B. Craps, T. Hertog, and N. Turok, Phys. Rev. **D86**, 043513 (2012), arXiv:0712.4180 [hep-th] .

[126] B. Craps, F. De Roo, and O. Evnin, JHEP **04**, 036 (2008), arXiv:0801.4536 [hep-th] .

[127] N. Engelhardt, T. Hertog, and G. T. Horowitz, JHEP **07**, 044 (2015), arXiv:1503.08838 [hep-th] .

[128] R. H. Brandenberger, E. G. M. Ferreira, I. A. Morrison, Y.-F. Cai, S. R. Das, and Y. Wang, Phys. Rev. **D94**, 083508 (2016), arXiv:1601.00231 [hep-th] .

[129] S. P. Kumar and V. Vaganov, JHEP **02**, 026 (2016), arXiv:1510.03281 [hep-th] .

[130] M. Gasperini and G. Veneziano, Phys. Rept. **373**, 1 (2003), arXiv:hep-th/0207130 [hep-th] .

[131] F. Quevedo, *The quantum structure of space-time and the geometric nature of fundamental interactions. Proceedings, RTN European Winter School, RTN 2002, Utrecht, Netherlands, January 17-22, 2002*, Class. Quant. Grav. **19**, 5721 (2002), arXiv:hep-th/0210292 [hep-th] .

[132] S. Kachru, R. Kallosh, A. D. Linde, and S. P. Trivedi, Phys. Rev. **D68**, 046005 (2003), arXiv:hep-th/0301240 [hep-th] .

[133] L. McAllister and E. Silverstein, Gen. Rel. Grav. **40**, 565 (2008), arXiv:0710.2951 [hep-th] .

[134] A. M. Polyakov, Physics Letters B **103**, 207 (1981).

[135] Y. Nakayama, Int. J. Mod. Phys. **A19**, 2771 (2004), arXiv:hep-th/0402009 [hep-th] .

[136] D. J. Gross and I. Klebanov, Nuclear Physics B **344**, 475 (1990).

[137] A. M. Polyakov, Physics Letters B **103**, 211 (1981).

[138] D. Kutasov and N. Seiberg, Physics Letters B **251**, 67 (1990).

[139] P. Di Francesco and D. Kutasov, Nucl. Phys. **B375**, 119 (1992), arXiv:hep-th/9109005 [hep-th] .

[140] T. Takayanagi and N. Toumbas, JHEP **07**, 064 (2003), arXiv:hep-th/0307083 [hep-th] .

[141] D. Kutasov and N. Seiberg, Nuclear Physics B **358**, 600 (1991).

[142] T. Banks, W. Fischler, S. H. Shenker, and L. Susskind, Phys. Rev. **D55**, 5112 (1997), arXiv:hep-th/9610043 [hep-th] .

[143] S. Yu. Alexandrov, V. A. Kazakov, and D. Kutasov, JHEP **09**, 057 (2003), arXiv:hep-th/0306177 [hep-th] .

[144] E. J. Martinec, (2003), arXiv:hep-th/0305148 [hep-th] .

[145] V. A. Kazakov and I. K. Kostov, , 1864 (2004), arXiv:hep-th/0403152 [hep-th] .

[146] S. Yu. Alexandrov and I. K. Kostov, JHEP **02**, 023 (2005), arXiv:hep-th/0412223 [hep-th] .

[147] V. A. Kazakov, I. Kostov, and A. Migdal, Physics Letters B **157**, 295 (1985).

[148] D. Boulatov, V. Kazakov, I. Kostov, and A. Migdal, Randomly Triangulated Surfaces In Two-Dimensions, Phys. Lett. B **159**, 303 (1985).

[149] V. Kazakov and A. Migdal, Nuclear Physics B **311**, 171 (1988).

[150] E. Brezin, V. Kazakov, and A. B. Zamolodchikov, Nuclear Physics B **338**, 673 (1990).

[151] G. 't Hooft, The Large N Expansion in Quantum Field Theory and Statistical Physics. Edited by BREZIN E ET AL. Published by World Scientific Publishing Co. Pte. Ltd., 1993. ISBN# 9789814365802, pp. 80-92 , 80 (1993).

[152] J. McGreevy and H. L. Verlinde, JHEP **12**, 054 (2003), arXiv:hep-th/0304224 [hep-th] .

[153] I. R. Klebanov, J. M. Maldacena, and N. Seiberg, JHEP **07**, 045 (2003), arXiv:hep-th/0305159 [hep-th] .

[154] A. B. Zamolodchikov and A. B. Zamolodchikov, (2001), arXiv:hep-th/0101152 [hep-th] .

[155] U. Gursoy and H. Liu, unpublished (2005).

[156] V. Kazakov, I. K. Kostov, and D. Kutasov, Nucl. Phys. **B622**, 141 (2002), arXiv:hep-th/0101011 [hep-th] .

[157] P. H. Ginsparg, in *Les Houches Summer School in Theoretical Physics: Fields, Strings, Critical Phenomena Les Houches, France, June 28-August 5, 1988* (1988) pp. 1–168, arXiv:hep-th/9108028 [hep-th] .

[158] M. Bershadsky and I. R. Klebanov, Physical review letters **65**, 3088 (1990).

[159] P. Ginsparg, Nuclear Physics B **295**, 153 (1988).

[160] L. Dixon, P. Ginsparg, and J. Harvey, Nuclear Physics B **306**, 470 (1988).

[161] P. Di Francesco, H. Saleur, and J.-B. Zuber, Nuclear Physics B **300**, 393 (1988).

[162] N. Seiberg, JHEP **03**, 010 (2005), arXiv:hep-th/0502156 [hep-th] .

[163] P. H. Ginsparg and G. W. Moore, in *Theoretical Advanced Study Institute (TASI 92): From Black Holes and Strings to Particles Boulder, Colorado, June 3-28, 1992* (1993) pp. 277–469, [,277(1993)], arXiv:hep-th/9304011 [hep-th] .

[164] S. Ramgoolam and D. Waldram, JHEP **07**, 009 (1998), arXiv:hep-th/9805191 [hep-th] .

[165] G. Moore, Nuclear Physics B **368**, 557 (1992).

[166] B. Eynard, T. Kimura, and S. Ribault, (2015), arXiv:1510.04430 [math-ph] .

[167] I. K. Kostov, *Recent developments in statistical mechanics and quantum field theory. Proceedings, Conference, Trieste, Italy, April 10-12, 1995*, Nucl. Phys. Proc. Suppl. **45A**, 13 (1996), arXiv:hep-th/9509124 [hep-th] .

[168] S. Kharchev, A. Marshakov, A. Mironov, A. Morozov, and S. Pakuliak, Nucl. Phys. **B404**, 717 (1993), arXiv:hep-th/9208044 [hep-th] .

[169] V. A. Kazakov, I. K. Kostov, and N. A. Nekrasov, Nucl. Phys. **B557**, 413 (1999), arXiv:hep-th/9810035 [hep-th] .

[170] R. Dijkgraaf and C. Vafa, (2002), arXiv:hep-th/0208048 [hep-th] .

[171] R. Dijkgraaf and C. Vafa, Nucl. Phys. **B644**, 21 (2002), arXiv:hep-th/0207106 [hep-th] .

[172] R. Dijkgraaf and C. Vafa, (2003), arXiv:hep-th/0302011 [hep-th] .

[173] S. Moriyama and T. Nosaka, JHEP **09**, 054 (2015), arXiv:1504.07710 [hep-th] .

[174] C. Vafa, (2014), arXiv:1409.1603 [hep-th] .

[175] G. Moore, N. Seiberg, and M. Staudacher, Nuclear Physics B **362**, 665 (1991).

[176] D. Kutasov, K. Okuyama, J.-w. Park, N. Seiberg, and D. Shih, JHEP **08**, 026 (2004), arXiv:hep-th/0406030 [hep-th] .

[177] J. M. Maldacena, G. W. Moore, N. Seiberg, and D. Shih, JHEP **10**, 020 (2004), arXiv:hep-th/0408039 [hep-th] .

[178] A. Morozov, Phys. Usp. **37**, 1 (1994), arXiv:hep-th/9303139 [hep-th] .

[179] A. Mukherjee and S. Mukhi, JHEP **10**, 099 (2005), arXiv:hep-th/0505180 [hep-th] .

[180] S. Mukhi, in *IPM String School and Workshop 2003 Caspian Sea, Iran, September 29-October 9, 2003* (2003) arXiv:hep-th/0310287 [hep-th] .

[181] J. A. Minahan, Int. J. Mod. Phys. **A8**, 3599 (1993), arXiv:hep-th/9204013 [hep-th] .

[182] M. Mehta, Communications in Mathematical Physics **79**, 327 (1981).

[183] V. Kazakov, Physics Letters A **119**, 140 (1986).

[184] H. Kleinert, *Path integrals in quantum mechanics, statistics, polymer physics, and financial markets* (World scientific, 2009).

[185] S. Matsumoto and S. Moriyama, JHEP **03**, 079 (2014), arXiv:1310.8051 [hep-th] .

[186] N. De Bruijn, J. Indian Math. Soc **19**, 133 (1955).

[187] H. Saleur, Journal of Physics A: Mathematical and General **20**, L1127 (1987).

[188] R. Dijkgraaf, E. Verlinde, and H. Verlinde, Communications in Mathematical Physics **115**, 649 (1988).

[189] N. Arkani-Hamed, A. G. Cohen, and H. Georgi, Phys. Rev. Lett. **86**, 4757 (2001), arXiv:hep-th/0104005 [hep-th] .

[190] I. K. Kostov, Phys. Lett. **B297**, 74 (1992), arXiv:hep-th/9208053 [hep-th] .

[191] M. Marino and P. Putrov, J. Stat. Mech. **1203**, P03001 (2012), arXiv:1110.4066 [hep-th] .

[192] D. J. Gross and E. Witten, Physical Review D **21**, 446 (1980).

[193] V. Periwal and D. Shevitz, Physical review letters **64**, 1326 (1990).

[194] A. Mironov, A. Morozov, and G. W. Semenoff, Int. J. Mod. Phys. **A11**, 5031 (1996), arXiv:hep-th/9404005 [hep-th] .

[195] J. Hoppe, V. Kazakov, and I. K. Kostov, Nucl. Phys. **B571**, 479 (2000), arXiv:hep-th/9907058 [hep-th] .

[196] S. Mukherji, S. Mukhi, and A. Sen, Physics Letters B **275**, 39 (1992).

[197] P. K. Mukherjee and A. Wahile, Journal of ethnopharmacology **103**, 25 (2006).

[198] M. Jimbo and T. Miwa, Publications of the Research Institute for Mathematical Sciences **19**, 943 (1983).

[199] J. W. van de Leur and A. Y. Orlov, Letters in Mathematical Physics **105**, 1499 (2015).

[200] A. Orlov, T. Shiota, and K. Takasaki, arXiv preprint arXiv:1611.02244 (2016).

[201] F. D. M. Haldane, Physical review letters **67**, 937 (1991).

[202] Y.-S. Wu, Physical review letters **73**, 922 (1994).

[203] J. Gomis and A. Kapustin, JHEP **06**, 002 (2004), arXiv:hep-th/0310195 [hep-th] .

[204] A. Borodin and E. Kanzieper, Journal of Physics A: Mathematical and Theoretical **40**, F849 (2007).

[205] G. Moore, Progress of Theoretical Physics Supplement **102**, 255 (1990).

[206] A. S. Fokas, A. Its, and A. Kitaev, Communications in Mathematical Physics **147**, 395 (1992).

[207] A. B. Zamolodchikov, Sov. Phys.-JETP **63**, 1061 (1986).

[208] R. J. Baxter, *Exactly solved models in statistical mechanics* (Elsevier, 1982).

[209] R. Baxter, Journal of Statistical Physics **145**, 518 (2011).

[210] D. F. Lawden, *Elliptic functions and applications*, Vol. 80 (Springer Science & Business Media, 2013).

[211] I. Affleck, Physical Review Letters **46**, 388 (1981).

[212] F. J. Dyson, Communications in Mathematical Physics **47**, 171 (1976).

[213] P. A. Deift, A. R. Its, and X. Zhou, Annals of mathematics **146**, 149 (1997).

[214] R. Dijgraaf, H. Verlinde, and E. Verlinde, Nuclear Physics B **371**, 269 (1992).

[215] A. Giveon, M. Porrati, and E. Rabinovici, Phys. Rept. **244**, 77 (1994), arXiv:hep-th/9401139 [hep-th] .

[216] A. A. Tseytlin and C. Vafa, Nucl. Phys. **B372**, 443 (1992), arXiv:hep-th/9109048 [hep-th] .

[217] E. Witten, Physical Review D **44**, 314 (1991).

[218] G. Mandal, A. M. Sengupta, and S. R. Wadia, Modern Physics Letters A **6**, 1685 (1991).

[219] P. Betzios, N. Gaddam, and O. Papadoulaki, Journal of High Energy Physics **2016**, 131 (2016).

[220] S. Sachdev, Ann. Rev. Condensed Matter Phys. **3**, 9 (2012), arXiv:1108.1197 [cond-mat.str-el] .

[221] M. J. Duff and J. T. Liu, Nucl. Phys. **B554**, 237 (1999), arXiv:hep-th/9901149 [hep-th] .

[222] M. Cvetic, M. J. Duff, P. Hoxha, J. T. Liu, H. Lu, J. X. Lu, R. Martinez-Acosta, C. N. Pope, H. Sati, and T. A. Tran, Nucl. Phys. **B558**, 96 (1999), arXiv:hep-th/9903214 [hep-th] .

[223] L. Andrianopoli, M. Bertolini, A. Ceresole, R. D'Auria, S. Ferrara, P. Fre, and T. Magri, J. Geom. Phys. **23**, 111 (1997), arXiv:hep-th/9605032 [hep-th] .

[224] A. Donos, J. P. Gauntlett, and C. Pantelidou, JHEP **01**, 061 (2012), arXiv:1109.0471 [hep-th] .

[225] A. Donos, J. P. Gauntlett, and C. Pantelidou, Class. Quant. Grav. **29**, 194006 (2012), arXiv:1112.4195 [hep-th] .

[226] A. Almuhairi and J. Polchinski, (2011), arXiv:1108.1213 [hep-th] .

[227] S. L. Cacciatori and D. Klemm, JHEP **01**, 085 (2010), arXiv:0911.4926 [hep-th] .

[228] D. Klemm and O. Vaughan, JHEP **01**, 053 (2013), arXiv:1207.2679 [hep-th] .

[229] C. Toldo and S. Vandoren, JHEP **09**, 048 (2012), arXiv:1207.3014 [hep-th] .

[230] N. Jokela, A. V. Ramallo, and D. Zoakos, JHEP **02**, 021 (2014), arXiv:1311.6265 [hep-th] .

[231] Y. Bea, N. Jokela, and A. V. Ramallo, (2016), arXiv:1604.03665 [hep-th] .

[232] K. Goldstein, S. Kachru, S. Prakash, and S. P. Trivedi, JHEP **08**, 078 (2010), arXiv:0911.3586 [hep-th] .

[233] K. Goldstein, N. Iizuka, S. Kachru, S. Prakash, S. P. Trivedi, and A. Westphal, JHEP **10**, 027 (2010), arXiv:1007.2490 [hep-th] .

[234] A. Amoretti, M. Baggioli, N. Magnoli, and D. Musso, (2016), arXiv:1603.03029 [hep-th] .

[235] S. S. Gubser, Adv. Theor. Math. Phys. **4**, 679 (2000), arXiv:hep-th/0002160 [hep-th] .

[236] I. Papadimitriou, JHEP **05**, 075 (2007), arXiv:hep-th/0703152 [hep-th] .

[237] A. Gnecchi and C. Toldo, JHEP **10**, 075 (2014), arXiv:1406.0666 [hep-th] .

[238] E. Witten, (2001), arXiv:hep-th/0112258 [hep-th] .

[239] M. Berkooz, A. Sever, and A. Shomer, JHEP **05**, 034 (2002), arXiv:hep-th/0112264 [hep-th] .

[240] T. Hertog and G. T. Horowitz, Phys. Rev. Lett. **94**, 221301 (2005), arXiv:hep-th/0412169 [hep-th] .

[241] D. Z. Freedman and S. S. Pufu, JHEP **03**, 135 (2014), arXiv:1302.7310 [hep-th] .

[242] S. M. Carroll, (1997), arXiv:gr-qc/9712019 [gr-qc] .

[243] V. A. Miransky and I. A. Shovkovy, Phys. Rept. **576**, 1 (2015), arXiv:1503.00732 [hep-ph] .

[244] V. P. Gusynin, V. A. Miransky, and I. A. Shovkovy, Phys. Rev. Lett. **73**, 3499 (1994), [Erratum: Phys. Rev. Lett.76,1005(1996)], arXiv:hep-ph/9405262 [hep-ph] .

[245] V. P. Gusynin, V. A. Miransky, and I. A. Shovkovy, Nucl. Phys. **B462**, 249 (1996), arXiv:hep-ph/9509320 [hep-ph] .

[246] R. D. Pisarski, Phys. Rev. **D29**, 2423 (1984).

[247] T. W. Appelquist, M. J. Bowick, D. Karabali, and L. C. R. Wijewardhana, Phys. Rev. **D33**, 3704 (1986).

[248] I. R. Klebanov and E. Witten, Nucl. Phys. **B556**, 89 (1999), arXiv:hep-th/9905104 [hep-th] .

[249] E. Berti, V. Cardoso, and A. O. Starinets, Class. Quant. Grav. **26**, 163001 (2009), arXiv:0905.2975 [gr-qc] .

[250] A. O. Starinets, Phys. Rev. **D66**, 124013 (2002), arXiv:hep-th/0207133 [hep-th] .

[251] M. Edalati, J. I. Jottar, and R. G. Leigh, JHEP **04**, 075 (2010), arXiv:1001.0779 [hep-th] .

[252] E. Witten, Adv. Theor. Math. Phys. **2**, 505 (1998), arXiv:hep-th/9803131 [hep-th] .

[253] J. M. Maldacena, Phys. Rev. Lett. **80**, 4859 (1998), arXiv:hep-th/9803002 [hep-th] .

[254] S.-J. Rey and J.-T. Yee, Eur. Phys. J. **C22**, 379 (2001), arXiv:hep-th/9803001 [hep-th] .

[255] S. Ryu and T. Takayanagi, Phys. Rev. Lett. **96**, 181602 (2006), arXiv:hep-th/0603001 [hep-th] .

[256] I. R. Klebanov, D. Kutasov, and A. Murugan, Nucl. Phys. **B796**, 274 (2008), arXiv:0709.2140 [hep-th] .

[257] G. S. Bali, F. Bruckmann, G. Endrodi, Z. Fodor, S. D. Katz, and A. Schafer, Phys. Rev. **D86**, 071502 (2012), arXiv:1206.4205 [hep-lat] .

[258] F. Preis, A. Rebhan, and A. Schmitt, JHEP **03**, 033 (2011), arXiv:1012.4785 [hep-th] .

[259] F. Preis, A. Rebhan, and A. Schmitt, Lect. Notes Phys. **871**, 51 (2013), arXiv:1208.0536 [hep-ph] .

[260] K. A. Mamo, JHEP **05**, 121 (2015), arXiv:1501.03262 [hep-th] .

[261] M. Ferreira, P. Costa, O. Lourenï¿œo, T. Frederico, and C. Providï¿œencia, Phys. Rev. **D89**, 116011 (2014), arXiv:1404.5577 [hep-ph] .

[262] J. McGreevy, Adv. High Energy Phys. **2010**, 723105 (2010), arXiv:0909.0518 [hep-th] .

[263] C. P. Herzog, *Spring School on Superstring Theory and Related Topics Miramare, Trieste, Italy, March 23-31, 2009*, J. Phys. **A42**, 343001 (2009), arXiv:0904.1975 [hep-th] .

[264] S. Sachdev, *5th Aegean Summer School: FROM GRAVITY TO THERMAL GAUGE THEORIES: THE AdS/CFT CORRESPONDENCE Adamas, Milos Island, Greece, September 21-26, 2009*, (2010), 10.1007/978-3-642-04864-7-9, [Lect. Notes Phys.828,273(2011)], arXiv:1002.2947 [hep-th] .

[265] G. Dall'Agata and A. Gnecchi, JHEP **03**, 037 (2011), arXiv:1012.3756 [hep-th] .

[266] K. Hristov and S. Vandoren, JHEP **04**, 047 (2011), arXiv:1012.4314 [hep-th] .

[267] G. Dall'Agata, G. Inverso, and M. Trigiante, Phys. Rev. Lett. **109**, 201301 (2012), arXiv:1209.0760 [hep-th] .

[268] C. V. Johnson, A. W. Peet, and J. Polchinski, Phys. Rev. **D61**, 086001 (2000), arXiv:hep-th/9911161 [hep-th] .

[269] A. Jeffrey and D. Zwillinger, *Table of integrals, series, and products* (Academic Press, 2007).

[270] M. Caselle and U. Magnea, Phys. Rept. **394**, 41 (2004), arXiv:cond-mat/0304363 [cond-mat] .

[271] H. Osborn, Lecture notes http://www.damtp.cam.ac.uk/user/ho/GNotes.pdf .

[272] J. Schur, Journal für die reine und angewandte Mathematik **139**, 155 (1911).

[273] M. Ishikawa, H. Kawamuko, and S. Okada, JOURNAL OF COMBINATORICS **12**, N9 (2005).

[274] G. Akemann and E. Kanzieper, J. Statist. Phys. **129**, 1159 (2007), arXiv:math-ph/0703019 [math-ph] .

[275] G. E. Andrews, Advances in Mathematics **191**, 408 (2005).

[276] K. Huang, *Introduction to statistical physics* (CRC Press, 2009).

[277] F. W. King, *Hilbert transforms*, Vol. 2 (Cambridge University Press Cambridge, 2009).

[278] P. Forrester and S. Warnaar, Bulletin of the American Mathematical Society **45**, 489 (2008).

[279] E. Basor and P. Forrester, Mathematische Nachrichten **170**, 5 (1994).

[280] M. L. Mehta, *Random matrices*, Vol. 142 (Academic press, 2004).

[281] E. Basor and P. Forrester, Mathematische Nachrichten **170**, 5 (1994).

[282] J. de Boer, E. P. Verlinde, and H. L. Verlinde, JHEP **08**, 003 (2000), arXiv:hep-th/9912012 [hep-th] .

[283] S. de Haro, S. N. Solodukhin, and K. Skenderis, Commun. Math. Phys. **217**, 595 (2001), arXiv:hep-th/0002230 [hep-th] .

[284] M. Bianchi, D. Z. Freedman, and K. Skenderis, Nucl. Phys. **B631**, 159 (2002), arXiv:hep-th/0112119 [hep-th] .

[285] I. Papadimitriou and K. Skenderis, JHEP **08**, 004 (2005), arXiv:hep-th/0505190 [hep-th] .

[286] A. Batrachenko, J. T. Liu, R. McNees, W. A. Sabra, and W. Y. Wen, JHEP **05**, 034 (2005), arXiv:hep-th/0408205 [hep-th] .

[287] S. W. Hawking and S. F. Ross, Phys. Rev. **D52**, 5865 (1995), arXiv:hep-th/9504019 [hep-th] .

[288] A. Ashtekar and A. Magnon, Class. Quant. Grav. **1**, L39 (1984).

[289] A. Ashtekar and S. Das, Class. Quant. Grav. **17**, L17 (2000), arXiv:hep-th/9911230 [hep-th] .

[290] Y. Kinar, E. Schreiber, and J. Sonnenschein, Nucl. Phys. **B566**, 103 (2000), arXiv:hep-th/9811192 [hep-th] .